Anatomical and Functional Analysis of microRNAs in Human Cornea Epithelial Progenitor Cells

LEE, Sharon Ka-wai

A Thesis Submitted in Partial Fulfillment of the Requirements for the Degree
of
Doctor of Philosophy
in
Ophthalmology and Visual Sciences

The Chinese University of Hong Kong
December 2009

ProQuest LLC
789 East Eisenhower Parkway
P.O. Box 1346
Ann Arbor, MI 48106-1346

Thesis/Assessment Committee

Prof Calvin Chi Pui PANG (Chair, thesis supervisor)
Prof Gary Hin Fai YAM (Thesis supervisor)
Prof Christopher Kai Shun LEUNG (Committee member)
Prof Richard Kwong Wah CHOY (Committee member)
Prof Herman S CHEUNG (External Examiner)

Abstract

Abstract of thesis entitled:

Anatomical and Functional Analysis of microRNAs in Human Cornea Epithelial Progenitor Cells

Sumbitted by LEE, Sharon Ka-wai

for the degree of Doctor of Philosophy in Ophthalmology and Visual Sciences

at the Chinese University of Hong Kong (December 2009)

MicroRNAs is a family of small non-coding RNAs that, in human, binds imperfectly to the 3' untranslated region (UTR) of target mRNAs for translational repression or negative regulation. Recent studies have shown that such negative regulatory pathways may play pivotal roles in the maintenance of asymmetric cell division in embryonic and tissue specific stem cells. Human corneal epithelial progenitor cells (CEPC), a tissue specific stem cell lineage residing between cornea and conjunctiva in the Palisade of Vogt of the limbus region, is known to maintain corneal homeostasis throughout human life. They respond to injury and normal wearing by rapid proliferation and differentiation into transit amplifying cells (TACs) and eventually corneal epithelial cells, though the biological factors controlling this homeostatic switch are still largely unknown. Here I hypothesized that microRNAs can participate in CEPC regulation. Experiments elucidating the anatomical distribution and functional roles of microRNAs on the human cornea rims were performed to testify this proposition.

This study begins with the phenotypic validation of human cornea rims recruited from the Chinese Hong Kong population using immunohistochemistry. Conventional CEPC markers (p63, EGFR, cytochrome oxidase and cytokeratin 15), embryonic stem

cell marker (stat1) and cancer stem cell markers (p73, MDM2 and pStat1) were expressed in the limbus region, suggesting that these specimens contained a source of CEPC for attesting our hypothesis.

Protocols aim at enriching the CEPC population were then devised. For the first time a four parameter cell sorting system utilizing ABCG2, Connexin 43, Notch 1 and pyronin Y as markers was established for the prospective in vitro study. Nevertheless, manual microdissection isolating the limbus region and the cornea region was employed for the present study of microRNAs.

By performing microRNA microarrays to globally detect any novel miRNAs in the limbus, eleven microRNAs (hsa-miR-136, hsa-miR-373*, hsa-miR-150, hsa-miR-143, hsa-miR-455, hsa-miR-145, hsa-miR-381, hsa-miR-224, hsa-miR-338, hsa-miR-154, hsa-miR-377) were found to be upregulated while two microRNAs (hsa-miR-122a and hsa-miR-425-3p) were identified as downregulated by more than 2 folds. Among these, hsa-miR-143 and hsa-miR-145 were distingushed to be the most significantly up-regulated limbal miRNAs. Individual assessement of the microarray results of a recently reported stem cell specific microRNA, hsa-miR-21, were also upregulated by more than two thousand fold when comparing limbus and cornea. miR-21, miR-143 and miR-145 were therefore selected as the most likely microRNA candidates in the present study. The expression level of these miRNA candidates were validated and confirmed by quantitative reverse transcription polymerase chain reaction (qRT-PCR). To localize these candidates, we performed *in situ* hybridization on frozen corneal rim sections using locked nucleic acid (LNA)-modified oligonucleotide probes. Results showed that miR-21, 143 and 145 were confined in the

limbal region with gradation of expression level along the basal-suprabasal line.

Functional roles of these microRNAs were then deciphered by overexpressing human corneal epithelial cell line (HCE) with precursor microRNAs (pre-miRs) through lipophilic transfection. Results showed that high endogenous level of miR-145 could inhibit cell proliferation by 3.5 fold as shown from MTT proliferation assay at day 5, and could generate discrete spherical colonies that resembles the morphology of holoclones at day 8, but not the other two candidate miRNAs.

To determine the mRNA targets of candidate microRNAs in HCE cells, Whole Human Genome Oligo Microarray Kits (Agilent Technologies) which contained 41K human genes and transcripts were employed. When compared to the scrambled control, HCE cells over-expressed with hsa-miR-21, 143 or 145 revealed differential expression of genes that participate in cell activation, motility and proliferation. Of note, interferon beta 1 fibroblast (IFNB1), a gene that is often deleted or rearranged in cancers, was significantly upregulated by a medium of 1093 fold in pre-miR-145 treated cells as confirmed by real time PCR assays.

In conclusion, I have identified three novel microRNAs (hsa-miR-21, 143, 145) which were precisely upregulated in the limbus region, while miR-145 was being the most limbal specific. In addition, the functions of miR-145 were found to be inhibitory on cell proliferation, possibly through the indirect regulation of IFNB1. These unprecedented results may suggest a therapeutic potential of miR-145 on limbal stem cell deficiency and limbal tumors because miR-145 can affect cell survival and proliferation.

摘要

此摘要取自論文題
《MicroRNA 在人角膜上皮祖細胞的解剖及功能分析》
於 二零零九年十二月
呈交自 李嘉慧
作爲 香港中文大學眼科及視覺神經學哲學博士學位 的結業所需

microRNA 是一類非編碼的小分子核糖核酸，在人體中，microRNA 通過與目標 mRNA 3'非編碼區的不完全結合來抑制或降低 mRNA 的翻譯。最新研究表明這種負性調節在保持胚胎及組織幹細胞的不對稱分裂中起到了關鍵作用。人角膜上皮祖細胞是一組織特定幹細胞系，存在於角結膜之間角膜緣區的 Vogt 欄柵，保持人體角膜平衡狀態。在損傷應答及修復過程中，人角膜上皮祖細胞可以快速增殖及分化成爲短暫擴充細胞，最終則成爲角膜上皮細胞，然而，調控此平衡轉換的生物因數尚且未知。在本論文中，我假設 microRNA 參與了人角膜上皮祖細胞的調控過程。爲了印證此觀點，我鑒定了 microRNA 在人角膜的解剖分佈及功能。

本研究的角膜樣本取自中國香港人口，以免疫組化確定其表型。結果顯示角膜緣基底細胞能夠表達角膜上皮祖細胞標記物（P63，EGFR，細胞色素氧化酶及角蛋白 15），胚胎幹細胞標記物（Stat1），以及癌幹細胞標記物（p73, MDM2 and pStat1）。這均說明是項研究所用的角膜樣本含有角膜上皮祖細胞。爲了提高角膜上皮祖細胞的濃度，我設計了以 ABCG2，連接蛋白 43，Notch 1 及 pyronin Y 作爲標記的四象流式細胞分離，是爲一創新方法用以細胞培植之研究。然而，本論文則僱用手工顯微切割以分離角膜緣及角

膜地區，以用作 microRNA 的研究。

透過 microRNA 微矩陣，全域性 microRNA 在角膜緣中的表達可以被探測。結果發現，在角膜緣地區有十一種 microRNAs (hsa-miR-136, hsa-miR-373*, hsa-miR-150, hsa-miR-143, hsa-miR-455, hsa-miR-145, hsa-miR-381, hsa-miR-224, hsa-miR-338, hsa-miR-154, hsa-miR-377)的表達提高了，而有兩種的 microRNAs (hsa-miR-122a ，hsa-miR-425-3p)表達則減低。在這其中，hsa-miR-143 與 hsa-miR-145 是上調表達最爲明顯的角膜緣特異性 miRNA。此外，近日的研究報導，通過單獨分析幹細胞特異性 microRNA 微矩陣結果，發現 miR-21 同樣在角膜緣中有較高表達。因此，在本研究中，miR-21, miR-143 and miR-145 被選定爲角膜緣幹細胞的候選 microRNA。應用 qRT-PCR 再次印證了其表達水準在角膜緣區域較角膜中央較高。冰凍角膜切片的原位雜交確定了其空間分佈位於角膜緣部的基底和副基底部。

在功能分析中，通過轉染 MicroRNA 前體入人角膜上皮細胞來提高 miR145 的表達，發現高水準內源性 miR-145 會抑制細胞增殖，並且形成少量球形分離性細胞團，包含小型增殖細胞。其後應用 Human Genome Oligo Microarray Kit (Agilent Technologies) 探測目的 mRNA，對比對照組，參與細胞動力，活化，增殖的基因在超表達 hsa-miR-21, 143 or 145 的人角膜上皮細胞表達有所差別。Real time PCR 顯示，腫瘤細胞中被檢測到變異的基因干擾素 1 在 miR-145 轉染的細胞中表達上升。

總的來說，我發現了三種新的 microRNA (hsa-miR-21, 143, 145)在角膜緣的表達有所提升。此外，也發現了 miR – 145 的職能爲抑制細胞增殖，可能通過間接調控的 IFNB1。因爲 miR - 145 能夠影響細胞的存活和增殖，這些前所未有的結果可能建議一個潛在的治療——以 miR – 145 醫治角膜緣幹細胞缺乏症和角膜腫瘤。

Acknowledgement

Studying a PhD includes two essential elements, the acquisition of knowledge and the learning from people. While the succeeding chapters log the scientific knowledge that I have acquired during the past three years, this acknowledgement is dedicated to the people that have intellectually and spiritually inspired me. Indeed I am very much privileged to study alongside with many talented people; I am more than grateful to have my life overlapped with many respectable others. Here, as part of the permanent record of my study, I wish to thank them one by one in words.

I would like to thank Prof Chi-pui Pang for his mentorship and critical review of my thesis. I am very much obliged to Prof Gary Yam for his speedy and valuable advice on my work. Thanks must also be due to Prof Richard Choy for granting me access to learn the state-of-the-art microarray experiments, and to Prof Chun-kwok Wong for allowing me to use all the flow cytometry equipments in his laboratory. I must also thank Prof Christopher Leung and Prof Herman Cheung for their cogent comments which have excelled my thesis. My thanks to them are beyond descriptions.

I am grateful to my labmates for their steady support. Thanks must be due to Dr Wai-ying Li and Ms Pancy Tam for their timely order of the animals and reagents, respectively, and to Dr Kai-on Chu, Mr Kwok-ping Chan, Ms Sylvia Chiang, Dr Ling-ping Cen, Dr Li-jia Chen, Mr Bo Gong, Dr Zhi-wei Li, Dr Huang-ming Liu, Dr

Xu Li, Mr Michael Ng, Dr Yu-fei Teng, Dr Li-ming Cao, Dr Jing Liu, Dr Enne Leung, Dr Zhang Xin, Mr Nathan Choi, Dr Shirley Liu, Miss Gilda Lai, Miss Nancy Liu, Miss Michelle Lai and Miss Rachel Cheung for their friendship, support and discussion. I am equally obliged to the previous lab members including Dr Josephine Lau, Dr Li-yun Jia, Dr Yvonne Ho, Dr Li-yun Zhang and Dr Hai-tao Li for being some wonderful companions during my first year of PhD study and for extending their friendship beyond.

My colleagues, ex-colleagues and friends in the Prince of Wales Hospital (PWH) remain affectionate throughout these years. I must thank Mr Kenneth Wong for his always kind support in the microarray experiments. I am grateful to Ms Carol Szeto and Ms Eve Choi for being very helpful especially in booking various machines for me. I feel myself fortunate to have the encouragement and friendship from Ms Bellise Chung, Dr Samantha Lun, Ms Priscilla Law, Dr Tao Tang and Dr Phyllis Cheung, whom have all made my PhD life fruitful and contented. Thanks must be due to Prof Chun-kwok Wong and his family again for their visits, friendship and caring. I am indebted to Dr Priscilla Poon - without her recommendation, I would have never begun my study here in this department.

For words like grateful, thankful and obliged are not sufficient to describe my feelings to my family. Without my parents, I would have never existed on this Earth. Without my sister, I would have never known how to act like an adult. Without my husband, I would have never completed. Without my son, I would have never understood how to

love. They are the pillar of my life and my study. My thesis is dedicated to them for teaching me things that I can never learn from books.

Publications and Academic Awards

Manuscript in preparation

Lee, S.K., Yam, G.H., Wong, K.H., Choy, R.K., Pang C.P. The role of miR-143 and miR-145 in corneal epithelial progenitor cells.

Conference publication

Lee, S.K., Yam, G.H., Wong, K.H., Choy, R.K., Pang C.P. MicroRNA profiling in human corneal progenitor cells. International Society for Stem Cell Research 7th Annual Meeting, July 8-11 2009, Barcelona, Spain. Thursday Poster Session Abstracts p244 (poster number 1503).

Academic awards

The Chinese University of Hong Kong Postgraduate Student Grants for Overseas Academic Activities (First Batch of Awards, 2009-2010).

Table of Content

Abbreviation

ABC	ATP binding cassette transporters
ABCG2	ATP binding cassette transporters, G family
BASC	Bronchioalveolar stem cells
Bcl-2	B-cell CLL/lymphoma 2
bESCs	Bulge epithelial stem cells
bFGF	basic fibroblast growth factor
BMI-1	B-cell-specific Moloney murine leukemia virus insertion site 1
BMP4	Bone morphogenetic protein 4
BRCP1	Breast cancer resistance protein 1
BSA	Bovine serum albumin
CD	Cell differentiation
CDCP1	CUB domain-containing protein 1
Cdk	Cyclin-dependent kinase
CEPC	Corneal epithelial progenitor cells
CE-RSCs	Ciliary epithelium-derived retinal stem cells
CFS	Colony stimulating factor
CFU	Colony forming unit
CK	Cytokeratin
CSCs	Cardiac stem cells
Ct	Cycle threshold
Cx43	Connexin 43
DAPI	4'6'-diamidino-2-phenyindole
DGCR8	DiGeorge syndrome critical region 8
EC	Embryonic cancer
EDTA	Ethylenediaminetetraacetic acid
EF	Elongation factor
EG	Embryonal carcinoma
eIF	Eukaryotic initiation factor
eNCSCs	Epidermal neural crest stem cells
EPCs	Endothelial progenitor cells
ES	Embryonic stem

FACS	Florescenced activated cell sorting
FITC	Fluorescein isothiocyanate
Foxd3	Forkhead box D3
FSP	Focal stromal projections (FSPs)
GDNF	Glial cell-derived neurotrophic factor
GFRα1	Glial cell-derived neurotrophic family alpha 1
GSCs	Gastric stem cells
GTP	Guanosine triphosphate
HOCs	Hepatic oval cells
HSCs	Hematopoietic stem cells
ICM	Inner cell mass
IE-RSCs	Iris-epithelium derived retina stem cells
IFNB1	Interferon beta 1
Ig	Immunoglobulin
IL-6	Interleukin 6
iPS	Induced pluripotent stem
ISCs	Intestinal stem cells
IVF	In vitro fertilization
JSIEC	Joint Shantou International Eye Center
K3	Keratin 3
KSCs	Keratinocyte stem cells
LC	Limbal crypts
LEC	Limbal epithelial crypts
LSCD	Limbal stem cell deficiency
m7G	7-methylguanosine
MDM2	Murine double minute 2
MDR1	Multi-drug resistance gene 1
MDSCs	Muscle-derived stem cells
miRISC	miRNA-induced silencing complex
miRNA	microRNA
M-RSCs	Müller glial derived retina stem cells
MSCs	Mesenchymal stem cells
NGF R	Nerve growth factor receptor
NSCs	Neural stem cells

OCP	Ocular cicatricial pemphigoid
OCT	Optimal cutting temperature
OCT4	Octomer 4
PBS	Phosphate buffered saline
PGC	Primordial germ cells
PSCs	Pancreatic stem cells
RIN	RNA integrity number
RNA	Ribonucleic acid
SCs	Stem cells
Sox2	Sex determining region Y-box 2
SP	Side population
STAT1	Signal Transducers and Activators of Transcription 1
UTR	Untranslated region
ABC	ATP binding cassette transporters

List of Figures

List of Tables

Part I
General Introduction

1

Prelude

1.1. Stem cells and progenitor cells

Stem cells, as defined by their functional attributes, are undifferentiated and unspecialized cells capable of indefinite self-renewal, proliferation and generation of progeny with wide range of differential potentials. Progenitor cells are essentially stem cells that have diminished power of potency, or differential potential as mentioned. Any cells that have potency less than the multipotent stage are generally regarded as progenitor cells.

1.2. Significance of progenitor cells

Progenitor cells, like stem cells, possess a special growth hierarchy bestowing by both the symmetric and asymmetric cell division, in which the former either generates two unaltered daughter progenitor cells or two daughter transit cells, and the latter produces one unaltered daughter progenitor cell and one daughter transit cell. The transit daughter cells in turn differentiate into the mature cells which have no further differential potential but serving to replace dying or damaged cells throughout the life cycle of an individual. It has been demonstrated that nearly every organ in the body

possesses its own population of progenitor cells (Table 1.1). The significance of progenitor cells therefore lies on their ability to indefinitely regenerate tissue in a specific organ especially after injury. A better understanding of progenitor cell biology has been envisaged as a basic requirement to develop novel and promising cell based therapy. This thesis aims at elucidating the molecular basis of progenitor cells in the epithelium of the human cornea. I shall begin here by introducing where this ocular progenitor cells reside.

Table 1.1. Progenitor cells and their therapeutic applications in disease treatment. BASCs = bronchioalveolar stem cells, bESCs = bulge epithelial stem cells, CE-RSCs = ciliary epithelium-retinal stem cells, M-RSCs = Müller glial derived retina stem cells, IE-RSCs = iris epithelium derived retina stem cells, CEPCs = corneal epithelial progenitor cells, CSCs = cardiac stem cells, EPCs = endothelial progenitor cells, eNCSCs = epidermal neural crest stem cells, GSCs = gastric stem cells, HOCs = hepatic oval cells, HSCs = hematopoietic stem cells, ISCs = intestinal stem cells, KSCs = keratinocyte stem cells, MDSCs = muscle-derived stem cells, MSCs = mesenchymal stem cells, NSCs = neural stem cells, PSCs = pancreatic stem cells, SCs = stem cells (Mimeault and Batra, 2008).

Progenitor cell source and type	Differentiated cells	Treated degenerative disorders and diseases
Eye		
CEPC	Corneal epithelial cells	Corneal disorders
Conjunctival SCs	Conjunctival epithelial cells	Conjunctival epithelial injury
CE-RSCs, M-RSC, IE-RSCs	Retinal progenitor cells	Retinal disorders
BM and vascular walls		
HSCs	Myleloid and lymphoid cells, platelets	Autoimmune diseases, anemias, thrombocytopenia, leukemias, aggressive solid tumors
MSCs	Osteoblasts	Osteoporosis, Osteogenesis imperfecta
	Chondrocytes	Cartilage disorders,
	Muscular cells	osteoarthritis
		Muscular disorders
HSCs, MSCs	Neural cells	Nervous system disorders
	Cardiomyocytes	Heart disorders
	Insulin-producing beta cells	Type 1 or 2 diabetes mellitus
	Hepatocytes	Liver disorders
EPCs	Endothelial cells	Vascular disorders
Adipose tissue/ skeletal		

muscle		
ADSCs and MDSCs	Muscle cells	Muscular disorders (muscular Duchenne and Becker dystrophies, neuromuscular disorders)
	Osteoblasts	Osteoporosis, Osteogenesis imperfecta
	Chondrocytes	Cartilage disorders, osteoarthritis
	Endothelial cells	Vascular disorders
	Cardiomyocytes	Heart disorders
	Neural cells	Nervous system disorders
ADSCs	Insulin-producing beta cells	Type 1 or 2 diabetes mellitus
	Hepatocytes	Liver disorders
Heart		
CSCs	Cardiomyocytes	Heart disorders
Brain		
NSCs	Neurons, Astrocytes	Nervous system disorders
	Oligodentrocytes	Myelin disorders
	Insulin-producing beta cells	Type 1 or 2 diabetes mellitus
Skin		
KSCs, bESCs and eNCSCs	Skin cells	Skin and hair disorders
Gastroinestinal tract		
ISCs and GSCs	Intestinal and stomach cells	Chronic inflammatory bowel diseases, ulcers
Pancreas		
PSCs	Insulin-producing beta cells	Type 1 or 2 diabetes mellitus
	Hepatocytes	Liver disorders
Liver		
HOCs	Hepatocytes, cholangiocytes	Hepatitis, acute liver failure, cirrhosis
	Cardiomyocytes	Heart failures
Lung		

BASCs	Lung cells (Bronchiolar Clara Cells and alveolar cells	Interstitial lung diseases, cystic fibrosis, asthma, chronic bronchitis, emphysema

2

The cornea epithelial progenitor cell

2.1. The human cornea and the cornea epithelium

The human cornea is situated at the most anterior part of the eye that touches posteriorly the aqueous in the anterior chamber (Figure 2.1). Functionally, it is the most refractive tissue contributing 2/3 refraction of the eye. This powerful role of the cornea is furnished by its unique integrity and transparency through the orchestration of five strata of specialized cells, in which the innermost being the endothelium, followed anteriorly by the Descemet's membrane, the stroma, the Bowman's membrane and the outermost epithelium (Figure 2.2).

Anatomically the epithelium is itself five-layered squamous comprising a single basal layer of cuboidal to columnar cells, two layers of wing cells immediately above, and another two layers of suprabasal or superficial cells which are more flattened and denser with some loss of cell organelles (Figure 2.3). All these five cellular layers does not contain papillary or vascular strucuture and are morphologically flat, supporting corneal transparency and thereby normal vision (Schermer et al., 1986). It has been suggested that the basal layer at the limbus region contains a population of progenitor cells.

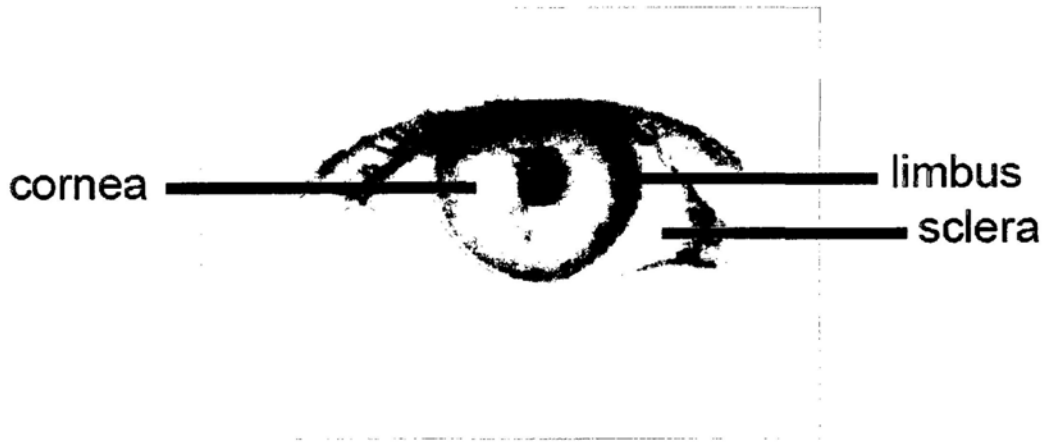

Figure 2.1. Location of cornea and limbus on the ocular surface of a Caucasian. Photo by Sharon K Lee, copyright 2009.

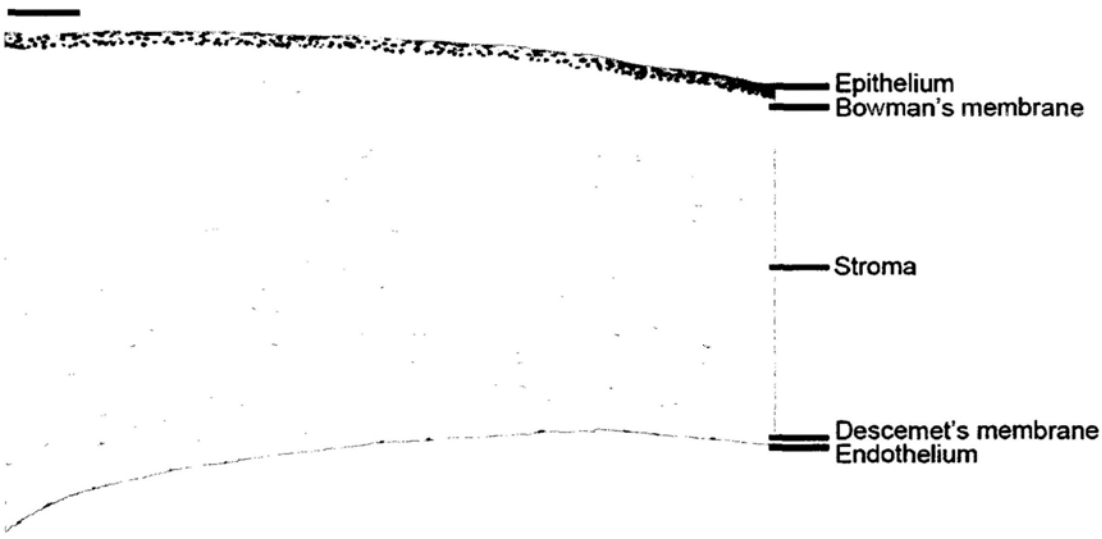

Figure 2.2. The five layers of human cornea epithelium, haematoxylin and eosin stained. Most of the endothelial cells were lost because this cornea rim was obtained after endothelial keratoplasty, the endothelium transplantation surgery that can better preserve the corneal shape, strength and focusing power of the eye when comparing to the conventional penetrating keratoplasty. Bar, 100 μm. Photo by Sharon K Lee, copyright 2009.

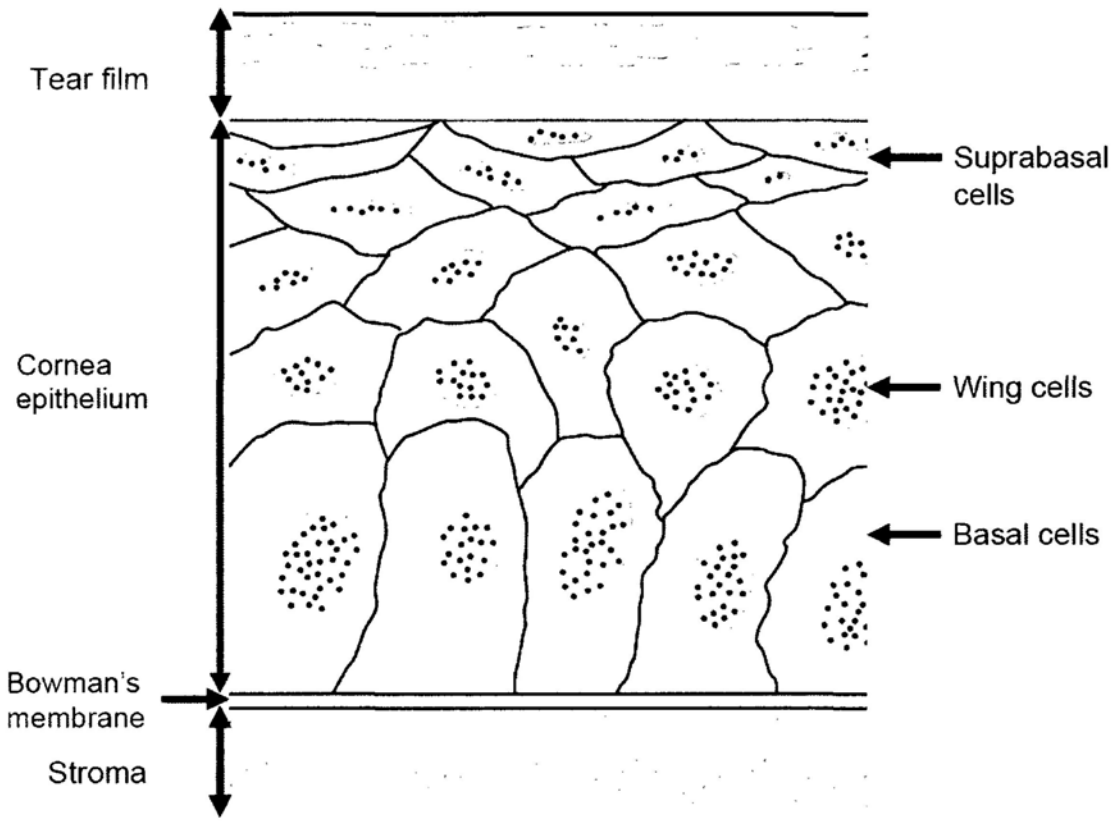

Figure 2.3. Schematic diagram showing the five cellular layers of human corneal epithelium. Photo modified from the Dictionary of Optometry and Visual Science, 2009.

2.2. Limbus as the location where cornea epithelial progenitor cells reside

The corneal limbus is defined as an annulus tissue approximately 1.5 mm wide situated at the vascularised junction between the transparent cornea and the opaque sclera. In the epithelium layer, this region is morphologically different from the central cornea region by being heavily pigmented and undulated. These features are necessary for protecting the progenitor cells at the basal layer because the epithelium is the outermost stratum of the cornea which frequently exposes to environmental challenges such as ultraviolet light and ionization. I postulate that it is also these daily stimuli which evolutionarises the cornea epithelium to possess its own population of progenitor cells for combating with the constant cell damages and cell death that may hinder normal vision.

At present, tremendous reports have suggested that the cornea epithelial progenitor cell resides at limbus. Davanger and Evensen are the first to propose limbus as the regenerative region for corneal epithelial cells (Davanger and Evensen, 1971). This notion was further substantiated by experiments on rabbit (Kinoshita et al., 1982), murine (Buck, 1979) and human (Lemp and Mathers, 1989) corneas by other groups. Although recently there are some reports suggesting a small portion of cornea epithelial progenitor cells may reside at the central cornea (Dua et al., 2009; Majo et al., 2008), the evidence are rather insufficient, especially when comparing to the enormous amount of circumstantial evidences obtained from both clinical and basic studies supporting limbus as the canonical residence for corneal epithelial progenitor

cells (Levis and Daniels, 2009).

2.3. The appellation of human cornea epithelial progenitor cells (CEPC)

Here in this context I shall use the term corneal epithelial progenitor cells, or CEPC in short, (Qi et al., 2008; Wang et al., 2009b) for a more explicit and specific description for the progenitor cell population of the cornea epithelium. This term is equivalent to other appellations including corneal limbal epithelial progenitor cells (Higa et al., 2009), limbal epithelial progenitor cells (Chen et al., 2007b; Li et al., 2007b; Miyashita et al., 2007), limbal epithelial stem cells (Hayashi et al., 2007; Rauz and Saw, 2009; Shortt et al., 2008), and limbal stem cells (Dua et al., 2009; Soliman Mahdy and Bhatia, 2009; Wylegala et al., 2008).

The rationale for chosing this CEPC appellation is that (1) the term limbus is not a specific term for the eye ; in anatomy, limbus actually refers to any distinctive border between two regions, for example, limbus may denote limbus of fossa ovalis (annulus ovalis), a prominent oval margin between left and right atrium of the heart ; and (2) If we use the noun adjective corneal instead of limbal to describe this epithelial progenitor cells, the fate of these cells is better implicated, which is to regenerate and replenish the corneal epithelial cells that wear off at the central cornea.

2.4. Functional characteristics of the cornea epithelial progenitor cells

Attributes of the cornea epithelial progenitor cells (CEPC) are functional and are defined through experiments. These experimental evidences also confirm the limbus location for this population of progenitor cells.

2.4.1. Proliferative and self-renewal capacity

One of the working definitions of stem / progenitor cells is being proliferative and self-renewing. Matsuda et al observed that the closer the wound to the limbus region, the faster the healing rate, indicating the proliferative potential of the peripheral corneal epithelium was greater than that of the central cornea (Matsuda et al., 1985). In the attempts to culture human limbal explants, it has been shown that peripheral corneal epithelium grew better than the central corneal epithelium (Ebato et al., 1987), yet limbal epithelium grew even better than the peripheral corneal epithelium (Ebato et al., 1988). In essence, the limbal epithelium has the greatest proliferative capacity, followed by the peripheral cornea and finally the central cornea (Chee et al., 2006). Besides, Pellegrini et al also showed that cultured limbal epithelium is able to generate holoclones which is comparable to other tissue specific stem cells such as epidermal progenitor cells (Pellegrini et al., 1999). The generation of holoclones has been regarded as an experimental indicator of self-renwal.

2.4.2. Slow cell cycle

Most progenitor cells are at mitotic quiescence in contrast to the genuine totipotent embryonic stem cells. In the resting stage, Cotsarelis et al demonstrated that corneal epithelial progenitor cells are slow-cycling as identified from the label retaining experiments (Cotsarelis et al., 1989).

2.4.3. Special growth hierarchy and centripetal migration

In 1983, Thoft and Friend proposed a mathematical formula, X + Y = Z, which clearly depicts the growth hierarchy of cornea epithelial progenitor cells. Literally this equation means that the epithelial cell loss from the surface (Z) is replaced by the proliferation of basal epithelial cells (X) and the centripetal movement of peripheral cells (Y) (Thoft and Friend, 1983). In line with this, Schermer et al observed that keratin 3 (K3), a differentiation marker, was exclusively expressed throughout the entire corneal epithelium, but was neither detected in the limbal basal epithelium nor the adjacent conjunctiva (Schermer et al., 1986). The centripetal migration model is therefore proposed, in which the undifferentiated progenitor cells at the limbus region can proliferate, differentiate and migrate into the transit amplifying cells at the basal epithelium of the cornea region. The transit amplifying cells eventually become the terminal epithelial cells, constituting the suprabasal layers at the central cornea epithelium (Figure 2.4).

2.5. Clinical implication of cornea epithelial progenitor cells

The functional characteristics and centripetal migration model suggests that aberrant regulation or depletion of corneal epithelial progenitor cells can result in disease conditions, respectively cornea epithelial tumors and limbal stem cell deficiency. These disease conditions also provide an indirect evidence supporting limbus as the location where cornea epithelial progenitor cell resides.

2.5.1. Cornea epithelial dysplasia and neoplasms

Cornea epithelial dysplasia and neoplasms are rare but the majority of them involve the limbal region (Dooley, 1958; Odom, 1954; Olasode et al., 1996; Park et al., 2009b; Rasteiro and Cunha-Vaz, 1976; Seale, 1953; Shirzadeh, 2008; Swan et al., 1948, 1950; Veasey, 1907). Their recurrent rate is high especially when the tumors are removed simply by mechanical debridement without excision of the neighbouring limbal tissue (Roberson, 1984). Together with the observation that these recurrences usually happen near the originally involved limbal area (Waring et al., 1984), an ancestral cell locating at the limbus region which is highly proliferative and self-renewing but is aberrantly regulated may have been involved. Naturally, corneal epithelial progenitor cell is a speculated ancestral cell and the cause for this tumorigenic condition.

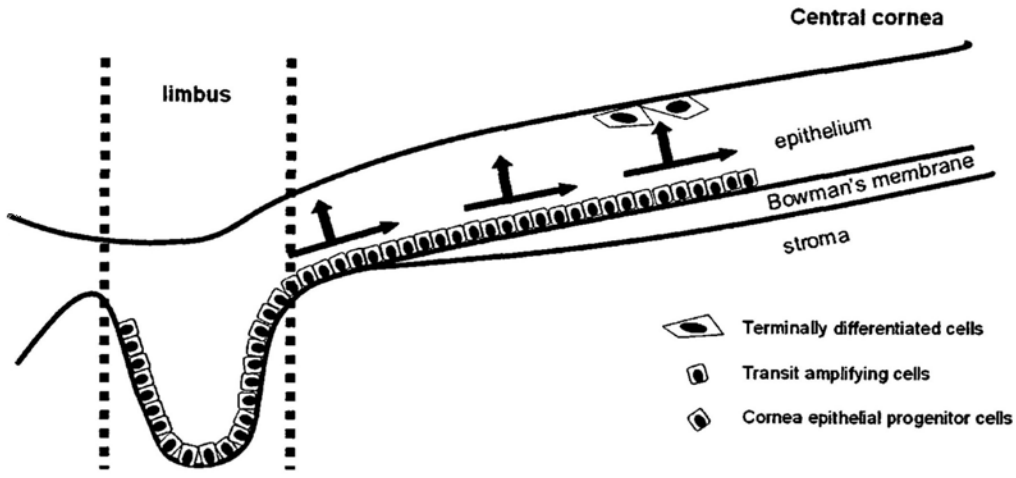

Figure 2.4. Schematic diagram showing the centripetal migration of cornea epithelial progenitor cells in the cornea epithelial maintenance. Drawn by Sharon K Lee, copyright 2009.

2.5.2. Limbal stem cell deficiency (LSCD)

Limbal stem cell deficiency (LSCD) is a complication caused primary by the insufficient stromal microenvironment to support CEPC function, such as in the condition of aniridia, congenital erythrokerato-dermia, chronic limbitis, neurotrophic keratopathy, and keratitis associated with multiple endocrine deficiencies. LSCD can also occur secondary by the destruction of CEPC through external factors, including but not exclusive to chemical burns, thermal injuries, Stevens-Johnson syndrome, ocular cicatricial pemphigoid (OCP), multiple surgeries or cryotherapies, contact lens wear, or extensive microbial infection (Dua et al., 2000). Patients with LSCD are normally presented with conjunctivalisation, the migration of vascular conjunctiva epithelium to the avascular corneal epithelium that can greatly hinder normal vision and deflate quality of life (Tseng, 1989).

Because the problem of LSCD patients is an insufficiency of progenitor cells at the peripheral cornea, conventional corneal keratoplasty cannot correct LSCD condition and offers little relief in LSCD patients (Revoltella et al., 2007). In 1989, Kenyon and Tseng presented two landmark studies in which transplanted CEPC was used to treat LSCD. The operation involves the autologous transfer of two free grafts of limbal tissue from the uninjured or less injured donor eye to the severely injured recipient eye. Patients undergone the operation showed improved visual acuity, rapid re-epithelialization with a smooth and stable corneal surface, healing of persistent epithelial defects and regression of neovascularization. Impression cytology also

confirmed the restoration of corneal epithelial phenotype (Kenyon, 1989; Kenyon and Tseng, 1989). Subsequently, others have adapted Kenyon and Tseng's technique and expanded the clinical use to bilateral LSCD condition. These techniques includes allograft transplantation (Tsai and Tseng, 1994; Tsubota et al., 1999), CEPC expansion before transplantation (Pellegrini et al., 1997), CEPC transplantation combined with amniotic membrane transplantation (Tseng et al., 1998), and CEPC expansion on amniotic membrane before transplantation (Koizumi et al., 2001a, b; Shimazaki et al., 2002). The clinical results of these studies have been promising, though the regulation of the corneal epithelial progenitor cells is still far from well understood.

2.6. Regulation of cornea epithelial progenitor cells

Within the limited knowledge on CEPC regulation, it has been known that the microenvironment niche, being the external factor, and the expression of various proteins, which is the intrinsic signals, are the two participants maintaining CEPC homeostasis.

2.6.1. External factor: The microenvironment niche

Niche represents a defined anatomical compartment that provides signals to the progenitor cells in the form of secreted and cell surface molecules, with the aim to control the rate of progenitor cell proliferation, to determine the fate of progenitor cell daughters, and to protect progenitor cells from exhaustion or death (Jones and Wagers, 2008). The three known niches for the cornea epithelial progenitor cells are all within the limbus regions, including the classical limbal palisades of Vogt (Goldberg and Bron, 1982) (Figure 2.5), limbal epithelial crypts (LEC) (Dua et al., 2005) (Figure 2.6), and the limbal crypts and focal stromal projections (FSPs) (Shortt et al., 2007). Anatomically these niches are rather well defined but functionally the signals secreted by these niches have not been extensively investigated.

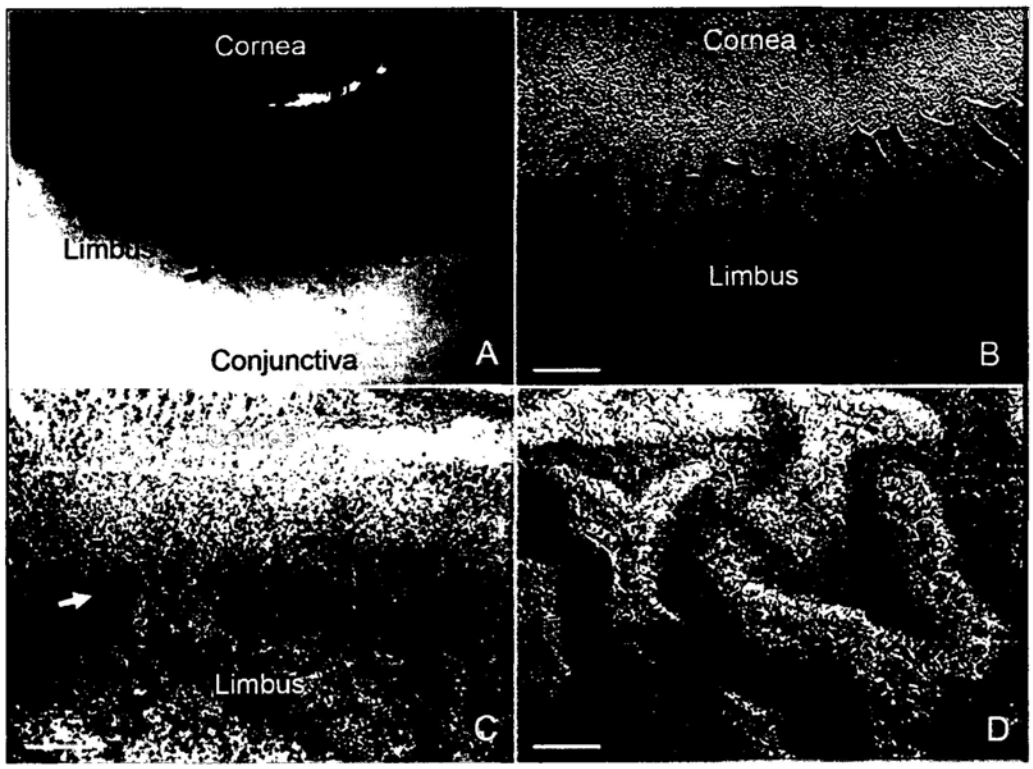

Figure 2.5. The limbal palisades of Vogt. The structure (A) on the ocular surface and (B) on the flat mount preparation of Dispase-isolated human limbal epithelial sheets. (C) It is heavily pigmented in donors with a darker skin. (D) The undulated epithelial papillae (stars) as shown in higher magnification. Bar represents 500 μm in A and B, 200 μm in C, and 50 μm in D. Reprinted by permission from Macmillan Publishers Ltd: Cell Res (Li et al., 2007a), copyright (2009).

2.6.2. Internal factor: Proteins

The known internal signals regulating corneal epithelial progenitor cells are mostly protein, as shown in Tabel 2.1. Most of the mentioned proteins are reported as phenotypic markers rather than having a precise dissection of its regulatory roles in cornea epithelial maintenance. p63, ABCG2, Connexin 43 and Notch 1 are the few proteins whose regulatory roles in cornea epithelial cells have been convincingly presented.

2.6.2.1. p63

p63 is the transcription factor essential for initiating epithelial stratification during development and for maintaining proliferative potential of basal keratinocytes in mature epidermis (Koster et al., 2004; Koster et al., 2005). Mice bearing phenotype of $p63^{-/-}$ displayed fundamental defect in stratified epithelial lineage development (Mills et al., 1999; Yang et al., 1999), which can be ascribed to a failure to maintain stem cells (Pellegrini et al., 2001). p63 expresison in the limbal basal epithelium is therefore critical in maintaining the progenitor-cell populations that are necessary to sustain corneal epithelial development and morphogenesis.

Table 2.1. Protein expression in limbal epithelium and corneal epithelium.

Positive markers	Limbal epithelium		Corneal epithelium	
	basal	suprabasal	basal	suprabasal
p63	+++	+/-	+/-	-
Δp63α	++	-	-	-
ABCG2	+++	+/-	-	-
Cytochrome oxidase and ATPase	+++	-	-	-
EGF R	+++	-	-	-
Importin 13	+++	-	-	-
Integrin α9	+++	+/-	-	-
NGF R (TrkA)	+++	++	+++	++
α-enolase	+++	+	++	+
Vimentin	+++	+/-	-	-
Keratin 19	++	-	-	-
Keratin 5 / 14	+++	-	-	-
Integrin β1	+++	++	++	+
N-Cadherin	++	-	-	-
GDNF	+++	++	-	-
GFRα-1	+++	++	-	-
Keratin 15	++	++	-	-
KGF-R	+/-	-	-	-
Notch1	+++	-	-	-
Negative markers				
Keratin 3/12	-	+++	+++	+++
Connexin 43	-	+++	+	+++
Connexin 50	-	+++	-	+++
Involucrin	-	+++	+	+++
NGFR ($p75^{NTR}$)	-	+++	+++	+++
E-cadeherin	+/-	+++	+++	+++
Integrin α2	- or +++	++	+++	+++
Integrin α6	- or +++	++	+++	+++
Integrin β4	- or +++	++	+++	+++

2.6.2.2. ABCG2

ABCG2, the G subfamily of the ATP Binding Cassette transporters, functions as a high capacity drug transporter with wide substrate specificity. This protein can transport large, hydrophobic, and both positively or negatively charged molecules, including cytotoxic compounds (mitoxantrone, topotecan, flavopiridol, methotrexate), fluorescent dyes (e.g., Hoechst 33342) and different toxic compounds found in normal food (2-amino-1-methyl-6-phenylimidazo[4,5-b]pyridine, PhIP) or pheophorbide A (Sarkadi et al., 2004). It mediates the extrusion of the transported compounds towards the extracellular space through a process energized by ATP hydrolysis (Nakagawa et al., 2002). From the stem cell perspective, this function is important to protect the cells from external stimulus and so maintain the undisturbed state of the stem cells. This view is supported by the facts that ABCG2 is expressed in a wide variety of stem cells (Zhou et al., 2001) besides in corneal epithelial progenitor cells (Budak et al., 2005).

2.6.2.3. Connexin 43

The connexins are a family of membrane proteins that typically aggregate to form a hexamer known as connexon. These connexons then join with sister connexons with adjacent cells to form an intercellular channel, or the so-called gap junction, which can enable passage of small molecules and therefore allow intercellular communication (Danesh-Meyer and Green, 2008). The absence of Connexin 43 in CEPC is important to isolate progenitor cells from the rest of the progeny, possibly for protecting and

maintaining the stemness (Matic et al., 1997). This is in agreement with epidermal stem cells (Matic et al., 2002) but not in hematopoietic stem cells (Cancelas et al., 2000; Rosendaal et al., 1994).

2.6.2.4. Notch 1

Notch 1 is a highly-conserved, ligand-activated transmembrane receptor known to play crucial roles in determining cell fates and developmental processes through cell to cell interactions (Thomas et al., 2007). Over-expression of Notch 1 receptor in the limbal epithelial cells in rat (Umemoto et al., 2005) and mice (Thomas et al., 2007) can help to maintain cornea epithelial progenitor cells at an undifferentiated states, as in hematopoietic stem cells (Duncan et al., 2005; Weber and Calvi, 2009), neural presuror cells (Crawford and Roelink, 2007) and the crypts of intestinal cells (Fre et al., 2005).

2.7. Current knowledge gap

Although CEPC has been used as a promising therapy in treating LSCD, functional myths like how CEPC determine its fate and maintain corneal homeostasis remain largely unknown. By studying a novel group of molecules, the microRNAs, we hope to further unravel the regulatory role of CEPC in cornea epithelial maintenance.

3

The microRNAs

3.1. History of microRNA discovery

The central dogma of molecular biology, first proposed by Francis Crick in year 1957 in one of his landmark lectures suggested that the transfer of information in cell flows from DNA to RNA and then to protein: DNA is the material for storage of genetic information in a stable form, protein is the functional participants of all the cellular activities, but RNA is only regarded as a middle man in this genetic information transfer (Crick, 1970; Crick, 1958). Such concept of 'genes control protein' (Crick, 1970) remained a canon until the discovery of small RNA.

The earliest discovery of small RNA can be dated back to 1993 when Victor Ambros (Figure 3.1A) and colleagues discovered *lin-4,* a gene controlling larval developmental timing in nematode *Caenorhabditis elegans,* did not encode a protein but produced two small RNAs approximately 61 and 22 nucleotides (nt) in length. While the longer transcript was predicted to fold into a stem loop and was likely the precursor of the shorter one, these transcripts in general contained sequences complementary to multiple sites in the 3' untranslated region (UTR) of *lin-14* mRNA (Lee et al., 1993). Ruvkun (Figure 3.2C) suggested that the *lin-4* RNAs pair to sites in the *lin-14* 3'UTR

to form multiple RNA duplexes that down-regulate *lin-14* translation (Wightman et al., 1991; Wightman et al., 1993). These papers, giving visionary hints on the microRNA biogenesis pathways and mechanisms, was at first underappreciated because the occurrence of these small functional RNA was not seen for six years in *C. elegans*, let alone in species other than nematodes. Perception of this apparent obscure concept began to change in 1999 when David Baulcombe (Figure 3.2B) announced the presence of "25-nt anti-sense RNA species" in tomatoes (Hamilton and Baulcombe, 1999), together with the discovery of the second small RNA *let-7* in *C. elegans* by Ruvkun. The pioneer research on the *C elegans* RNA reported in the early nineties was brought under the limelight. Similar to its precedent, *let-7* encodes a temporally regulated 21 nts RNA that is complementary to the multiple sites in the 3' UTR of several heterochronic genes (Reinhart et al., 2000). Loss-of-function experiments have confirmed the 3' UTR of one of these heterochronic genes, *lin-41*, is temporally and negatively regulated in a *let-7*-dependent manner (Slack et al., 2000). Northern blot analyses have revealed that expression of *let-7* RNAs were identified not only in *C. elegans*, but also in human and Drosophila and were developmentally regulated in lophotrochozoans and deuterostomes (Pasquinelli et al., 2000). Because both *let-7* and *lin-4* have common roles in developmental timing in bilateral animals and "their size is central" to their regulatory function, they were first proposed as short temporal RNAs (stRNAs), with anticipation that additional regulatory RNAs of this type would be unmasked (Pasquinelli et al., 2000). In 2001, less than a year after the *let-7* discovery, Tuschl, Bartel, and Ambros cloned small RNAs of 21-25 nts from three different organisms, detecting over 100 novel tiny RNAs (Lagos-Quintana et al., 2001; Lau et

al., 2001; Lee and Ambros, 2001). A more systematic nomenclature was therefore urgently needed. From this year onwards, any tiny endogenous non-coding RNAs which "are about 20-24 nts in length and are processed from fold-back structures" have been referred to as "microRNA, abbreviated miRNAs, with individual miRNAs and their genes designated miR-# and mir-#, respectively" (Lau et al., 2001).

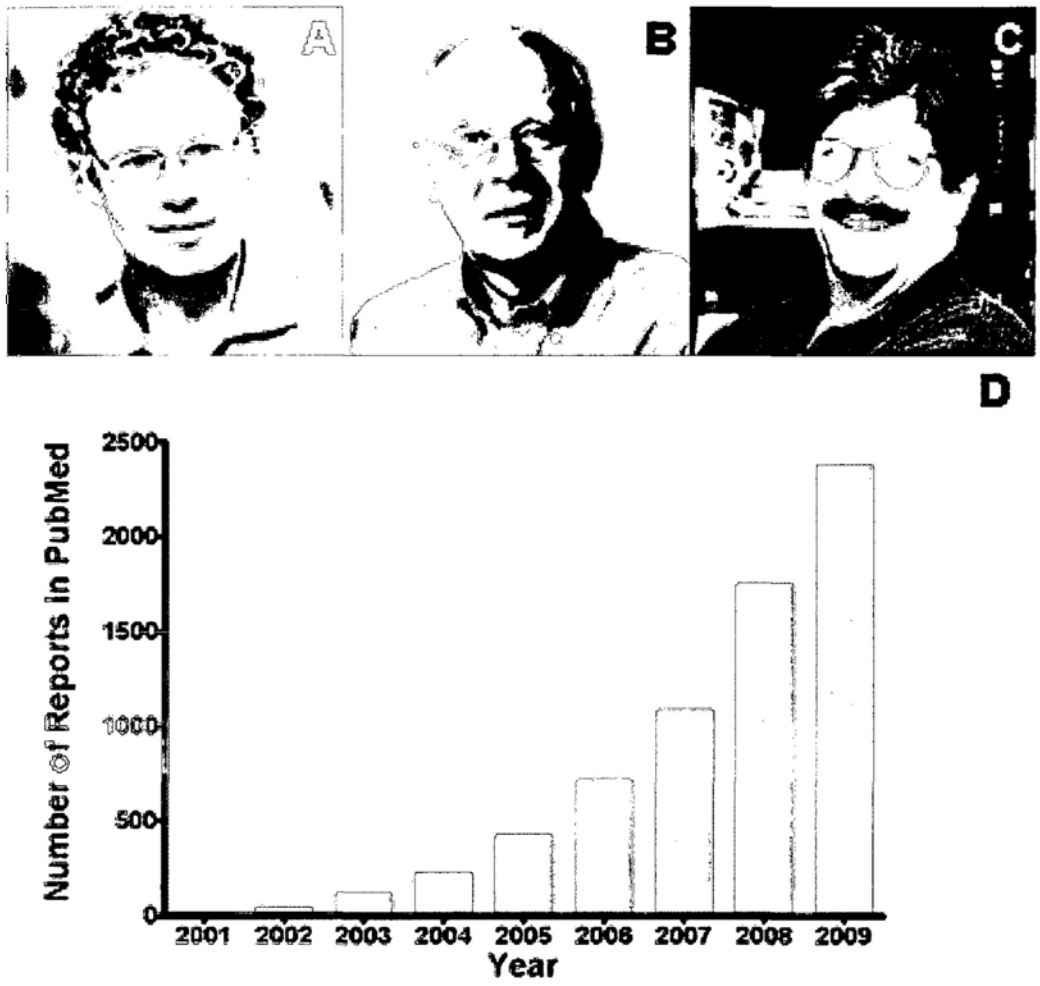

Figure 3.1. History and discovery of microRNAs. (A-C) Major contributors to the early discovery of microRNA: Victor Ambros (A), David Baulcomb (B) and Gary Ruvkun (C). (D) Research on microRNA has grown exponentially from 2001, the year that the second miRNA let-7 was discovered. (Photos in A,B and C were modified from Lasker Foundation. www.laskerfoundation.org. Data in D were obtained from PubMed on Friday, December 25, 2009).

3.2. Biogenesis of microRNA

The short history of microRNAs suggests that it is a novel group of molecules with uncountable possibilities and is therefore the center of some of the most enchating scientific puzzles that entails solution today (Figure 3.1D). Much efforts have therefore been invested in understanding miRNAs, with the primary focus on decoding its biogenesis pathway. At present, miRNA biogenesis is known to comprise of three major steps in various cell compartments: (1) transcription and maturation in the nucleus, (2) export from the nucleus to the cytoplasm, and (3) subsequent processing and maturation in the cytoplasm (Singh et al., 2008b) (Figure 3.2).

The biogenesis of miRNA begins in the nucleus when microRNA genes are transcribed into long (usually > 1000 nts) primary microRNA transcripts (pri-miRNA) by either RNA polymerase II (pol II) (Brennecke et al., 2003; Lee et al., 2004) or RNA polymerase III (pol III) (Borchert et al., 2006). The choice of RNA polymerase (pol) for miRNA gene transcription occurs at a miRNA-dependent manner. pol II transcribes miRNA that was processed from the introns of protein coding genes (Bartel, 2004) and it regulates cellular development (Cai et al., 2004); while pol III transcribes the largest human miRNA cluster, C19MC (Borchert et al., 2006). Nevertheless, a single pri-miRNA transcript often contains sequences for several different miRNAs (Filipowicz et al., 2008), in which the expression of selected miRNAs may be controlled by transcription factors, including c-Myc or p53 (He et al., 2007; O'Donnell et al., 2005), or relies on the methylation stage of their promoter

sequences (Brueckner et al., 2007; Lujambio et al., 2008; Saito et al., 2006; Weber et al., 2007). Although 50 % of the miRNAs are found to be located in the same genomic clusters, they can be transcribed and regulated independently (Song et al., 2008). The long duplex pri-miRNAs is then folded into hairpin structures containing imperfectly base-paired stems in which the base are cleaved with a typical staggered cut by the RNase III endonuclease class 2 Drosha (Basyuk et al., 2003; Lee et al., 2003) and its partner co-factor, either DiGeorge syndrome critical region gene 8 (DGCR8) in mammals (Han et al., 2004; Han et al., 2006) or Pasha (Partner of Drosha) in *Drosophila melanogaster* (Yeom et al., 2006), thereby liberating the ~ 60-70 hair-pin intermediates that bears a 5' phosphate and ~2 nt 3' overhang called miRNA precursor (pre-miRNA) (Lee et al., 2003; Zeng et al., 2003). This pre-miRNA then awaits active transport from nucleus into the cytoplasm by Ran-GTP *via* the nuclear export receptor Exportin-5 (Bohnsack et al., 2004; Lund et al., 2004; Yi et al., 2003).

While the amputation by Drosha complex in the nucleus defines one end of the mature miRNA, the other end is excised by the ATP-dependent multidomain RNase III endonuclease class 3 Dicer (Bernstein et al., 2001; Grishok et al., 2001; Hutvagner et al., 2001; Ketting et al., 2001), which is coupled by the double strand RNA (dsRNA) binding protein partner, TAR RNA-binding protein (TRBP) in the cytoplasm of human (Chendrimada et al., 2005). This Dicer protein composes of two major functional domains, namely, PAZ and RNase III (Macrae et al., 2006). PAZ domains are specialized to bind RNA ends, especially duplex terminus with short (~ 2 nt) 3' overhangs. The pre-miRNA, with one end engaging to the Dicer PAZ domain (Figure

3.3), extends approximately two helical turns (~ 22 bp) along the surface of the Dicer protein before it reaches a single processing center involving two RNase III domains. Each active site of these domains cleaves one of the two pre-miRNA strands, leading to a staggered short-lived duplex scission that bears a 5' monophosphate and a new end with ~2 nt 3' overhangs (Carthew and Sontheimer, 2009). The distance between PAZ domain and the RNase III processing center dictates the length of the mature microRNAs (MacRae et al., 2007).

The transient miRNA duplex is then unwound by helicase(s) and is separated into mature miRNA and its opposing arm, miRNA*, which is usually degraded by an unknown nuclease. Thermodynamic criteria influence the choice of miRNA versus miRNA*, that is, the strand with the less stable 5' end (for instance, G:U pair versus G:C pair) usually survives (Khvorova et al., 2003; Schwarz et al., 2003). Moreover, miRNAs can arise from either arm of the pre-miRNA stem. While occasionally some pre-miRNAs produce mature miRNAs from both arms, other pre-miRNAs show pronounced thermodynamic asymmetry that the miRNA* is rarely detected (Ruby et al., 2006). The functional miRNA strand is finally loaded with Argonaute protein 2 (Ago 2) and glycine(G)-tryptophan(W) bodies at molecular size 182 kDa (GW182) into a ribonucleoprotein complex, known as miRNA-induced silencing complex (miRISC), for the downstream mechanisms in which their regulatory effects are exerted.

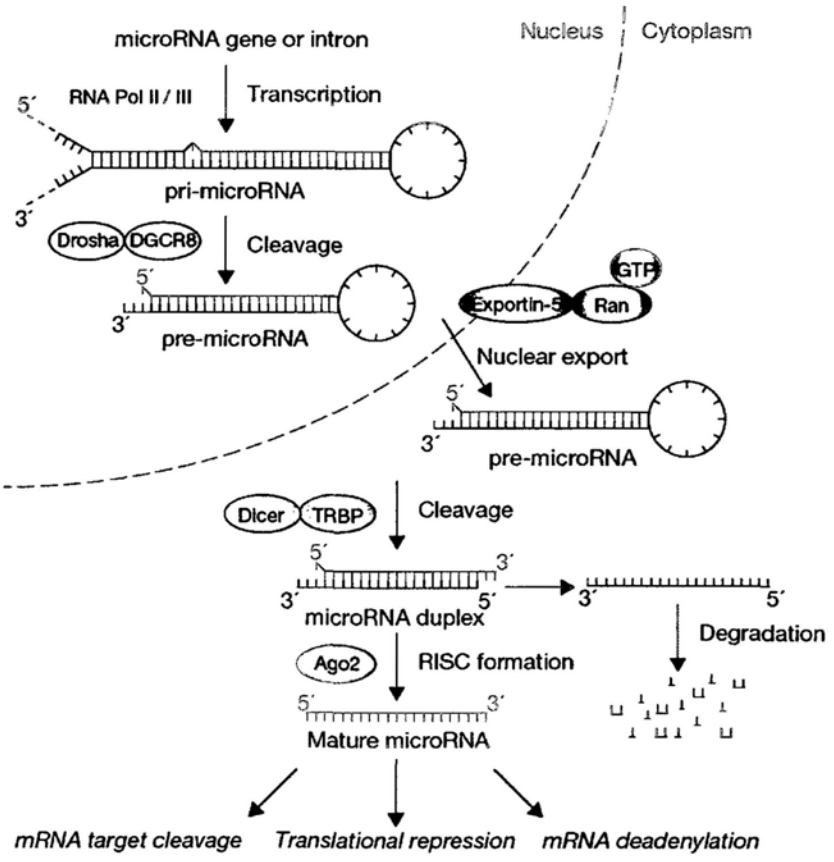

Figure 3.2. The 'linear' canonical pathway of microRNA processing. Adapted with permission from Macmillan Publishers Ltd: Nature Cell Biology (Winter et al., 2009), copyright (2009).

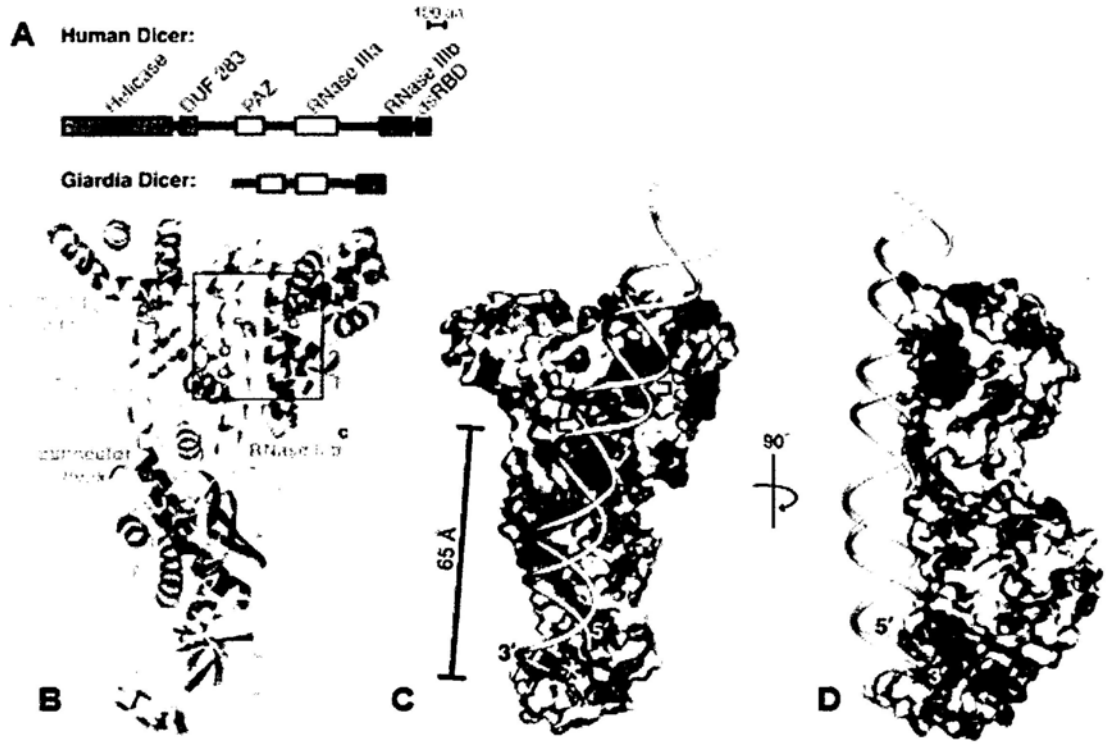

Figure 3.3. Structure of Dicer protein. (A) Schematic representation of the primary sequence of human and *Giardia* Dicers. (B) Crystal structure of *Giardia* Dicer, front view. (C-D) A model for dsRNA processing by Dicer: front view (C) and side view (D). Adapted with permission from the American Association for the Advancement of Science: Science (Macrae et al., 2006), copyright (2009).

3.3. Regulatory mechanisms of microRNA

microRNAs exerts its negative regulation by inhibiting the initiation and post-initiation phase of translation, and by triggering mRNA decay.

3.3.1. Inhibition at the initiation phase

3.3.1.1. Competition for the cap structure

It has been reported that at the very early stage of translation, Ago2 of the miRISC can compete with the eukaryotic initation factor eIF4E for binding to the mRNA 5'-terminal 7-methylguanosine (m7G) cap structure (Kiriakidou et al., 2007). Because the interaction of eIF4E and the m7G is actually the key to switch on the entire translation process, all the downstream translation steps are inhibited by the Ago2 competition and therefore microRNAs (Figure 3.4A).

3.3.1.2. Inhibition of ribosomal subunit joining

Similarly, eIF6 participates in the biogenesis and maturation of 60S ribosomal subunits. It is also known as an anti-association factor that binds to the 60S subunit, prevents the tethering between 40S and 60S ribosomes, thus precludes the productive assembly of 80S ribosomes (Ceci et al., 2003; Filipowicz et al., 2008; Sanvito et al., 1999). Chendrimada et al. identified eIF6 and 60S ribosomal subunits in association with

AGO2-Dicer-TRBP (RISC complex) in human cells, suggesting the RISC complex may recruit the eIF6 bound 60S for preventing the assembly of translationally competent 80S ribosome which results in translation repression (Chendrimada et al., 2007) (Figure 3.4B).

3.3.1.3. Inhibition of mRNA circularisation

Wakiyama et al in 2007 further reported a strict requirement for both the 5' m7G cap structure and 3' polyA tail in silencing (Wakiyama et al., 2007). They utilized a cell free system prepared from rabbit reticulocyte and human HEK293F cell lysate and proposed that miRNA might have bestowed the repression of capped mRNAs by impairing the eIF4G-mediated mRNA circularization via deadenylation at the 3' terminus (Eulalio et al., 2008) (Figure 3.4C).

3.3.2. Inhibition at the post-initiation phase

3.3.2.1. Ribosomal drop-off

Petersen et al. proposed that miRNAs represses translation by causing ribosomes to exit prematurely from their associated mRNAs (Figure 3.4D). They suggested that the miRISC imperfectly binds at the 3' UTR of a target mRNA and acts at a distance to cause drop-off of translating ribosomes at multiple sites within the open reading frame (ORF). A tiny increase in drop off frequency at multiple sites would significantly

diminish the synthesis of full-length polypeptides (Petersen et al., 2006). Though there are no precedents similar to Petersen et al's proposal in the ORF of eukaryotic cells, earlier studies have established the mechanism of ribosomal drop-off repression in prokaryotic cells (Jorgensen and Kurland, 1990; Manley, 1978; von Hippel and Yager, 1991). Besides, independent reports have also suggested possible role of miRNA in slowing down ribosomal elongation besides causing drop-off (Filipowicz et al., 2008; Mootz et al., 2004; Ruegsegger et al., 2001).

3.3.2.2. Co-translational protein degradation

miRNA degrades nascent polypeptides while it is actively translated (Figure 3.4E). Maroney et al arbitrarily chose three representative miRNAs (miR-21, miR-16 and let-7a) and demonstrated that the vast majority of them are associated with actively translating mRNA in polyribosomes (Maroney et al., 2006). Similarly, Nottrott et al. also indicated that let-7a miRNA inhibits actively translating polyribosomes and interferes with the accumulation of growing polypeptides (Nottrott et al., 2006).

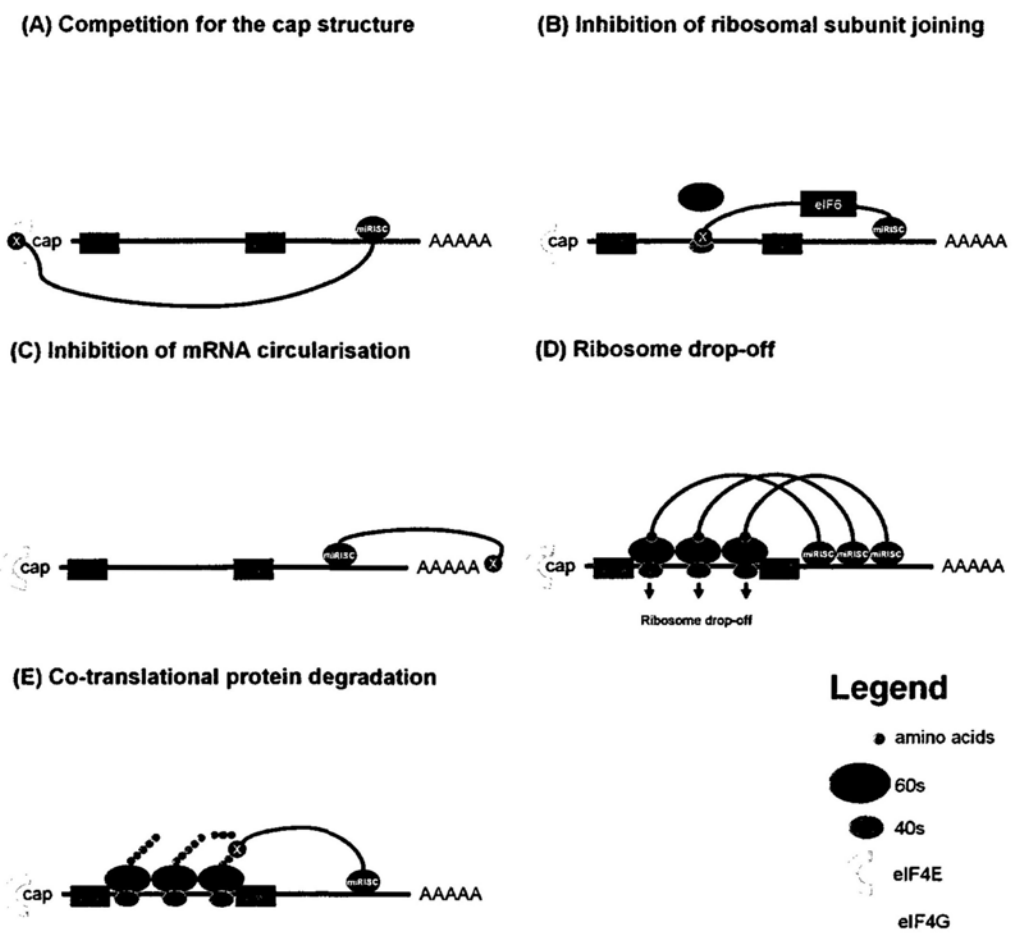

Figure 3.4. Mechanisms of miRNA-mediated gene silencing. Drawn by Sharon K Lee, copyright 2009.

3.3.3. mRNA degradation

Unlike plants, animal miRNAs usually bind imperfectly to the target mRNA and degrade mRNA through shortening of the polyA tail at the 3' terminus by mRNA deadenylases (Bagga et al., 2005). Either one of the two consequences then follow: (1) a decapping enzyme consisting of two subunits (Dcp1p and Dcp2p) dislodges the 5' cap structure, thereby exposing the transcript to digestion by a 5' to 3' exonuclease, Xrn1p; or (2) the cytoplasmic exosome degrades the mRNA in a 3' to 5' direction, in which the remaining oligonucleotide cap is then hydrolysed by the DcpS scavenger decapping enzyme (Eulalio et al., 2007). The degraded mRNA was eventually sent to P-bodies for sequestration (Wu et al., 2006).

3.4. *Computational prediction of target mRNAs*

The regulatory mechanisms described above implied that each miRNA has its own set of target sites to which the negative regulatory effects can be exerted. Large scale validation experiments on the microRNA targets are usually time consuming and labor intensive, as one single miRNA can effectively bind with thousands mRNAs targets. Hence, computational predictions based on sequence properties of a miRNA/mRNA target duplex serve as an extremely useful first-step tool to filter out any likely candidates of miRNA target gens. Currently, there are a number of algorithms available for testing the prediction of miRNAs, including the largest of its type, miRBase.

3.5. Diversity and Broad Functions of microRNAs

The discovery of second microRNA, let-7, triggered large scale searches for miRNAs in various organisms. At least 100-200 miRNAs per species have already been identified experimentally in *C. elegans, D. melanogaster, D. rerio, M. musculus* and *H. sapiens*, many of them being conserved over large evolutionary distances (Table 3.1), suggesting broad cellular functions of miRNAs. Indeed, miRNAs are now found participating in a variety of functions, including neuronal patterning, apoptosis, adipogenesis metabolism, tumorigenesis, infectious diseases, hematopoiesis, and developmental transition , in which the lattermost associates with stem and progenitor cells.

Table 3.1. The diversity of miRNAs. Data obtained from miRBase Release 13.0.

Metazoa	Bilateria	Deuterostoma	Chordata	Cephalochordata				*Branchiostoma floridae*	78
				Urochordata				*Ciona intestinalis*	34
								Ciona savignyi	27
								Oikopleura dioica	66
				Vertebrata	Amphibia			*Xenopus laevis*	7
								Xenopus tropicalis	184
					Aves			*Gallus gallus*	474
					Mammalia	Carnivora		*Canis familiaris*	321
						Metatheria		*Monodelphis domestica*	119
						Primates	Atelidae	*Ateles geoffroyi*	60
								Lagothrix lagotricha	48
							Cebidae	*Saguinus labiatus*	42
							Cercopithecidae	*Macaca mulatta*	463
								Macaca nemestrina	75
								Pygathrix bieti	11
							Hominidae	*Gorilla gorilla*	86
								Homo sapiens	**706**
								Pan paniscus	89
								Pan troglodytes	594
								Pongo pygmaeus	84

								Symphalangus syndactylus	11
							Lemuridae	*Lemur catta*	16
						Prototheria		*Ornithorhynchus anatinus*	331
						Rodentia		*Cricetulus griseus*	1
								Mus musculus	547
								Rattus norvegicus	286
						Ruminantia		*Bos taurus*	356
								Ovis aries	4
						Suina		*Sus scrofa*	77
					Pisces			*Danio rerio*	336
								Fugu rubripes	131
								Tetraodon nigroviridis	132
			Echinodermata					*Strongylocentrotus purpuratus*	45
			Hemichordata					*Saccoglossus kowalevskii*	43
		Ecdysozoa	Arthropoda	Chelicerata				*Ixodes scapularis*	1
				Hexapoda				*Anopheles gambiae*	66
								Apis mellifera	62
								Bombyx mori	55
								Drosophila ananassae	76
								Drosophila erecta	81
								Drosophila grimshawi	82
								Drosophila melanogaster	152

					Drosophila mojavensis	71
					Drosophila persimilis	75
					Drosophila pseudoobscura	73
					Drosophila sechellia	78
					Drosophila simulans	70
					Drosophila virilis	74
					Drosophila willistoni	77
					Drosophila yakuba	80
					Locusta migratoria	7
					Tribolium castaneum	55
			Nematoda		*Caenorhabditis briggsae*	95
					Caenorhabditis elegans	155
			Platyhelminthes		*Schistosoma japonicum*	5
					Schistosoma mansoni	5
					Schmidtea mediterranea	63
		Lophotrochozoa	Annelida		*Capitella sp. I*	71
			Molusca		*Haliotis rufescens*	5
					Lottia gigantea	59
			Nemertea		*Cerebratulus lacteus*	2
	Cnidaria				*Hydra magnipapillata*	1
					Nematostella vectensis	40
	Porifera				*Amphimedon queenslandica*	8

Mycetozoa				*Dictyostelium discoideum*	2
Viridiplantae	Chlorophyta			*Chlamydomonas reinhardtii*	49
	Coniferophyta			*Pinus taeda*	37
	Embryophyta			*Physcomitrella patens*	230
				Selaginella moellendorffii	58
	Magnoliophyta	eudicotyledons	Brassicaceae	*Arabidopsis thaliana*	187
				Brassica napus	44
				Brassica oleracea	6
				Brassica rapa	17
			Caricaceae	*Carica papaya*	1
			Fabaceae	*Glycine max*	78
				Lotus japonicus	2
				Medicago truncatula	38
				Vigna unguiculata	1
			Malvaceae	*Gossypium herbecium*	1
				Gossypium hirsutum	13
				Gossypium rammindii	2
			Salicaceae	*Populus trichocarpa*	234
			Solanaceae	*Solanum lycopersicum*	30
			Vitaceae	*Vitis vinifera*	140
		monocotyledons		*Oryza sativa*	377
				Saccharum officinarum	16

			Sorghum bicolor	72
			Triticum aestivum	32
			Zea mays	98
Viruses			*BK polyomavirus*	1
			Epstein Barr virus	25
			Herpes Simplex Virus 1	6
			Herpes Simplex Virus 2	3
			Human cytomegalovirus	11
			Human immunodeficiency virus 1	3
			JC polyomavirus	1
			Kaposi sarcoma-associated herpesvirus	13
			Mareks disease virus	14
			Mareks disease virus type 2	17
			Merkel cell polyomavirus	1
			Mouse cytomegalovirus	18
			Mouse gammaherpesvirus 68	9
			Rhesus lymphocryptovirus	16
			Rhesus monkey rhadinovirus	7
			Simian virus 40	1

4

The Relationship between microRNAs and stem Cells

As mentioned in Chapter 1, asymmetric cell division is a hallmark of stem cells. It generates one daughter cell that retains stem cell properties, and another daughter cell that is committed to specialized functions. External and internal factors are known to regulate such unique cell division pattern, which have been exemplified by the niche and intracellular signals in our tissue specific stem cell model using corneal epithelial progenitor cells. microRNA is a recently emerged intracellular molecule which acts by negatively regulate its target mRNA, together with the increasing evidence that microRNAs associate with cell development and stem cells, we postulate that microRNA is capable to regulate tissue specific stem cells, including the corneal epithelial progenitor cells that we are interested of. In this chapter, evidences which support microRNA as a regulator for the general stem cells will be presented.

4.1. The DGCR8 and Dicer knockout model

DGCR8 and Dicer are the two critical proteins associated with the production of mature miRNAs. It has been shown that Dicer is essential for early mouse development, as its absence leads to embryos depleted of stem cells and so embryonic

lethality (Bernstein et al., 2003). In an *in vitro* system, Dicer-null ES cells fail to express differentiation markers, including hepatocyte nuclear factor 4A (HNf4A; which is endodermal) and brachyury, bone morphogenetic protein 4 (BMP4) and GATA1 (which are mesodermal), even after the induction of differentiation (Kanellopoulou et al., 2005). Although Dicer is associated with both miRNA and siRNA pathways, in the absence of Dicer, only the profiles of miRNAs change in ES cells, but not of other small RNAs (Calabrese et al., 2007). On the other hand, DGCR8 knockout ES cells show a stable but subtle proliferation defect by not completely silencing the pluripotency markers *Oct4*, *Rex1*, *Sox2* and *Nanog* (Wang et al., 2007b). These reports suggest that the microRNA pathway indeed participates in stem cell maintenance and related cellular processes.

4.2. Stem cells has a distinct signature of microRNAs

The relationship between microRNAs and stem cells is put forward by the distinct microRNA signature found in both embryonic stem cells and tissue specific stem cells, the latter actually being the progenitor cells that we have been discussing. Table 4.1 shows a summary of the key microRNAs that are specifically expressed in various stem or progenitor cells. Of note, epidermal stem cells, which are the close relative of cornea epithelial progenitor cells, have shown to express miR-203 in mice. This microRNA has been found to target p63 expression, which is the proteins that similarly expressed in the limbal epithelium (Yi et al., 2008). These observations provide a strong hint that cornea epithelial progenitor cells may too be regulated by microRNAs.

Table 4.1. microRNAs identified in various types of stem cells.

Stem cell process	Cell type or lineage	miRNAs involved	Targets	References
Embryonicstem cells				
Self-renewal	Mouse ES cells	miR-290–295 cluster, miR-296, miR-302;	N/A	(Calabrese et al., 2007);
		miR-17–92 cluster, miR-15b–16 cluster;		
		miR-302-367 cluster	N/A	(Houbaviy et al., 2003);
			N/A	(Barroso-del Jesus et al., 2009)
	Human ES cells	miR-371, miR-372, miR-373*–373,	N/A	(Suh et al., 2004)
		miR-200c, miR-368 and miR-154*		
Differentiation	Mouse ES cells	miR-21 and miR-22	miR-21 targets Nanog and Sox2	(Houbaviy et al., 2003; Singh et al., 2008a)
	Human ES cells	miR-301, miR-374, miR-21, miR-29b and	No targets identified	(Suh et al., 2004)
		miR-29		
Tissue specific stem cells				
Haematopoiesis	Progenitor cells	miR-128, miR-181, miR-16, miR-103 and	No targets identified	(Georgantas et al., 2007)
		miR-107		
	Pro-T lymphoid cells	miR-150	No targets identified	(Zhou et al., 2007)
	Pro-B lymphoid cells	miR-181, miR-155, miR-24, miR-17,	No targets identified	(Georgantas et al., 2007)
		miR-16, miR-103 and miR-107		
	Erythroid myeloid cells	miR-150, miR-155, miR-221, miR-222,	miR-24 targets human ALK4; and miR-221 and	(Bruchova et al., 2007; Felli et

		miR-451, miR-16 and miR-24	miR-222 target human KIT	al., 2005; Georgantas et al., 2007; Wang et al., 2008a; Wang et al., 2008b)
	Monocytes	miR-17-5p, miR-20a, miR-106a, miR-16, miR-103 and miR-107	miR-17-5p, miR-20a and miR-106a target AML1	(Fontana et al., 2007)
	Granulocytes	miRNA-155, miR-24, miR-17, miR-223, miR-16, miR-103 and miR-107	miR-223 targets mice Mef2c	(Georgantas et al., 2007) (Johnnidis et al., 2008)
	Megakaryocytes	miR-155, miR-24, and miR-17	miR-155 targets human Ets-1 and Meis1	(Georgantas et al., 2007; Romania et al., 2008)
Myogenesis	Skeletal cells	miR-1, miR-133, miR-206 and miR-26a	miR-1 targets mouse Hdac4; miR-133 targets mouse Srf; miR-1 and miR-206 target mouse connexin 43 (also known as Gja1); and miR-26a targets mouse Ezh2	(Chen et al., 2006; Kim et al., 2006) (Anderson et al., 2006)
		microRNA-27b	miR-27b targets mice Pax3	(Crist et al., 2009)
Neurogenesis	Neuronal	miR-124 and miR-128	miR-124 targets chicken SCP1	(Krichevsky et al., 2006; Smirnova et al., 2005; Visvanathan et al., 2007)
			miR-124 targets mice Sox9	(Cheng et al., 2009)
	Astrocytes	miR-26, miR-29, miR-23	No targets identified	(Smirnova et al., 2005)
Osteogenesis	Osteoblasts	miR-125b and miR-26a	miR-26a targets human SMAD	(Mizuno et al., 2008)
		miR-141 and -200a	miR-141 and -200a targets mice Dlx5	(Itoh et al., 2009)
Skin development	Keratinocytes	miR-203	miR-203 targets mouse p63	(Lena et al., 2008; Yi et al., 2008)

5

Our Study - Hypothesis, Goals, Significance and Plan

5.1. Hypothesis

The evidence of microRNA in embryonic and tissue specific stem cell provide a solid foundation of our hypothesis: microRNAs can participate in the regulation of corneal epithelial progenitor cells, the tissue specific stem cells for the cornea epithelium.

5.2. Immediate and long term goal

As stated in Chapter 2, functional biology of the corneal epithelial progenitor cells (CEPC) remains largely unknown. By delineating the role of microRNAs in CEPC, we hope to better understand CEPC biology, with a long-term objective to devise novel therapy for effective treatment of patients with limbal stem cell deficiency and cornea surface injuries. The potential clinical significance of this study is discussed below.

5.2.1. Help in the development of microRNA eyedrops

Small RNAs has been anticipated as a new category of drugs. Small interfering RNAs

(siRNAs), one of the close relatives of microRNAs, is exceedingly promising for successful clinical application (Love et al., 2008). To date, at least 7 clinical trials use siRNAs for treating a variety of diseases. Among these, 3 siRNAs are known for ophthalmic treatment, namely, Bevasiranib, Sirna-027/AGN211745 and RTP801i-14 - the former two targets at Vascular endothelial growth factor (VEGF), while the latter targets at Hypoxia-inducible gene (RTP801), all with the hope to treat wet age-related macular degeneration (AMD) (Love et al., 2008). The reasons why nearly half of the trials focus at eye diseases is that (1) a number of eye diseases is currently no cure, (2) cell therapy in bilateral eye diseases is much constrainted due to the limited supply of tissues for allogenic transplant, (3) the blood brain barrier renders eye as a rather isolated compartment, which can sustain small RNAs delivered in the eye and enable higher efficiency in drug absorption and assimilation. Because microRNAs prevails over siRNAs in that they can target multiple genes rather than a single target, and their repression mechanism is more subtle than that of siRNA, miRNA is now considered as a novel class of small RNA drug that can combat complicated diseases including cornea surface complications. Limbal stem cell deficiency is an ocular disease perplexed with the loss of CEPC at the cornea periphery. Current treatment using amniotic membrane provides the niche for the proliferation of CEPC but there are a number of drawbacks associated with its use as a substrate in corneal repair, including the maintenance of a reliable supply of membranes, considerable variation amongst donors, costly donor screening which cannot completely avoid the risk of viral agent transmission and ultimately lack of optimal transparency (Levis and Daniels, 2009). Better alternative treatment is needed. Unlike conventional gene therapy whose

delivery is coupled with virus vector, microRNAs can be delivered naked as an eyedrop onto the cornea surface with considerable level of uptake. Immunological problems caused by the viral vector is thus tremendously reduced. With the better understanding of CEPC biology, we hope to devise microRNA eyedrops for efficiently and conveniently treating limbal stem cell deficiency and cornea surface injuries.

5.2.2. Help in the cell-based therapy

Cell based therapy have been providing realistic hope for restoring tissue function and therefore treating the root cause of degenerative diseases in the currently aging population. MicroRNAs, together with other small molecules, e.g. LIN28, OCT4, SOX2, is envisaged as the candidate molecules for reprogramming tissue specific stem cells into its pluripotent state. Besides, Lavker and Sun have proposed that CEPC is the ideal model for studying epithelial stem cell biology. This present study may therefore provide clues for the specific microRNAs which associate in reprogramming CEPC into its pluripotent state.

5.2.3. Help in the understanding of cancer biology

Cancer is originated from stem cells that have been aberrantly regulated. From the observation that orbit and eye cancers have the lowest prevalence comparing to cancers in other parts of the body (Table 5.1), it is tempting to speculate that ocular stem cells may possess a unique system for combating with any harmful external

stimulus. In addition to the possible stimulus like alcohol and nicotine, the cornea surface is also exposed to ultraviolet irradiation. This means that cornea does not receive less harmful external stimulus than the rest of the body but their cancer prevalence remains exceptionally low. By comparing CEPC at the limbus region with other normal tissue specific stem cells, and by comparing the limbal squamous cell carcinoma with other cancers, we may speculate a protective mechanism of corneal epithelial progenitor cells for resisting the mutation and thus the emergence of aberrant stem cells.

5.3. Study plan

In order to prove the hypothesis and achieve the aim, this study is divided into five sections. The first section concerns mostly on the validation of tissue samples, the second section discusses the best isolation methods for CEPC, the third part identifies candidate microRNAs in CEPC, the forth part aims at confirming the candidates that have been identified, and the final section elucidates the functional roles of these microRNAs in cornea epithelial maintenance. With all these, we hope to open up a novel avenue for ocular progenitor cell research.

Table 5.1. Prevalence of cancer in the human body. (Data obtained from http://seer.cancer.gov/index.html)

Cancer	Age-adjusted incidence rate (per 100,000 individual per year)
Anus	1.6
Bones and joints	0.9
Brain and other nervous system	6.4
Breast	123.8
Cervix uteri	8.2
Colon and rectum	49.1
Corpus and uterus, NOS	23.3
Esophagus	4.5
Eye and orbit	**0.8**
Kidney and renal pelvis	13.6
Larynx	3.5
Leukemia	12.2
Liver and intrahepatic bile duct	6.6
Lung and bronchus	63.1
Lymphoma	22.3
Myeloma	5.6
Oral cavity and pharynx	10.4
Ovary	13.1
Pancreas	11.7
Prostate	159.3
Skin (excl. basal and squamous)	21.4
Small intestine	1.9
Soft tissue including heart	3.1
Stomach	7.9
Testis	5.4
Thyroid	9.6
Urinary bladder	21
Vulva	2.2

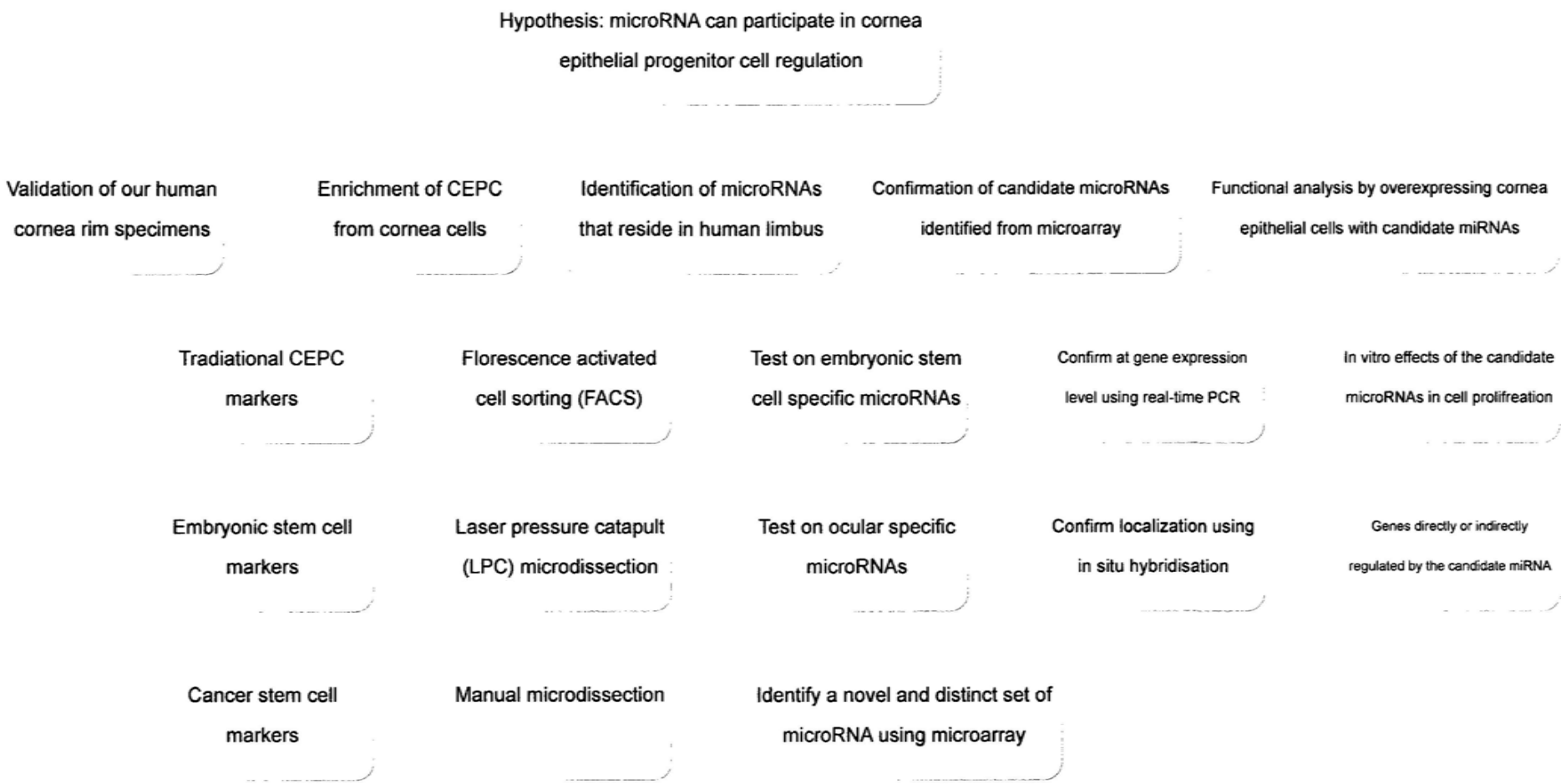

Figure 5.1. Study plan of the thesis.

Part II
General Methodology

6 Materials

6.1. Animals

All animal experiments were conducted in compliance with the ARVO Statement for the Use of Animals in Ophthalmic and Vision Research. Approval of all animal experimentation procedures was obtained from the Animal Experimentation Ethics Committee of The Chinese University of Hong Kong.

The principles of laboratory animal care set forth by the NIH were followed. Male BALB/c mice aged 3-4 weeks of age and weighed approximately 20-22 g were obtained from the Laboratory Animal Services Centre, The Chinese University of Hong Kong (Hong Kong, SAR, China). The mice were kept under a 12:12 h light-dark cycle in a humidity-controlled room and fed with irradiated LabDiet for rodents (PMI Nutrition, Richmond, Ind., USA) and ozone-sterilised tap water.

6.2. Cells

Human corneal epithelial cells (HCE) cells were cultured in DMEM/F12 medium supplemented with 5 % FBS. It was maintained in 37 °C humidified CO_2 incubator

and passaged every 3 days.

6.3. Tissue specimens

Fresh human cornea rims disposed after cornea transplant were used in the present study. The specimens were preserved under cold storage conditions in Optisol before surgery. The study protocol complied with the provisions of the Declaration of Helsinki and was reviewed and approved by the Ethics Committee of the Chinese University of Hong Kong. Informed consent was obtained from individuals.

6.4. *List of commonly used reagents in the thesis*

Reagent name	Company
Sucrose	Fluka
Paraformaldehyde (PFA)	Sigma-Aldrich
Formamide	Riedel
Diethylpyrocarbonate (DEPC)	Fluka
Triethanolamine	Fluka
Conc. HCl	Riedel
Acetic anhydride	Sigma-Aldrich
50X Denhardt's	Sigma-Aldrich
Yeast tRNA	Sigma-Aldrich
Salmon sperm DNA	Sigma-Aldrich
Blocking reagent	Roche
Anti-digoxigenin antibody	Roche
Levamisol	Sigma-Aldrich
BCIP	Roche
NBT	Roche
Tissue Tek OTC	Sakura
Fast Red Substrate	Dako
10% (w/w) CHAPS	Sigma-Aldrich
10% and 20% (w/w) Tween	Fluka
5 M NaCl	Merck
1 M MgCl2	Fluka
Tris-HCl	Sigma-Aldrich
Optimal cutting temperature (OCT) tissue freezing medium	Tissue-Tek
Haematoxylin	Sigma-Aldrich
Scott's tap water	Sigma-Aldrich
Eosin	Sigma-Aldrich
Triton X-100 (Sigma-Aldrich)	Sigma-Aldrich
4',6'-diamidino-2-phenyindole (DAPI)	Sigma-Aldrich
BSA	Sigma-Aldrich
Dispase II	Roche Diagnostics

D-sorbitol	Sigma-Aldrich

6.5. List of antibodies

Antibody name	Company	Cat no.
p73 (H-79), rabbit pAb IgG	Santa Cruz	sc-7957
EGFR (31G7), mouse mAb, IgG1	Zymed	28-0005
Anti-human cytochrome oxidase subunit II, mouse mAb 12C4-F12	MolecularProbes	A-21363
Cytokeratin 3/12 (AE5), mouse mAb	LifeSpan Biosciences	LS-C84884-200
Connexin43, mouse mAb IgG	Zymed	13-8300
Nanog (Clone 98-195) mouse Ab	Abnova	H00079923-M02
Notch1 (C-20), goat pAb IgG	SantaCruz	sc-6014
Oct-4 (C-10),mouse mAb IgG2a	SantaCruz	sc-5279
Stat3 Ab	Cell Signalling	9132
STAT1 Ab	Cell Signal	9172
Phospho-Stat1 (Tyr701) (58D6) Rabbit mAb	Cell Signal	9167s
CDCP1 (E-20) goat pAb IgG	Santa Cruz	sc-32844
Cytokeratin 15 (LHK15), mouse mAb	abcam	ab2414-500
Anti-BMI-1 Clone F6, mouse monoclonal IgG1	Upstate	05-637
MDM2 (SMP14), mouse mAb IgG1	Santa Cruz	sc-965

6.6. List of primers used in polymerase chain reaction

Gene Name	Orientation	Primer Sequence	Tm (°C)	Product (bp)
ABCG2	Forward	TCACAGTCGTACTGGGACTGGTT	60	108
ABCG2	Reverse	GGTTGGTCGTCAGGAAGAAGAGA	61	
ANXA13-1	Forward	GCAATCGTCATGCTAAAGCG	61.82	144
ANXA13-1	Reverse	GCCTCTCATCTGATGTCCTGC	62.3	
ANXA13-2	Forward	CTAAAGGGGACTCCCAACCC	61.93	180
ANXA13-2	Reverse	TGATGGCTGCTTCATTGGTC	62.17	

BCRP1	Forward	GGTTTCCAAGCGTTCATTCAAA	59.9	88
BCRP1	Reverse	AACCAGTCCCAGTACGACTGTGAC	60.3	
CD34	Forward	AGCCACCAGAGCTATTCCCAA	60	149
CD34	Reverse	GTGTAATAAGGGTCTTCGCCCA	59	
CD71	Forward	GCCACTGAATGGCTAGAGGGATA	60	112
CD71	Reverse	GGCTGGCAGAAACCTTGAAGTT	61	
CFH	Forward	ATGTCAGAAAAGGCCCTGTG	60.11	170
CFH	Reverse	TGGTCCATCCATCTGTGTCA	60.98	
CFHR1	Forward	ATGTGTAGAACGGGGCTGGT	61.72	186
CFHR1	Reverse	CACATCACTTCTTCATCCCCA	60.91	
CK12	Forward	GCAGATGCTTCACAGAGCGATT	60	144
CK12	Reverse	CATCCTGAAGTCCTCAGCAGCTA	60	
CK13	Forward	ATTGAAGAGCTCCGGGACAA	58	124
CK13	Reverse	GGGCCAGCTCATTCTCATACTT	58	
CK3	Forward	GGACCTGGTGGAAGACTTCAAGA	60	140
CK3	Reverse	CATCCACTTTGGCCTGAAGCT	60	
connexin 43	Forward	GTACCAAACAGCAGCGGAGTTT	59	141
connexin 43	Reverse	CTGGGCACCACTCTTTTGCTTA	60	
desmoglein 3	Forward	GCCTGCCGTATGGAGTATCACA	61	134
desmoglein 3	Reverse	GTGGCATCTCACACCGATTGTT	61	
EGFR	Forward	GTGAGGTGGTCCTTGGGAATTT	60	112
EGFR	Reverse	GTGTTGAGGGCAATGAGGACA	60	
FGF14	Forward	ATGGAACCAAGGATGACAGC	59.93	148
FGF14	Reverse	GGGGTAAAAAGTTCTGATGGG	59.69	
FMO1	Forward	TTGGAATGGGAAATTCTGGC	62.06	192
FMO1	Reverse	AAGTCACAATTGGGGTTGGG	61.92	
IFNB1	Forward	GCATTACCTGAAGGCCAAGG	61.87	150
IFNB1	Reverse	GCAATTGTCCAGTCCCAGAG	60.66	
IGF1R	Forward	GCTTGTCCAACGAGCAAGTC	60.99	134
IGF1R	Reverse	GAAGGAAGGCCTCATCTTGG	61.1	
Intregrin alpha 6	Forward	CCGAAAATATCAGGCTGCCA	60	108
Intregrin alpha 6	Reverse	CCACTAGGATGATCCACCAAGGT	60	
KRT15	Forward	ATAAAGACACGGCTGGAGCA	60.8	176
KRT15	Reverse	TTGTGGGAAGAAACCACCTG	60.92	

KRT2	Forward	ACCAGGAGCTGATGAACGTG	61.28	135
KRT2	Reverse	TGGTGCTGCTTGTCACAGAC	61.11	
MAPK7	Forward	GGGATGACACATTCCCAGAG	60.33	125
MAPK7	Reverse	GCCGTCTTCCTCCTTCAGAG	61.44	
Nanog	Forward	ATGCCTGTGATTTGTGGGCC	60	403
Nanog	Reverse	GCCAGTTGTTTTTCTGCCAC	60	
NFIB	Forward	ACATTGCACAAACCCAGCAC	61.97	143
NFIB	Reverse	TCTTGGCAGGATCATTGTGG	62.02	
OCT4	Forward	AGC CCT CAT TTC ACC AGG CC	63	456
OCT4	Reverse	CAA AAC CCG GAG GAG TCC CA	63	
p73H	Forward	GATGAACCGCCGTCCAATTT	61	114
p73H	Reverse	TTCCTGTCTCTTCCTGGGCAA	61	
PCNA	Forward	ACGTCTCTTTGGTGCAGCTCA	60	123
PCNA	Reverse	CATTGCCGGCGCATTTTA	60	
PITX2	Forward	GCCGGGATCGTAGGACCTT	59.9	79
PITX2	Reverse	GTGCCCACGACCTTCTAGCA	59.8	
RARA-1	Forward	GGGAATCCTGAATCGAGCTG	62.03	142
RARA-1	Reverse	AAAGATGCCACTCCTAGATGGG	61.69	
S100A12	Forward	ACATTCCTGTGCATTGAGGG	60.92	172
S100A12	Reverse	GGTGTTTGCAAGCTCCTTTG	60.81	
SOHLH2	Forward	CCTCGGTACTGCACTTCTGG	60.84	182
SOHLH2	Reverse	GGTCTTTGGGTGGAGCTTTC	61	
Sox2	Forward	CCCCCCTGTGGTTACCTCTT	59	137
Sox2	Reverse	GCTGGGACATGTGAAGTCTGC	59	
vimentin	Forward	TGGATTCACTCCCTCTGGTTGA	60	142
vimentin	Reverse	GCTGCACTGAGTGTGTGCAATT	60	
WNT7A	Forward	CTGGAACTGCTCTGCACTGG	62.17	185
WNT7A	Reverse	GGTGGTACTGGCCTTGCTTC	61.97	

6.7. List of primers used in Taqman microRNA microarray

microRNA primer	Target sequence	Company
hsa-miR-21	UAGCUUAUCAGACUGAUGUUGA	ABI
hsa-miR-184	UGGACGGAGAACUGAUAAGGGU	ABI
hsa-miR-143	UGAGAUGAAGCACUGUAGCUC	ABI
has-mIR-145	GUCCAGUUUUCCCAGGAAUCCCU	ABI
hsa-let-7a	UGAGGUAGUAGGUUGUAUAGUU	ABI
hsa-miR-16	UAGCAGCACGUAAAUAUUGGCG	ABI
hsa-miR-26b	UUCAAGUAAUUCAGGAUAGGUU	ABI
hsa-miR-302a	UAAGUGCUUCCAUGUUUUGGUGA	ABI
hsa-miR-302d	UAAGUGCUUCCAUGUUUGAGUGU	ABI
hsa-miR-320	AAAAGCUGGGUUGAGAGGGCGAA	ABI
hsa-miR-338	UCCAGCAUCAGUGAUUUUGUUGA	ABI
hsa-miR-371	GUGCCGCCAUCUUUUGAGUGU	ABI
hsa-miR-372	AAAGUGCUGCGACAUUUGAGCGU	ABI
hsa-miR-373	GAAGUGCUUCGAUUUUGGGGUGU	ABI
hsa-miR-373#	ACUCAAAAUGGGGGCGCUUUCC	ABI
hsa-miR-182	UUUGGCAAUGGUAGAACUCACA	ABI
hsa-miR-204	UUCCCUUUGUCAUCCUAUGCCU	ABI
hsa-miR-184	UGGACGGAGAACUGAUAAGGGU	ABI

7

Methods

7.1. Cryosectioning

Cornea rims were fixed in paraformaldehye (4 %) for 1 hour at room temperature before sectioning into small pieces at 50 mm x 50 mm using surgical blade. The small sections were immersed in 20 % sucrose for 2 hours at room temperature to reduce the possible formation of ice upon freezing and were then embedded in optimal cutting temperature (OCT) tissue freezing medium. For cryosectioning, it was cut at 8 μm in cryostat that has been adjusted at -20°C. The sections were captured using superfrost slides (Thermo Scientific). All the embedded tissues were freezed at -80°C for storage.

7.2. Haematoxylin and Eosin Staining

Slides containing the human cornea rim sections were stained in haematoxylin for 10 mins at room temperature. The nucleus were then differentiated by immersing slides in acid alcohol for 30 secs, followed by the blueing up process using Scott's tap water for another 1 min. The cytoplasms were further stained by eosin for 10 mins. The slides were then washed and dehydrated in 50, 70, 80, 90 and 100 % alcohol, each for 5 mins, before mount.

7.3. Immunostaining

Sections on slides were post-fixed in 4% paraformaldehyde, rinsed with PBS and incubated in 0.1% Triton X-100-PBS for 30 min. Non-specific fixation sites were saturated with 5% bovine serum albumin in PBS for 1 hour, and then incubated with suitable primary antibodies at RT for 2 hours. After incubation with the specific primary antibodies, the sections were rinsed (3 times 5 min each) with PBS, incubated for 1 h at room temperature with appropriate secondary antibody and 4',6'-diamidino-2-phenyindole (DAPI) diluted in PBS containing 1% BSA. The sections were mounted and were examined with a fluorescent microscope coupled to a digital camera.

7.4. Flow cytometric assays

7.4.1. Annexin V apoptosis Assay

Cornea epithelial cells at 5 x 10^5 cells/tube were stained with Annexin V-FITC and propidium iodide (PI) for 15 min at RT by using a commercial kit (BD Pharmingen, USA). Cells were washed twice with PBS and re-suspended in buffer solution. Stained cells were analyzed with a flow cytometer (BD, FACSAria™) within 1 hour of staining, as described in the manufacturer's manual. Data were analysed using FACSDiva™ software.

7.4.2. ABCG2 staining

Mouse cornea epithelial cells at 5 x 10^5 cells/tube were blocked in purified rat anti-mouse CD16/CD32 (BD Biosciences) for 15 mins at RT. Florescence conjugate were developed to the antibodies using Zenon ® Alexa Fluor ® 488 Mouse IgG2a labeling kit (Invitrogen) as according to manufacturer's protocol. The cells were then stained with the conjugated rat monoclonal antibody against ABCG2 clone BXP-53 (Abcam) or its conjugated isotype control IgG2a for 30 min at RT. Stained cells were analysed by a flow cytometer (BD, FACSAria™). Data were analysed using FACSDiva™ software.

7.4.3. Pyronin Y optimization

Mouse cornea epithelial cells at 5 x 10^5 cells/tube were stained in 1 μL pyronin Y (Invitrogen) (250 ng) for 15, 30, and 45 mins. The cells were briefly washed in PBS by centrifugation at 300 g for 3 mins at 4°C. The staining efficiency were analysed immediately using a flow cytometer (BD, FACSAria™). Data were analysed using FACSDiva™ software.

7.4.4. Rhodamine 123 optimisation

Mouse cornea epithelial cells at 5 x 10^5 cells/tube were stained in 10 ng/mL

Rhodamine 123 (Invitrogen) for 15, 30, and 45 mins. The cells were briefly washed in PBS by centrifugation at 300 g for 3 mins at 4°C to reduce the background. The staining efficiency were analysed immediately using a flow cytometer (BD, FACSAria™). Data were analysed using FACSDiva™ software.

7.4.5. Four parameter sorting of corneal epithelial progenitor cells

Singlet mouse cornea epithelial cells were blocked in purified rat anti-mouse CD16/CD32 (BD Biosciences) for 15 mins at RT. The cells were distributed at a proportion of 20 % and 80 % in two separate tubes. The one with fewer cells were for isotype staining, while the other one were for staining with the antibodies of interest. To stain the cells, florescence were first conjugated to the appropriate antibody. Rat monoclonal antibody against ABCG2 clone BXP-53 (Abcam, ab24115) and its isotype control rat IgG2a (Abcam, ab11671) were conjugated by Zenon ® Alexa Fluor ® 488 Mouse IgG2a labeling kit (Invitrogen, Z25102); mouse anti-Notch1 antibody (Zymed, 41-3500) and its isotype control mouse IgG1 (Abcam, ab18447) were conjugated by Zenon ® Alexa Fluor ® 660 Mouse IgG1 labeling kit (Invitrogen, Z25009); mouse anti-connexin 43 (Zymed, 13-8300) and its isotype control mouse IgG (Abcam, ab37355) were conjugated by Zenon ® Allophycocyanin Mouse IgG1 labeling kit (Invitrogen, Z25051). All conjugations were performed as per manufacturer's protocol. The conjugated rat monoclonal antibody against ABCG2 clone BXP-53 or its isotype control rat IgG2a, conjugated mouse anti-Notch1 antibody or its isotype control mouse IgG1, conjugated mouse anti-connexin 43 or its isotype control mouse IgG, and

pyronin Y (250 ng) or its control PBS buffer, were incubated with cells for 30 min at RT. The stained cells were analysed and sorted by a flow cytometer (BD, FACSAria™). Data were analysed using FACSDiva™ software.

7.4.6. Cell cycle analysis

Harvested cells (5 x 10^5) were fixed in ice cold 75 % ethanol for 4 hours at -20°C. Propidium iodide (50 µg/ml) and RNase A (0.1 mg/mL) diluted in cold PBS were then incubated with the samples for 30 mins at 4°C. Excess staining was removed by centrifugation at 1500 rpm for 5 mins. The cells were resuspended in 500 µl PBS for flow cytometric analysis using BD FACS Calibur. Data were analysed using FACSDiva™ software.

7.5. RNA extraction

For every 1 x 10^7 cells, add 700 µl Trizol ® Reagent (Invitrogen) for lysis. The cells were homogenized by pipetting up and down in Trizol ® Reagent > 15 times and were left on benchtop at room temperature for 5 mins. For every 700 µl homoegenate, add 140 µl chloroform, shake the tube vigorously by hands for 15 s and stand for 3 mins. The tube was then centrifuge for 15 min at 12,000 x g at 4°C. The upper aqueous phase was collected and transferred to a new collection tube. One and a half volumes (usually 525 µl) of 100% ethanol were added and mixed thoroughly by pipetting up and down 5 times. The total RNA was then purified according to the cleanup protocol

suggested by miRNeasy Mini Handbook (Qiagen). Briefly, 700 µl of the sample was pipetted into an RNeasy Mini spin column in a 2 ml collection tube, which were then centrifuging at ≥8000 x g for 15 s at RT. Any flow through were discarded. Buffer RWT (700 µl) were then added to the RNeasy Mini spin column. Close the lid gently, centrifuge for another 15 s at 8000 x g to wash the column, and discard the flow-through. This is followed by adding Buffer RPE (500 µl) onto the RNeasy Mini spin column to wash the column. The column membrane was then dried by centrifugation for 2 min at 8000 x g. Transfer the dried RNeasy Mini spin column to a new 1.5 ml collection tube. Pipet 30 µl RNase-free water directly onto the RNeasy Mini spin column membrane. Close the lid gently and centrifuge for 1 min at 8000 x g to elute the RNA.

7.6. RNA integrity check

7.6.1. Bioanalyser

The RNA 6000 Pico Chip Kit (Agilen) was used for Bioanalyser measurement (Agilent) and was carried out as per manufacturer's protocol. Briefly, the gel was filtered by centrifugation at 1500 x g for 10 mins at RT and was loaded at 65 µL in a 0.5 mL RNAase-free microfuge tubes. The vortexed dye concentrate was then added at 65 µL in the same tube. This is followed by spinning the gel-dye mix at 13000 x g for 10 mins at RT and loading at 9 µL on a new RNA 6000 Pico chip that has been put on the chip priming station. The conditioning solution and marker were pipetted at 9 µL

and 5 μL respectively into the appropriate marked wells. Pipette 1 μL each of the heat denatured ladder and diluted RNA sample (5 ng/μL) into appropriate wells. After vortexing the chip for 1 mins at 2400 rpm, the chip could be run in the Agilent 2100 bioanalyser machine (Agilent) for assessing RNA integrity.

7.6.2. Nanodrop

RNA concentrations were verified by measuring absorbance (A260) on the NanoDrop Spectrophotometer ND-1000 (NanoDrop). 28S/18S ratios in the typical range of 1.1–1.8 for RNA isolated from limbus and cornea tissues were used in the experiments.

7.7. Taqman microRNA assay using quantitative polymerase chain reaction

7.7.1. Procedures

cDNA was reverse transcribed from RNA using High Capacity cDNA Reverse Transcription Kit (Applied Biosystem, Cat No. 4368813) as per manufacturer's protocol. Briefly, a cocktail containg 10x reverse transcription buffer (0.5 μl), 100 mM dNTP mix (0.05 μl), recombinant RNase inhibitor (0.063 μl), 50 U/μL Multiscribe reverse transcriptase (0.35 μl), 5x Taqman® miRNA RT primer RT (1 μl); 10 ng/μL RNA (1 μl), and nuclease-free water (3.037 μl) were assayed in thermal cycler at 16°C for 30 min, 42°C for 30 min, 85°C for 5 min for termination and 4°C for storage. The

cDNA products were then quantitated by real time PCR, in which one reaction contains 20x TaqMan MicroRNA Assay Primer (0.5 μL), 1:3 diluted cDNA (1.4 μl), TaqMan 2x Universal PCR Master Mix (2.5 μl), and nuclease-free water (0.6 μl). Real-time PCR reactions was performed at least duplicate and was assayed in an optical 96-well plates using ABI PRISM® 7900HT Sequence Detection System (ABI) with the following conditions - 10 min at 95°C, 40 cycles each of 15 s at 95°C and 1 min at 60°C. The emitted fluorescence signal was converted into numerical values by SDS 2.1 software (Applied Biosystems).

7.7.2. Statistical analysis

The expression level of the miRNA was analysed by the SDS 2.1 software (ABI). The relative expression of each target miRNA was determined by dividing the target amount by endogenous control U6 amount to obtain a normalized target value (ΔCT). Then the normalized values of the target miRNAs were compared between samples. Data were analysed using GraphPad Prism v5.0. $p < 0..05$ is considered statistical significant.

7.8. microRNA microarray

Agilent™ Human MicroRNA Microarray Kit v1 (Agilent, cat no. G4470A) which probes with 470 human miRNA and 64 viral miRNAs according to Sanger database version 9.1 was used in the present microarray analysis. Briefly, a total of 100 ng of

total RNA was dephosphorylated (calf intestinal alkaline phosphatase; GE Healthcare, Munich, Germany) and labeled by ligation (T4 RNA ligase; NEB Biolabs, Frankfurt, Germany) with one cyanine 3-pCp molecule to the 3' end of the RNA molecules using Agilent's miRNA labeling reagent and hybridization kit (Agilent Technologies). Labeled miRNAs were desalted with Micro Bio-Spin Chromatography Columns (BioRad Laboratories) as described by Agilent Technologies. Hybridization (20 hours at 55°C), microarray washing, and detection of the labeled miRNA on the microarray were performed according to the manufacturer's instructions. Microarray results were extracted using Agilent Feature Extraction software (v9.5.3.1) and analyzed using Gene-Spring GX 7.3.1 software (Agilent Technologies). Following Agilent recommendations, no interarray normalization was applied, because the similarity between matched limbus and cornea sample arrays was unknown. Quality of all data sets was tested.

7.9. miRNA Target Prediction Methods

The miRNA database miRBase (http://www.mirbase.org/) was used to identify potential miRNA targets and our candidate miRNA sequences across species. In the miRBase, the miRanda algorithm was used to scan all available miRNA sequences for a given genome against 3' UTR sequences of that genome. The algorithm uses dynamic programming to search for maximal local complementary alignments, which correspond to a double-stranded antiparallel duplex. A positive score is given for complementary base pairing, and a negative score is given to mismatches, gap opening,

and gap extension. Importantly, scores derived from the 5' end of the miRNA were multiplied by a scaling factor to reflect the apparent importance of perfect Watson-crick base pairing, which has been observed experimentally. Subsequently, Karlin-Altschul normalization was performed.

7.10. In situ hybridization

In situ hybridsation were performed on frozen sections as previously described (Obernosterer et al., 2007). Briefly, human cornea rims were pre-fixed in 4 % paraformaldehyde for 30 mins, followed by 30 % sucrose overnight at 4°C. The tissues were then embedded and immersed in tissue Tek OCT medium and were sectioned at 10 μm using cryostat. The section were then post-fixed in 4% paraformaldehyde for 10 mins and acetylated in acetic anhydride/triethanolamine for another 10 mins. The sections were treated with proteinase K at 5 μg/mL for 10 mins to increase membrane permeability for the subsequent hybridisation. After thorough washing, the tissue were pre-hybridized in hybridization solution (50% formamide, 5× SSC, 200 μg/mL yeast tRNA, 1× Denhardt's solution, 500 μg/mL salmon sperm DNA and 0.4 g Roche blocking reagent) at RT (below the predicted T m value of the LNA probe) for 4 hours. Probes (3 pmol) denatured at 80°C for 5 mins (LNA miRCURY probe; Exiqon) were DIG-labeled (DIG Oligonucleotide 3′ Tailing Kit; Roche Applied Sciences) and hybridized to the sections overnight at 60°C. After post-hybridization wash in 0.1× SSC at 55°C, the in situ hybridization signals were detected using the NBT/BCIP developer solution (BCIP, Roche, cat no. 1383221; NBT, Roche, 1383213). Slides

were mounted, observed under microscope coupled with an Olympus digital camera.

7.11. Transfection using Pre-miRs

HCE cells were plated to 80 % confluency and allowed to adhere overnight. After 24 hours, pre-miR 21, 143, 145 or a scrambled pre-miR control (Ambion) was reverse transfected (50 or 100 nM) using siPORT NeoFX transfection (Ambion, Austin, TX) into cells in growth media following manufacturer's recommendation. Following 48 hs, cells were harvested for RNA extraction. The cells were incubated longer for MTT or morphological study until day 8.

7.12. MTT proliferation assay

Cells were reverse transfected with pre-miR-21, 143, 145 or scrambled pre-miR. MTT assay was performed with the modified Mosmann's method (Mosmann, 1983).

7.13. Gene expression microarray

Whole Human Genome Oligo Microarray Kit (Agilent Technologies) which contains 41K human genes and transcripts were used to screen for the candidate targets of miR-21, 143 and 145. The procedures were performed according to manufacturer's protocol. The resulting images were visualized and digitalized by Feature Extraction software v 9.5.3.1 (Agilent Technologies, Santa Clara, CA, USA),

in which background signal, non-uniform signal and the average raw signal on each probe were automatically calculated. The resulting data files were generated and transferred to GeneSpring GX version 7.3.1 (Agilent Technologies, Santa Clara, CA, USA) for further analysis. In order to compare samples on different arrays and obtain meaningful data, several normalization methods in GeneSpring were applied including per gene (normalize to median) normalization and per chip (normalize to 50th percentatile) normalization. The cut-off value for the differential change of gene expression was set as 2 fold for the data analysis. Pathway analysis was performed with references to the pathway information downloaded from KEGG database (ftp://ftp.genome.jp/pub/kegg/).

7.14. Western blot

7.14.1. Summary of procedures

Cell lysate was prepared using RIPA Buffer with protease inhibitors and quantified using protein assay. Protein (20 μg) was loaded onto a 10% SDS–PAGE gel then transferred onto nitrocellulose and incubated with mouse monoclonal Notch1 antibody (Santa Cruz) at 4 °C overnight in blocker (1% non-fat dry milk in TTBS), followed by incubation with HRP-conjugated secondary anti mouse. Blots were then developed using ECL Substrate (Amersham) following manufacturer's instructions. HRP-conjugated GAPDH was incubated further for normalization. The blots were again developed using ECL substrate.

7.14.2. Reagent Preparation

7.14.3. RIPA buffer for protein extraction

Stock reagent	Working	Volume / Amount
1M Tris-HCI (PH 7.4)	50mM	0.5 ml
(SIGMA, TRIZA® BASE)		
5M NaCl	150mM	0.3 mL
(GIBCO BRL)		
NP-40	1%	0.1 mL
(Fluka, Nonidet® P40 Substitute)		
H2O		9.1 mL
5% sodium deoxycholate	0.25%	50µl
(SIGMA-ALDRICH)		
Protease inhibitor cocktail		1 tablet
with EDTA		
(Roche)		
PhosphatesSTOP		1 tablet
100mM PMSF	1mM	10µl
(SIGMA, phenylmathlsulfonyl fluoride, p-7626)		

7.14.4. 5X DTT/SDS Loading Buffer

Reagent	Volume / Amount
Tris HCL (pH 6.8)	250mM
Glycerol	50%
SDS (Sodium dodecyl sulfate)	10%
Bromophenol blue	0.01%
DTT (Dithiothreitol)	250mM
ß-mercaptoethanol	25%

7.14.5. Gel preparation

Reagent	Volume / Amount
Resolving gel solution	*(20ml for 2 gel; 1.5mm thick)*
30% acrylamide/ Bis solution 29:1 (3.3% C) (BIO-RAD)	6.7ml
dd H2O	8.2ml
10% ammonium persulphate	100µl
TEMED (AMRESCO)	20µl
Stacking gel solution (4% arylamide; 10ml for 4 gels)	*1.5mm thick (10ml)*
30% acrylamide/ Bis solution 29:1 (3.3% C)	1.33ml
4 X Tris-Hcl-SDS PH 6.8	2.5ml
dd H2O	6.1ml
10% ammonium persulphate	50µl
TEMED	10µl

7.14.6. Running buffer, 10x

Reagent	Volume / Amount
Tris base	30.3g
Glycine	144g
SDS	10g
H2O	1L

7.14.7. Transfer buffer, 10x

Reagent	Volume / Amount
Tris base	30.3g
Glycine	144.167g
H2O	1L

7.14.8. TBS

Reagent	Volume / Amount
1M Tris base (PH7.4)	20ml
5M Nacl	30ml
H2O	950ml

7.14.9. TBST

Reagent	Volume / Amount
TBS	1000ml
Tween 20 (SIGMA)	500µl

Part III
Results and Discussion

8

Validating human cornea rims in our study

Ethnic variations have been reported in ocular anatomy and in the prevalence and severity of eye diseases (Blake et al., 2003). The human cornea rims described in this thesis originated from the Chinese Hong Kong population. However, there are currently no reports characterizing it in details. As a first step to confirm our hypothesis and to validate our studied samples, we here investigated the morphology and protein expression of the human cornea rims recruited in our study.

8.1. Gen eral morphology of the cornea rim specimen

Figure 8.1 shows the morphology of our human cornea rim in cross section. The rim consists of three visually identical parts at the epithelial layer, the bulbar conjunctiva, the thick limbus region, and the thin cornea region. The thickness of the limbus is nearly doubled when comparing to the cornea region as described elsewhere (Feng and Simpson, 2008). Essentially we focused on the limbal and cornea regions for the protein expression study.

8.2. Expression of limbal and cornea specific proteins

As mentioned, a distinct set of proteins have been postulated to regulate the corneal epithelial progenitor cells (CEPC) either extrinsically or intrinsically. The extrinsic protein or niche is out of our study capacity here because the human cornea rim was collected ex vivo and after surgery. We here studied a number of proteins which we believed are the intrinsic regulators or markers of the CEPC and the results are summarized in Table 8.1. From our results, we found that the limbal specific proteins, p63 (Figure 8.2), EGFR (Figure 8.3), cytochrome oxidase (Figure 8.4) and cytokeratin (CK) 15 (Figure 8.6) were highly expressed at the limbal region when comparing to the central cornea, while the expression of the cornea specific protein, such as cytokeratin (CK) 3/12 (Figure 8.5) and connexin (Cx) 43 (Figure 8.7) were higher at the central cornea when compared to the limbal region.

Previous reports have shown that p63 was an undifferentiation marker of epithelium that can initiate epithelial stratification and therefore its expression in the basal cells of the limbal region (Koster et al., 2004). EGFR is important for the EGF-signaling in corneal epithelial cell growth and proliferation and was therefore located at the basal limbal epithelium (Murata et al., 1993). As one of the terminal enzymes of the respiratory chain, cytochrome oxidase accelerates cornea epithelial cell renewal by increasing metabolic rate of the cells at the basal limbus (Hayashi and Kenyon, 1988). Cytokeratin (CK) 15 belongs to the type 1 family of cytoskeletal component proteins of epithelial cells and have been shown to express by limbal and conjunctival epithelia,

but not by corneal epithelium (Yoshida et al., 2006). Another pairs of cytokeratin (CK), the basic cytokeratin 3 and acidic cytokeratin 12, and connexin 43, are known as corneal differentiation markers and they exhibited intensive expression in the cornea (Matic et al., 1997; Yoshida et al., 2006). In summary, the expression pattern of our human cornea rim was similar to the recognized phenotype that has been previously reported (Chen et al., 2004).

8.3. Expression of embryonic stem cell specific proteins

With an endeavor to suggest any similarities or differences between CEPC and embryonic stem (ES) cells, or CEPC and cancer stem (CS) cells, we have also analysed the proteins which is specific for ES or CS cells in our tissues. Nanog, Oct4, Sox2, and Notch 1 have been regarded as the canonical ES cell markers. However, we could not obtain observable expression at the basal limbus, let alone the cornea region (Table 8.2). STAT1 and STAT3 are the members of the signal transducers and activator of transcription (STAT) proteins, which together forms homodimers or heterodimers for regulating broad spectrum of cell growth, differentiation and survival. The expression of STAT1 appears critical for ES cells because disruption of STAT1 gene disabled cells from responding to interferon (Durbin et al., 1996), a cytokine for activating stem cells (Essers et al., 2009). In our tissue, STAT1 was expressed more strongly at the basal limbus and weakly at the suprabasal cornea, but STAT3 was expressed in neither region (Durbin et al., 1996) (Figure 8.8 and Table 8.2). Our results indicated that the corneal epithelial progenitor cells may resemble embryonic

stem cells at little extent, confirming the underlying difference between tissue specific stem cells and ES cells.

8.4. Expression of cancer stem cell specific proteins

In Chapter 5, we have suggested the feasibility of understanding cancer biology using CEPC as a model. To test whether CEPC possesses features similar to cancer stem cells, we investigated the expression of several cancer specific proteins. We identified that p73, MDM2, and phospho-STAT1 were highly expressed in the basal limbus when compared to basal cornea, but this was reversed for CDCP1 expression (Table 8.3). However, we did not observe any expression of BMI-1 and Stat3 in both the limbus and cornea regions (Table 8.3). p73, together with the previously mentioned p63, are members of the p53 tumor suppressor family which bind to the p53 DNA-binding sites, transactivate p53-responsive genes and induce cell cycle arrest or apoptosis (Jost et al., 1997), though overexpression of p73 has also been observed in a wide range of tumors (Stiewe and Putzer, 2002) (Figure 8.10). Similar to p73, MDM2 relates to p53 in the sense that it negatively regulates p53. Recently, MDM2 was proposed as a small molecule target for anti-cancer therapeutics (Dickens et al., 2009) (Figure 8.11). phospho-STAT1, activated by Janus-activated kinases, has been recommended as a biomarker in melanoma prognosis (Wang et al., 2007a). Interestingly, both phospho-STAT1 and STAT1 were expressed stronger in the limbus when compared to the cornea in our specimens (Figure 8.8 and 8.13). CDCP1 is a novel cancer stem cell marker which is expressed in CD34-positive haematopoietic

stem cells, mesenchymal stem/progenitor cells, and several other types of cancers (Ikeda et al., 2006). However, instead of expressing at the basal layer of limbal region, CDCP1 was expressed in the cornea basal epithelium in our tissues (Figure 8.9). Whether this is a hint for explaining the low prevalence of limbal tumors requires further elucidation. BMI-1, a polycomb gene family member which plays an important role in the general cell cycle regulation, cell immortalization, and cell senescence, is involved in the regulation of self-renewal and differentiation of stem cells (Jiang et al., 2009), though neither cornea nor limbus in our tissues positively expressed BMI-1 (Table 8.3). In conclusion, basal cells at the limbus region, or functionally CEPC, possesses properties similar to cancer cells especially the overexpression of p73, MDM2 and phospho-STAT1 but different to other cancer stem cell like the negative expression of CDCP1 at the limbus region. Further study is pending for dissecting these unique qualities of CEPC.

8.5. Expression of proteins phenotyped for tissue specific stem / progenitor cells

Because CEPC belongs to the population of tissue specific stem cells, we briefly tested whether CEPC expressed c-Kit receptor, a tyrosine kinase receptor that have been frequently used as a marker for hematopoietic stem and progenitor cells, probably the most well known and historic tissue specific stem cells in the human body (Edling and Hallberg, 2007). As shown in Figure 6.13, c-kit receptor was strongly expressed in the basal layer of limbus, which is the location where CEPC resides.

8.6. *Brief conclusion*

By possessing qualities similar to the limbal tissues from other human populations and to other tissue specific stem cells, we conclude that the human cornea rim tissue that we collected is eligible for our study.

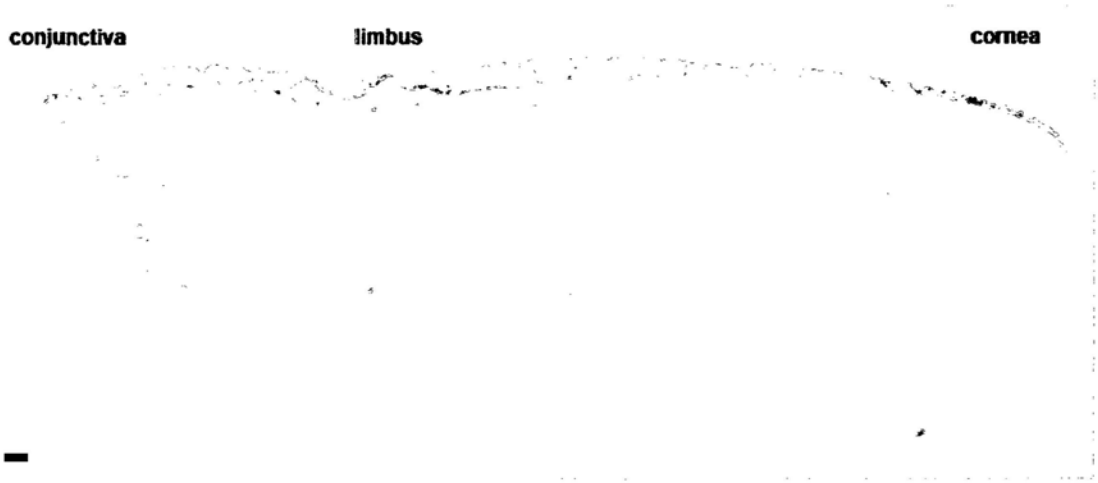

Figure 8.1. A representative human cornea rim collected in our study, cross section, haematoxylin and eosin stain. Bar, 100 μm.

Table 8.1. Expression of reported corneal epithelial progenitor cell (CEPC) marker in the human cornea rim of our study.

Marker	Staining site	Limbal basal	Corneal basal
p63	Nuclear	+++	+
EGFR	Cell surface	++	+/-
Cytochrome oxidase	Cytoplasmic	++	-
Cytokeratin 15	Cytoplasmic	+++	-
Cytokeratin 3/12	Cytoplasmic	-	++
Connexin 43	Cell surface	-	++

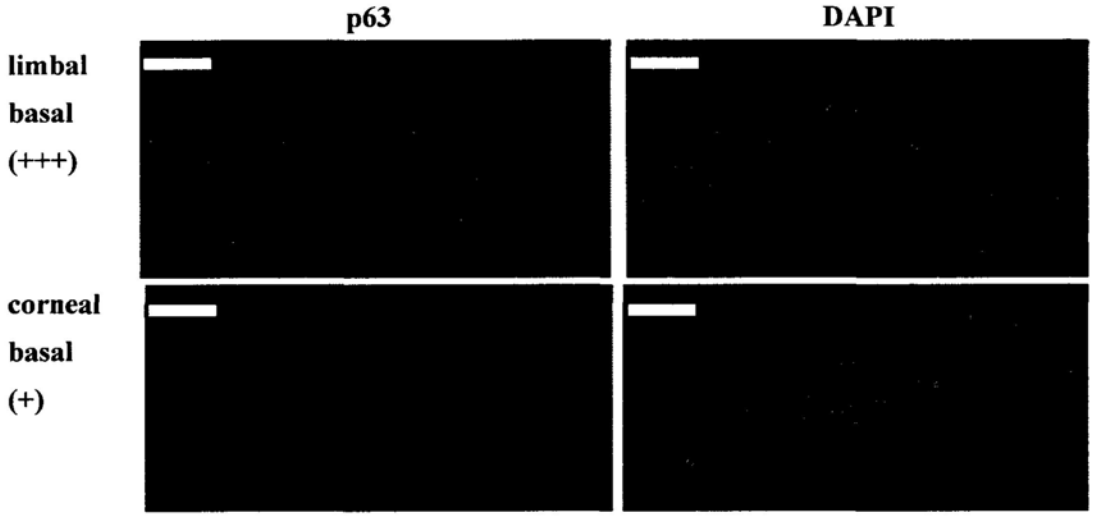

Figure 8.2. Expression of p63 in the limbal and corneal basal region of our corneal rim. The nucleus was stained with DAPI. Florescence intensity was denoted by '+'. Bar, 100 μm.

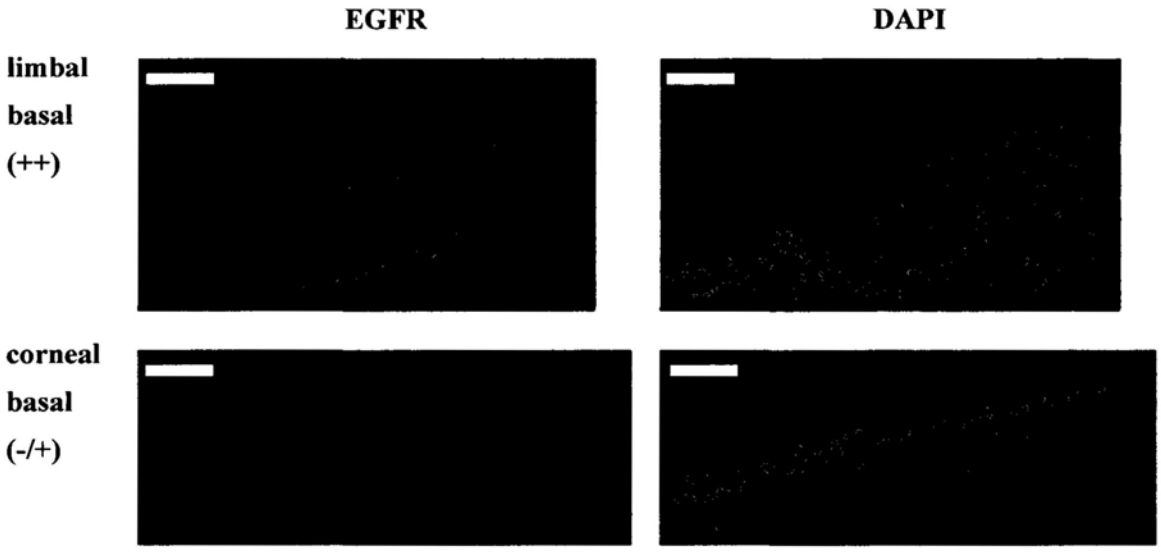

Figure 8.3. Expression of epidermal growth factor receptor (EGFR) in the limbal and corneal basal region of our corneal rim. The nucleus was stained with DAPI. Florescence intensity was denoted by '+' or '-'. Bar, 50 μm.

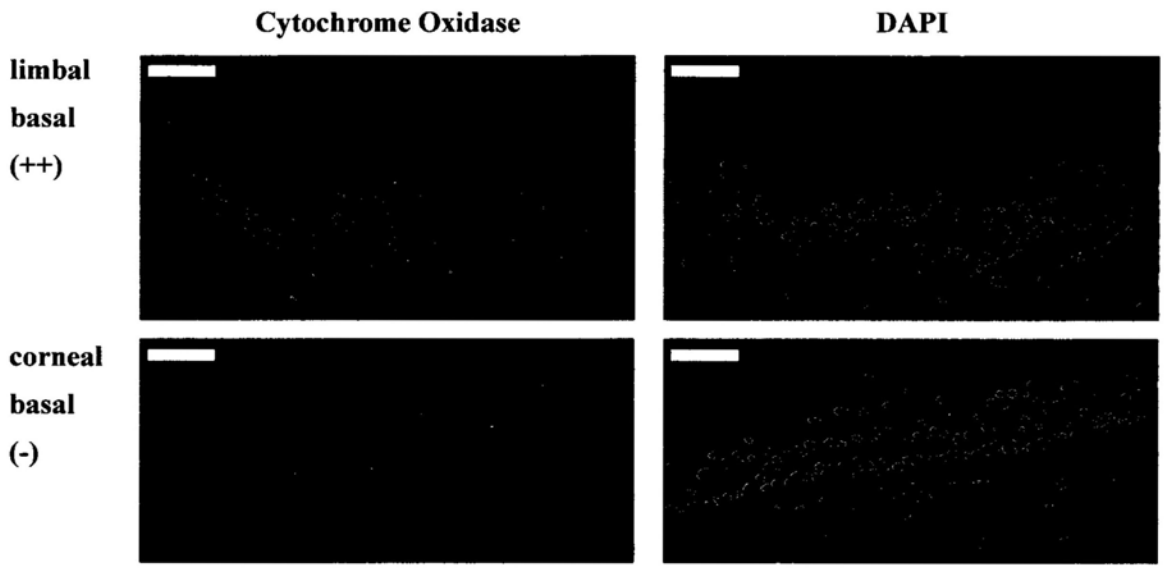

Figure 8.4. Expression of cytochrome oxidase in the limbal and corneal basal region of our corneal rim. The nucleus was stained with DAPI. Florescence intensity was denoted by '+' or '-'. Bar, 50 μm.

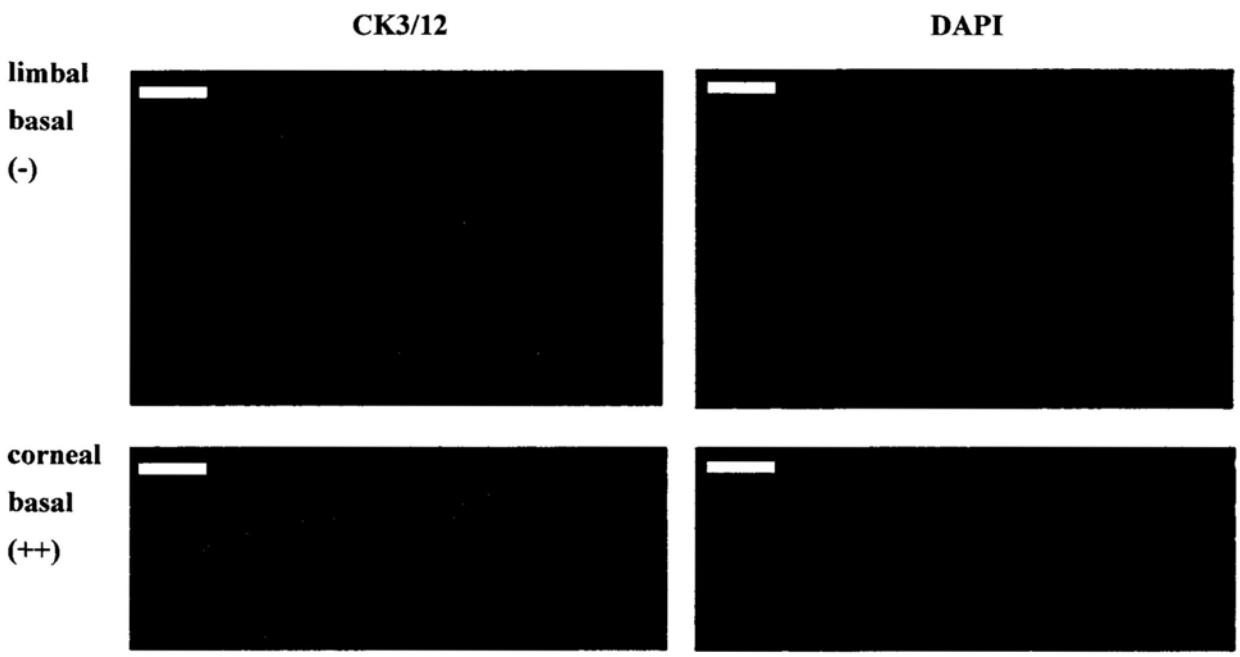

Figure 8.5. Expression of cytokeratin 3/12 (CK3/12) in the limbal and corneal basal region of our corneal rim. The nucleus was stained with DAPI. Florescence intensity was denoted by '+' or '-'. Bar, 50 μm.

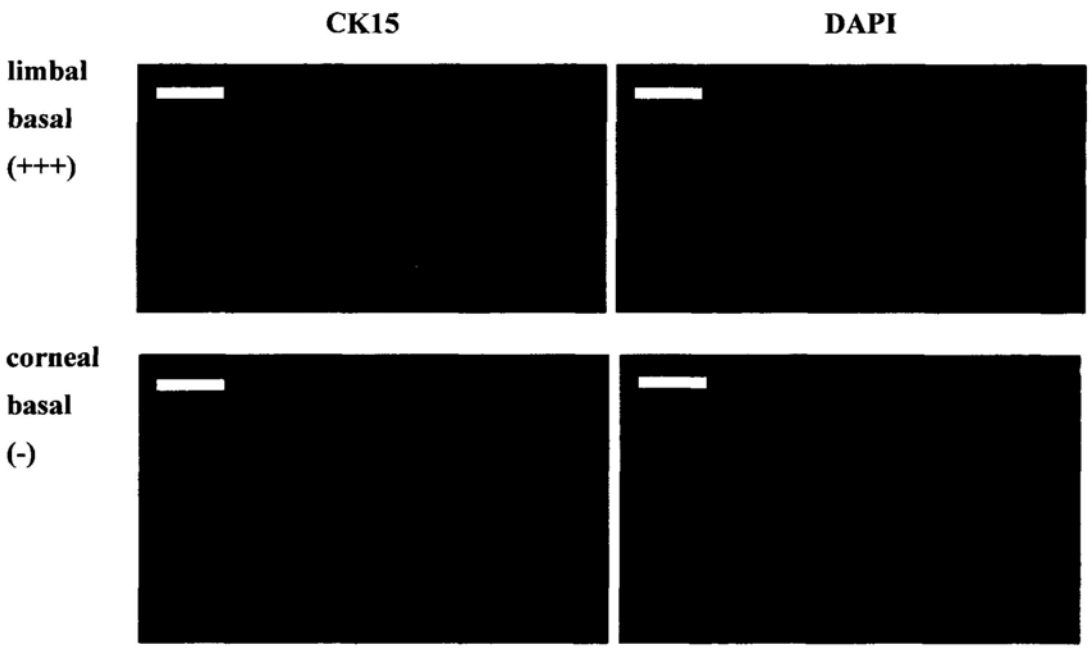

Figure 8.6. Expression of cytokeratin 15 (CK15) in the limbal and corneal basal region of our corneal rim. The nucleus was stained with DAPI. Florescence intensity was denoted by '+' or '-'. Bar, 50 μm.

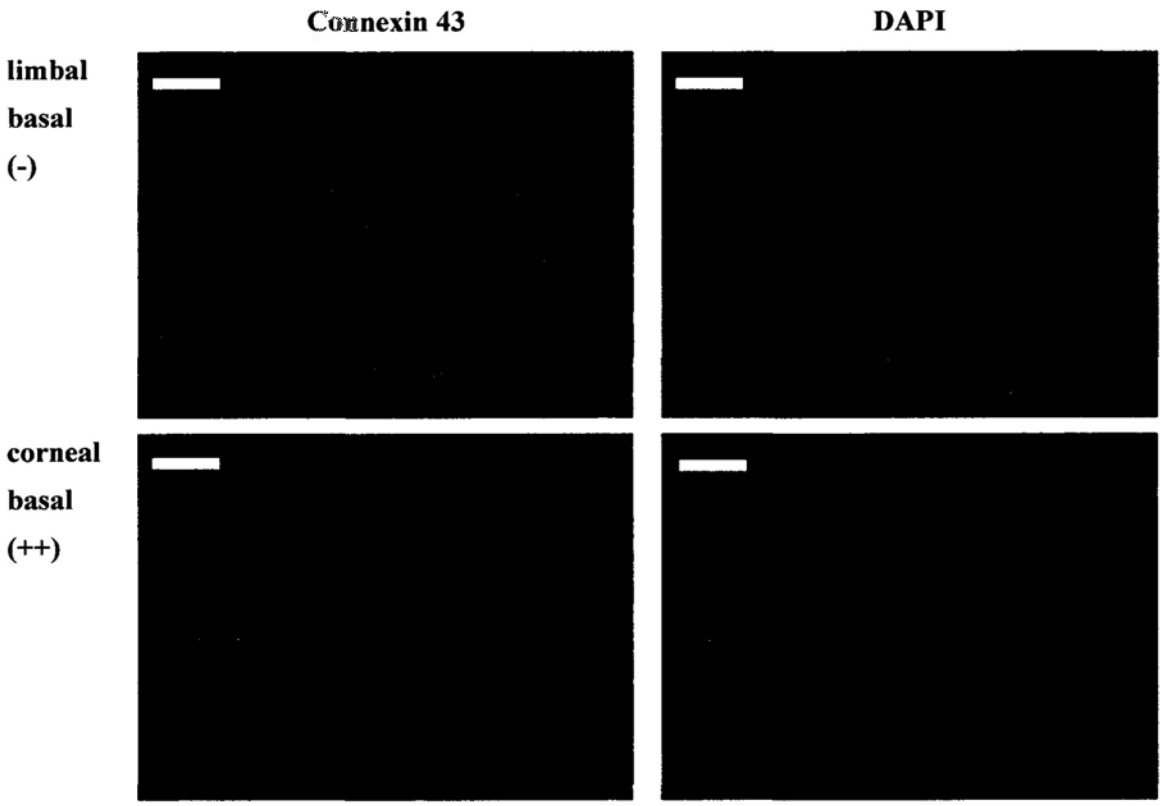

Figure 8.7. Expression of connexin 43 in the limbal and corneal basal region of our corneal rim. The nucleus was stained with DAPI. Florescence intensity was denoted by '+' or '-'. Bar, 25 μm.

Table 8.2. Expression of reported embryonic stem cell (ESc) marker in the human cornea rim of our study.

Marker	Staining site	Limbal basal	Corneal basal
Nanog	Nuclear	-	-
Oct4	Nuclear	-	-
Sox2	Nuclear	-	-
Stat1	Cytoplasmic – surface	++	+
Stat3	Cytoplasmic	-	-
Notch1	Cell surface - nuclear	-	-

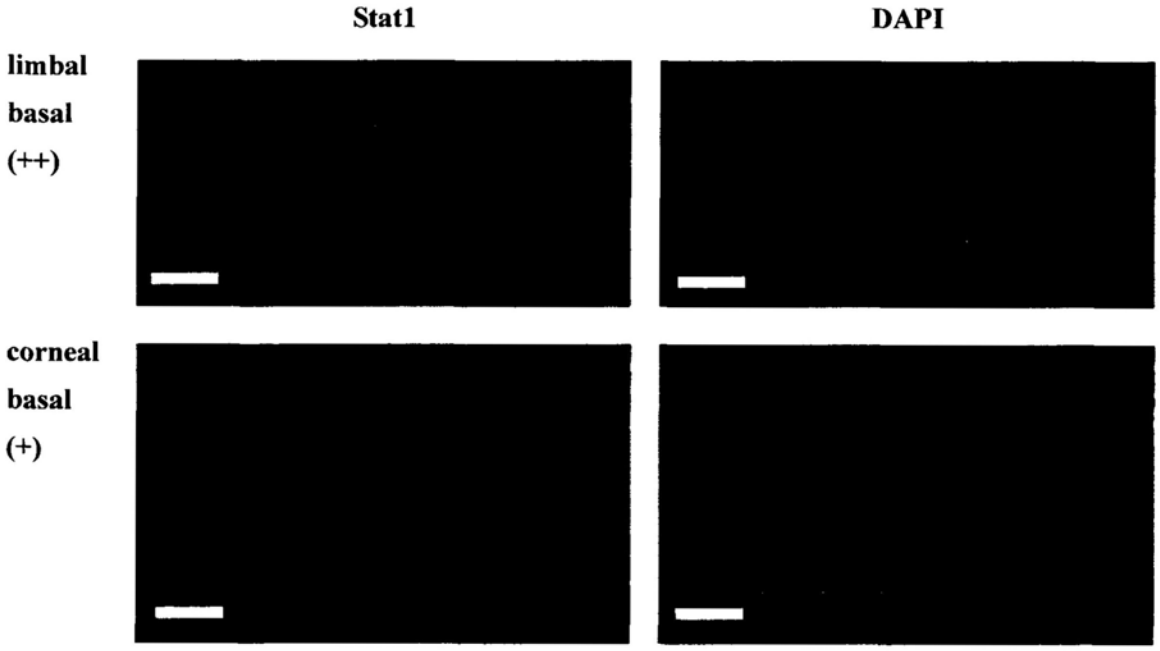

Figure 8.8. Expression of stat1 in the limbal and corneal basal region of our corneal rim. The nucleus was stained with DAPI. Florescence intensity was denoted by '+'. Bar, 25 μm.

Table 8.3. Expression of reported cancer stem cell (ESc) marker in the human cornea rim of our study.

Marker	Staining site	Limbal basal	Corneal basal
CDCP1	Cytoplasmic	-	+
BMI-1	Nuclear	-	-
p73	Cytoplasmic	+++	++
MDM2	Cytoplasmic	+++	-
P Stat1	Cytoplasmic – surface	+/++	-
Stat3	Cytoplasmic	-	-

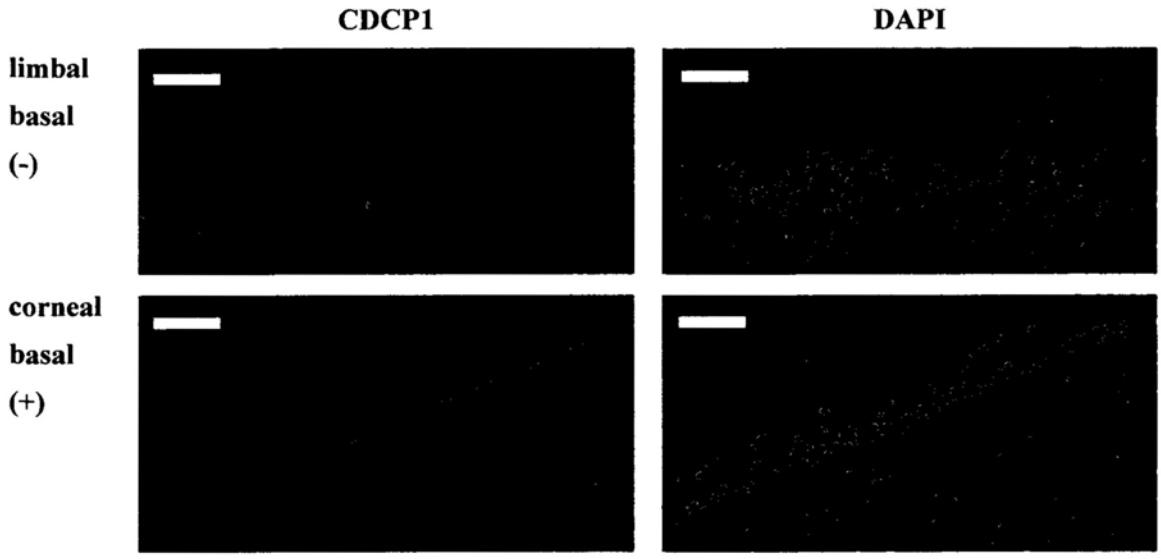

Figure 8.9. Expression of CDCP1 in the limbal and corneal basal region of our corneal rim. The nucleus was stained with DAPI. Florescence intensity was denoted by '+' or '-'. Bar, 50 μm.

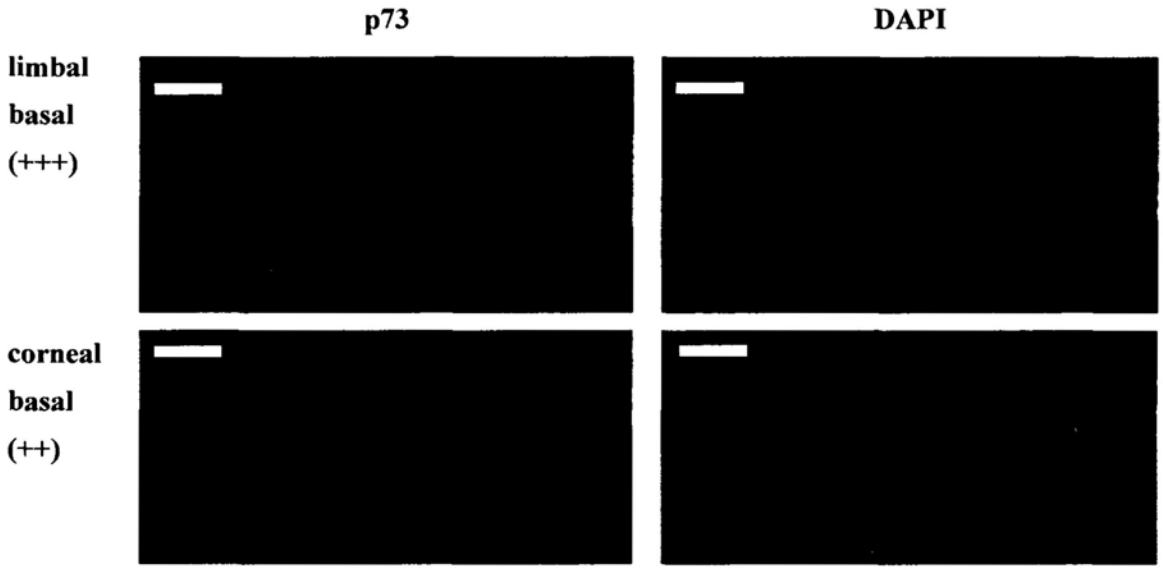

Figure 8.10. Expression of p73 in the limbal and corneal basal region of our corneal rim. The nucleus was stained with DAPI. Florescence intensity was denoted by '+'. Bar, 50 μm.

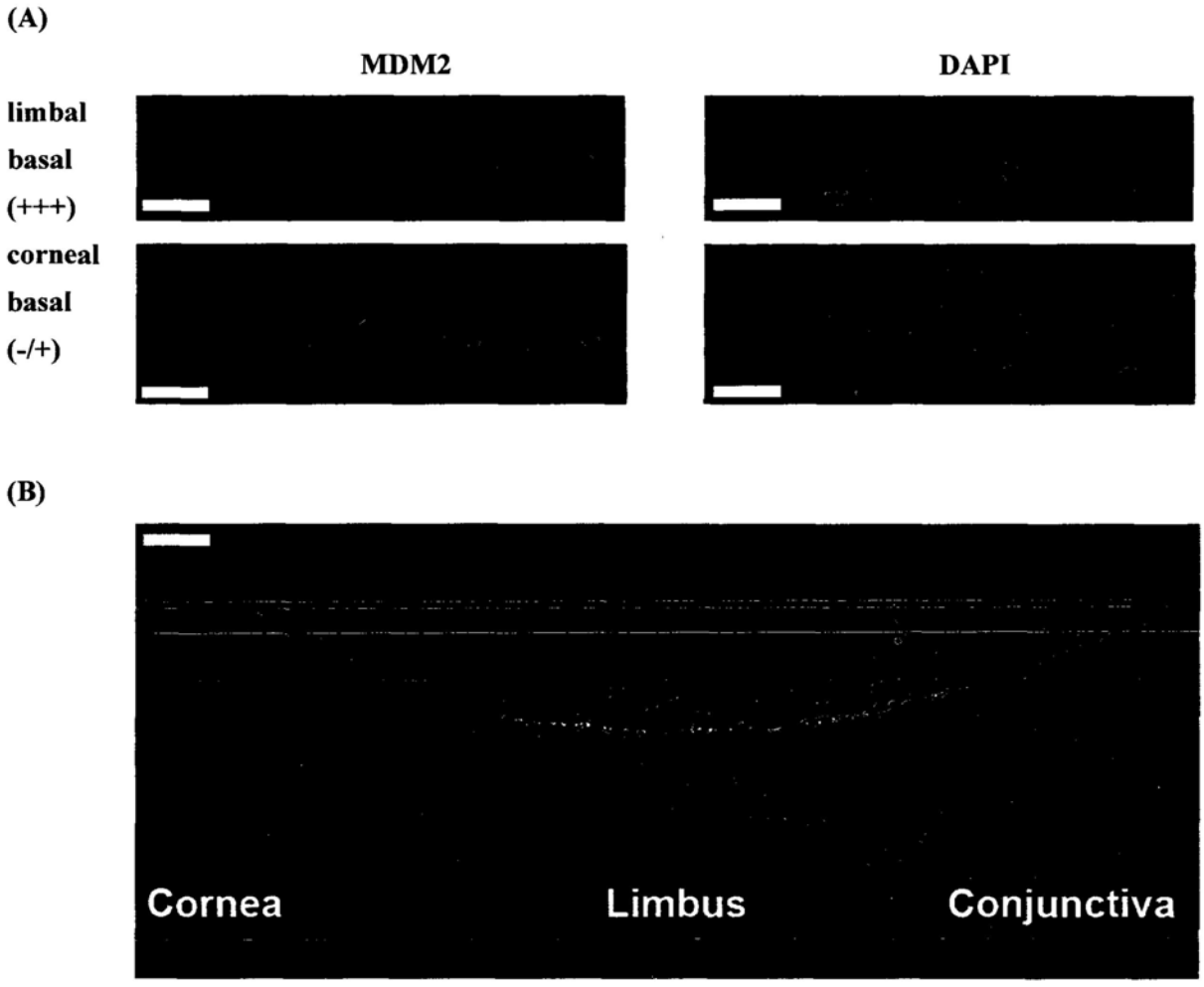

Figure 8.11. Expression of MDM2 in the limbal and corneal basal region of our corneal rim. Florescence intensity was denoted by '+'. The nucleus was stained with DAPI, MDM2 was stained in Rhodamine Red. Bars in A, 25 μm. Bars in B, 100 μm.

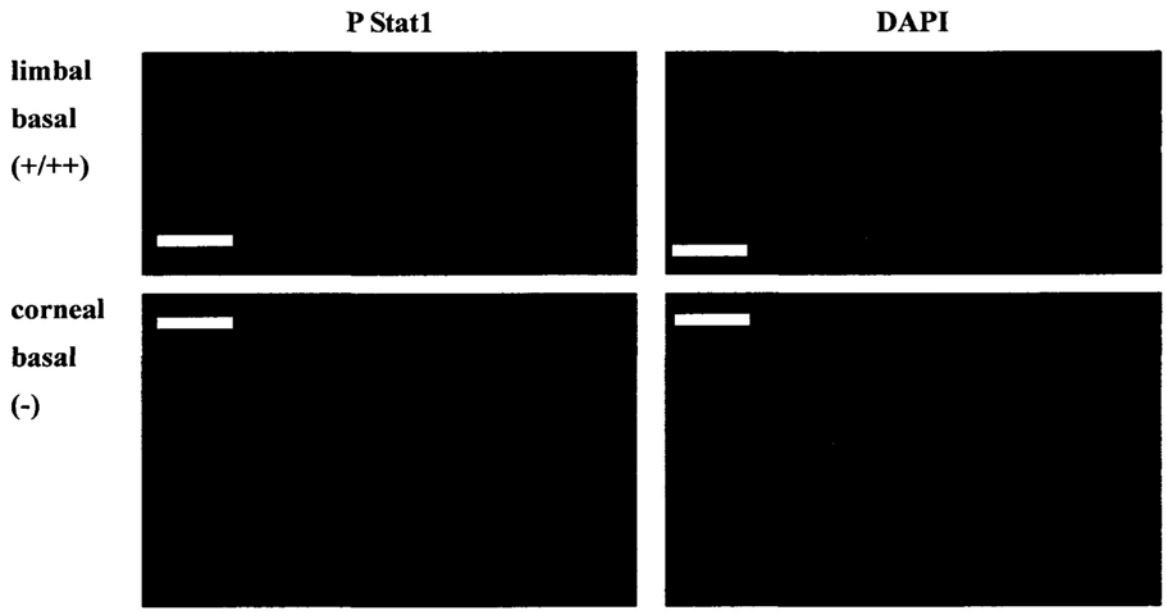

Figure 8.12. Expression of P Stat1 in the limbal and corneal basal region of our corneal rim. The nucleus is stained with DAPI. Florescence intensity was denoted by '+'. Bar, 50 μm.

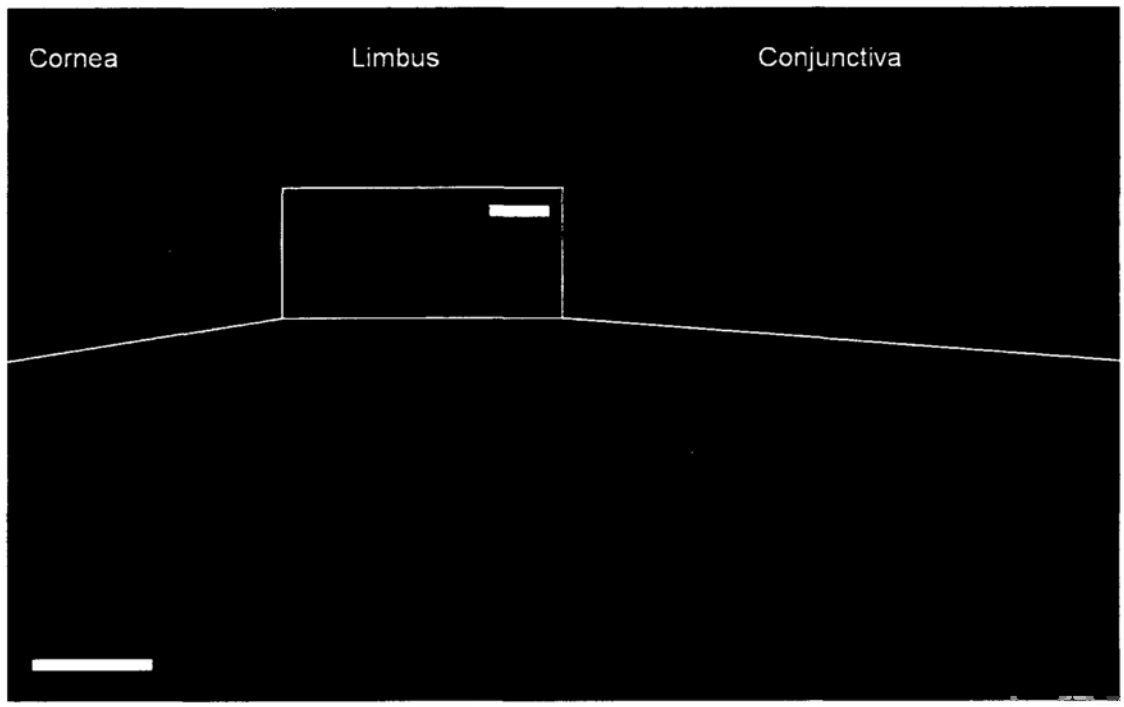

Figure 8.13. Expression pattern of c-kit receptor in the human cornea rim. Bar in upper image, 100 μm; bar in lower image, 25 μm

9

Protocols for enriching the population of corneal epithelial progenitor cells

Because tissue specific stem cells including cornea epithelial progenitor cells generally exist at low occurrence, it is necessary to enrich this population of cells from the cornea rim before study. This chapter describes the several enrichment protocols that we have devised, beginning with the isolation of single cells, the protocol utilising flow cytometry, laser pressure catapult system and finally manual microdissection, with an aim to determine a method which gives the most genuine microRNA profiling pattern as described in Chapter 10.

9.1. Isolation of single cells from cornea tissue

To obtain singlet CEPC for further assays, we optimized our isolation method using cow's eye ball, which was purchased freshly from a local butcher. As shown in Figure 9.1, the extraocular muscles on the eyeball were removed, which was followed by the isolation of anterior ocular segment. Lens, iris and cornea endothelium were then scraped away gently by a round surgical blade. The central cornea and peripheral cornea were isolated manually by dissection. The tissue was then washed with phosphate-buffered saline and was incubated in 50 mg/ml Dispase II (Roche

Diagnostics, Basel, Switzerland) in the presence of D-sorbitol (100 mM) at 4°C for 16 hours. The epithelium was loosened readily from the underlying stroma and was collected for single cell isolation. By incubating and pipetting up and down in pre-warmed 0.05% trypsin (1:250) and 0.53 mM ethylenediaminetetraacetic acid (EDTA), single cell suspension is obtained. The action of trypsin was neutralized by adding ice-cold trypsin inhibitor cocktail diluted at 1 mg/mL in corneal epithelium culture medium. The cell suspension was then passed through a 40 μm nylon mesh to collect the singlet cell population in the flow-through (Figure 9.2). In addition, the corneal epithelial cell culture medium is composed of Dulbecco modified Eagle medium:F12 basal media in a 2:1 ratio containing 5% heat-activated fetal bovine serum (European Directorate on the Quality of Medicines compliant), hydrocortisone 0.4 μg/mL, cholera toxin 0.1 nmol, recombinant human insulin 5 μg/mL, selenite A (6.7 ng/mL), transferrin (5.5μg/mL), basic fibroblast growth factor (10 ng/mL) and epidermal growth factor 10 ng/mL. The antimicrobials penicillin (100 IU/mL), streptomycin (100 μg/mL), and amphotericin B (0.25 μg/mL) were added at all the washing and incubation steps.

Because it has been shown that CEPC is the smallest epithelial cells in the cornea (Romano et al., 2003), we examined the size of the singlet cell population that we obtained from the cow's cornea to validate our procedures. As shown in Figure 9.3A and B, singlet cells isolated from the peripheral cornea had smaller cell size when compared to those from the central cornea. Since apoptotic cells usually shrink and become compact when compared to viable population, we also investigated the

percentage of cell apoptosis in the small sized cell population from the peripheral cornea using flow cytometric analysis. We found that the percentage of early apoptotic cells at the peripheral cornea and central cornea were similar, with the values of 20.4 ± 1.5 and 21.9 ± 0.7, respectively (Figure 9.3D, E), indicating most small-sized cells from peripheral cornea were not apoptotic cells and the isolation procedure could maintain the viability of target cells. Instead, this population of cells should be the corneal epithelial progenitor cells as suggested by other reports (Arpitha et al., 2008a, b; Romano et al., 2003; Umemoto et al., 2006).

This procedure has been confirmed applicable to the isolation of murine, porcine and human singlet CEPC, respectively. The mouse eyeballs were collected from BALB/c mice aged 4 to 8 weeks; the eyeballs from pig were again freshly purchased from local butcher, the human eyeballs were obtained from Joint Shantou International Eye Center (JSIEC), Shantou, China. For the human cornea rim collected in the Hong Kong Eye Hospital and Prince of Wales Hospital, Hong Kong, the isolation step began by manually dissecting the more central cornea and the peripheral cornea, followed by the immersion in Dispase II overnight at 4°C. The procedures were then followed likewise.

9.2. Enrichment of corneal epithelial progenitor cells using Florescence Activated Cell Sorting (FACS)

We attempted to use the florescence activated cell sorting (FACS) for isolating a purer

population of CEPC. This usually involves a panel of positive or negative markers to select the target population. It has been shown that stem or progenitor cells exhibits a Hoechst 33342-low side population (SP) phenotype through the effluxing of the supravital dye Hoechst 33342 by membrane efflux activity of the ATP-binding cassette (ABC) transporter superfamily, including multidrug resistance 1 (Mdr1a/1b, mouse; MDR1, human) (Schinkel et al., 1997) and breast cancer resistance protein 1 (Bcrp1)/ATP-binding cassette, subfamily G (WHITE), member 2 (ABCG2) (Zhou et al., 2001). This SP phenotype was originally described in murine bone marrow preparations and was later used as a gold standard for purifying stem cells (Goodell et al., 1996; Lin and Goodell, 2006). However, the excitation of Hoechst requires the installation of expensive ultraviolet lamp in the FACS machine, which may not be affordable in normal laboratory settings. Based on the principle that Hoechst was effluxed through the ABC transporter superfamily, it is possible to sort prospective stem cells by the surface marker, ABCG2. Indeed, several reports have successfully utilized ABCG2 as a marker for sorting CEPC that is slow cycling (Budak et al., 2005; de Paiva et al., 2005). To validate our set up and procedures, we have also utilized ABCG2 as a marker for sorting CEPC (Figure 9.4). By using murine cornea epithelial cells, we found that $ABCG2^+$ cells appeared small (Figure 9.4C) and engaged 15 ± 3.555 % of the total cell population (Figure 9.4D). Since other tissue specific stem cell, for example hematopoietic stem cells, generally exists at 0.01 – 0.05 % out of the concerned cell population (Challen et al., 2009), our percentage of $ABCG2^+$ cells appeared higher than expected. Indeed, it has been shown that different tissue SP cells may use different transporters and ABCG2 is not the exclusive markers for the SP

phenotype (Challen and Little, 2006). Furthermore, functional data also do not support the sole use of ABCG2 for stem cell purification (Naylor et al., 2005). We therefore include additional markers in the FACS isolation.

Because CEPC are generally slow cycling in condition without external stimuli, it is possible to isolate CEPC by its characteristic quiescent state, which can be measured by pyronin Y and rhodamine 123. Pyronin Y is a cationic dye capable of forming fluorescent complexes with double-stranded RNA and DNA (Kapuscinski and Darzynkiewicz, 1987). It has been reported that PY^{-} represents cells in the G0 phases of the cell cycle when DNA is blocked by other dyes (Huttmann et al., 2001). Rhodamine 123, a fluorescent cationic dye labels mitochondria in living cells and effluxed by MDR1 (Kim et al., 1998), has been reported as a replacement of Hoechst 33342, with an advantage that it is excited at 505 nm and therefore eases the requirement for an expensive ultraviolet lamp in the FACS machine. Indeed there is an increasing trend of using Rhodamine 123 as a marker for isolating tissue specific stem cells (Lo et al., 2005; McKenzie et al., 2007; Wagner-Souza et al., 2008). Based on these reports, we have also tested the validity of using these two markers for purifying CEPC. Figure 9.5 shows the staining efficiency of pyronin Y (250 ng/μl) (Bhatt et al., 2003). Necrotic and apoptotic cells were differentiated from the viable cells by the uptake of propidium iodide. We found that pyronin Y at this concentration possessed little cytoxicity on the corneal epithelial cells and 15 mins incubation time is already sufficient for an efficient stain up. Similarly, Figure 9.6 shows the staining efficiency of Rhodamine 123 (10 ng/ml). This concentration is actually ten times lower than the

one suggested by McKenzie et al in 2007. However, we noticed that rhodamine 123 possessed observable cytotoxicity if the incubation is longer than 45 mins in corneal epithelial cells. Although rhodamine 123 could satisfactorily stain up the cells within 15 mins, the time required for sorting a rare cell population is much beyond 45 mins. Because of the possible cytotoxicty induced by rhodamine 123, we abandon the use of it in purifying CEPC.

Besides ABCG2 and pyronin Y, we introduced two additional markers in the enrichment protocol, which are Connexin 43, the cornea differentiation marker, and Notch1, the marker for CEPC (Djalilian et al., 2008). These two markers were chosen because they are the rare surface antigens that are known in CEPC. And surface antigens are selected because viable cell staining is enabled and viable cells can be sorted for *in vitro* experiments. Figure 9.7 shows the results of the enrichment protocol gating low Connexin 43, high ABCG2, high Notch1 and low Pyronin Y cells. In a typical sorting experiment, we obtained 0.7 % cells with low Connexin 43, high ABCG2, high Notch1 and low Pyronin Y phenotype. This percentage appears reasonable for CEPC and this novel protocol is ready for further *in vitro* testing which will be carried out in further study.

9.3. Enrichment of corneal epithelial progenitor cells using laser pressure catapult microdissection

Although the FACS protocol is useful for isolating cells for culture, it is far from

desire in the identification of microRNAs in the CEPC. Two reasons for this, first, the cells were manipulated in enzymes, medium, antibodies and buffers for around 24 hours before the actual sorting. Such manipulation may induce undesirable side effects on the profiling of microRNAs; second, the number of cells isolated by the four parameter protocols are scarce, which means that a higher number of initial cells is demanded for RNA isolation and microarray studies. This appears impossible for a human cornea tissue because the cornea donation in Hong Kong is insufficient for medication, let alone those for scientific research. To profile microRNAs from human cornea rim, we must devise another enrichment method for CEPC.

We tackle this by recruiting the non-contact laser-capture microdissection system (P.A.L.M., Bernried, Germany). Cornea tissues were cryosectioned at 8 μm and mounted onto a 1.35 μm thin polyethylene naphthalene membrane attaching onto a normal slide. The MicroBeam ejected from the system cut both the specimen and the underlying membrane at the desired location. The specimens were then catapulted in a non-contact micromanipulation manner (Huang et al., 2003). Figure 7.8 shows the location of cells that we intended to collect for microRNA profiling. We attempted to obtain cells at the basal layers in both the limbus (Figure 9.8A) and cornea (Figure 9.8B) regions. However, we encountered a dilemma which is that for collecting good quality of RNA, the tissue should be fresh and so be prepared in frozen section instead of the dry paraffin sections. The moisture inevitably increased the tissue's weight, rendering difficulty in catapulting the section. We therefore abandoned this enrichment protocol because it may take up to 4 hours to collect one single section which is

already much manipulated and dried on repeated irradiation.

9.4. Enrichment of corneal epithelial progenitor cells using manual microdissection

With an aim to reduce the manipulation time but preserve the natural nucleic acid profile as much as possible, we finally utilized manual microdissection as our isolation method. We isolate the periperhal cornea from the close to central cornea in freshly collected human cornea rims. We regard the peripheral cornea as the limbus tissue, while the close to central cornea as the cornea tissue. Although the population of CEPC is not homogenous, the limbus tissue is much enriched with CEPC when compare to the cornea tissue. We believe the most prominently expressed microRNAs will be revealed in the identification process, as discussed in Chapter 10.

Because degraded RNA appears as short fragment and may affect microRNA identification, we evaluated the RNA integrity of the cornea and limbal tissues using bioanalyser before the actual experiments. As shown in Figure 9.9, the typical integrity of our RNA samples usually bears a more than 1.3 ratio of 28S to 18S, and an RNA integrity number (RIN) above 7. This value appears reasonable for the human cornea specimen, which was generally stored in Optisol at 4°C for a few days before the cornea transplant. In addition, purity of the RNA samples was assessed using Nanodrop 1000. We proceeded only those RNA samples with OD260/280 ~ 2 and OD260/230 > 2 for the identication experiments, as described in Chatper 10.

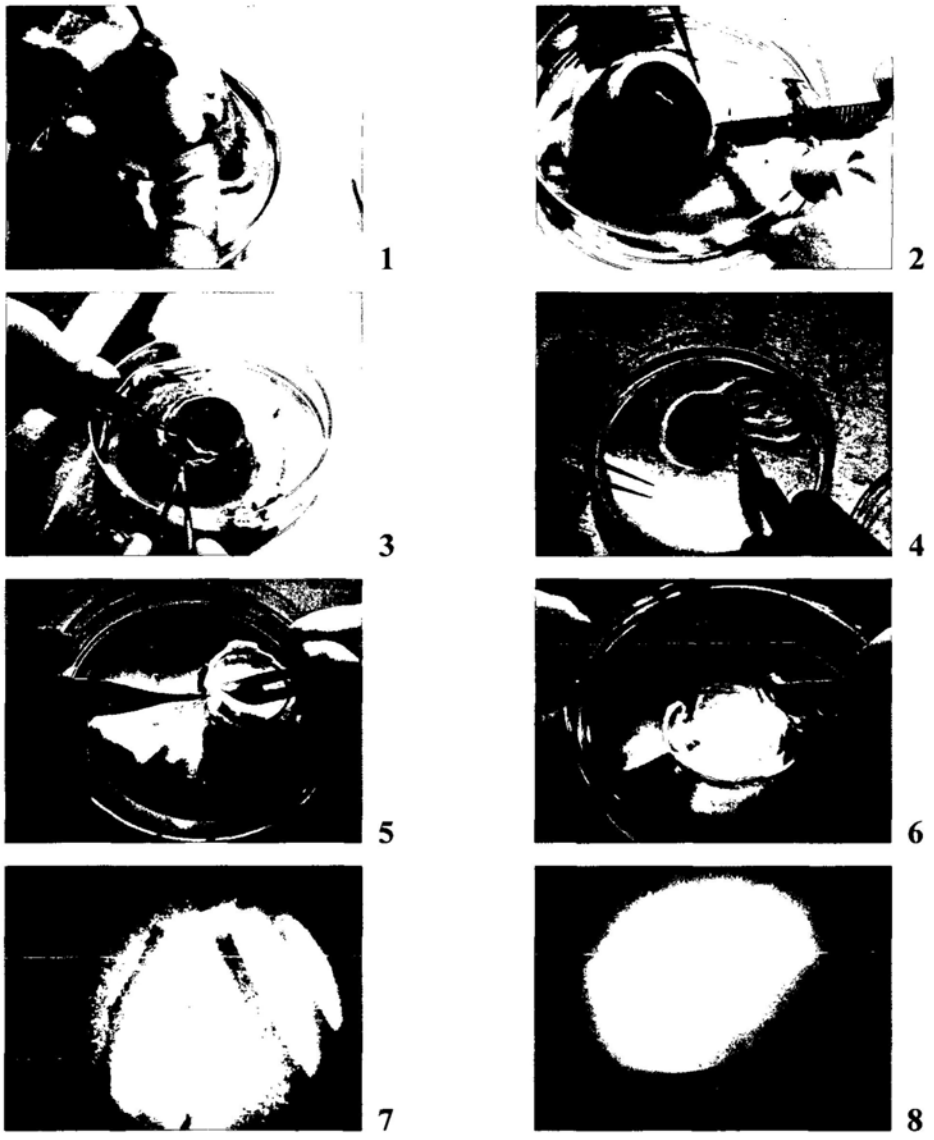

Figure 9.1. Schematic diagrams showing the isolation of corneal epithelial progenitor cells from the cornea tissue. Cow's eyes were used in demonstrating this method for easy visualization. (1) Remove extraocular muscle and other connective tissues on the eyeballs. (2) Make a slit on the sclera. (3) Collect anterior segment. (4) Remove lens and iris. (5) Remove endothelium. (6) Separate central cornea and peripheral cornea. (7) and (8) Incubate tissue at dispase for 16 hours at 4°C to collect corneal epithelium and limbal epithelium, respectively.

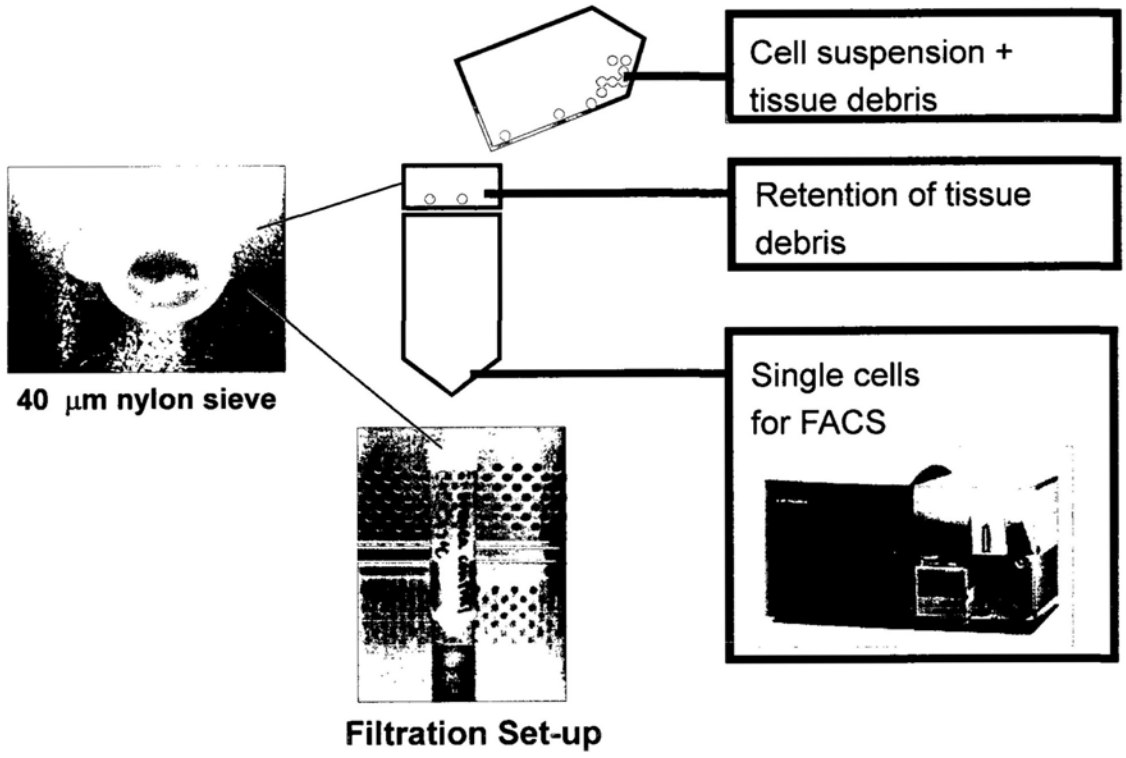

Figure 9.2. Schematic diagram showing the set-up for collecting a cell population enriched with single corneal epithelial progenitor cells.

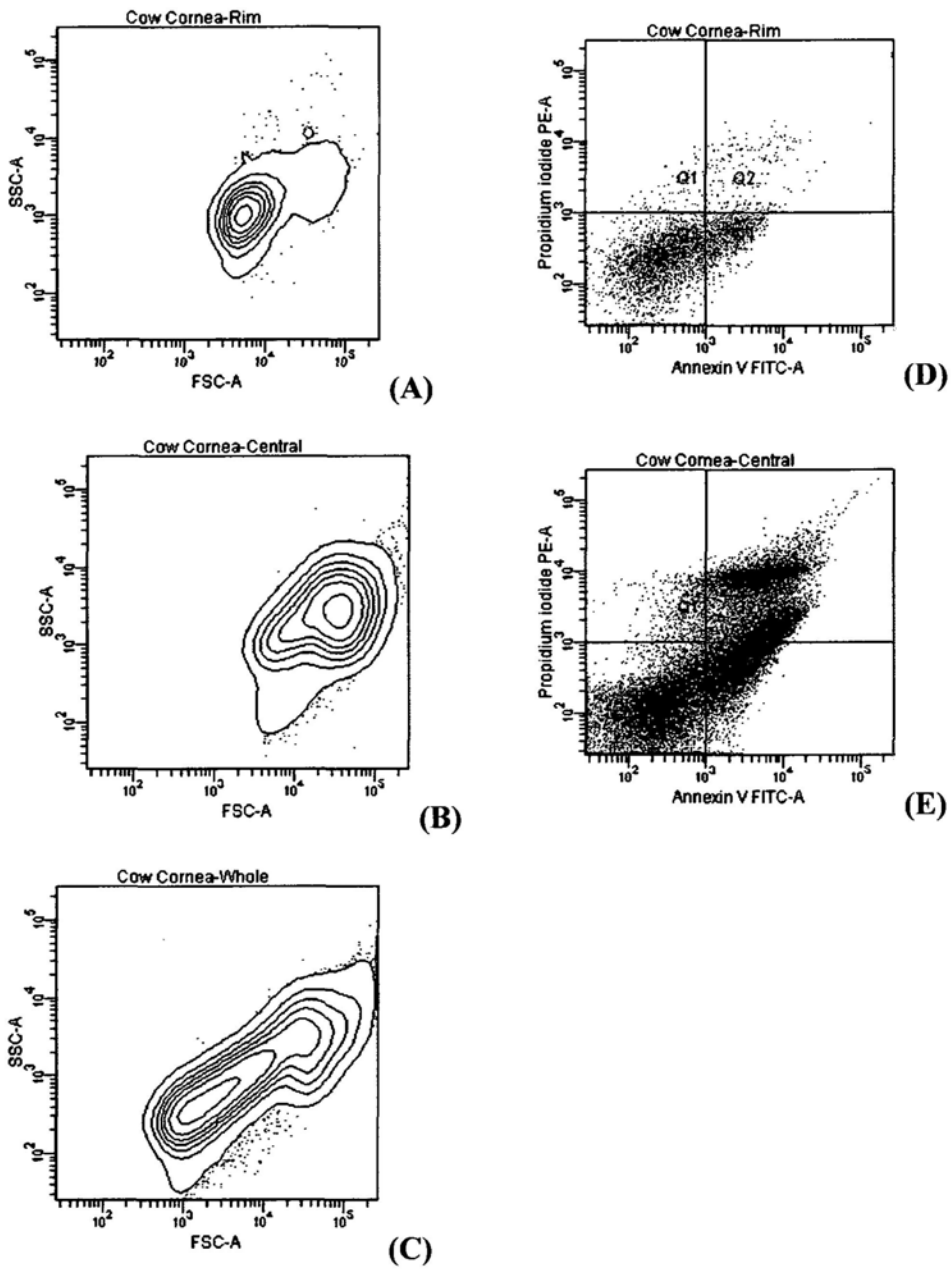

Figure 9.3. Cell size and apoptosis pattern of the isolated single cells. Representative results showing size of the single cells collected from (A) peripheral and (B) central cornea regions, and apoptosis pattern of cells collected from (D) peripheral and (E) central cornea. (C) Scatter plot denoting the size of single cells collected from intact cornea. Quadrants Q1, debris; Q2, late apoptosis; Q3, viable; Q4, early apoptosis.

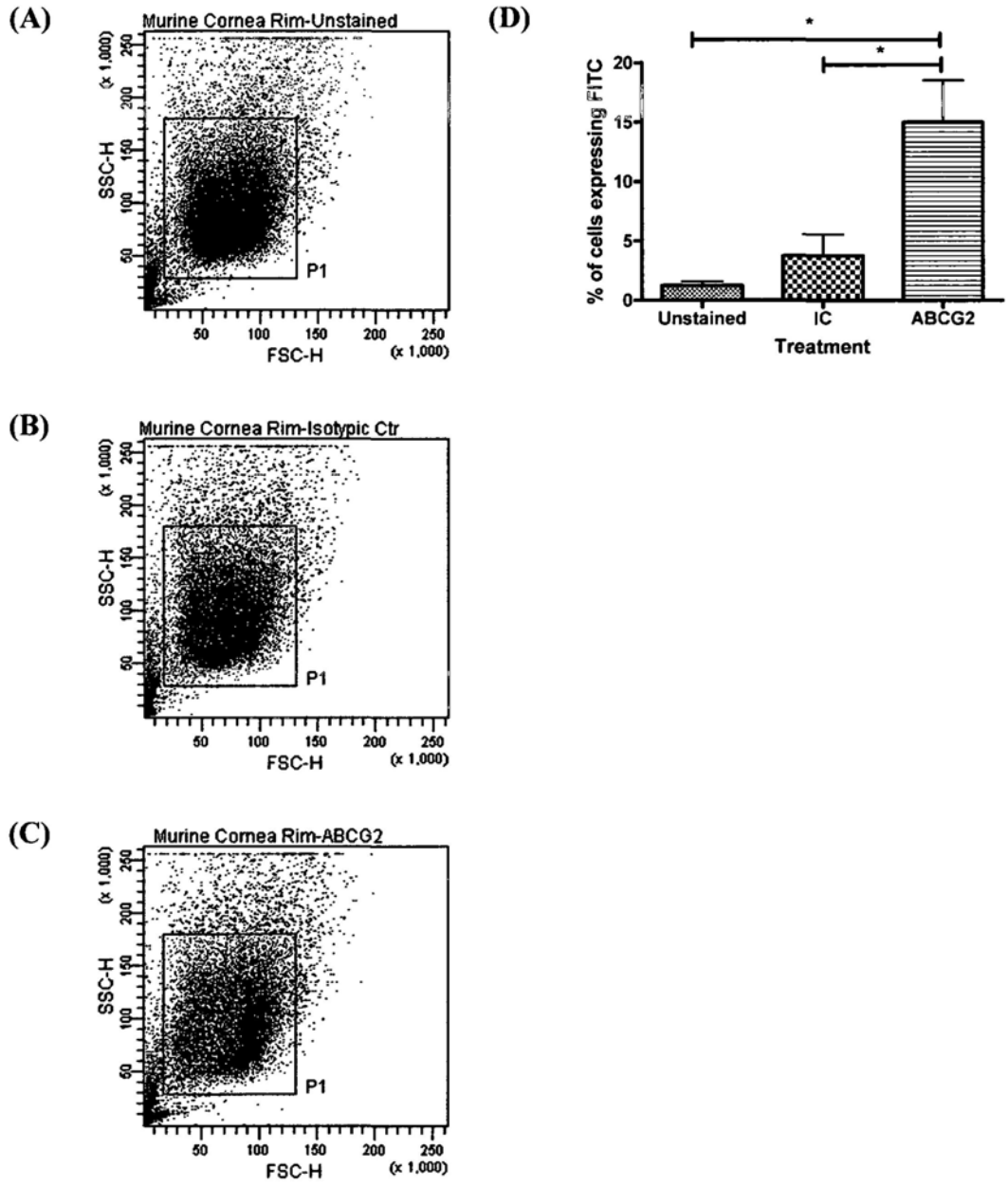

Figure 9.4. ABCG2 staining on cornea epithelial cells. (A-C) The size of cornea epithelial progenitor cells stained with ABCG2 (FITC) were small. (A) unstained control; (B) isotypic control; (C) ABCG2 stained cells. (D) Bar graphs showing the percentage of FITC positive cells in the unstained, isotypic control (IC) and ABCG2 treated cells. * $p < 0.05$, n =3, One Way ANOVA with Bonferroni's Multiple Comparison.

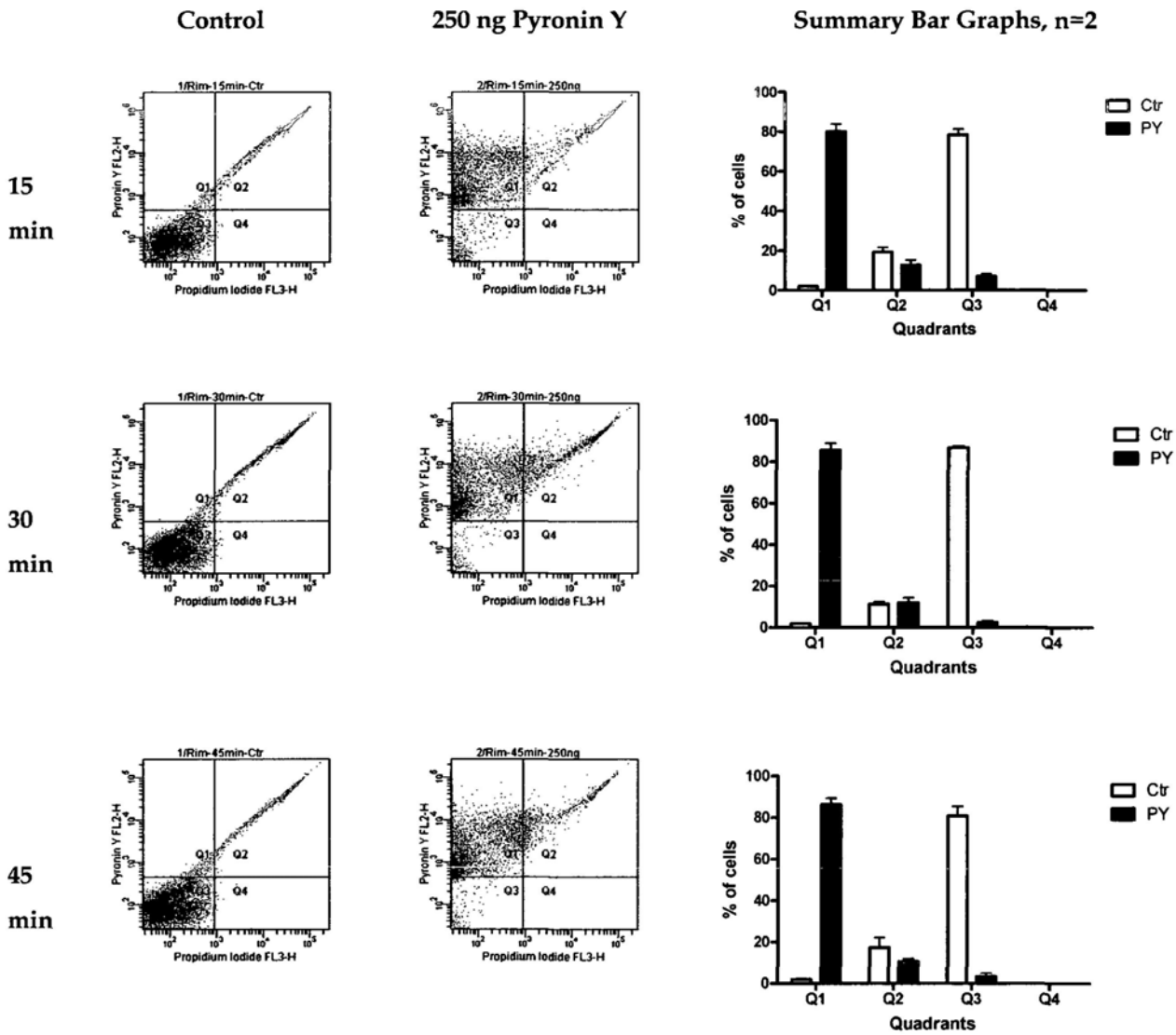

Figure 9.5. Efficiency of Pyronin Y (PY, 250 ng) staining at 15, 30 and 45 mins. Quadrants Q1, PY+PI- cells; Q2, PY+PI+ cells; Q3, PY-PI- cells; Q4, PY-PI+ cells. Treatments Ctr, Control; PY, Pyronin Y.

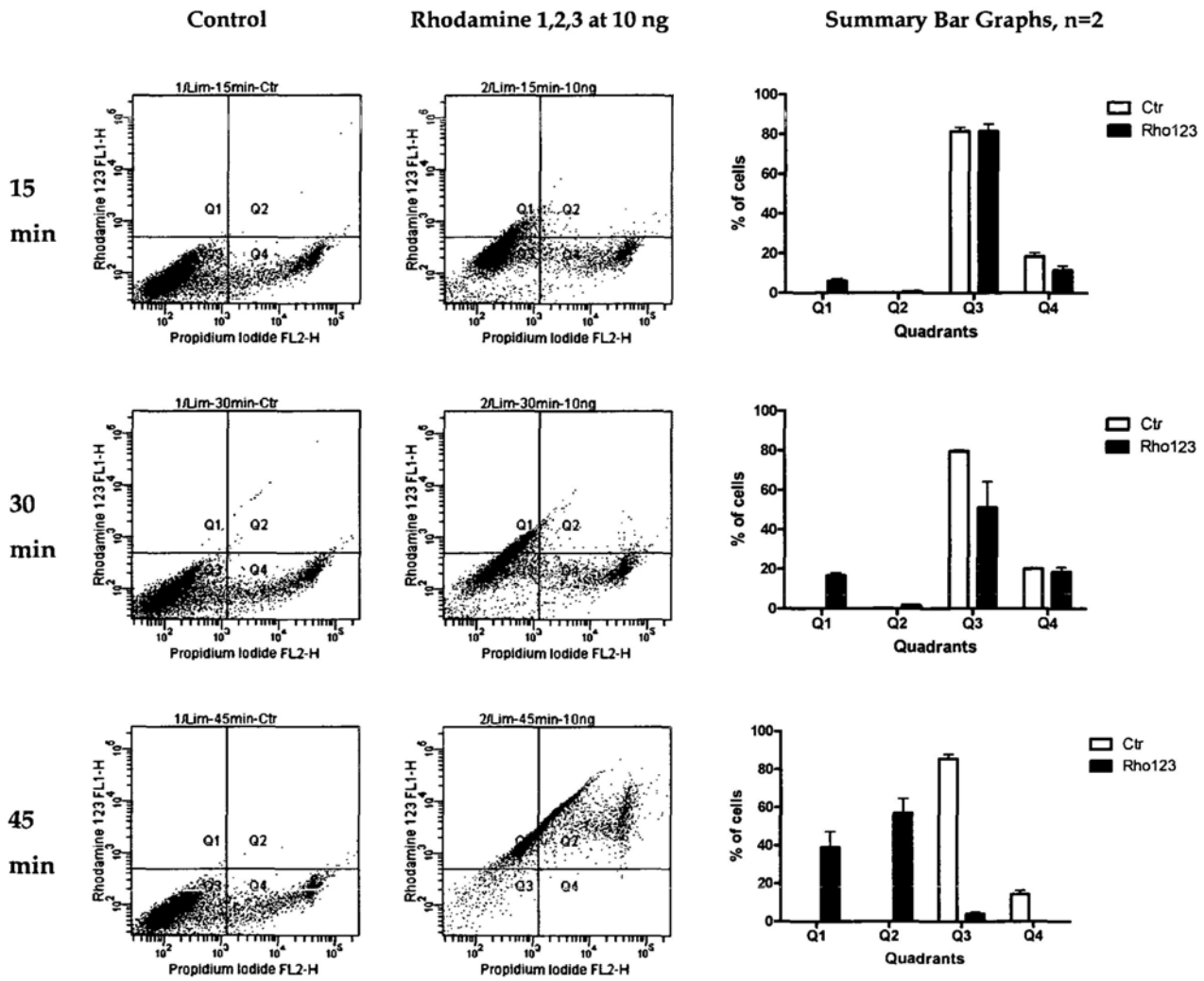

Figure 9.6. Efficiency of Rhodamine 1,2,3 (10 ng) staining at 15, 30, and 45 mins. Quadrants Q1, Rho123+PI- cells; Q2, Rho123+PI+ cells; Q3, Rho123-PI- cells; Q4, Rho123-PI+ cells. Treatments Ctr, Control; Rhodamine-1,2,3, Rho123.

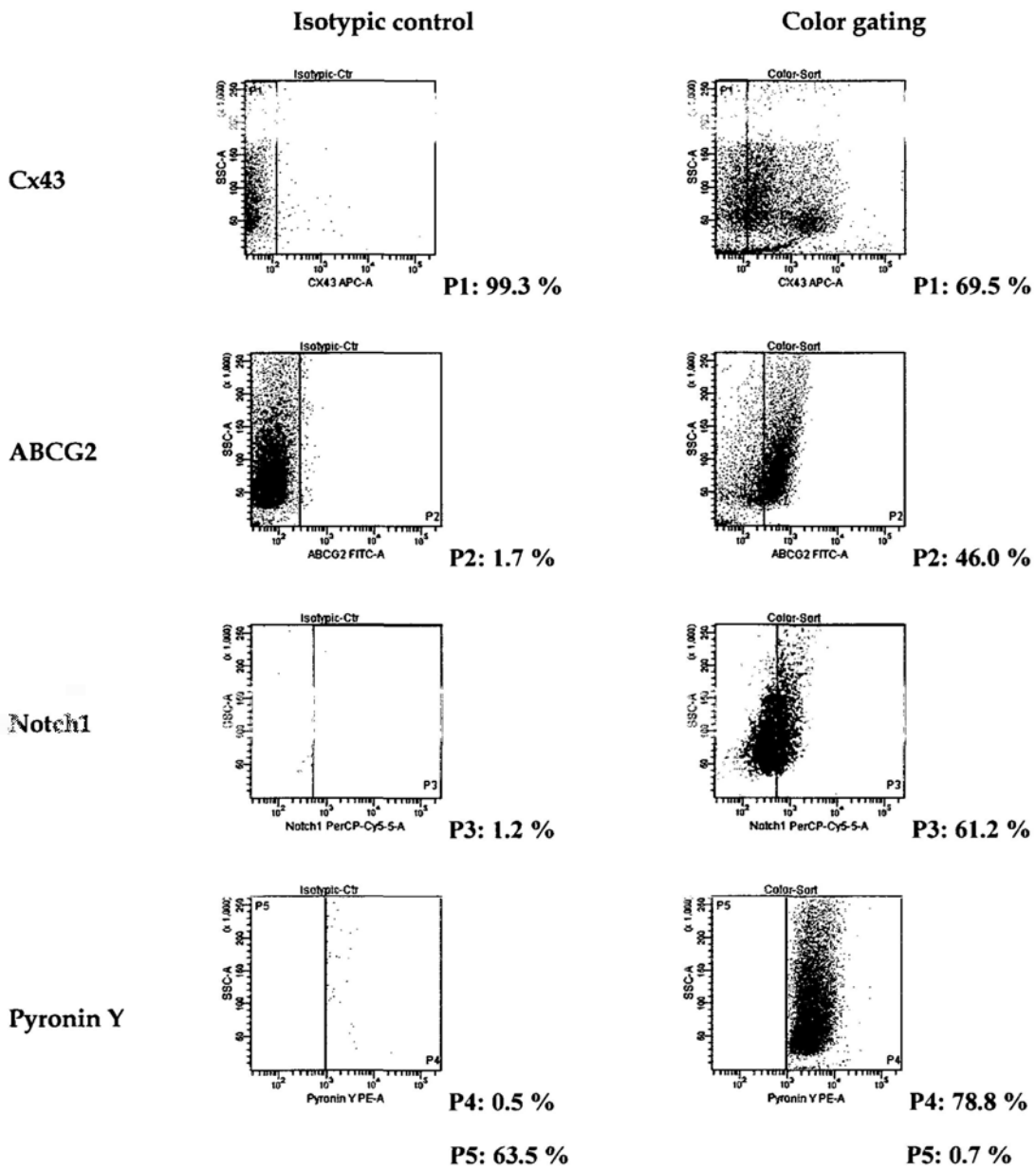

Figure 9.7. The four parameter gating for isolating corneal epithelial progenitor cells from mouse. P1, gate for all cells negatively expressing connexin 43; P2, gate for all P1 cells that positively expressing ABCG2; P3, gate for all P2 cells that positively expressing Notch1; P4, gate for all P3 cells that positively expressing pyronin Y; P5, gate for all P3 cells that negatively expressing pyronin Y.

(A)

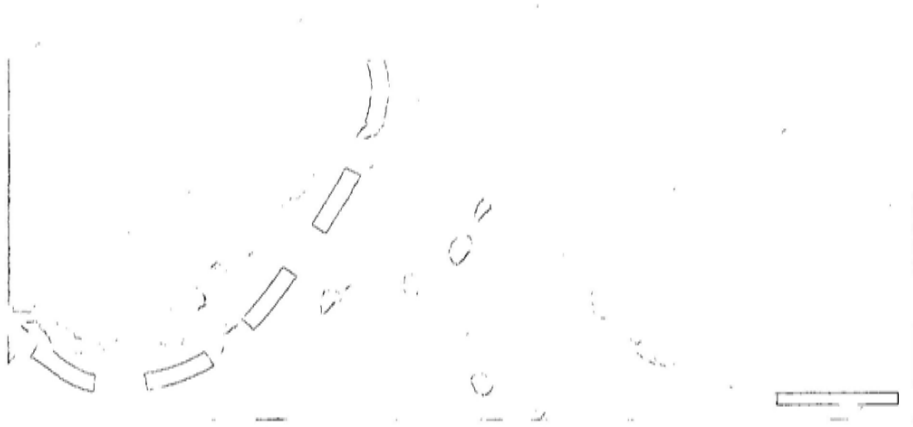

(B)

Figure 9.8. Diagrams showing the human (A) basal limbus and (B) basal corneal regions excised by the laser pressure catapult system. Bar, 25 μm.

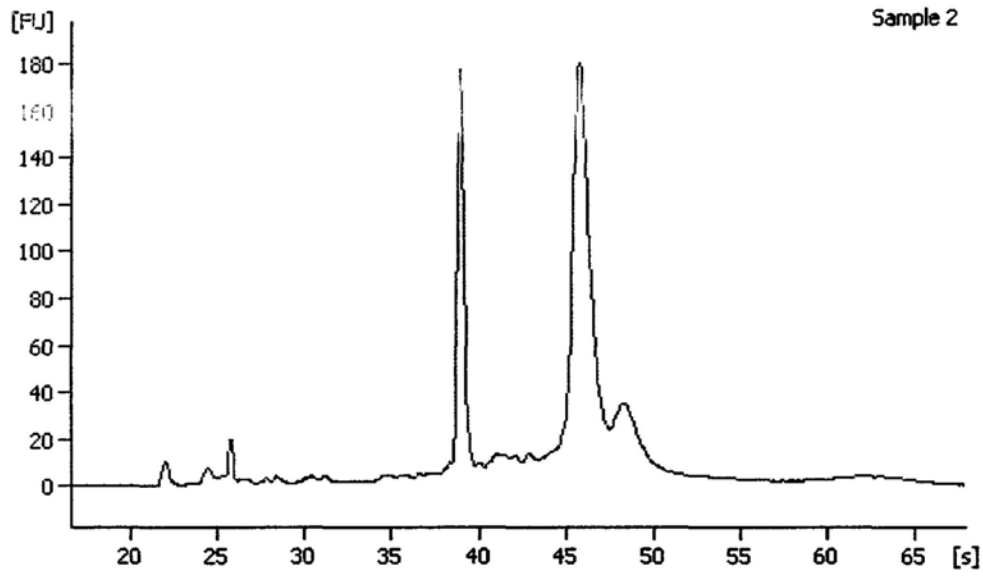

Figure 9.9. Chromatogram showing the RNA integrity of our human cornea rim sample. The ribosomal RNA 18S and 28S peaks are located at around 39 and 46 seconds on the x-axis, respectively. FU: florescence unit, s: time in second.

10

Identification of microRNAs in the limbus

10.1. Housekeeping microRNAs are present in limbus

To identify limbal specific microRNAs, we first evaluated whether microRNAs were actually present in the limbus and cornea regions. We assessed the level of several housekeeping microRNAs, including hsa-let-7a, hsa-miR-16, and hsa-miR-26b (Davoren et al., 2008) using real time polymerase chain reaction (qPCR). As shown in Figure 10.1, 10.2, and 10.3, which respectively represents the qPCR results of hsa-let-7a, hsa-miR-16, and hsa-miR-26b, the housekeeping microRNAs expressed as early as the threshold cycle (CT) 21, indicating the presence of microRNAs in the human cornea rim.

10.2. Selected embryonic stem cells specific microRNAs are not present in limbus

We next evaluated whether limbus contains any ES cell specific microRNAs. We selected several ES cell specific microRNAs for our study (Houbaviy et al., 2003; Suh et al., 2004), namely, hsa-miR-302a (Card et al., 2008), hsa-miR-302d (Li et al., 2009b; Tsai et al., 2009), hsa-miR-320, hsa-miR-338, hsa-miR-371 (Wilson et al., 2009),

hsa-miR-372, hsa-miR-373 and hsa-miR-373# (Qi et al., 2009). However, we could detect neither their expression in the limbus nor cornea region (Table 10.1). Together with the immunostaining results, CEPC may not possess phenotypes that pertain to embryonic stem cells.

10.3. Ocular specific microRNAs are not differentially expressed in limbus

Human cornea rim is part of the ocular tissues. We further assessed whether ocular specific microRNAs were expressed in our limbus and cornea specimens. We selected three microRNAs, including miR-182, miR-184, and miR-204 whose expression in eyes have been reported in different mammalian systems. In mouse embryos, miR-204 and miR-184 could express in the retina (Deo et al., 2006; Karali et al., 2007) and corneal epithelium, respectively (Karali et al., 2007). In adult mouse, it has been demonstrated that miR-182 expressed in the retina (Jin et al., 2009; Ryan et al., 2006), miR-184 in the basal and the immediately suprabasal cells of corneal epithelium, and miR-204 in lens epithelial cells (Ryan et al., 2006). In a human system using cultured epidermal keratinocytes, high expression of miR-184 was identified (Yu et al., 2008). Although these microRNAs have been reported in both murine and human system, and in both embryonic and adult tissues, their expression and specificity in the limbal region is yet unknown. Here we showed that the expression of miR-182 was higher in limbus when compared to cornea, though no statistical significance could be obtained ($p = 0.3865$) (Figure 10.4). Conversely, we detected no observable and statistical difference in the expression of miR-204 between cornea and limbus tissues ($p > 0.05$)

(Figure 10.5). For the expression of miR-184, we observed an observable difference in cornea when compared to the limbus, but such difference was not statistically significant ($p > 0.05$) (Figure 10.6). In summary, the currently known ocular specific microRNAs did not differentially express in limbus of the human cornea.

10.4. Identification of novel microRNAs differentially expressed in limbus

Based on the mentioned results, we postulated that limbus residing the CEPC might contain a novel and distinct set of microRNAs. We performed microRNA microarray to identify the possible microRNA candidates in the limbus region. By analyzing four sets of microRNA microarray experiments and by plotting a volcano plot that arrange genes along dimensions of biological and statistical significance (Figure 10.7), we found that eleven microRNAs (hsa-miR-136, hsa-miR-373*, hsa-miR-150, hsa-miR-143, hsa-miR-455, hsa-miR-145, hsa-miR-381, hsa-miR-224, hsa-miR-338, hsa-miR-154, hsa-miR-377) were downregulated by more than 2 folds in the cornea when compared to limbus, while two microRNAs (hsa-miR-122a and hsa-miR-425-3p) were upregulated by more than 2 folds when comparing cornea to limbus likewise.

The functions of these microRNAs have been individually reviewed. miR-136 is known to involve in early erythroid commitment (Choong et al., 2007) and is highly expressed in parthenotes (Cui et al., 2009). These two reports have suggested a possible role of miR-136 in stem cells and have been supported recently by Liu et al, whom successfully associate miR-136 to embryonic stem cell regulation (Liu et al.,

2009a). miR-373* is cancer specific because it is downregulated in childhood B-cell precursor acute lymphoblastic leukemia (Ju et al., 2009) but highly expressed in retinoblastoma (Zhao et al., 2009). miR-338 is essentially another cancer specific microRNA. Reports have suggested that it is downregulated in hepatocellular carcinoma (Huang et al., 2009), is upregulated in oral carcinogenesis in hamster model (Yu et al., 2009), is upregulated in squamous cell carcinoma (SCC) of the tongue (Wong et al., 2008), and is closely associated with relapse-free and overall survival among patients with gastric cancer (Xu et al., 2009b). Over-expression of miR-338 in the axon also markedly decreases cytochrome c oxidase IV expression, mitochondrial functional activity, and the uptake of neurotransmitter into the axon (Aschrafi et al., 2008; Kaplan et al., 2009). miR-150 has been studied in a variety of dieases. Reports have suggested that it is differentially expressed in sepsis, (Vasilescu et al., 2009) upregulated in hepatocellular carcinoma (Magrelli et al., 2009), downregulated in circulating leukocytes in an *in vivo* model of acute inflammation (Schmidt et al., 2009), downregulated in polycythemia vera (Bruchova et al., 2007; Bruchova et al., 2009), and is upregulated in B-cell chronic lymphocytic leukaemia/small lymphocytic lymphoma (Wang et al., 2008a). Its relation with stem cell can be exemplified by the observation that overexpression of miR-150 in hematopoietic stem cells could greatly impair mature B cell formation or function (Zhou et al., 2007). Besides, miR-150 has also been reported as a crucial partner for c-Myb for embryonic development (Lin et al., 2008). miR-455 and miR-381 have been known for their roles in cell maintenance. miR-455 has been shown to participate in cell development through its enhanced expression during brown adipocyte differentiation (Walden et al., 2009), while

miR-381 is essential for activity-dependent dendritic outgrowth of hippocampal neurons (Khudayberdiev et al., 2009). miR-224 has been reported in both cancers and stem cells. Studies have shown that increased expression of miR-224 could associate with colorectal cancer progression (Arndt et al., 2009), could be detected in highly invasive and metastaticpancreatic ductal adenocarcinomas (Mees et al., 2009), and could enhance the migration and invasion of HepG2 cells in an in vitro system (Li et al., 2009a). miR-224 could also express in prostate cancer by perineural cancer cells (Prueitt et al., 2008) and in benign and malignant hepatocellular tumors (Ladeiro et al., 2008). Besides, osteogenesis of the unrestricted somatic stem cells has also been correlated to miR-224 (Schaap-Oziemlak et al., 2009). miR-154 is similar to miR-224 by link up with tumors and stem cells. It is up-regulated in squamous cell carcinoma (SCC) of the tongue (Wong et al., 2008) and associated with karyotype in acute myeloid leukaemia (Dixon-McIver et al., 2008). Their stem cell relation can be demonstrated by its downregulation in fetal brains with prenatal ethanol exposure (Wang et al., 2009c), the participation in common myeloid/erythroid progenitor commitment (Choong et al., 2007) and upregulating in neonatal mouse and fetal human lung (Williams et al., 2007). Likewise, miR-377 is related to cell maintenance by being upregulated in lung tumors (Melkamu et al., 2009) and upregulated during growth arrest states (Maes et al., 2009). In addition, overexpression of miR-377 in diabetic nephropathy can indirectly lead to increased fibronectin protein production (Wang et al., 2008c). miR-143 and 145, on the other hand, are the only clustered microRNAs that we have identified in our microarray experiments. This clustered gene has been known for its specificity in cancers, especially they are down-regulated in

oral squamous cell carcinoma (Yu et al., 2009), human gastric cancers (Takagi et al., 2009), nasopharyngeal carcinoma (Chen et al., 2009a) and colorectal cancers (Motoyama et al., 2009; Wang et al., 2009a). They also involve in the regulation of smooth muscle cells by switching its quiescent versus proliferative phenotype (Cordes et al., 2009), modulate cytoskeletal dynamics and responsiveness of smooth muscle cells to injury (Xin et al., 2009), and reverse its differentiation phenotype that occurs during vascular disease (Elia et al., 2009). They partake in other cellular maintenance processes which include prolonging the cell survival of hematopoietic stem cell of the umbilical cord blood (UCB) cell lineages by being downregulated (Merkerova et al., 2009), and associating with endometriosis via its upregulation (Ohlsson Teague et al., 2009). On the contrary, miR-122a is one of the two microRNAs that are upregulated in the cornea tissue from our microarray results. Reports have shown that it is hepato-specific and is down-regulated in human hepatocellular carcinoma (HCC) by targeting the cyclin G1 mRNA (Gramantieri et al., 2007). However, there is no known report suggesting the functions of miR-425-3p, another cornea specific microRNA in our experiment; though its major form, miR-425, may guard brain differentiation (Gal et al., 2008).

Because the thirteen microRNAs generated from our microarray results have shown to engage in various cellular maintenance processes including those sustaining the homeostasis of stem cells, it is possible that all of them may actually participate in cornea epithelial progenitor cell regulation. Nevertheless, by investigating individual microarray data (Figure 10.10 to 10.16), we observed that hsa-miR-143 (Figure 10.8)

and hsa-miR-145 (Figure 10.9) were the most differentially expressed when compared limbus to cornea; numerically, there was more than 1000 fold changes in three of the four pairs of specimens. We therefore speculated that hsa-miR-143 and hsa-miR-145 are the most likely microRNA candidates for regulating CEPC. Further literatures supporting their biological roles were presented in Table 10.4 and 10.5.

miR-21 is a well studied microRNAs that has been known as cancer specific (Table 10.2) and can involve in a number of biological processes (Table 10.3). Recently, it has been reported as a stem cell specific microRNA (Singh et al., 2008a). From our results, it was differentially upregulated in limbus in three of the six pairs of sample; the numerical values of such differential expression were also more than two thousand fold in two of the samples (Figure 10.6). We have therefore included it in our study likewise.

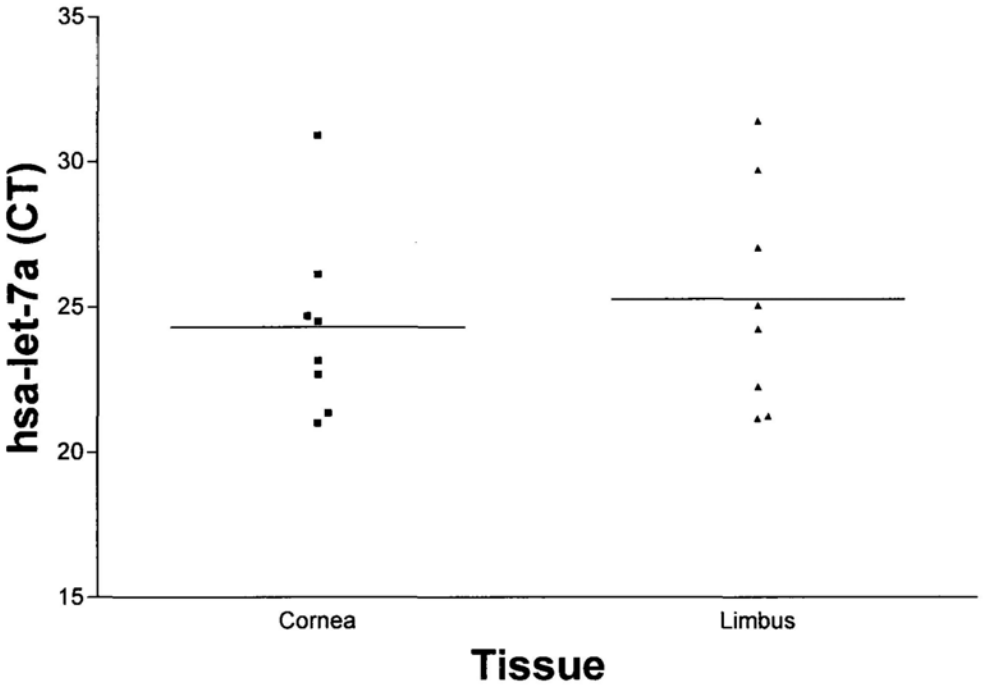

Figure 10.1. Expression of the housekeeping microRNA hsa-let-7a in cornea and limbal tissue, n = 8.

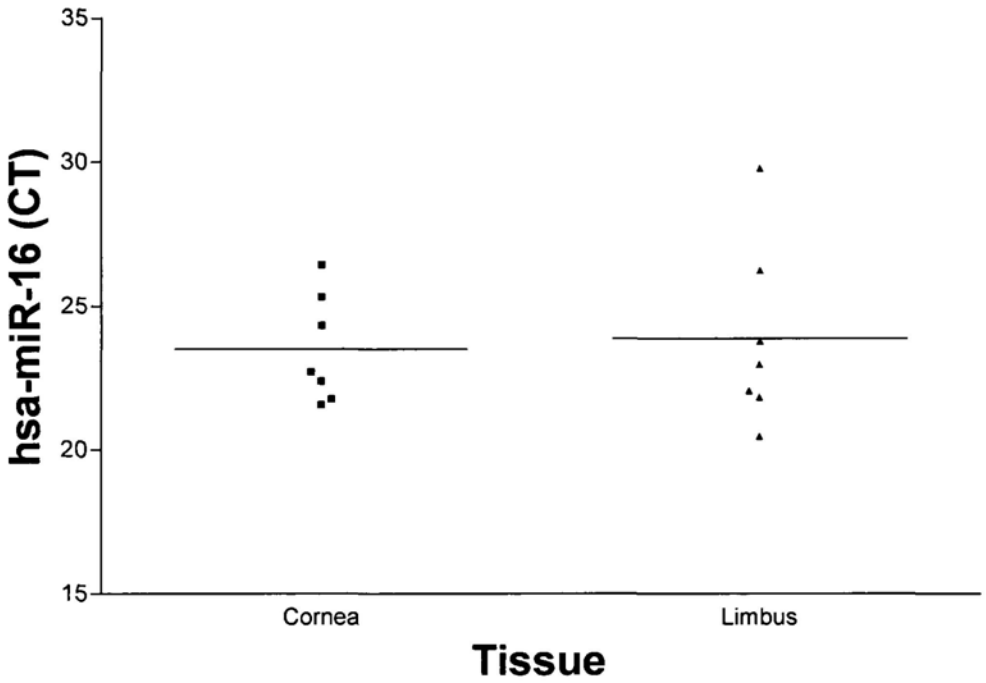

Figure 10.2. Expression of the housekeeping microRNA hsa-miR-16 in cornea and limbal tissue, n = 8.

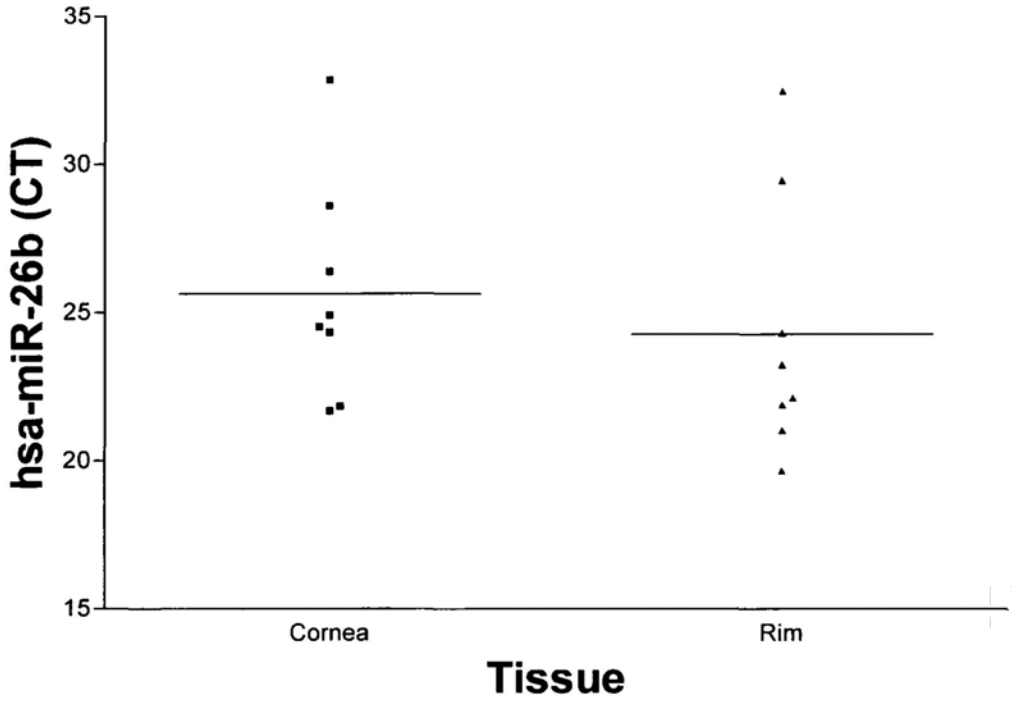

Figure 10.3. Expression of the housekeeping microRNA hsa-miR-26b in cornea and limbal tissue, n = 8.

Table 10.1. The expression of several ESc specific microRNAs were undetectable.

microRNA	Reference	Threshold cycle
hsa-miR-302a	(Suh et al., 2004)	Undetectable
hsa-miR-302d	(Suh et al., 2004)	Undetectable
hsa-miR-320	(Suh et al., 2004)	Undetectable
hsa-miR-338	(Suh et al., 2004)	Undetectable
hsa-miR-371	(Suh et al., 2004)	Undetectable
hsa-miR-372	(Suh et al., 2004)	Undetectable
hsa-miR-373	(Suh et al., 2004)	Undetectable
hsa-miR-373#	(Suh et al., 2004)	Undetectable

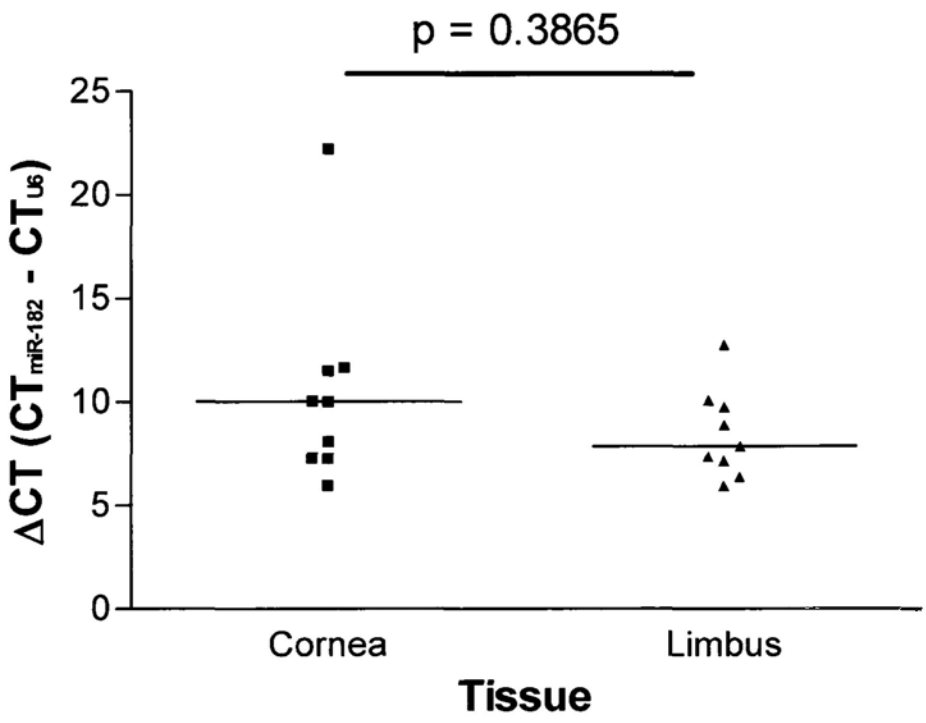

Figure 10.4. Real time PCR quantification of the ocular specific hsa-miR-182 in human cornea and limbal tissue. Mann Whitney U-test, $p < 0.05$ considered statistical significant.

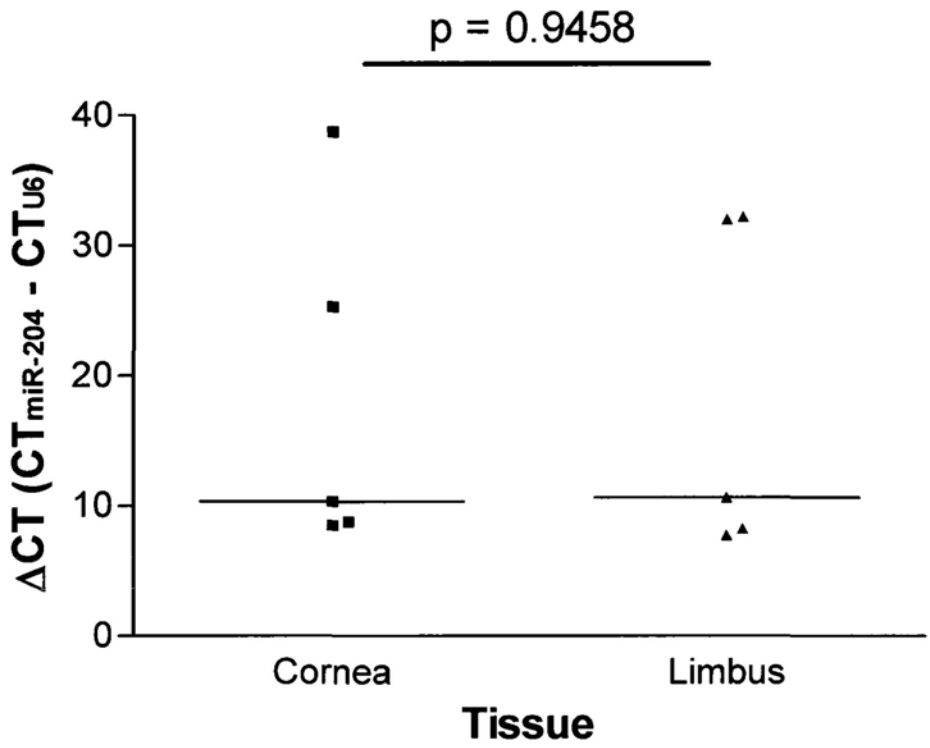

Figure 10.5. Real time PCR quantification of the ocular specific hsa-miR-204 in human cornea and limbal tissue. Mann Whitney U-test, $p < 0.05$ considered statistical significant.

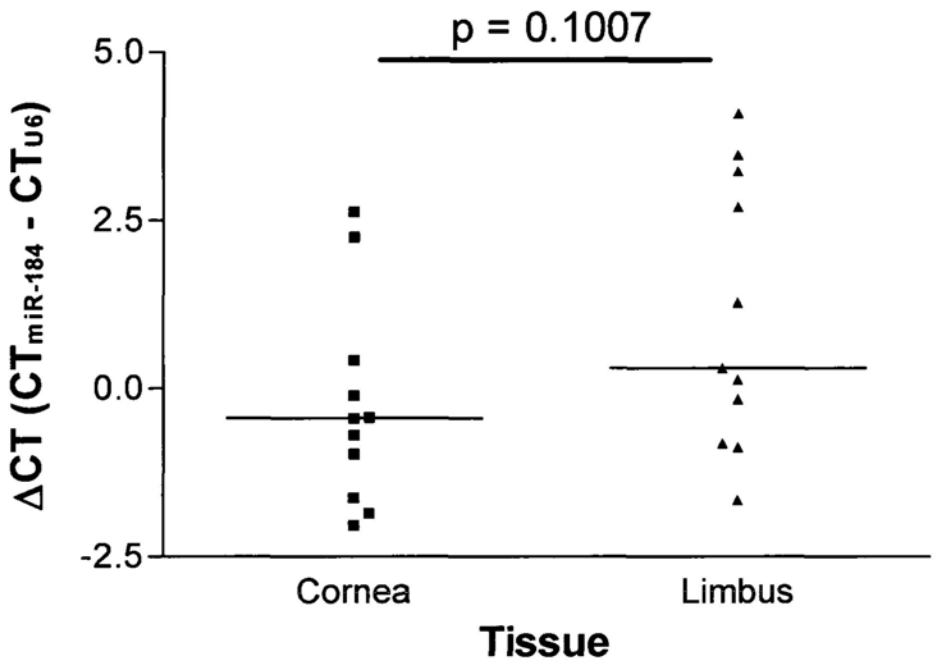

Figure 10.6. Real time PCR quantification of the ocular specific hsa-miR-184 in human cornea and limbal tissue. Mann Whitney U-test, $p < 0.05$ considered statistical significant.

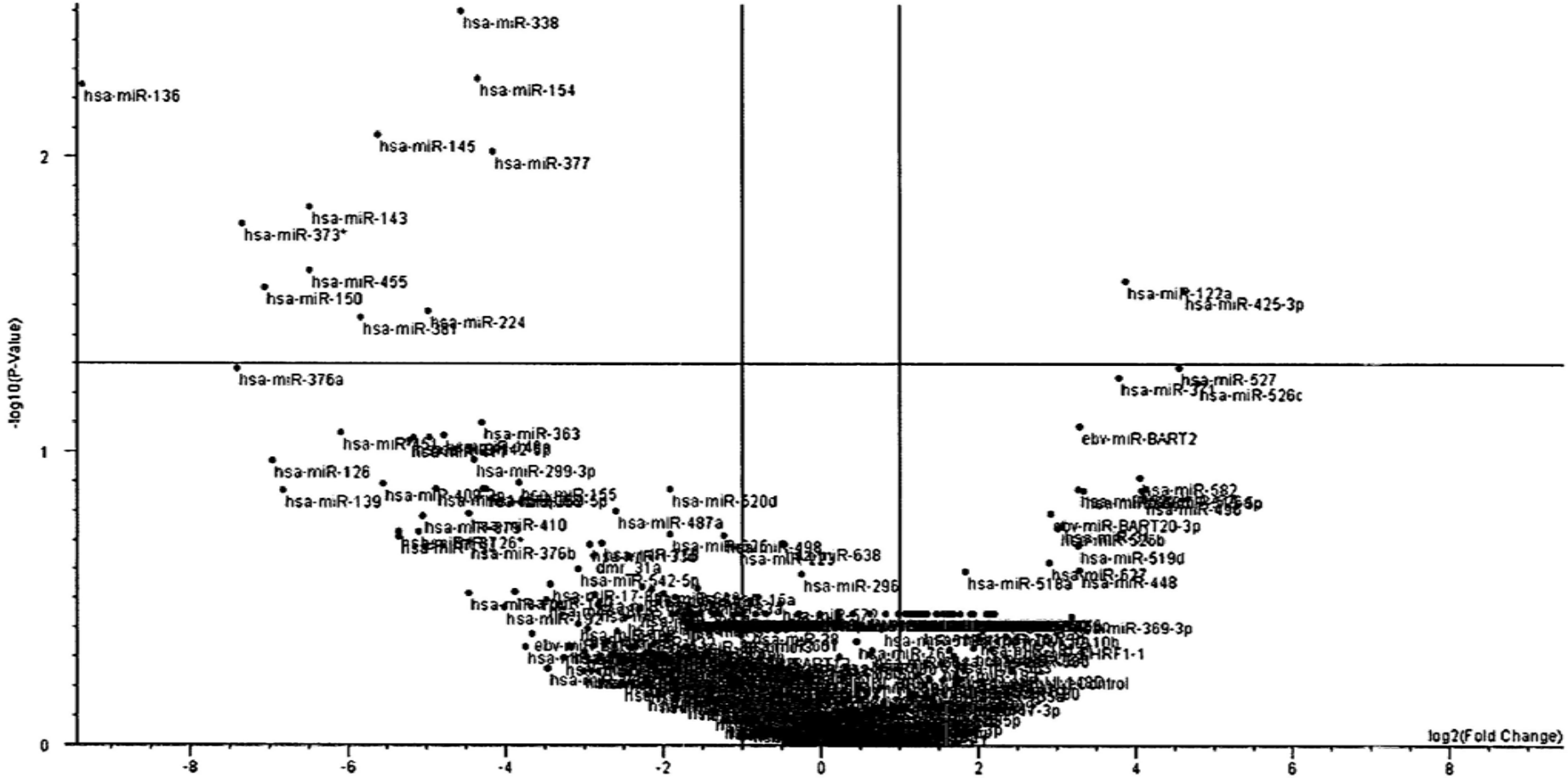

Figure 10.7. Volcano plot generated by comparing four pairs of corneal and limbal RNA.

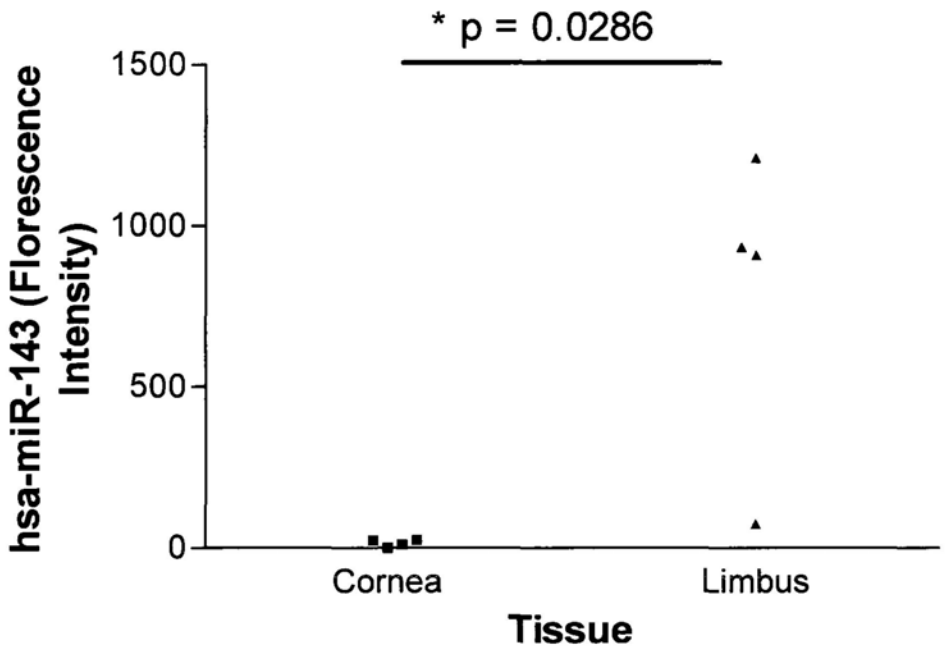

Figure 10.8. Scatter plot comparing the expression of hsa-miR-143 in four pairs of cornea and limbal RNA. * $p < 0.05$, Mann Whitney U Test.

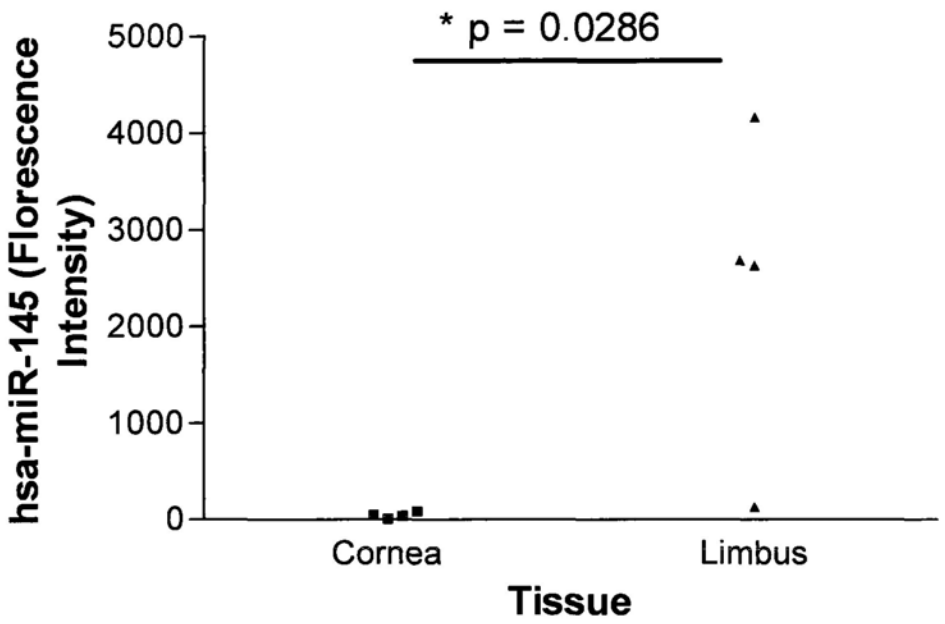

Figure 10.9. Scatter plot comparing the expression of hsa-miR-145 in four pairs of cornea and limbal RNA. * $p < 0.05$, Mann Whitney U Test.

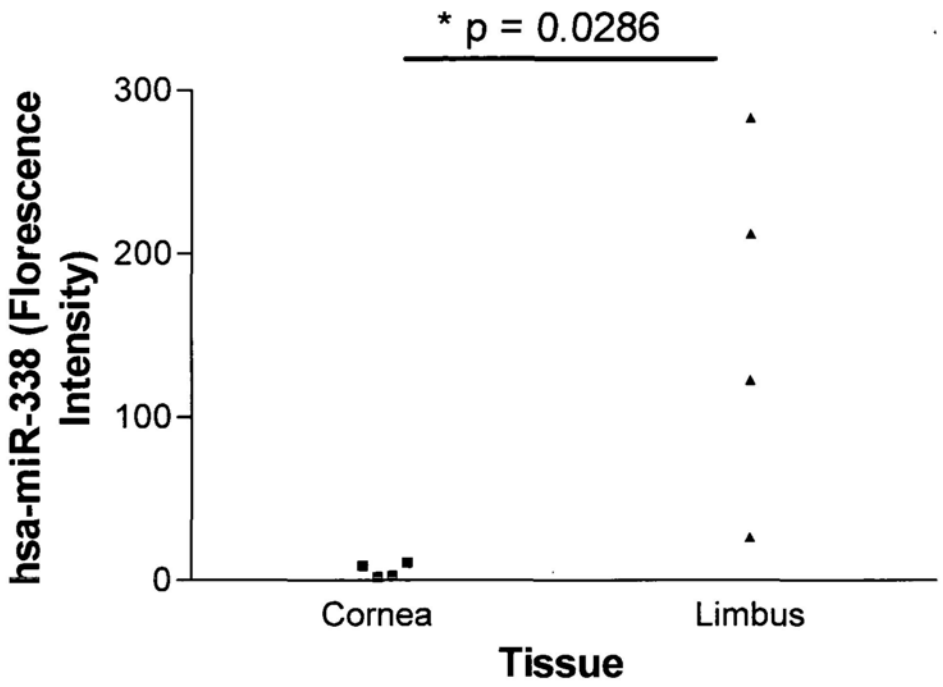

Figure 10.10. Scatter plot comparing the expression of hsa-miR-338 in four pairs of cornea and limbal RNA. * $p < 0.05$, Mann Whitney U Test.

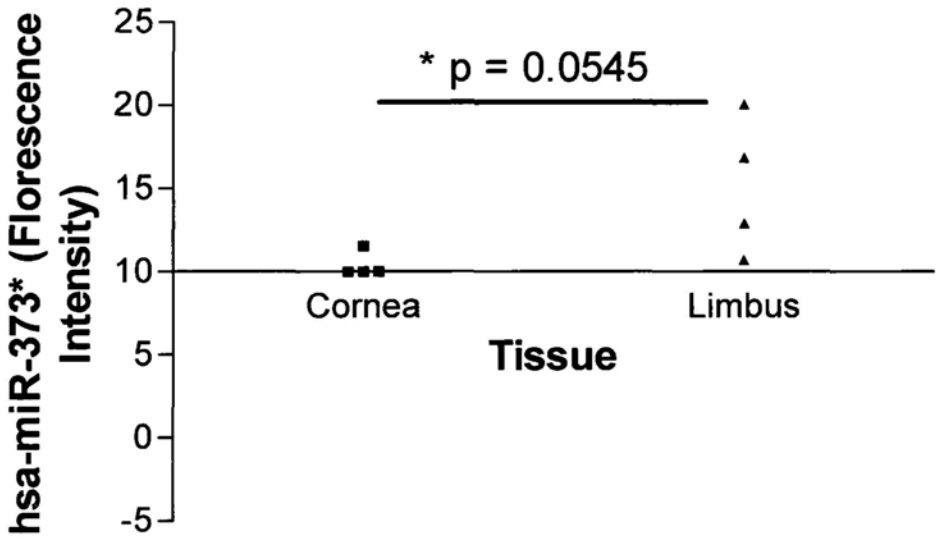

Figure 10.11. Scatter plot comparing the expression of hsa-miR-373* in four pairs of cornea and limbal RNA. * $p < 0.05$, Mann Whitney U Test.

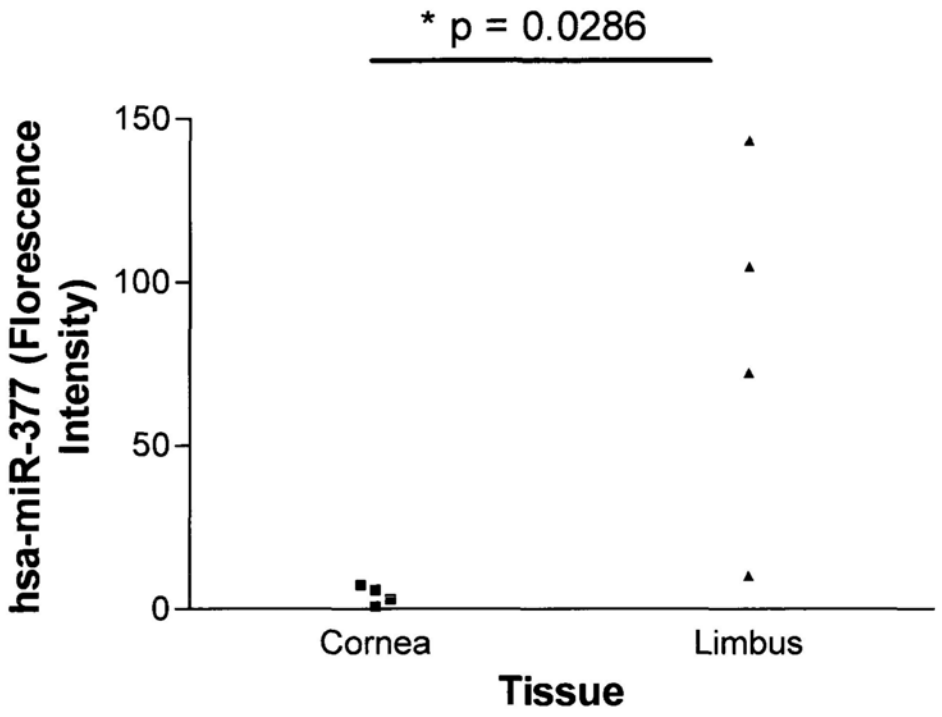

Figure 10.12. Scatter plot comparing the expression of hsa-miR-377 in four pairs of cornea and limbal RNA. * $p < 0.05$, Mann Whitney U Test.

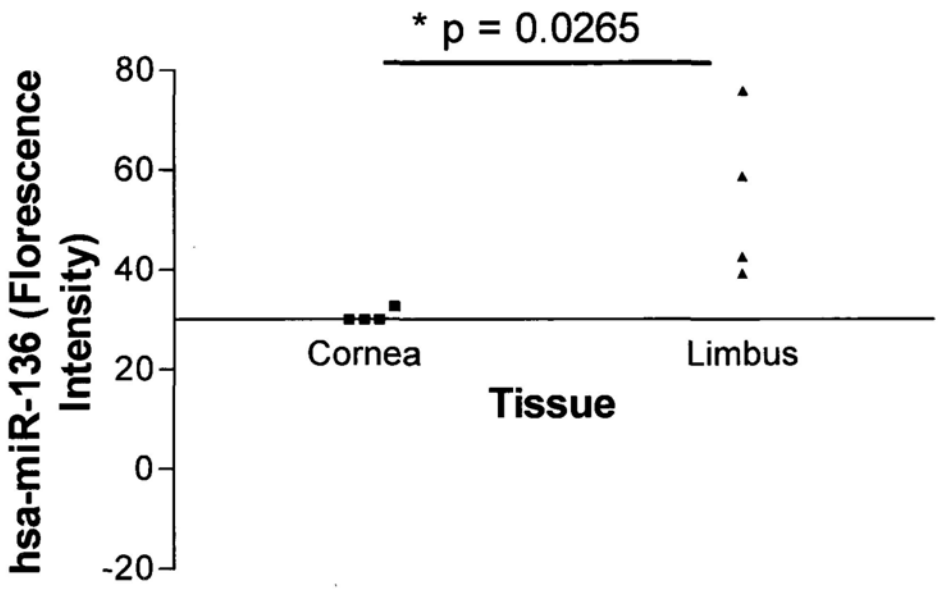

Figure10.13. Scatter plot comparing the expression of hsa-miR-136 in four pairs of cornea and limbal RNA. * $p < 0.05$, Mann Whitney U Test.

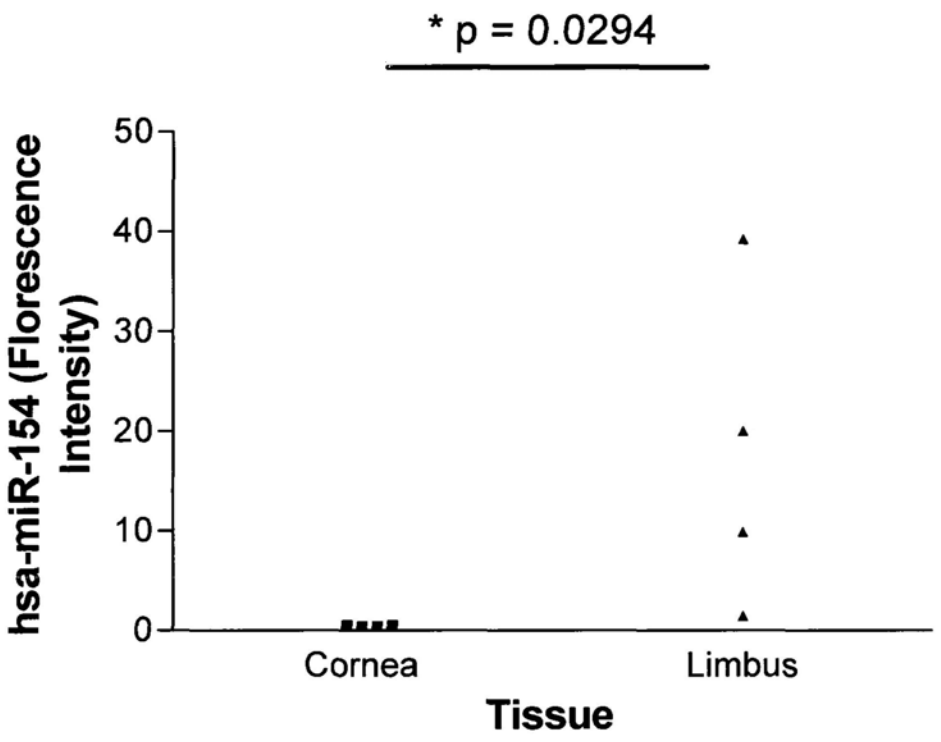

Figure 10.14. Scatter plot comparing the expression of hsa-miR-154 in four pairs of cornea and limbal RNA. * $p < 0.05$, Mann Whitney U Test.

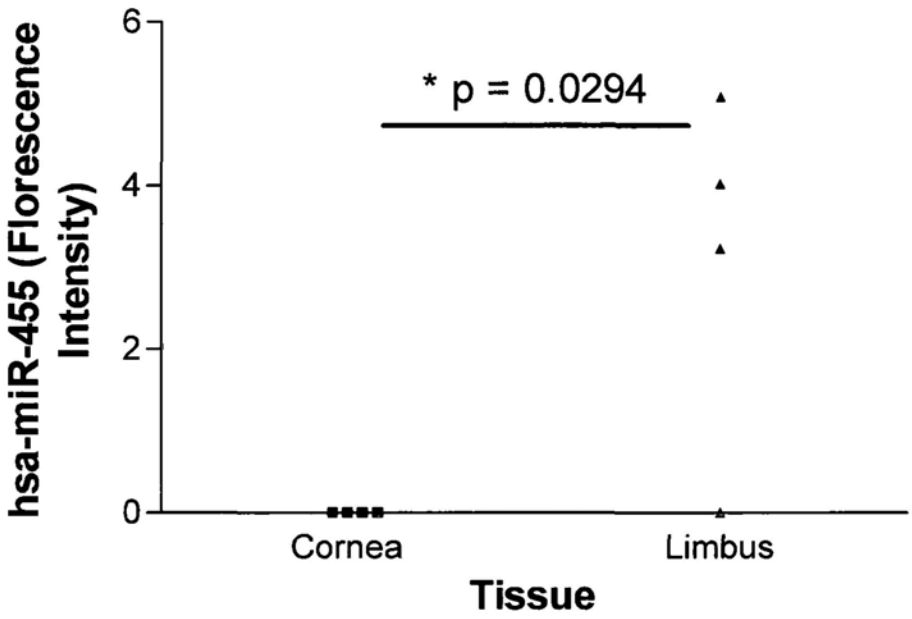

Figure 10.15. Scatter plot comparing the expression of hsa-miR-445 in four pairs of cornea and limbal RNA. * $p < 0.05$, Mann Whitney U Test.

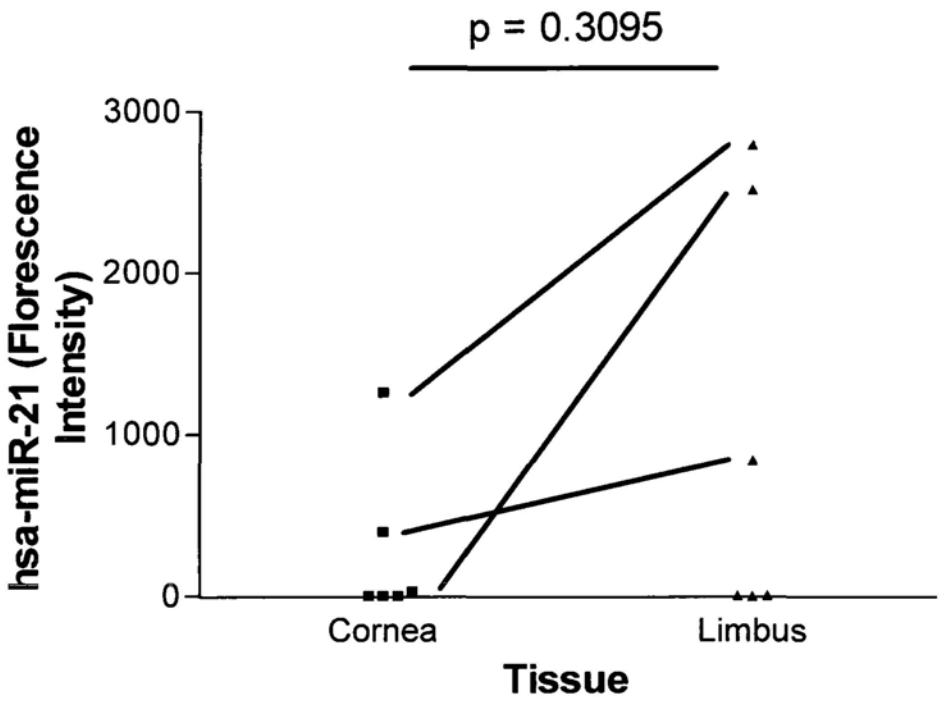

Figure 10.16. Scatter plot comparing the expression of hsa-miR-21 in six pairs of cornea and limbal RNA. * $p < 0.05$, Mann Whitney U Test.

Table 10.2. Functions of miR-21 in cancers from key references.

Cancer	miR-21 expression	miR-21 involvement in biological process	miR-21 targets	References
Glioma	Up-regulation in GBM tumors, primary cells and glioma cell lines	Invasion and cell growth	PDCD4, RECK, NFIB	(Chan et al., 2005; Ciafre et al., 2005; Gabriely et al., 2008)
Breast cancer	Up-regulation	Cell growth, apoptosis, Angiogenesis and invasion	PDCD4, TPM1, maspin	(Frankel et al., 2008; Iorio et al., 2005; Volinia et al., 2006; Zhu et al., 2007; Zhu et al., 2008)
Ovarian cancer	Up-regulation Down-regulation			(Iorio et al., 2007; Nam et al., 2008) (Dahiya et al., 2008)
Colorectal cancer	Up-regulation	Cellular outgrowth, migration, invasion and metastasis	PDCD4, NFIB, SPRY2, cdc25A	(Asangani et al., 2008; Fujita et al., 2008; Sayed et al., 2008; Slaby et al., 2007; Volinia et al., 2006; Wang et al., 2009a; Wang et al., 2009d)
Stomach/gastric cancer	Up-regulation		RECK	(Chan et al., 2008; Volinia et al., 2006; Zhang et al., 2008)
Hepatocellular carcinoma	Up-regulation	Cell migration and invasion and Cell proliferation		(Kutay et al., 2006; Meng et al., 2007)
Prostate cancer	Up-regulation			(Ribas et al., 2009; Volinia et al., 2006)
Pancreas cancer	Up-regulation			(Lee et al., 2007; Park et al., 2009a; Volinia et al., 2006)

Lung cancer	Up-regulation	(Markou et al., 2008; Volinia et al., 2006)
Head and neck cancer	Up-regulation	(Avissar et al., 2009; Tran et al., 2007)
Esophageal canceer	Up-regulation	(Feber et al., 2008; Mathe et al., 2009)
Thyroid carcinoma	Up-regulation	(Tetzlaff et al., 2007)
Cervical cancer	Up-regulation	(Lui et al., 2007)
Cholangiocarcinoma	Up-regulation	(Meng et al., 2006)
Leukemia	Up-regulation in CLL and AML patients	(Fulci et al., 2007; Jongen-Lavrencic et al., 2008)
B-cell and Hodgkin lymphoma	Up-regulation in patients and cell lines	(Lawrie et al., 2007; Navarro et al., 2008)

Table 10.3. Functions of miR-21 in various biological processes.

Biological process	miR-21 expression	miR-21 involvement	miR-21 targets	References
Adipogenesis	Upregulation	Adipogenic differentiation		(Kim et al., 2009)
Tumorigenesis	Upregulation	Anti-apoptotic, as oncogene		(Si et al., 2007)
Vascular neointimal lesion formation	Upregulation	Neointima formation after angioplasty	PTEN, Bcl-2	(Ji et al., 2007)
Cardiac hypertrophy	Upregulation Downregulation	Cardiac hypertrophy. Myocyte hypertrophy		(Cheng et al., 2007) (Tatsuguchi et al., 2007)
T cell differentiation	Upregulation	Regulate effector and memory T cells		(Wu et al., 2007)
Stem cell self-renewal	Downregulation	Repress self-renewal	REST	(Singh et al., 2008a)
Cellular outgrowth	Upregulation	Cell protrusion	Sprouty2	(Sayed et al., 2008)
Embryo implantation	Upregulation	Implantation		(Hu et al., 2008)

Table 10.4. Biological functions of miR-143.

Biological processes	miR-143 expression	miR-143 involvement	proposed targets	References
Colorectal tumorigenesis	Upregulation Downregulation		ERK5 KRAS	(Nakagawa et al., 2007) (Borralho et al., 2009; Chen et al., 2009b; Michael et al., 2003; Motoyama et al., 2009; Slaby et al., 2007; Wang et al., 2009a)
Gastric cancer	Downregulation			(Takagi et al., 2009)
Hepatocellular carcinogenesis	Upregulation		Fibronectin type III domain containing 3B (FNDC3B)	(Zhang et al., 2009)
Oral carcinogenesis	Downregulation	oral squamous cell carcinoma		(Yu et al., 2009)
B cell maligancies	Downregulation			(Akao et al., 2007)
Cervical tumorigenesis	Downregulation			(Lui et al., 2007; Wang et al., 2008d)
Polycythemia vera	Upregulation	regulate polycythemia vera mononuclear cells		(Bruchova et al., 2008)
Corticotrophic tumorigenesis	Downregulation			(Amaral et al., 2009)
Lung carcinogenesis	Downregulation			(Melkamu et al., 2009)
Rectal tumorigenesis	Downregulation			(Wang et al., 2009a)
Other tumorigenesis	Upregulation	Kaposi sarcoma		(O'Hara et al., 2009)

Nasopharyngeal carcinogenesis	Upregulation	nasopharyngeal carcinoma		(Chen et al., 2009a)
Prostate carcinogenesis	Downregulation		ERK5	(Clape et al., 2009)
Stem cell maintenance	Downregulation	prolonged survival of umbilical cord blood haematopoietic stem cell		(Merkerova et al., 2009)
	Upregulation	repress proliferation of smooth muscle cells		(Cordes et al., 2009)
Innate immunity	Upregulation			(Schmidt et al., 2009)
Apoptosis	Upregulation		ERK5	(Akao et al., 2009)
Adipocyte differentiation	Upregulation	differentiate adipocyte, elevated body weight and mesenteric fat weight	ERK5	(Esau et al., 2004; Takanabe et al., 2008; Xie et al., 2009)
Endometriosis	Upregulation			(Ohlsson Teague et al., 2009)
Development of Barrett's esophagus	Upregulation			(Dijckmeester et al., 2009)
Prolonged cell survival of umbilical cord blood				(Merkerova et al., 2009)

Table 10.5. Biological functions of miR-145.

Biological Processes	miR-145 expression	miR-145 involvement	proposed targets	Reference
Colorectal tumorigenesis	Upregulation			(Yantiss et al., 2009)
	Downregulation		KRAS	(Bandres et al., 2006; Borralho et al., 2009; Michael et al., 2003; Motoyama et al., 2009; Schepeler et al., 2008; Slaby et al., 2007; Wang et al., 2009a)
Breast tumorigenesis	Downregulation			(Iorio et al., 2005; Sempere et al., 2007)
Ovarian tumorigenesis	Downregulation			(Iorio et al., 2007; Nam et al., 2008)
Prostate tumorigenesis	Downregulation			(Ozen et al., 2008)
Hepatic tumorigenesis	Downregulation			(Varnholt et al., 2008)
Bone formation	Downregulation			(Palmieri et al., 2008)
Polycythemia vera	Upregulation	regulate polycythemia vera mononuclear cells		(Bruchova et al., 2008)
Cervical tumorigenesis	Downregulation			(Wang et al., 2008d)
ACTH-secreting pituitary tumorigenesis	Downregulation			(Amaral et al., 2009)
Endometriosis	Upregulation			(Ohlsson Teague et al., 2009)

Exposure to environmental risk factor	Upregulation			(Wang et al., 2009c)
p53 regulatory network				(Sachdeva et al., 2009)
Lung tumorigenesis	Downregulation			(Liu et al., 2009b)
Rectal cancer	Downregulation			(Wang et al., 2009a)
Nasopharyngeal carcinogenesis	Upregulation			(Chen et al., 2009a)
Bladder cancer	Downregulation			(Dyrskjot et al., 2009; Ichimi et al., 2009)
Stem cell maintenance			OCT3, SOX2, KLF4	(Xu et al., 2009a)
	Upregulation	repress proliferation of smooth muscle cells		(Cordes et al., 2009)
Prolonged cell survival of umbilical cord blood				(Merkerova et al., 2009)
Oral carcinogenesis	Downregulation	oral squamous cell carcinoma		(Yu et al., 2009)
Gastric cancer	Downregulation			(Takagi et al., 2009)
Controlling vascular neointimal lesion formation	Downregulation			(Cheng et al., 2009b)

11

Confirmation of candidate limbal microRNAs

11.1. Comparative Ct method is used in quantifying miRNA expression

To confirm the expression level of the three candidate microRNAs, we performed Taqman microRNA assay which utilized qPCR for validation. Figure 11.1 is a representative figure showing the cycle threshold of the housekeeping U6 and microRNA of interests. We adapted the comparative Ct method for calculating the expression level of microRNA, which is that Ct of U6 is subtracted by Ct of microRNA to obtain a ΔCt value. The ΔCt of a specific microRNA in the limbus and the cornea region is then plotted on a scatter plot. Because the lower the Ct value (also the normalized ΔCt), the stronger the expression, the scatter plots from Figure 11.2 to 11.5 and in the succeeding chapters will read like the lower the position of the dots, the higher the expression value. For Ct higher than 35, we regarded them as undetectable.

11.2. U6 is the most suitable housekeeping RNA

To select the most suitable housekeeping for our study, we compared different housekeeping microRNAs and small nucleolar RNA (snRNA) in eight different human

cornea rims. We found that U6, a non-coding snRNA, was the most stable amongst the eight pairs of specimens (Figure 11.2), numerically the Ct values were 19.91 ± 2.142 in the cornea tissue and 19.95 ± 2.133 in limbal region. The Ct values of hsa-let-7a, hsa-miR-16 and hsa-miR-26b, however, were 24.30 ± 1.12 and 25.26 ± 1.36, 23.50 ± 1.88 and 23.87 ± 3.17, and 25.65 ± 3.68 and 24.27 ± 4.43 in cornea and limbus tissues, respectively. We therefore favored U6 as our housekeeping RNA and will applied in all microRNA qPCR assays.

11.3. Confirming the expression level of candidate miRNAs

Expression levels of the candidate microRNAs in limbus and cornea were confirmed by qPCR. Results showed that the ΔCT of hsa-miR-143 is 5.89 ± 0.80 in the limbal epithelium and 11.09 ± 0.87 in the cornea epithelium ($p = 0.0006$, Mann Whitney U-test) (Figure 11.4), while that of hsa-miR-145 is 4.53 ± 0.72 and 10.19 ± 0.66 ($p = 0.0004$, Mann Whitney U-test) (Figure 11.5) in the limbal and cornea epithelium, respectively. Biologically these ΔCT values represented an upregulation of miR-143 and miR-145 in the limbus region by an average of more than 700 fold, confirming the microarray results that we have previously obtained. Although the expression of hsa-miR-21 was not statistically significant as shown from our microarray results, we could secure a significant difference in the ΔCT values of limbus (2.79 ± 0.35) and cornea (7.44 ± 1.55) ($p = 0.0028$, Mann Whitney U-test). This has a biological meaning that upregulation of miR-21 was observed in limbus when compared to the cornea.

11.4. Confirming the spatial distribution of candidate miRNAs

To localize the three candidate microRNAs, we performed *in situ* hybridization on the frozen cornea rim sections using locked nucleic acid (LNA)-modified oligonucleotide probes. Results showed that miR-21, 143 and 145 were distributed in the limbal region with gradation of expression level along the basal-suprabasal line. In particular, the expression of miR-21, when comparing to the other two candidate microRNAs, appeared relatively strong in both the cornea and limbus regions, which is inconcordance with the qPCR results (with low ΔCTs respectively of 6.09 ± 4.64 and 3.04 ± 1.04 in the cornea and limbal epithelium). On the contrary, the expression of miR-143 was fairly subtle in both the cornea and limbus, as respectively agreed by the median ΔCTs of 10.72 ± 2.87 and 7.05 ± 2.65. When comparing the expression of miR-145 to miR-21, the expression was equally potent but more specific in the limbal region (hsa-miR-145: ΔCTs of 4.28 ± 2.38 in limbus, hsa-miR-21: ΔCTs of 3.04 ± 1.04 in limbus). This suggests that miR-145 may be a more faithful microRNA in stem cell regulation when comparing to miR-21 and 143. Indeed reports have suggested that miR-21 participates in a wide range of cancers and biological activities, and is therefore a more general microRNA in cellular processes (See the review in Table 10.2 to 10.3). Although miR-143 and miR-145 is in the same cluster and often co-expresses in colorectal cancer, their pathway does not overlap (Arndt et al., 2009). This indicates the different functions of miR-143 and miR-145 even though they are co-express in a single tissue and even single cell. Because our results showed that the expression of miR-145 is far more specific and potent than miR-143 in the limbal basal and

suprabasal regions, miR-145 may be the chief CEPC regulator of the miR-143/145 cluster. To further elucidate the role of the microRNA candidates especially miR-145 in cornea epithelial cells, we performed the functional studies in Chapter 12.

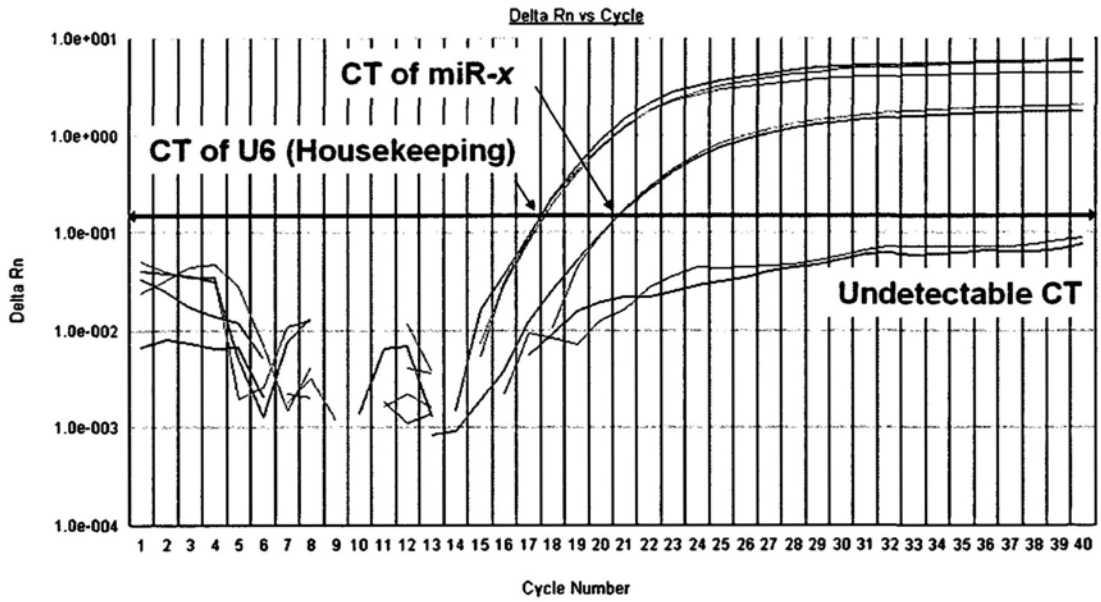

Figure 11.1. Representative real time PCR results showing the expression level of the housekeeping RNA, U6 and candidate microRNA, miR-x. CT, cycle threshold.

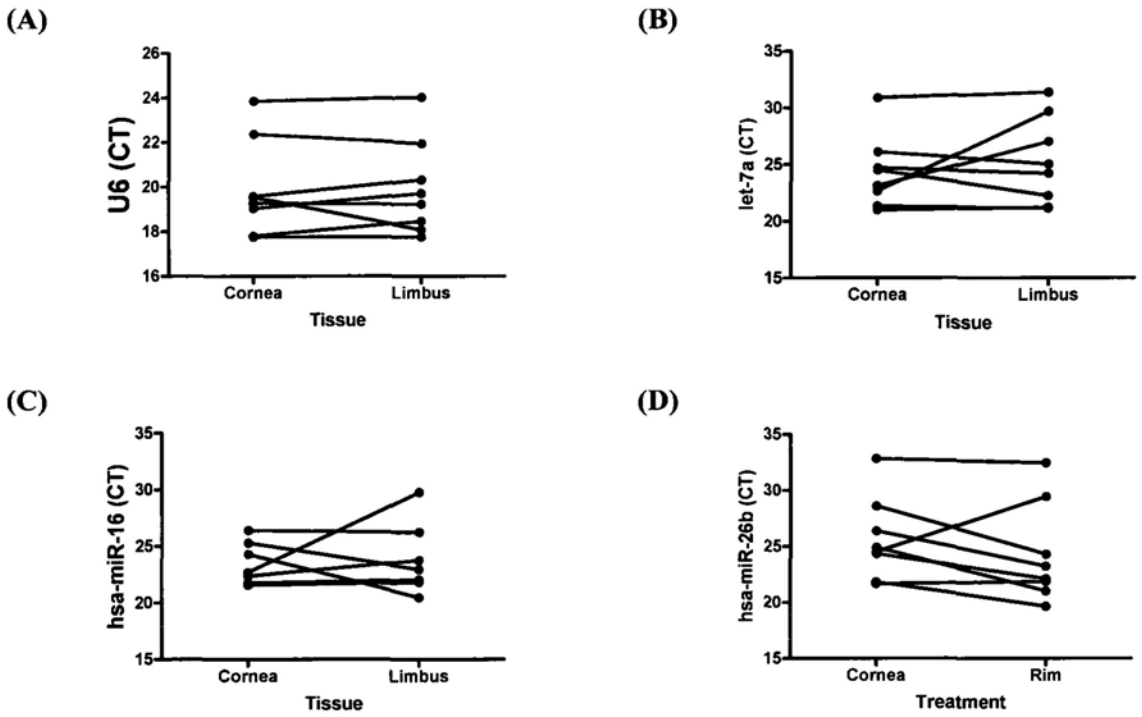

Figure 11.2. Expression level of reported housekeeping (A) small nuclear RNA and (B-D) microRNAs in cornea and limbus. CT, cycle threshold.

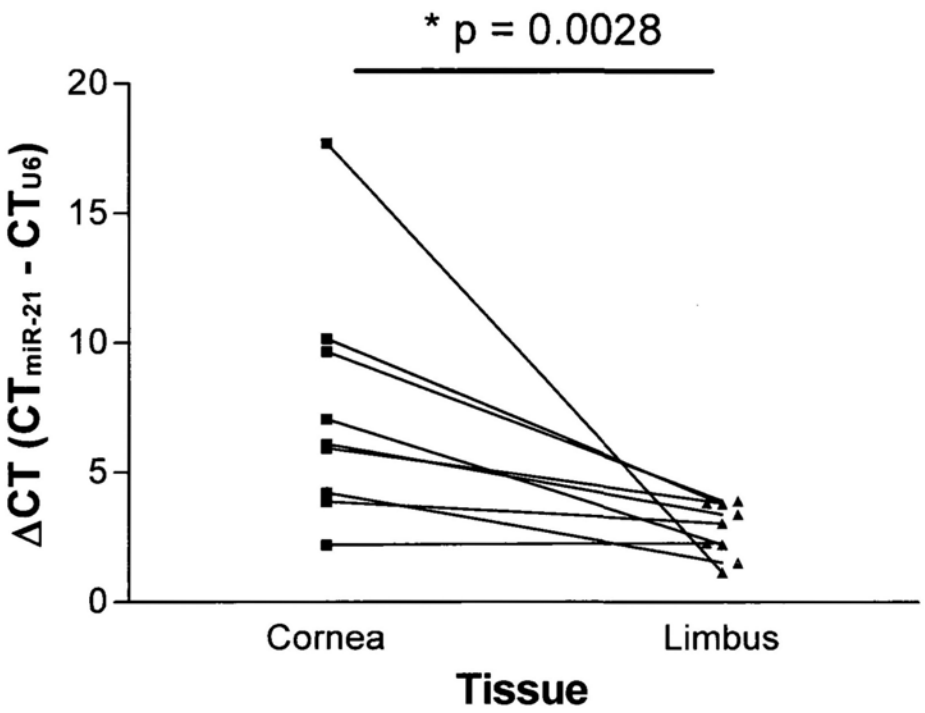

Figure 11.3. Expression level of hsa-miR-21 in the cornea and limbus region, illustrated by ΔCT. * $p < 0.05$, Mann Whitney U test.

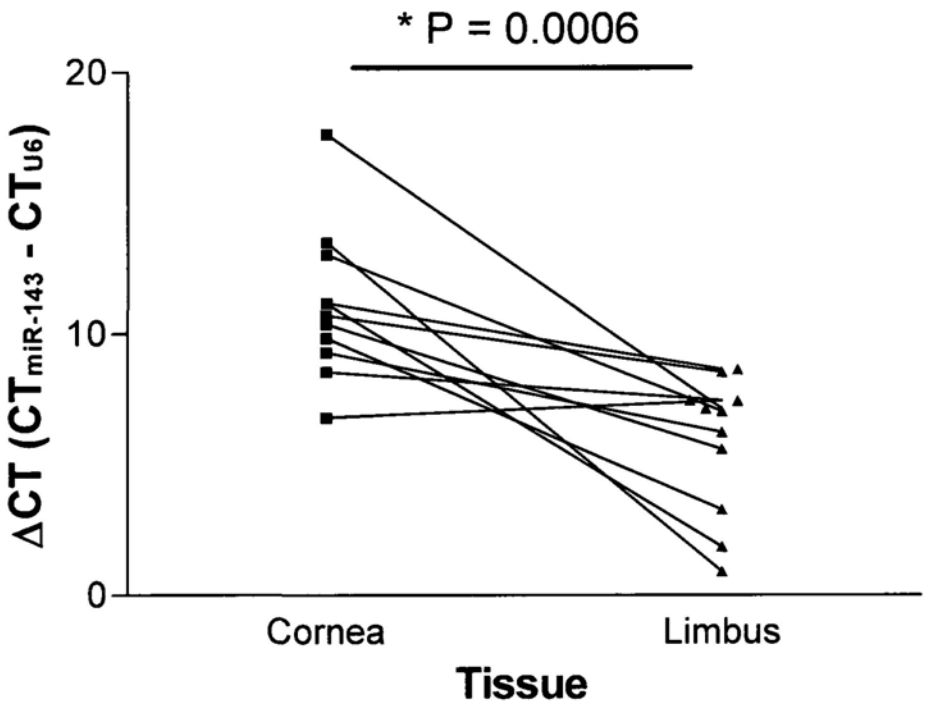

Figure 11.4. Expression level of hsa-miR-143 in the cornea and limbus region illustrated by ΔCT. * $p < 0.05$, Mann Whitney U test.

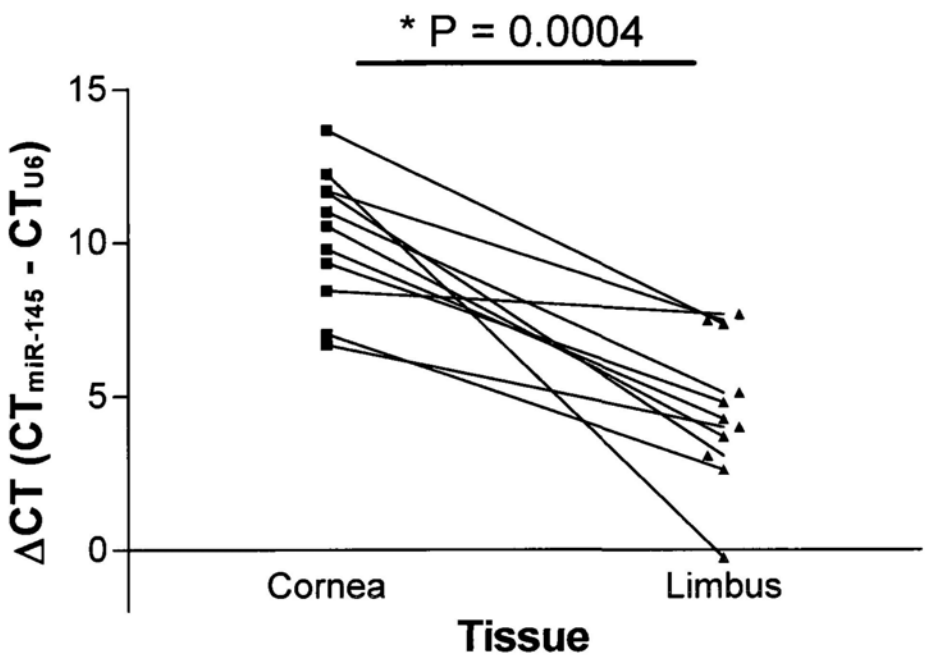

Figure 11.5. Expression level of hsa-miR-145 in the cornea and limbus region illustrated by ΔCT. * $p < 0.05$, Mann Whitney U test.

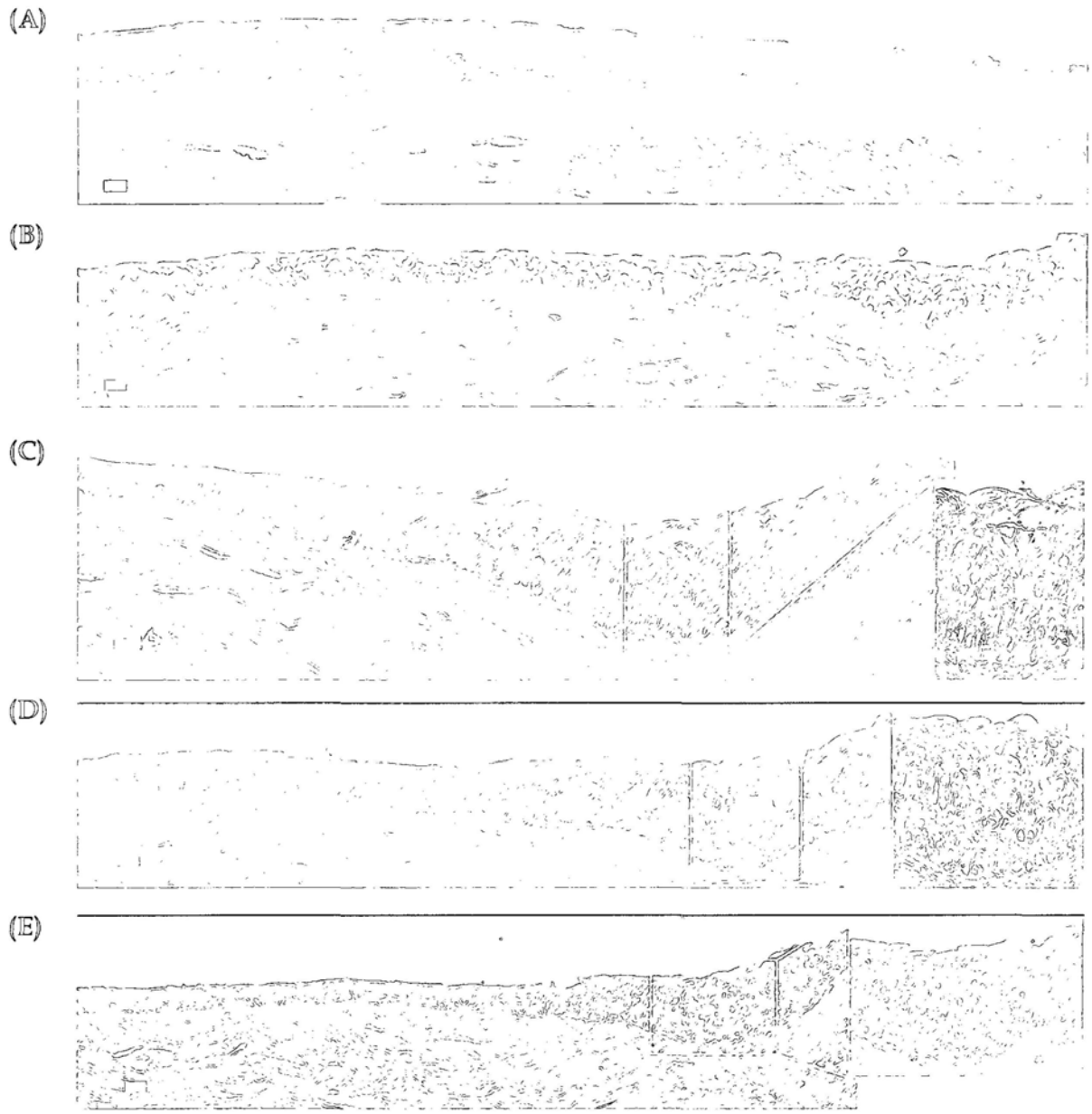

Figure 11.6. Spatial expression of miR-21, 143 and 145 in cornea rim sections. Representative in situ hybridisation results showing the cross section of cornea rim that has been incubated with (A) scrambled LNA, (B) U6 LNA, (C) hsa-miR-145 LNA, (D) hsa-miR-143 LNA and (E) hsa-miR-21 LNA. Bar in A-D, 50 μm, E, 100 μm.

12

Functional analyses of candidate microRNAs in human corneal epithelial cells

In this chapter, we performed bioinformatic and literature search and overexpression experiments to better understand the functions of the candidate microRNAs.

12.1. From bioinformatics search

It has been known that the mature sequences of miR-21 (Table 12.1), 143 (Table 12.2) and 145 (Table 12.3) are perfectly conserved across mammals, as many other miRNAs are, and are encoded by single (as in miR-21) to several genes (as in miR-143 and 145). The human miR-21 gene is relatively well characterised and has been mapped to chromosome 17q23.2 (Table 12.4), where it overlaps with the protein-coding gene VMP1 (or TMEM49), a human homologue of rat vacuole membrane protein (Cai et al., 2004; Fujita et al., 2008). The human miR-143 and miR-145 genes are clustered together within the same chromosomal region 5q31-33 (Table 12.4) and are therefore originated from the same transcriptional unit (Akao et al., 2007; Johannsdottir et al., 2006). It is therefore not surprising for us to observe simultaneous expression of miR-143 and 145 at the limbus region. The precursor hair-pin sequences of these

candidate microRNAs are presented in Figure 12.1.

12.2. From literature search

It has been proposed that microRNAs are ubiquitous in function. Table 10.2 to 10.5 presents the broad biological functions of miR-21, 143 and 145. Noticeably, most functions of miR-143 and 145 are overlapped because they exist in cluster, which is in concordance with our current finding that limbus also co-expresses both miR-143 and 145. Because most of the known functions of miR-21, 143 and 145 involve tumorigenesis, we speculated that these microRNAs may too affect cell proliferation in the limbus region for maintaining homeostasis of CEPC. We therefore performed the below overexpression study for the better elucidation of our candidates.

12.3. From over-expression experiments of miR-21, 143 and 145 in human corneal epithelial cells

Because of the scarcity of human cornea rim tissues, we utilized human corneal epithelial cell transformed by Adeno-12/SV-40 viral sequences, abbreviated below as HCE, for our study. Figure 12.2 presents the typical morphology of HCE in culture, which resembled cobblestone appearance and was cohesively organized in small colonies as described by Liu et al (Liu et al., 2007). The expression levels of miR-143 and 145 were undetectable, while that of miR-21 remains low when comparing to the housekeeping U6 expression (Figure 12.3).

We attempted to over-express precursor microRNAs (Pre-miRs) in HCE cells, with the rationale that they are small and so are easily transfectable. As assessed by qPCR, the transfection efficiency of pre-miR-21, 143 and 145 were respectively around 50, 1000 and 1000 folds (Figure 12.3).

By establishing the transfection method, we next evaluated the *in vitro* effects of the over-expressed candidates in cell proliferation and morphology. As shown in Figure 12.4, miR-145 suppressed cell proliferation of HCE, while scramble control, miR-21 and miR-143 did not show inhibitory effects on cell growth. By culturing transfected cells for seven days (Figure 12.5), colonies resembling those of holoclones were formed in cells transfected with pre-miR-145. The number of pre-miR-145 treated cells, as counted by Trypan blue exclusion assay, was found to be 50 % less when comparing to the control. Whether miR-145 transforms the differentiated human corneal epithelial cells to become more quiescent requires further elucidation.

To fully confirm the functions of miR-145, we carried out microarray to evaluate the gene and transcript expression of miR-21, miR-143 or miR-145 overexpressed HCE cells. We performed two independent sets of microarray experiments in which the results were summarized by principle component analyses (PCA) using transfection experiment as the variables (Figure 12.5, 12.6). PCA on either one of the two set microarray displayed a dispersed expression of scrambled pre-miR, pre-miR- 21, 143 and 145 transfected cells (Figure 12.5); while PCA on both microarray experiments

indicated a more segregated expression among the four treatments in experiment 2 (Abbreviated as Expt-2 in Figure 12.6). We therefore selected experiment 2 for further analysis. By performing cluster analysis to demonstrate how the gene and transcript expression pattern relates between the four treatments in experiment 2, we found that pre-miR- 143 and 145 transfected cells looked more alike to each other but more differed to scrambled pre-miR and pre-miR-21 treated cells (Figure 12.7). This is in concordance with the proposal that miR-143 and 145 exist in cluster with overlapping functions and downstream genes. By associating the expression pattern of the pre-miR- 21, 143, 145 treatments to the scramble control, we obtained a list of differentially expressed genes, or entities to be more specific. Numerically, among the total 41,078 entities of the microarray, we distinguished a total of 7,089 entities with fold change more than 2. When individually comparing the pre-miR-21 treatment with the scrambled pre-miR, there was 1,508 entities bearing 2 or more fold change, while the pre-miR-143 and pre-miR-145 treated cells respectively generated 1,721 and 3,860 entities with 2 or more fold change when associating with the scrambled. These numbers implicated that miR-145 possessed the strongest alteration to the gene expression profile of HCE cells when comparing to the other two microRNA candidates. This agreed with our cellular experiments in which miR-145 appeared critical in silencing cell proliferation in the human corneal epithelial cells but not miR-21 and miR-143.

Next, we manually correlated these differentially expressed entities with the predicted targets of the corresponding microRNA by searchng miRBase, the largest miRNA

prediction database to date. We distinguished from each of the pre-miR-21-scrambled, pre-miR-143-scramble, and pre-miR-145-scramble comparison, there was approximately 100 entities that were the prediction targets of the corresponding microRNA (Table 12.5, 12.6, 12.7). Among the list, we attempted to validate several which we regarded as highly possible targets by using qPCR, as highlighted in purple in Table 12.5, 12.6 and 12.7. For the prediction targets of miR-21, we selected FASLG, FGF14, PSCA, SOX2, CFH, CFHR1, NFIB and PITX2; for prediction targets of miR-143, we picked KRT2, SOHLH2, MAPK7; for prediction targets of miR-145, we chose IGF1R, PSCA, WNT7A, NFIB, IFNB1, and RARA for validation. Besides, we have also included several other genes which was not differentially expressed in the two microarray results, including, two canonical stem cell markers OCT4 and KLF4, two cancer stem cell markers MDM2 and MYC, and TGFBI, which involves in corneal dystrophy and corneal development and so is cornea specific. However, among all these genes, only the upregulation of IFNB1 could be verified (a median of 1093 folds in pre-miR-145 treated cells when compared to the control, $p < 0.05$) (Figure 10.9). For the other genes, we either could not obtain detectable expression in all the four treatments (we regard $CT > 35$ as undetectable) or could not discern statistical difference between the pre-miR-treated groups and the scrambled control ($p > 0.05$). qPCR results of KLF4, WNT7A, MDM2, TGFBI, and IGF1R were presented in Figure 12.10, 12.11, 12.12, 12.13, and 12.14, respectively; while qPCR results of the remaining prioritiesed genes were not shown because their expressions were either undetectable or could not discern observable expression difference among all the treatment groups.

IFNB1 is therefore of special interest to us. We discovered a statistically significant upregulation of IFNB1 in the presence of high endogenous miR-145, but not miR-21 or 143, we here speculated a highly possible relation between IFNB1 and miR-145, which has not been reported elsewhere. A number of studies have indicated the downregulation of miR-145 in cancers but upregulation in stem cell maintenance (Table 12.11), indicating the negative contribution of miR-145 in cell proliferation as literally suggested by Akao et al (2007). Other studies have revealed that the chromosomal location of IFNB1 at 9p21 is frequently deleted or rearranged in a number of human cancers, including leukemia, glioma, neuroblastoma, non-small-cell lung carcinoma, and melanoma (Center et al., 1993; Chen et al., 1996; Fountain et al., 1992a; Fountain et al., 1992b; Olopade et al., 1992a; Olopade et al., 1992b; Takita et al., 1997; Zhang et al., 1996) implicating the involvement of IFNB1 in regulating cell proliferation. We therefore postulate a novel correlation that miR-145 inhibit cell proliferation through the direct or indirect regulation of IFNB1. The terms direct and indirect are used here because IFNB1 is not a prediction target of miR-145, as disclosed by the miRBase target prediction algorithm, but microRNAs may activate gene expression under very special cellular conditions that we may not be aware of (Vasudevan et al., 2007). As mentioned, the relation between IFNB1 and miR-145 has actually never been established, although miR-145, often together with miR-143, is a colorectal cancer specific microRNA, and IFNB1 has been found as cytostatic factor (Zimmer and Thomas, 2002) and inhibitor for carcinoembryonic antigen (CEA) secretion in colorectal cancer (Toth and Thomas, 1990). We here are the first to

suggest that miR-145 may regulate IFNB1 for colorectal cancer metastasis and staging, but this is far from the scope that this thesis can be addressed in details. Besides, since STAT1 is the downstream target of IFNB1 in the IFNα/β signaling pathway, and we have shown that STAT1 was expressed strongly in the limbal epithelium (Chatper 6). We here therefore postulate the possible tight coordination between miR-145, IFNB1 and STAT1, though further experiments are necessary.

In summary, by using the overexpression miR-145 HCE model, we identified the function of miR-145, which is possibly through the upregulation of IFNB1, to inhibit cell proliferation for the critical maintainance stem cell queiscence. This study shed lights on further correlation study of miR-145 and IFNB1.

Table 12.1. Mature miR-21 sequences are perfectly conserved across species.

miRNA	Accession No.	Mature Sequence	Species (Scientific)	Species (Common)
ptr-miR-21	MIMAT0002321	**UAGCUUAUCAGACUGAUGUUGA**	*Pan troglodytes*	chimpanzee
mml-miR-21	MIMAT0002320	**UAGCUUAUCAGACUGAUGUUGA**	*Macaca mulatta*	rhesus monkey
oan-miR-21	MIMAT0007160	**UAGCUUAUCAGACUGAUGUUGA**	*Ornithorhynchus anatinus*	platypus
gga-miR-21	MIMAT0003774	**UAGCUUAUCAGACUGAUGUUGA**	*Gallus gallus*	chicken
age-miR-21	MIMAT0002325	**UAGCUUAUCAGACUGAUGUUGA**	*Ateles geoffroyi*	spider monkey
mdo-miR-21	MIMAT0004091	**UAGCUUAUCAGACUGAUGUUGA**	*Monodelphis domestica*	opossum
ppy-miR-21	MIMAT0002323	**UAGCUUAUCAGACUGAUGUUGA**	*Pongo pygmaeus*	orang-utan
tni-miR-21	MIMAT0003000	**UAGCUUAUCAGACUGGUGUUG**GC	*Tetraodon nigroviridis*	green spotted pufferfish
mmu-miR-21	MIMAT0000530	**UAGCUUAUCAGACUGAUGUUGA**	*Mus musculus*	mouse
fru-miR-21	MIMAT0002999	**UAGCUUAUCAGACUGGUGUUG**GC	*Fugu rubripes*	Japanese pufferfish
ssc-miR-21	MIMAT0002165	**UAGCUUAUCAGACUGAUGUUGA**	*Sus scrofa*	feral pigs
hsa-miR-21	MIMAT0000076	**UAGCUUAUCAGACUGAUGUUGA**	*Homo sapiens*	human
rno-miR-21	MIMAT0000790	**UAGCUUAUCAGACUGAUGUUGA**	*Rattus norvegicus*	rat
ppa-miR-21	MIMAT0002326	**UAGCUUAUCAGACUGAUGUUGA**	*Pan paniscus*	bonobo
ggo-miR-21	MIMAT0002322	**UAGCUUAUCAGACUGAUGUUGA**	*Gorilla gorilla*	gorilla
cgr-miR-21	MIMAT0004417	**UAGCUUAUCAGACUGAUGUUGA**	*Cricetulus griseus*	Chinese hamster
bta-miR-21	MIMAT0003528	**UAGCUUAUCAGACUGAUGUUGA**CU	*Bos Taurus*	domestic cow
mne-miR-21	MIMAT0002324	**UAGCUUAUCAGACUGAUGUUGA**	*Macaca nemestrina*	pigtail macaque
cfa-miR-21	MIMAT0006741	**UAGCUUAUCAGACUGAUGUUGA**	*Canis familiaris*	dog
eca-miR-21	MIMAT0013029	**UAGCUUAUCAGACUGAUGUUGA**	*Equus caballus*	horse

Table 12.2. Mature miR-143 sequences are perfectly conserved among various species.

miRNA	Accession No.	Mature Sequence	Species (Scientific)	Species (Common)
lla-miR-143	MIMAT0002260	**UGAGAUGAAGCACUGUAGCUC**A	*Lagothrix lagotricha*	woolly monkeys
xtr-miR-143	MIMAT0003686	**UGAGAUGAAGCACUGUAGCUC**G	*Xenopus tropicalis*	pipid frog
ggo-miR-143	MIMAT0002258	**UGAGAUGAAGCACUGUAGCUC**A	*Gorilla gorilla*	gorilla
mdo-miR-143	MIMAT0004113	**UGAGAUGAAGCACUGUAGCUC**G	*Monodelphis domestica*	opossum
ppy-miR-143	MIMAT0002259	**UGAGAUGAAGCACUGUAGCUC**A	*Pongo pygmaeus*	orang-utan
oan-miR-143	MIMAT0007144	**UGAGAUGAAGCACUGUAGCUC**	*Ornithorhynchus anatinus*	platypus
eca-miR-143	MIMAT0013063	**UGAGAUGAAGCACUGUAGCUC**	*Equus caballus*	horse
ptr-miR-143	MIMAT0002257	**UGAGAUGAAGCACUGUAGCUC**A	*Pan troglodytes*	chimpanzee
cfa-miR-143	MIMAT0006682	**UGAGAUGAAGCACUGUAGCUC**	*Canis familiaris*	dog
ppa-miR-143	MIMAT0002261	**UGAGAUGAAGCACUGUAGCUC**A	*Pan paniscus*	bonobo
bta-miR-143	MIMAT0009233	**UGAGAUGAAGCACUGUAGCUC**G	*Bos Taurus*	domestic cow
dre-miR-143	MIMAT0001840	**UGAGAUGAAGCACUGUAGCUC**	*Dario rerio*	zebrafish
hsa-miR-143	MIMAT0000435	**UGAGAUGAAGCACUGUAGCUC**	*Homo sapiens*	human
mmu-miR-143	MIMAT0000247	**UGAGAUGAAGCACUGUAGCUC**	*Mus musculus*	mouse
mml-miR-143	MIMAT0006201	**UGAGAUGAAGCACUGUAGCUC**	*Macaca mulatta*	rhesus monkey
rno-miR-143	MIMAT0000849	**UGAGAUGAAGCACUGUAGCUC**A	*Rattus norvegicus*	rat

Table 12.3. Mature sequences of miR-145 are conserved across various species.

miRNA	Accession No.	Mature Sequence	*Species (Scientific)*	Species (Common)
rno-miR-145	MIMAT0000851	**GUCCAGUUUUCCCAGGAAU**CCCU	*Rattus norvegicus*	rat
mdo-miR-145	MIMAT0004116	**GUCCAGUUUUCCCAGGAAU**CCCU	*Monodelphis domestica*	opossum
ggo-miR-145	MIMAT0002268	**GUCCAGUUUUCCCAGGAAU**CCCUU	*Gorilla gorilla*	gorilla
xtr-miR-145	MIMAT0003688	**GUCCAGUUUUCCCAGGAAU**CCCUU	*Xenopus tropicalis*	pipid frog
mmu-miR-145	MIMAT0000157	**GUCCAGUUUUCCCAGGAAU**CCCU	*Mus musculus*	mouse
mne-miR-145	MIMAT0002270	**GUCCAGUUUUCCCAGGAAU**CCCUU	*Macaca nemestrina*	pigtail macaque
dre-miR-145	MIMAT0001842	**GUCCAGUUUUCCCAGGAAU**CCC	*Dario rerio*	zebrafish
cfa-miR-145	MIMAT0009863	**GUCCAGUUUUCCCAGGAAU**CCCU	*Canis familiaris*	dog
ssc-miR-145	MIMAT0002123	**GUCCAGUUUUCCCAGGAAU**CCCUU	*Sus scrofa*	wild boar
bta-miR-145	MIMAT0003542	**GUCCAGUUUUCCCAGGAAU**CCCU	*Bos Taurus*	domestic cow
mml-miR-145	MIMAT0002266	**GUCCAGUUUUCCCAGGAAU**CCCUU	*Macaca mulatta*	rhesus monkey
ppy-miR-145	MIMAT0002269	**GUCCAGUUUUCCCAGGAAU**CCCUU	*Pongo pygmaeus*	orang-utan
ptr-miR-145	MIMAT0002267	**GUCCAGUUUUCCCAGGAAU**CCCUU	*Pan troglodytes*	chimpanzee
oan-miR-145	MIMAT0007141	**GUCCAGUUUUCCCAGGAAU**	*Ornithorhynchus anatinus*	platypus
eca-miR-145	MIMAT0013064	**GUCCAGUUUUCCCAGGAAU**CCCU	*Equus caballus*	horse
hsa-miR-145	MIMAT0000437	**GUCCAGUUUUCCCAGGAAU**CCCU	*Homo sapiens*	human

Table 12.4. Chromosomal coordinates of microRNAs according to UCSC Genome Browser.

microRNAs	Chromosomal coordinates
hsa-mir-145	5: 148,790,402-148,790,489 [+]
hsa-mir-143	5: 148,788,674-148,788,779 [+]
hsa-mir-21	17: 55,273,409-55,273,480 [+]

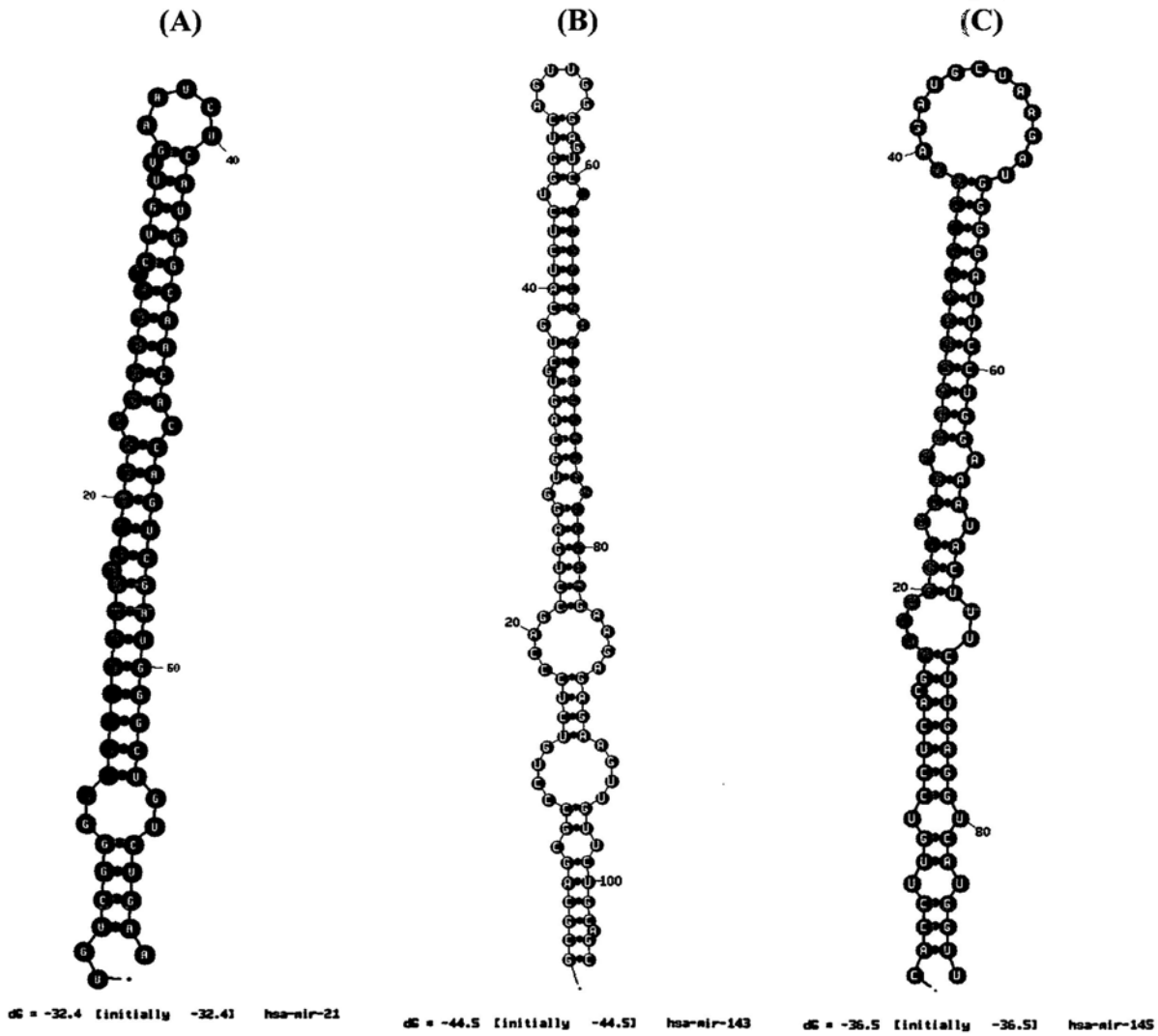

Figure 12.1. Precursor hair pin sequence of (A) hsa-miR-21, (B) hsa-miR-143 and (C) hsa-miR-145.

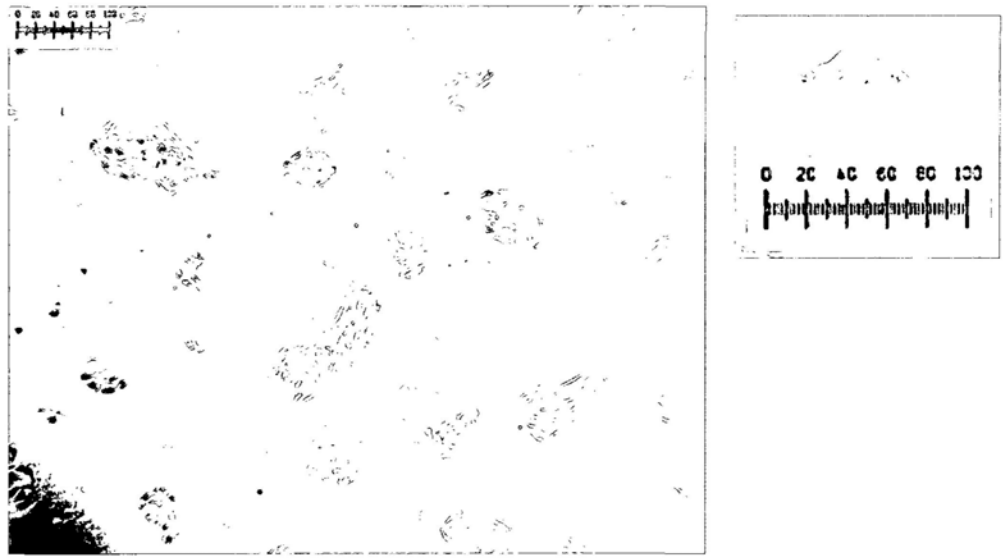

Figure 12.2. Morphology of human corneal epithelial cell line used in our study. Bar, 100 μm.

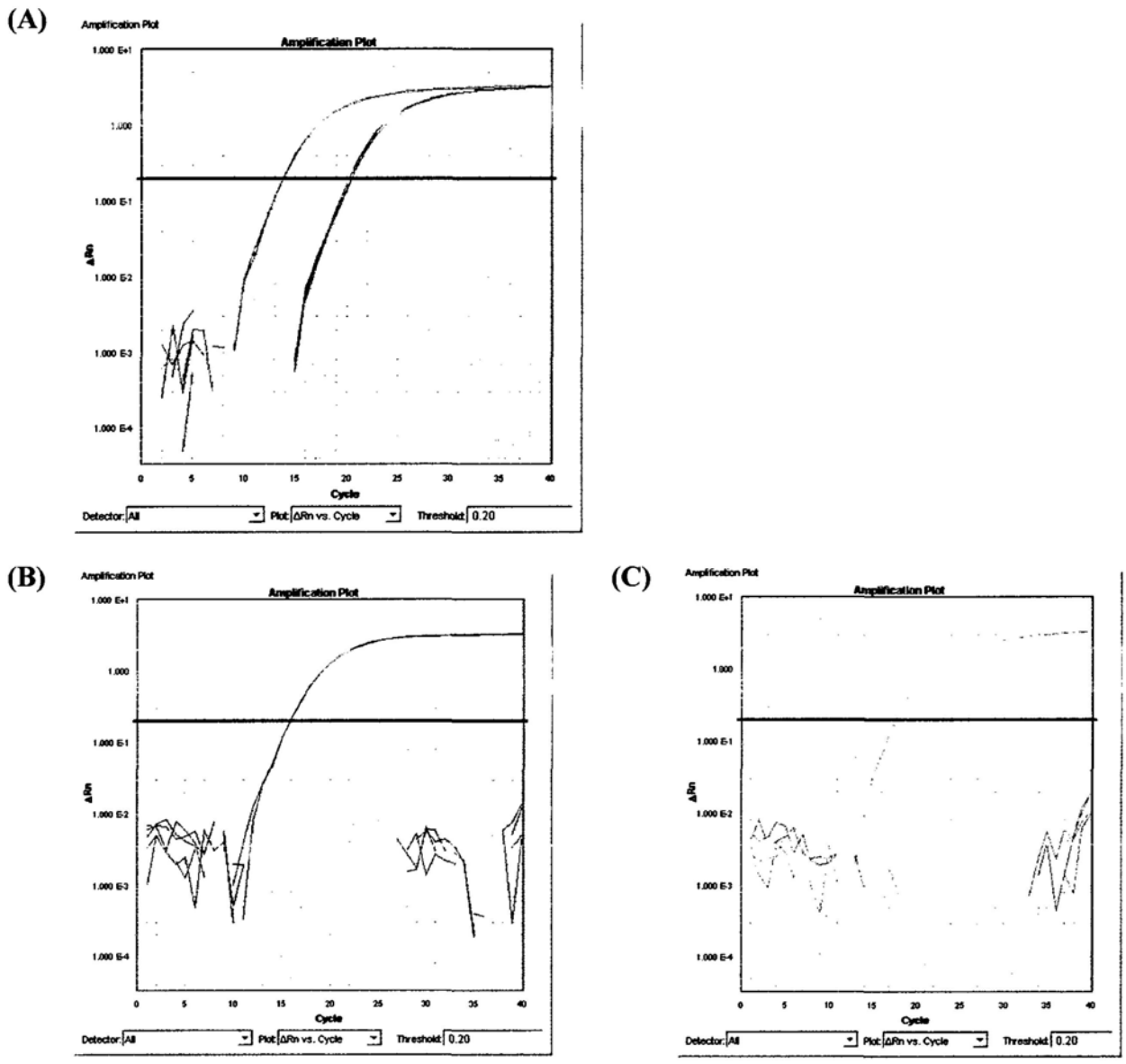

Figure 12.3. Transfection efficiency of Pre-miRs in human corneal epithelial cell line. Amplification plots comparing the expression level of (A) miR-21, (B) miR-143, and (C) miR-145 in transfected cells (left curves) and untreated HCE cells (right curves).

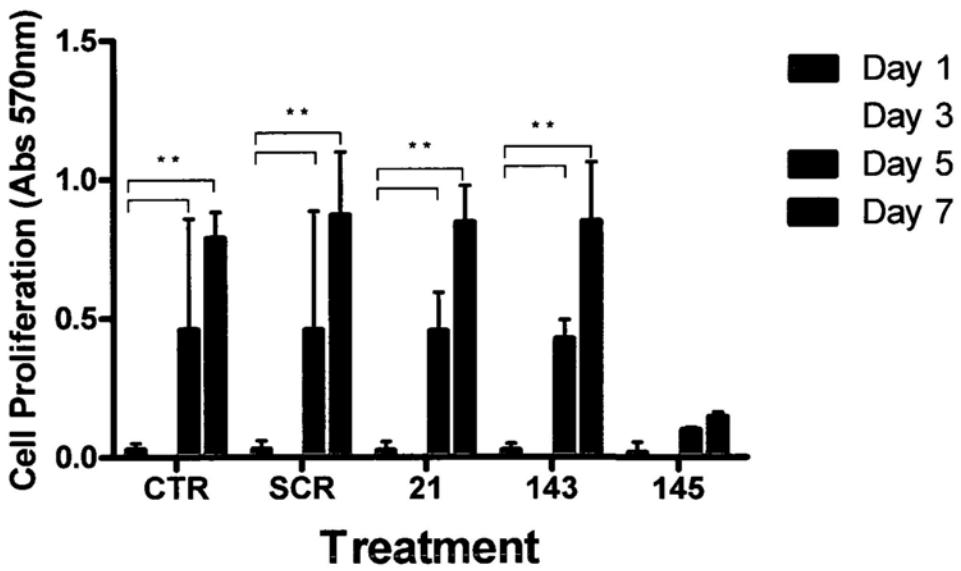

*** p < 0.001, Two-way ANOVA, with Bonferroni Post-test*

Figure 12.4. miR-145 affects cell proliferation in human corneal epithelial cells. One way ANOVA, p < 0.05.

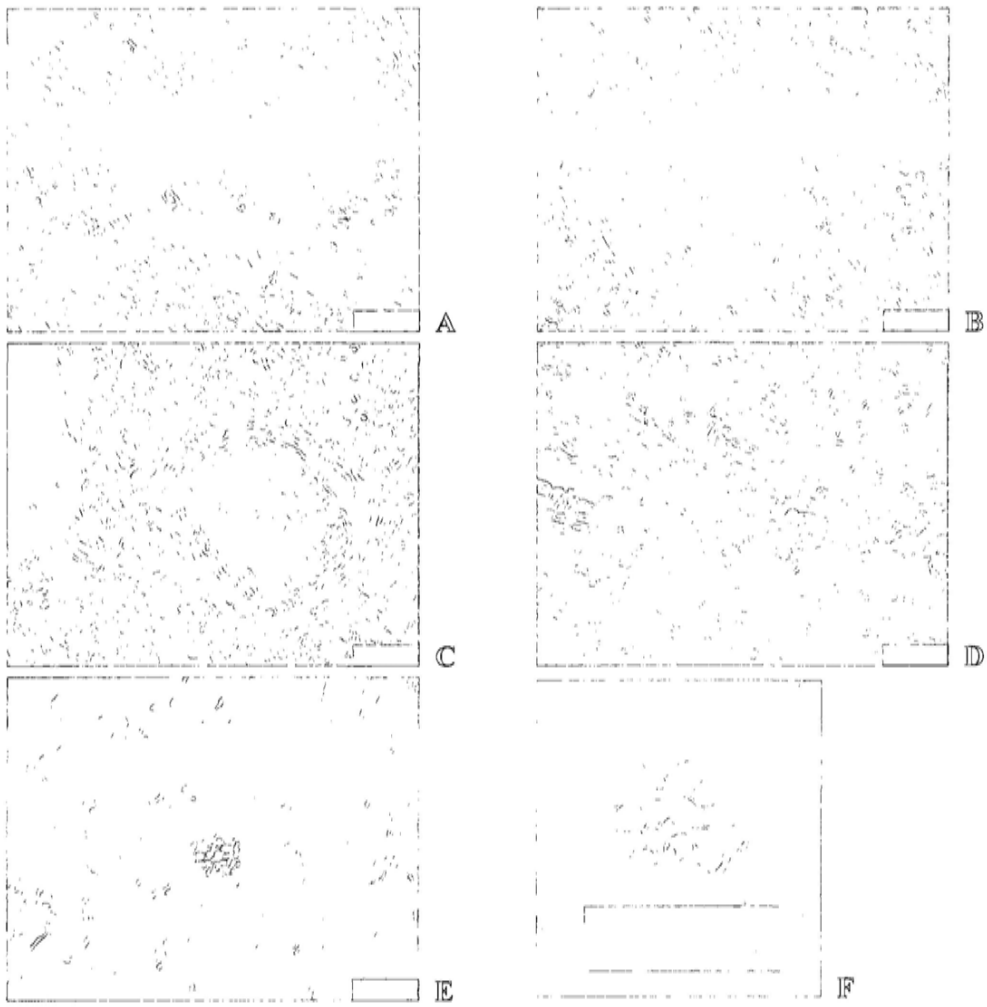

Figure 12.5. Morphological change after precursor miRs transfection. (A) untreated HCE, (B) scrambled, (C) miR-21, (D) miR-143, and (E, F) miR-145 treated control. The HCE cells were cultured for 7 days after transfection of the precursor miRs. Bar, 100 μm.

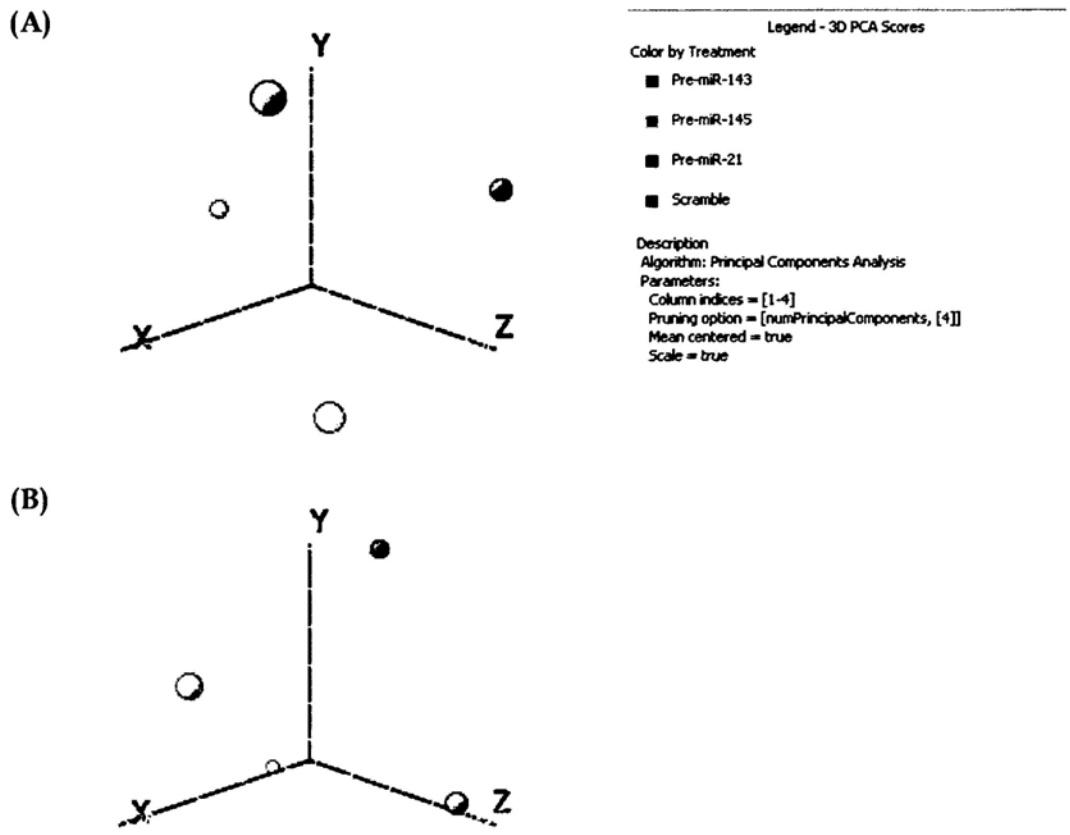

Figure 12.6. Principle Component Analysis of (A) Experiment 1 and (B) Experiment 2 microarray.

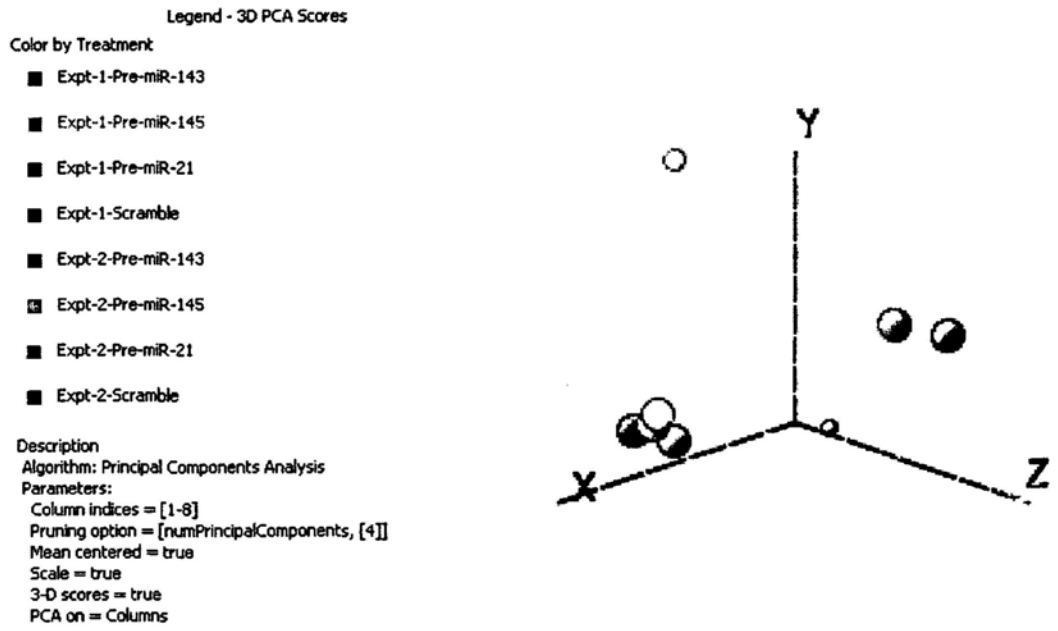

Figure 12.7. Principle Component Analysis of experiment 1 and experiment 2 microarrays.

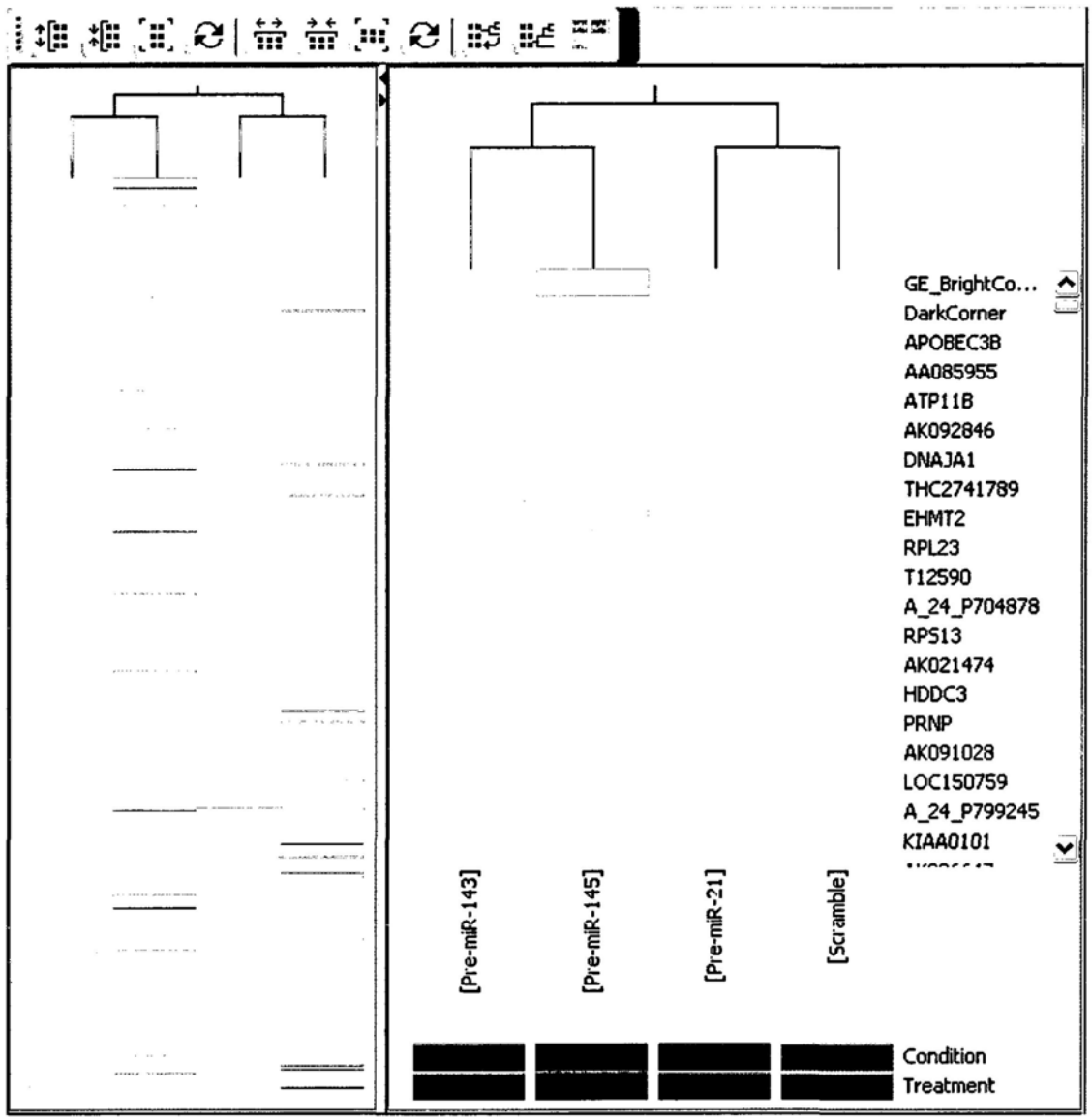

Figure 12.8. Cluster analysis of experiment 2 microarray.

Table 12.5. Prediction targets of miR-21 which has 2 or more fold change in expression when comparing microarray results of pre-miR-21 treated group to the scrambled pre-miR control.

GeneSymbol	Fold change	Regulation	Description
FASLG	30.756798	down	Homo sapiens Fas ligand (TNF superfamily, member 6) (FASLG), mRNA [NM_000639]
C2	17.100248	down	Homo sapiens complement component 2, mRNA (cDNA clone IMAGE:5183067), complete cds. [BC029781]
LYZ	14.3382435	down	Homo sapiens lysozyme (renal amyloidosis) (LYZ), mRNA [NM_000239]
RASSF6	12.094283	down	Homo sapiens Ras association (RalGDS/AF-6) domain family 6 (RASSF6), transcript variant 2, mRNA [NM_201431]
FGF14	9.983563	down	Homo sapiens fibroblast growth factor 14 (FGF14), transcript variant 2, mRNA [NM_175929]
PKHD1L1	9.683415	down	Homo sapiens polycystic kidney and hepatic disease 1 (autosomal recessive)-like 1 (PKHD1L1), mRNA [NM_177531]
BFSP2	7.976225	down	Homo sapiens beaded filament structural protein 2, phakinin (BFSP2), mRNA [NM_003571]
MYOZ1	5.9512005	down	Homo sapiens myozenin 1 (MYOZ1), mRNA [NM_021245]
PDLIM2	5.8758097	down	Homo sapiens PDZ and LIM domain 2 (mystique) (PDLIM2), transcript variant 1, mRNA [NM_176871]
PHOX2B	4.7115545	down	Homo sapiens paired-like homeobox 2b (PHOX2B), mRNA [NM_003924]
TMPRSS11B	3.6309516	down	Homo sapiens transmembrane protease, serine 11B (TMPRSS11B), mRNA [NM_182502]
ASPA	3.2223127	down	Homo sapiens aspartoacylase (Canavan disease) (ASPA), mRNA [NM_000049]
PSCA	3.0143023	down	Homo sapiens prostate stem cell antigen (PSCA), mRNA [NM_005672]
WFDC5	2.8827262	down	Homo sapiens WAP four-disulfide core domain 5 (WFDC5), mRNA [NM_145652]
ABCA1	2.6441383	down	Homo sapiens ATP-binding cassette, sub-family A (ABC1), member 1 (ABCA1), mRNA [NM_005502]
OBSCN	2.488633	down	Homo sapiens obscurin, cytoskeletal calmodulin and titin-interacting RhoGEF (OBSCN), mRNA [NM_052843]
SOX2	2.2245593	down	Homo sapiens SRY (sex determining region Y)-box 2 (SOX2), mRNA [NM_003106]
RNF180	2.1022487	down	Homo sapiens ring finger protein 180 (RNF180), mRNA [NM_178532]

GPRASP1	2.0842059	down	Homo sapiens G protein-coupled receptor associated sorting protein 1 (GPRASP1), mRNA [NM_014710]
MON2	2.0736325	down	Homo sapiens MON2 homolog (S. cerevisiae) (MON2), mRNA [NM_015026]
CFH	1.7724438	down	Homo sapiens complement factor H (CFH), transcript variant 1, mRNA [NM_000186]
DZIP1L	1.5392343	down	Homo sapiens DAZ interacting protein 1-like (DZIP1L), mRNA [NM_173543]
CFHR1	1.5232387	down	Homo sapiens complement factor H-related 1 (CFHR1), mRNA [NM_002113]
IL12A	1.2979609	down	Homo sapiens interleukin 12A (natural killer cell stimulatory factor 1, cytotoxic lymphocyte maturation factor 1, p35) (IL12A), mRNA [NM_000882]
SAMD9	1.2673316	down	Homo sapiens sterile alpha motif domain containing 9 (SAMD9), mRNA [NM_017654]
NPPB	1.2041534	down	Homo sapiens natriuretic peptide precursor B (NPPB), mRNA [NM_002521]
NFIB	1.1826209	down	Homo sapiens nuclear factor I/B (NFIB), mRNA [NM_005596]
TMEM27	1.1578189	down	Homo sapiens transmembrane protein 27 (TMEM27), mRNA [NM_020665]
SALL1	1.1534477	down	Homo sapiens sal-like 1 (Drosophila) (SALL1), mRNA [NM_002968]
TTC33	1.1443623	down	Homo sapiens tetratricopeptide repeat domain 33 (TTC33), mRNA [NM_012382]
MED28	1.1390672	down	Homo sapiens mediator of RNA polymerase II transcription, subunit 28 homolog (S. cerevisiae) (MED28), mRNA [NM_025205]
DYNC2H1	1.1277648	down	Homo sapiens dynein, cytoplasmic 2, heavy chain 1 (DYNC2H1), mRNA [NM_001080463]
PLK4	1.1216954	down	Homo sapiens polo-like kinase 4 (Drosophila) (PLK4), mRNA [NM_014264]
NIN	1.0837419	down	Homo sapiens ninein (GSK3B interacting protein) (NIN), transcript variant 4, mRNA [NM_016350]
C1QTNF3	1.066408	down	Homo sapiens C1q and tumor necrosis factor related protein 3 (C1QTNF3), transcript variant 2, mRNA [NM_181435]
TPSG1	1.0577645	down	Homo sapiens tryptase gamma 1 (TPSG1), mRNA [NM_012467]
C4orf16	1.0556518	down	Homo sapiens chromosome 4 open reading frame 16 (C4orf16), mRNA [NM_018569]
THBS1	1.0512879	down	Homo sapiens thrombospondin 1 (THBS1), mRNA [NM_003246]
GBP1	1.0501183	down	Homo sapiens guanylate binding protein 1, interferon-inducible, 67kDa (GBP1), mRNA [NM_002053]
PITX2	1.0440087	down	Homo sapiens paired-like homeodomain transcription factor 2 (PITX2), transcript variant 2, mRNA [NM_153426]

GAPVD1	1.0435616	down	Homo sapiens GTPase activating protein and VPS9 domains 1 (GAPVD1), mRNA [NM_015635]
CHDH	1.042861	down	Homo sapiens partial mRNA for choline dehydrogenase (chdh gene). [AJ272267]
UCRC	1.0211692	down	Homo sapiens ubiquinol-cytochrome c reductase complex (7.2 kD) (UCRC), transcript variant 2, mRNA [NM_001003684]
MR1	1.0161586	down	Homo sapiens major histocompatibility complex, class I-related (MR1), mRNA [NM_001531]
LRRTM2	1.0150509	down	Homo sapiens leucine rich repeat transmembrane neuronal 2 (LRRTM2), mRNA [NM_015564]
MERTK	1.0143	down	Human cellular proto-oncogene (c-mer) mRNA, complete cds. [U08023]
IFI30	1.0050286	down	Homo sapiens interferon, gamma-inducible protein 30 (IFI30), mRNA [NM_006332]
MATN2	1.0042455	down	Homo sapiens matrilin 2 (MATN2), transcript variant 2, mRNA [NM_030583]
FLJ23049	8.350039	up	Homo sapiens hypothetical protein FLJ23049 (FLJ23049), mRNA [NM_024687]
HBE1	7.1187153	up	Homo sapiens hemoglobin, epsilon 1 (HBE1), mRNA [NM_005330]
SLC10A1	5.676948	up	Homo sapiens solute carrier family 10 (sodium/bile acid cotransporter family), member 1 (SLC10A1), mRNA [NM_003049]
HPGD	5.5312757	up	Homo sapiens hydroxyprostaglandin dehydrogenase 15-(NAD) (HPGD), mRNA [NM_000860]
SESN1	4.89194	up	Homo sapiens sestrin 1 (SESN1), mRNA [NM_014454]
P2RY12	4.6683087	up	Homo sapiens purinergic receptor P2Y, G-protein coupled, 12 (P2RY12), transcript variant 1, mRNA [NM_022788]
PRTG	3.559601	up	Homo sapiens protogenin homolog (Gallus gallus) (PRTG), mRNA [NM_173814]
C2orf34	3.3418	up	Homo sapiens chromosome 2 open reading frame 34, mRNA (cDNA clone IMAGE:4673016), complete cds. [BC029359]
CART1	3.3257337	up	Homo sapiens cartilage paired-class homeoprotein 1 (CART1), mRNA [NM_006982]
GPR6	2.3933372	up	Homo sapiens G protein-coupled receptor 6 (GPR6), mRNA [NM_005284]
S100A12	2.3054564	up	Homo sapiens S100 calcium binding protein A12 (S100A12), mRNA [NM_005621]
KIF6	2.23255	up	Homo sapiens kinesin family member 6 (KIF6), mRNA [NM_145027]
PHTF1	2.1923935	up	Homo sapiens putative homeodomain transcription factor 1 (PHTF1), mRNA [NM_006608]
C14orf124	2.11005	up	Homo sapiens chromosome 14 open reading frame 124 (C14orf124), mRNA [NM_020195]
FABP4	1.8497595	up	Homo sapiens fatty acid binding protein 4, adipocyte (FABP4), mRNA [NM_001442]

GIPC3	1.6814344	up	Homo sapiens mRNA; cDNA DKFZp686J1198 (from clone DKFZp686J1198). [BX648927]
VGLL2	1.6504401	up	Homo sapiens vestigial like 2 (Drosophila) (VGLL2), transcript variant 2, mRNA [NM_153453]
LPA	1.5084004	up	Homo sapiens lipoprotein, Lp(a) (LPA), mRNA [NM_005577]
RUNX2	1.4512037	up	Homo sapiens runt-related transcription factor 2 (RUNX2), transcript variant 3, mRNA [NM_004348]
AOF1	1.3230029	up	Homo sapiens amine oxidase (flavin containing) domain 1 (AOF1), mRNA [NM_153042]
SLC13A4	1.3101876	up	Homo sapiens solute carrier family 13 (sodium/sulfate symporters), member 4 (SLC13A4), mRNA [NM_012450]
SUFU	1.2385826	up	Homo sapiens suppressor of fused homolog (Drosophila) (SUFU), mRNA [NM_016169]
EXOC6	1.1728877	up	Homo sapiens exocyst complex component 6 (EXOC6), transcript variant 2, mRNA [NM_001013848]
PIWIL4	1.1611315	up	Homo sapiens piwi-like 4 (Drosophila) (PIWIL4), mRNA [NM_152431]
RANBP3	1.1610793	up	H.sapiens mRNA for RanBP3, splice variant. [Y08699]
ENAH	1.1482252	up	Homo sapiens enabled homolog (Drosophila) (ENAH), transcript variant 2, mRNA [NM_018212]
C1orf96	1.1398543	up	Homo sapiens chromosome 1 open reading frame 96 (C1orf96), mRNA [NM_145257]
SPATA6	1.1385673	up	Spermatogenesis-associated protein 6 precursor. [Source:Uniprot/SWISSPROT;Acc:Q9NWH7] [ENST00000371847]
NPAL2	1.1359752	up	Homo sapiens NIPA-like domain containing 2 (NPAL2), mRNA [NM_024759]
ENST00000355049	1.1050383	up	similar to peptidylprolyl isomerase A isoform 1 (LOC126170), mRNA [Source:RefSeq_dna;Acc:XR_016157] [ENST00000355049]
BTK	1.0856843	up	Homo sapiens Bruton agammaglobulinemia tyrosine kinase (BTK), mRNA [NM_000061]
KIAA0090	1.0803887	up	Homo sapiens mRNA; cDNA DKFZp686M0947 (from clone DKFZp686M0947). [BX648708]
USP41	1.0793	up	Ubiquitin carboxyl-terminal hydrolase 41 (EC 3.1.2.15) (Ubiquitin thioesterase 41) (Ubiquitin-specific-processing protease 41) (Deubiquitinating enzyme 41) (Fragment). [Source:Uniprot/SPTREMBL;Acc:Q3LFD5] [ENST00000292729]
NPTN	1.0753732	up	Homo sapiens neuroplastin (NPTN), transcript variant beta, mRNA [NM_012428]
UMODL1	1.0694094	up	Homo sapiens uromodulin-like 1 (UMODL1), transcript variant 2, mRNA [NM_173568]
NUPL2	1.0652657	up	Homo sapiens nucleoporin like 2 (NUPL2), mRNA [NM_007342]
CD8B	1.0611724	up	Homo sapiens CD8b molecule (CD8B), transcript variant 4, mRNA [NM_172102]

MYO5A	1.0589598	up	Homo sapiens myosin VA (heavy chain 12, myoxin) (MYO5A), mRNA [NM_000259]
BANK1	1.0544065	up	Homo sapiens B-cell scaffold protein with ankyrin repeats 1 (BANK1), mRNA [NM_017935]
SNTB1	1.0499787	up	Homo sapiens Tax interaction protein 43 mRNA, partial cds. [AF028828]
SH2D1A	1.0455633	up	Homo sapiens SH2 domain protein 1A, Duncan's disease (lymphoproliferative syndrome) (SH2D1A), mRNA [NM_002351]
TOMM40	1.041468	up	Homo sapiens translocase of outer mitochondrial membrane 40 homolog (yeast) (TOMM40), mRNA [NM_006114]
FCRLB	1.0406319	up	Homo sapiens Fc receptor-like B, mRNA (cDNA clone MGC:71141 IMAGE:3529386), complete cds. [BC067080]
SLC39A11	1.0381653	up	Homo sapiens solute carrier family 39 (metal ion transporter), member 11 (SLC39A11), mRNA [NM_139177]
GIMAP2	1.0357541	up	Homo sapiens GTPase, IMAP family member 2 (GIMAP2), mRNA [NM_015660]
HIST1H4A	1.0346578	up	Homo sapiens histone cluster 1, H4a (HIST1H4A), mRNA [NM_003538]
RPS4Y2	1.0284082	up	Homo sapiens ribosomal protein S4, Y-linked 2 (RPS4Y2), mRNA [NM_001039567]
ZNF670	1.0143862	up	Homo sapiens zinc finger protein 670 (ZNF670), mRNA [NM_033213]
RNF122	1.0131947	up	Homo sapiens ring finger protein 122 (RNF122), mRNA [NM_024787]
MAP1LC3C	1.012965	up	Homo sapiens microtubule-associated protein 1 light chain 3 gamma (MAP1LC3C), mRNA [NM_001004343]
HLA-G	1.0112301	up	Homo sapiens HLA-G histocompatibility antigen, class I, G (HLA-G), mRNA [NM_002127]
ANG	1.0083485	up	Homo sapiens angiogenin, ribonuclease, RNase A family, 5 (ANG), mRNA [NM_001145]
LOH11CR2A	1.0017599	up	Homo sapiens loss of heterozygosity, 11, chromosomal region 2, gene A (LOH11CR2A), transcript variant 2, mRNA [NM_198315]

Table 12.6. Prediction targets of miR-143 which has 2 or more fold change in expression when comparing microarray results of pre-miR-143 treated group to the scrambled pre-miR control.

GeneSymbol	Fold change	Regulation	Description
TAC1	15.223206	down	Homo sapiens tachykinin, precursor 1 (substance K, substance P, neurokinin 1, neurokinin 2, neuromedin L, neurokinin alpha, neuropeptide K, neuropeptide gamma) (TAC1), transcript variant beta, mRNA [NM_003182]
PKHD1L1	12.396731	down	Homo sapiens polycystic kidney and hepatic disease 1 (autosomal recessive)-like 1 (PKHD1L1), mRNA [NM_177531]
KRT2	9.893273	down	Homo sapiens keratin 2 (epidermal ichthyosis bullosa of Siemens) (KRT2), mRNA [NM_000423]
FHAD1	9.598528	down	Homo sapiens cDNA FLJ36564 fis, clone TRACH2009851. [AK093883]
CCL23	8.18045	down	Homo sapiens chemokine (C-C motif) ligand 23 (CCL23), transcript variant CKbeta8-1, mRNA [NM_005064]
GRIK3	7.4723535	down	Homo sapiens glutamate receptor, ionotropic, kainate 3 (GRIK3), mRNA [NM_000831]
ATP10A	7.2163615	down	Homo sapiens ATPase, Class V, type 10A (ATP10A), mRNA [NM_024490]
CLDN10	7.0647273	down	Homo sapiens claudin 10 (CLDN10), transcript variant 1, mRNA [NM_182848]
SLFNL1	5.908156	down	Homo sapiens cDNA FLJ23878 fis, clone LNG13675. [AK074458]
ADAMTS6	5.7631207	down	Homo sapiens ADAM metallopeptidase with thrombospondin type 1 motif, 6 (ADAMTS6), mRNA [NM_197941]
SOHLH2	5.4052076	down	Homo sapiens spermatogenesis and oogenesis specific basic helix-loop-helix 2 (SOHLH2), mRNA [NM_017826]
MYOZ1	4.4368525	down	Homo sapiens myozenin 1 (MYOZ1), mRNA [NM_021245]
HTR3A	4.359153	down	Homo sapiens 5-hydroxytryptamine (serotonin) receptor 3A (HTR3A), transcript variant 1, mRNA [NM_213621]
FLOT2	3.2905853	down	Homo sapiens flotillin 2 (FLOT2), mRNA [NM_004475]
CCL7	3.150191	down	Homo sapiens chemokine (C-C motif) ligand 7 (CCL7), mRNA [NM_006273]
AZGP1	3.1411178	down	Homo sapiens alpha-2-glycoprotein 1, zinc-binding (AZGP1), mRNA [NM_001185]
SLC5A6	2.9173563	down	Homo sapiens solute carrier family 5 (sodium-dependent vitamin transporter), member 6 (SLC5A6), mRNA [NM_021095]

BPIL1	2.6329253	down	Homo sapiens bactericidal/permeability-increasing protein-like 1 (BPIL1), mRNA [NM_025227]
TXNDC6	2.4911397	down	Homo sapiens thioredoxin domain containing 6 (TXNDC6), mRNA [NM_178130]
C8orf45	2.3686004	down	Homo sapiens cDNA FLJ25692 fis, clone TST04461. [AK098558]
MAPK7	2.2231672	down	Homo sapiens mitogen-activated protein kinase 7 (MAPK7), transcript variant 1, mRNA [NM_139033]
FRY	2.2191963	down	Homo sapiens furry homolog (Drosophila) (FRY), mRNA [NM_023037]
EMID1	2.1697946	down	Homo sapiens EMI domain containing 1 (EMID1), mRNA [NM_133455]
EME1	2.1423292	down	Homo sapiens essential meiotic endonuclease 1 homolog 1 (S. pombe) (EME1), mRNA [NM_152463]
IFNG	2.0904121	down	Homo sapiens interferon, gamma (IFNG), mRNA [NM_000619]
OR7A17	1.9714923	down	Homo sapiens olfactory receptor, family 7, subfamily A, member 17 (OR7A17), mRNA [NM_030901]
ISLR2	1.9243379	down	Homo sapiens immunoglobulin superfamily containing leucine-rich repeat 2 (ISLR2), mRNA [NM_020851]
NFATC2	1.8163143	down	Homo sapiens nuclear factor of activated T-cells, cytoplasmic, calcineurin-dependent 2 (NFATC2), transcript variant 1, mRNA [NM_012340]
ICA1L	1.5003935	down	Homo sapiens islet cell autoantigen 1,69kDa-like (ICA1L), transcript variant 1, mRNA [NM_138468]
PRPS2	1.454856	down	Homo sapiens phosphoribosyl pyrophosphate synthetase 2 (PRPS2), transcript variant 2, mRNA [NM_002765]
ZCCHC7	1.4440186	down	Homo sapiens zinc finger, CCHC domain containing 7 (ZCCHC7), mRNA [NM_032226]
CALN1	1.3980949	down	Homo sapiens calneuron 1 (CALN1), transcript variant 1, mRNA [NM_031468]
GOLGA4	1.3975248	down	Homo sapiens golgi autoantigen, golgin subfamily a, 4 (GOLGA4), mRNA [NM_002078]
ARHGAP9	1.3836889	down	Homo sapiens Rho GTPase activating protein 9 (ARHGAP9), transcript variant 1, mRNA [NM_032496]
GIMAP4	1.3646493	down	Homo sapiens GTPase, IMAP family member 4 (GIMAP4), mRNA [NM_018326]
RUFY2	1.3600681	down	Homo sapiens RUN and FYVE domain containing 2 (RUFY2), transcript variant 1, mRNA [NM_017987]
MORN3	1.3564515	down	Homo sapiens MORN repeat containing 3 (MORN3), mRNA [NM_173855]
HERC5	1.3239083	down	Homo sapiens hect domain and RLD 5 (HERC5), mRNA [NM_016323]
MRO	1.274243	down	Homo sapiens maestro (MRO), mRNA [NM_031939]

PLA2G1B	1.2729473	down	Homo sapiens phospholipase A2, group IB (pancreas) (PLA2G1B), mRNA [NM_000928]
HS2ST1	1.2590948	down	Homo sapiens heparan sulfate 2-O-sulfotransferase 1 (HS2ST1), mRNA [NM_012262]
SCIN	1.2466595	down	Homo sapiens scinderin (SCIN), mRNA [NM_033128]
IFIT3	1.2434876	down	Homo sapiens interferon-induced protein with tetratricopeptide repeats 3 (IFIT3), mRNA [NM_001549]
IFIT1	1.1907158	down	Homo sapiens interferon-induced protein with tetratricopeptide repeats 1 (IFIT1), transcript variant 2, mRNA [NM_001548]
MYL2	1.1652602	down	Homo sapiens myosin, light chain 2, regulatory, cardiac, slow (MYL2), mRNA [NM_000432]
PCM1	1.1617657	down	Homo sapiens pericentriolar material 1 (PCM1), mRNA [NM_006197]
ZMYND12	1.1457781	down	Homo sapiens zinc finger, MYND-type containing 12 (ZMYND12), mRNA [NM_032257]
PGLYRP4	1.1456277	down	Homo sapiens peptidoglycan recognition protein 4 (PGLYRP4), mRNA [NM_020393]
TM7SF4	1.1320344	down	Homo sapiens transmembrane 7 superfamily member 4 (TM7SF4), mRNA [NM_030788]
LENEP	1.130775	down	Homo sapiens lens epithelial protein (LENEP), mRNA [NM_018655]
RXFP2	1.1206489	down	Homo sapiens relaxin/insulin-like family peptide receptor 2 (RXFP2), mRNA [NM_130806]
GDF10	1.0829333	down	Homo sapiens growth differentiation factor 10 (GDF10), mRNA [NM_004962]
DTNB	1.0755353	down	Homo sapiens dystrobrevin, beta (DTNB), transcript variant 3, mRNA [NM_033148]
DIAPH1	1.074235	down	Homo sapiens diaphanous homolog 1 (Drosophila) (DIAPH1), transcript variant 1, mRNA [NM_005219]
CASP8	1.0580918	down	Homo sapiens caspase 8, apoptosis-related cysteine peptidase (CASP8), transcript variant E, mRNA [NM_033358]
PLCG2	1.0496867	down	Homo sapiens phospholipase C, gamma 2 (phosphatidylinositol-specific) (PLCG2), mRNA [NM_002661]
IGF2R	1.0416766	down	Homo sapiens insulin-like growth factor 2 receptor (IGF2R), mRNA [NM_000876]
SCEL	1.0341574	down	Homo sapiens sciellin (SCEL), transcript variant 2, mRNA [NM_144777]
C9orf86	1.0174323	down	Homo sapiens chromosome 9 open reading frame 86 (C9orf86), mRNA [NM_024718]
SAMD1	1.0145578	down	Homo sapiens sterile alpha motif domain containing 1 (SAMD1), mRNA [NM_138352]
HS3ST2	1.0073991	down	Homo sapiens heparan sulfate (glucosamine) 3-O-sulfotransferase 2 (HS3ST2), mRNA [NM_006043]
TACR1	32.99328	up	Homo sapiens tachykinin receptor 1 (TACR1), transcript variant short, mRNA [NM_015727]

OPTC	17.717186	up	Homo sapiens opticin (OPTC), mRNA [NM_014359]
EYA3	9.711262	up	Homo sapiens mRNA; cDNA DKFZp686G0248 (from clone DKFZp686G0248). [BX648945]
CLEC4M	7.0306835	up	Homo sapiens C-type lectin domain family 4, member M (CLEC4M), transcript variant 2, mRNA [NM_214675]
DQX1	5.79971	up	Homo sapiens DEAQ box polypeptide 1 (RNA-dependent ATPase) (DQX1), mRNA [NM_133637]
INSL5	5.308491	up	Homo sapiens insulin-like 5 (INSL5), mRNA [NM_005478]
CCR2	5.037433	up	Homo sapiens chemokine (C-C motif) receptor 2 (CCR2), transcript variant A, mRNA [NM_000647]
FMO1	4.9491587	up	Homo sapiens flavin containing monooxygenase 1 (FMO1), mRNA [NM_002021]
CPB2	4.4702234	up	Homo sapiens carboxypeptidase B2 (plasma) (CPB2), transcript variant 1, mRNA [NM_001872]
LRFN2	3.7064536	up	Homo sapiens leucine rich repeat and fibronectin type III domain containing 2 (LRFN2), mRNA [NM_020737]
C10orf91	3.672813	up	Homo sapiens chromosome 10 open reading frame 91 (C10orf91), mRNA [NM_173541]
WDR16	3.0484776	up	Homo sapiens WD repeat domain 16 (WDR16), transcript variant 2, mRNA [NM_145054]
TKTL1	3.0339007	up	Homo sapiens transketolase-like 1 (TKTL1), mRNA [NM_012253]
SERPINI2	2.8685977	up	Homo sapiens serpin peptidase inhibitor, clade I (pancpin), member 2 (SERPINI2), mRNA [NM_006217]
LMAN1	2.375154	up	Homo sapiens lectin, mannose-binding, 1 (LMAN1), mRNA [NM_005570]
C1orf162	2.216766	up	Homo sapiens chromosome 1 open reading frame 162 (C1orf162), mRNA [NM_174896]
ACTL7B	2.020669	up	Homo sapiens actin-like 7B (ACTL7B), mRNA [NM_006686]
SMPDL3A	1.8295702	up	Homo sapiens sphingomyelin phosphodiesterase, acid-like 3A (SMPDL3A), mRNA [NM_006714]
RSRC2	1.8291602	up	Homo sapiens arginine/serine-rich coiled-coil 2 (RSRC2), transcript variant 2, mRNA [NM_198261]
RAPGEF4	1.6179972	up	Homo sapiens Rap guanine nucleotide exchange factor (GEF) 4 (RAPGEF4), mRNA [NM_007023]
C18orf34	1.5903953	up	Homo sapiens cDNA FLJ26445 fis, clone KDN02608. [AK129955]
WBSCR17	1.5051498	up	Homo sapiens Williams-Beuren syndrome chromosome region 17 (WBSCR17), mRNA [NM_022479]
ENST00000343756	1.4889143	up	similar to peptidyl-Pro cis trans isomerase (LOC121981), misc RNA [Source:RefSeq_dna;Acc:XR_017783] [ENST00000343756]
GOLGA	1.4569497	up	Homo sapiens golgin-like protein (GOLGA), mRNA [NM_018652]

PPIA	1.4364005	up	Homo sapiens peptidylprolyl isomerase A (cyclophilin A) (PPIA), mRNA [NM_021130]
SLC38A3	1.3575665	up	Homo sapiens solute carrier family 38, member 3 (SLC38A3), mRNA [NM_006841]
RND2	1.3147771	up	Homo sapiens Rho family GTPase 2 (RND2), mRNA [NM_005440]
HCCS	1.2975148	up	Homo sapiens holocytochrome c synthase (cytochrome c heme-lyase) (HCCS), mRNA [NM_005333]
FMO5	1.2728938	up	Homo sapiens flavin containing monooxygenase 5 (FMO5), mRNA [NM_001461]
ZSCAN20	1.2039906	up	Homo sapiens zinc finger and SCAN domain containing 20 (ZSCAN20), mRNA [NM_145238]
TMEM16B	1.1948388	up	Homo sapiens transmembrane protein 16B (TMEM16B), mRNA [NM_020373]
FABP3	1.1794945	up	602405126F1 NIH_MGC_21 Homo sapiens cDNA clone IMAGE:4542655 5', mRNA sequence [BG336702]
MERTK	1.1731211	up	Human cellular proto-oncogene (c-mer) mRNA, complete cds. [U08023]
TMPRSS3	1.1494467	up	Homo sapiens transmembrane protease, serine 3 (TMPRSS3), transcript variant D, mRNA [NM_032405]
CENTG1	1.0955405	up	Centaurin-gamma 1 (ARF-GAP with GTP-binding protein-like, ankyrin repeat and pleckstrin homology domains 2) (AGAP-2) (Phosphatidylinositol-3-kinase enhancer) (PIKE) (GTP-binding and GTPase-activating protein 2) (GGAP2)....
HLA-DRB5	1.0674367	up	Homo sapiens major histocompatibility complex, class II, DR beta 5 (HLA-DRB5), mRNA [NM_002125]
PRTG	1.0544076	up	Homo sapiens protogenin homolog (Gallus gallus) (PRTG), mRNA [NM_173814]
PRUNE2	1.0306809	up	Homo sapiens prune homolog 2 (Drosophila) (PRUNE2), mRNA [NM_138818]
GMPR	1.0017983	up	Homo sapiens guanosine monophosphate reductase (GMPR), mRNA [NM_006877]

Table 12.7. Prediction targets of miR-145 which has 2 or more fold change in expression when comparing microarray results of pre-miR-145 treated group to the scrambled pre-miR control.

GeneSymbol	Fold Change	Regulation	Description
GIP	21.076103	down	Homo sapiens gastric inhibitory polypeptide (GIP), mRNA [NM_004123]
IGF1R	16.451866	down	Homo sapiens clone 1900 unknown protein mRNA, complete cds. [AF020763]
APCS	15.544595	down	Homo sapiens amyloid P component, serum (APCS), mRNA [NM_001639]
ANGPT4	12.661437	down	Homo sapiens angiopoietin 4 (ANGPT4), mRNA [NM_015985]
GPR35	11.940191	down	Homo sapiens G protein-coupled receptor 35 (GPR35), mRNA [NM_005301]
PSCA	9.210029	down	Homo sapiens prostate stem cell antigen (PSCA), mRNA [NM_005672]
HTR6	7.464415	down	Homo sapiens 5-hydroxytryptamine (serotonin) receptor 6 (HTR6), mRNA [NM_000871]
EFNA2	7.332939	down	Homo sapiens ephrin-A2 (EFNA2), mRNA [NM_001405]
TTC18	6.478285	down	Homo sapiens tetratricopeptide repeat domain 18 (TTC18), mRNA [NM_145170]
ANXA13	6.244866	down	Homo sapiens annexin A13 (ANXA13), transcript variant 2, mRNA [NM_001003954]
GCG	5.806891	down	Homo sapiens glucagon (GCG), mRNA [NM_002054]
DTD1	5.4953995	down	Homo sapiens cDNA FLJ23724 fis, clone HEP13989. [AK074304]
KATNAL2	5.3615456	down	Homo sapiens katanin p60 subunit A-like 2 (KATNAL2), mRNA [NM_031303]
C14orf153	5.0207562	down	Homo sapiens chromosome 14 open reading frame 153 (C14orf153), mRNA [NM_032374]
SLAMF1	4.9234457	down	Homo sapiens signaling lymphocytic activation molecule family member 1 (SLAMF1), mRNA [NM_003037]
RETN	4.9025807	down	Homo sapiens resistin (RETN), mRNA [NM_020415]
ZFYVE9	4.8025184	down	Homo sapiens zinc finger, FYVE domain containing 9 (ZFYVE9), transcript variant 2, mRNA [NM_007323]
SLC39A2	3.9944472	down	Homo sapiens solute carrier family 39 (zinc transporter), member 2 (SLC39A2), mRNA [NM_014579]

CDH16	3.9292324	down	Homo sapiens cadherin 16, KSP-cadherin (CDH16), mRNA [NM_004062]
IL17C	3.5512366	down	Homo sapiens interleukin 17C (IL17C), mRNA [NM_013278]
SYNE2	3.2685766	down	Homo sapiens spectrin repeat containing, nuclear envelope 2 (SYNE2), transcript variant 1, mRNA [NM_015180]
C2orf51	3.160961	down	Homo sapiens chromosome 2 open reading frame 51 (C2orf51), mRNA [NM_152670]
CDR1	3.0015113	down	Homo sapiens cDNA FLJ30359 fis, clone BRACE2007760, highly similar to 40S RIBOSOMAL PROTEIN S15A. [AK054921]
BTBD7	2.9583948	down	Homo sapiens BTB (POZ) domain containing 7 (BTBD7), transcript variant 1, mRNA [NM_001002860]
PANX3	2.8774498	down	Homo sapiens pannexin 3 (PANX3), mRNA [NM_052959]
TLN2	2.5845218	down	Homo sapiens talin 2 (TLN2), mRNA [NM_015059]
GGTL3	2.5163667	down	Homo sapiens cDNA FLJ42798 fis, clone BRAWH3008931. [AK124788]
ITGB8	2.4963107	down	Homo sapiens integrin, beta 8 (ITGB8), mRNA [NM_002214]
NEUROG1	2.439907	down	Homo sapiens neurogenin 1 (NEUROG1), mRNA [NM_006161]
HNRPUL2	2.4030693	down	Homo sapiens heterogeneous nuclear ribonucleoprotein U-like 2 (HNRPUL2), mRNA [NM_001079559]
C20orf23	2.388433	down	Homo sapiens chromosome 20 open reading frame 23 (C20orf23), mRNA [NM_024704]
WNT7A	2.316022	down	Homo sapiens wingless-type MMTV integration site family, member 7A (WNT7A), mRNA [NM_004625]
SOCS7	2.2276409	down	Homo sapiens suppressor of cytokine signaling 7 (SOCS7), mRNA [NM_014598]
QPCTL	2.1723428	down	Homo sapiens glutaminyl-peptide cyclotransferase-like (QPCTL), mRNA [NM_017659]
CUEDC1	2.1606152	down	Homo sapiens CUE domain containing 1 (CUEDC1), mRNA [NM_017949]
FRMD4A	2.1551063	down	Homo sapiens FERM domain containing 4A (FRMD4A), mRNA [NM_018027]
HDGF	2.0840971	down	Homo sapiens hepatoma-derived growth factor (high-mobility group protein 1-like) (HDGF), mRNA [NM_004494]
ACAD8	2.05666	down	Homo sapiens acyl-Coenzyme A dehydrogenase family, member 8 (ACAD8), mRNA [NM_014384]
NFIB	2.050749	down	Homo sapiens nuclear factor I/B (NFIB), mRNA [NM_005596]
PTPN22	2.0369048	down	Homo sapiens protein tyrosine phosphatase, non-receptor type 22 (lymphoid) (PTPN22), transcript variant 1, mRNA [NM_015967]

LSS	2.0128546	down	Homo sapiens lanosterol synthase (2,3-oxidosqualene-lanosterol cyclase) (LSS), transcript variant 1, mRNA [NM_002340]
NIN	2.0111775	down	Homo sapiens ninein (GSK3B interacting protein) (NIN), transcript variant 4, mRNA [NM_016350]
ARHGAP30	1.7336707	down	Homo sapiens Rho GTPase activating protein 30 (ARHGAP30), transcript variant 2, mRNA [NM_181720]
FBN3	1.1888963	down	Homo sapiens fibrillin 3 (FBN3), mRNA [NM_032447]
ZNF169	1.185139	down	Homo sapiens zinc finger protein 169, mRNA (cDNA clone IMAGE:5259146), complete cds. [BC035060]
BNIPL	1.1462312	down	Homo sapiens BCL2/adenovirus E1B 19kD interacting protein like (BNIPL), mRNA [NM_138278]
LOH11CR2A	1.0501027	down	Homo sapiens loss of heterozygosity, 11, chromosomal region 2, gene A (LOH11CR2A), transcript variant 2, mRNA [NM_198315]
C10orf81	1.0167493	down	Homo sapiens chromosome 10 open reading frame 81 (C10orf81), mRNA [NM_024889]
IFNB1	**55.78875**	**up**	**Homo sapiens interferon, beta 1, fibroblast (IFNB1), mRNA [NM_002176]**
CHDH	27.732122	up	Homo sapiens partial mRNA for choline dehydrogenase (chdh gene). [AJ272267]
CMAH	12.456315	up	Homo sapiens cytidine monophosphate-N-acetylneuraminic acid hydroxylase (CMP-N-acetylneuraminate monooxygenase), mRNA (cDNA clone MGC:22537 IMAGE:4692226), complete cds. [BC022302]
CP	9.752202	up	Homo sapiens ceruloplasmin (ferroxidase) (CP), mRNA [NM_000096]
LOC255411	7.9762774	up	Homo sapiens cDNA FLJ27495 fis, clone TST03995. [AK131005]
ECE2	6.9579196	up	Homo sapiens endothelin converting enzyme 2 (ECE2), transcript variant 1, mRNA [NM_014693]
C1QL2	6.319045	up	Homo sapiens complement component 1, q subcomponent-like 2 (C1QL2), mRNA [NM_182528]
IRF7	5.130164	up	Homo sapiens interferon regulatory factor 7 (IRF7), transcript variant d, mRNA [NM_004031]
BATF	4.8547935	up	Homo sapiens basic leucine zipper transcription factor, ATF-like (BATF), mRNA [NM_006399]
NLRC5	4.48177	up	Homo sapiens NLR family, CARD domain containing 5 (NLRC5), mRNA [NM_032206]
TNFAIP6	4.0474105	up	Homo sapiens tumor necrosis factor, alpha-induced protein 6 (TNFAIP6), mRNA [NM_007115]
SSTR4	3.900703	up	Homo sapiens somatostatin receptor 4 (SSTR4), mRNA [NM_001052]
PLG	3.6215816	up	Homo sapiens plasminogen (PLG), mRNA [NM_000301]

MFSD2	3.3651447	up	Homo sapiens cDNA FLJ14490 fis, clone MAMMA1002886. [AK027396]
TMC2	3.279298	up	Homo sapiens transmembrane channel-like 2 (TMC2), mRNA [NM_080751]
ADAM28	3.2213213	up	Homo sapiens ADAM metallopeptidase domain 28 (ADAM28), transcript variant 3, mRNA [NM_021777]
NLRC5	3.1833043	up	Homo sapiens NLR family, CARD domain containing 5 (NLRC5), mRNA [NM_032206]
ACTB	3.067547	up	Homo sapiens actin, beta (ACTB), mRNA [NM_001101]
SAA4	3.0340161	up	Homo sapiens serum amyloid A4, constitutive (SAA4), mRNA [NM_006512]
LYZL2	2.6935203	up	Homo sapiens lysozyme-like 2 (LYZL2), mRNA [NM_183058]
LRRC16	2.595159	up	Homo sapiens leucine rich repeat containing 16 (LRRC16), mRNA [NM_017640]
SLC35B1	2.421991	up	Homo sapiens solute carrier family 35, member B1 (SLC35B1), mRNA [NM_005827]
IFI30	2.272975	up	Homo sapiens interferon, gamma-inducible protein 30 (IFI30), mRNA [NM_006332]
RARA	2.233152	up	Homo sapiens retinoic acid receptor, alpha (RARA), transcript variant 1, mRNA [NM_000964]
CDH18	2.20749	up	Homo sapiens cadherin 18, type 2 (CDH18), mRNA [NM_004934]
IL18BP	2.1755402	up	Homo sapiens interleukin 18 binding protein (IL18BP), transcript variant A, mRNA [NM_173042]
CCDC88	2.1727915	up	Homo sapiens coiled-coil domain containing 88 (CCDC88), mRNA [NM_032251]
FANCL	2.1639419	up	Homo sapiens Fanconi anemia, complementation group L (FANCL), mRNA [NM_018062]
RND2	2.1620588	up	Homo sapiens Rho family GTPase 2 (RND2), mRNA [NM_005440]
DFFB	2.120751	up	Homo sapiens DNA fragmentation factor, 40kDa, beta polypeptide (caspase-activated DNase) (DFFB), transcript variant 3, mRNA [NM_001004285]
ZNF226	2.1098883	up	Homo sapiens zinc finger protein 226 (ZNF226), transcript variant 1, mRNA [NM_001032372]
SLC25A41	2.0728123	up	Homo sapiens solute carrier family 25, member 41 (SLC25A41), mRNA [NM_173637]
SLC24A4	1.8376743	up	Homo sapiens solute carrier family 24 (sodium/potassium/calcium exchanger), member 4 (SLC24A4), transcript variant 1, mRNA [NM_153646]
TSHZ2	1.7069851	up	Homo sapiens teashirt family zinc finger 2 (TSHZ2), mRNA [NM_173485]

ALDH3B2	1.4894705	up	Homo sapiens aldehyde dehydrogenase 3 family, member B2 (ALDH3B2), transcript variant 1, mRNA [NM_000695]
APOC3	1.347286	up	Homo sapiens apolipoprotein C-III (APOC3), mRNA [NM_000040]
KIAA0922	1.1884731	up	Homo sapiens KIAA0922 (KIAA0922), mRNA [NM_015196]
ROPN1B	1.1833892	up	Homo sapiens ropporin, rhophilin associated protein 1B (ROPN1B), mRNA [NM_001012337]
C20orf186	1.1556878	up	Homo sapiens chromosome 20 open reading frame 186 (C20orf186), mRNA [NM_182519]
KCNE4	1.1377367	up	Homo sapiens potassium voltage-gated channel, Isk-related family, member 4 (KCNE4), mRNA [NM_080671]
C14orf49	1.1119845	up	Homo sapiens chromosome 14 open reading frame 49 (C14orf49), mRNA [NM_152592]
PTPRCAP	1.0318254	up	Homo sapiens protein tyrosine phosphatase, receptor type, C-associated protein (PTPRCAP), mRNA [NM_005608]

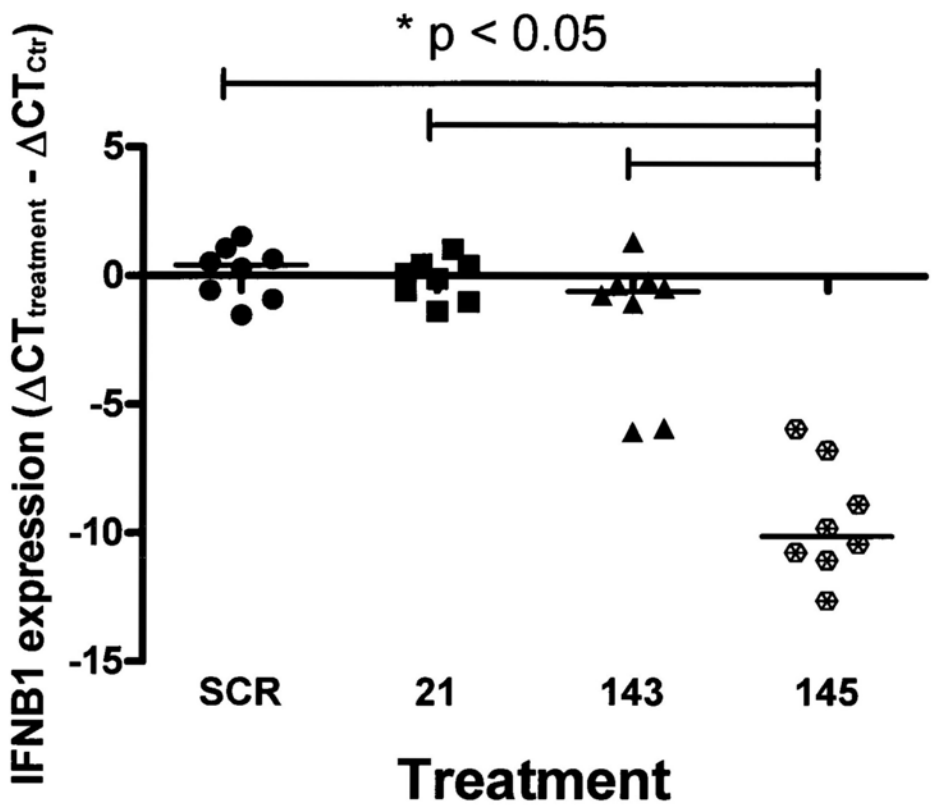

Figure 12.9. qPCR validation of IFNB1 expression in scrambled pre-miR (SCR), pre-miR-21 (21), pre-miR-143 (143) and pre-miR-145 (145) transfected HCE cells. Kruskal Wallis test, * $p < 0.05$.

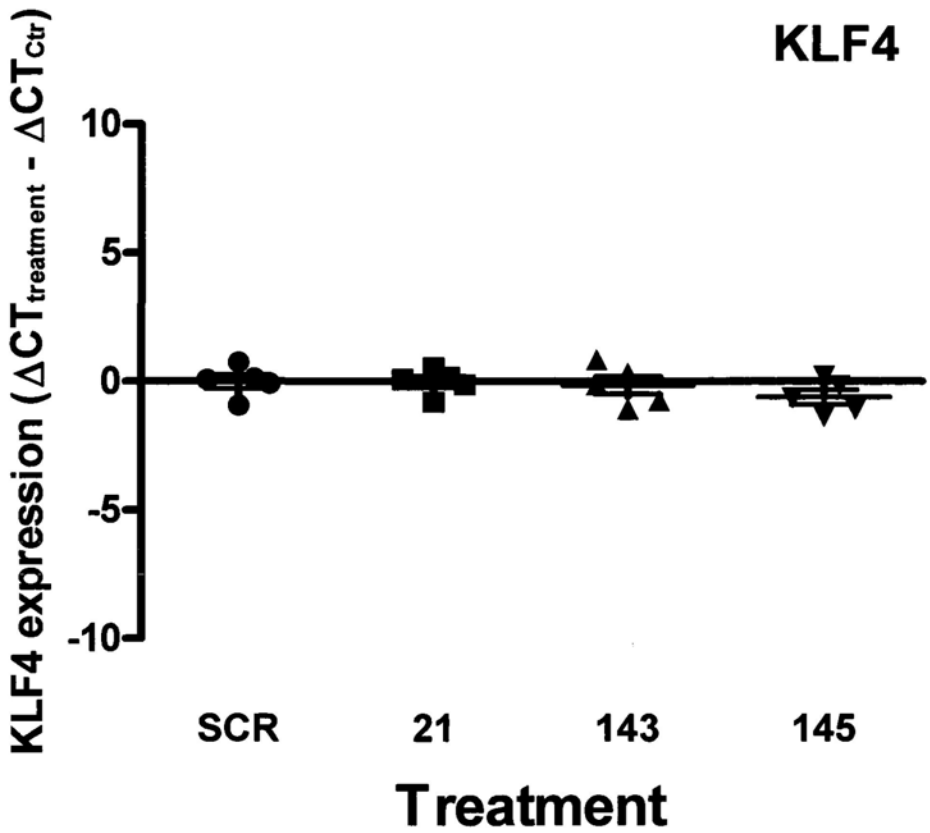

Figure 12.10. qPCR validation of KLF4 expression in scrambled pre-miR (SCR), pre-miR-21 (21), pre-miR-143 (143) and pre-miR-145 (145) transfected HCE cells. Kruskal Wallis test, * $p < 0.05$.

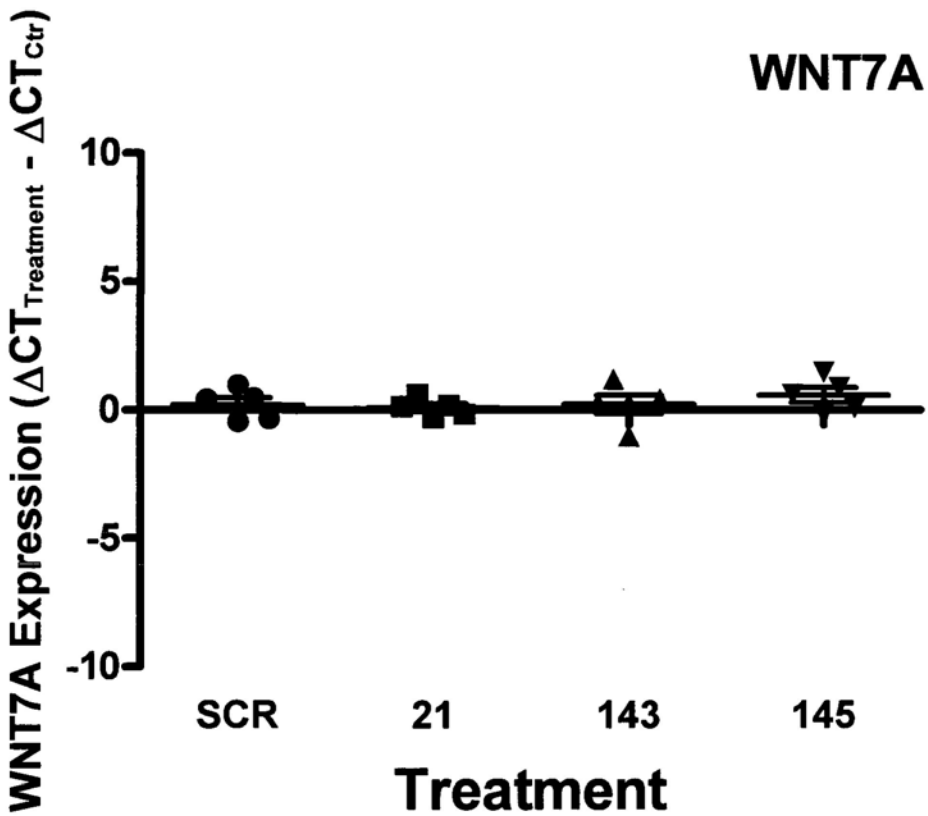

Figure 12.11. qPCR validation of WNT7a expression in scrambled pre-miR (SCR), pre-miR-21 (21), pre-miR-143 (143) and pre-miR-145 (145) transfected HCE cells. Kruskal Wallis test, * $p < 0.05$.

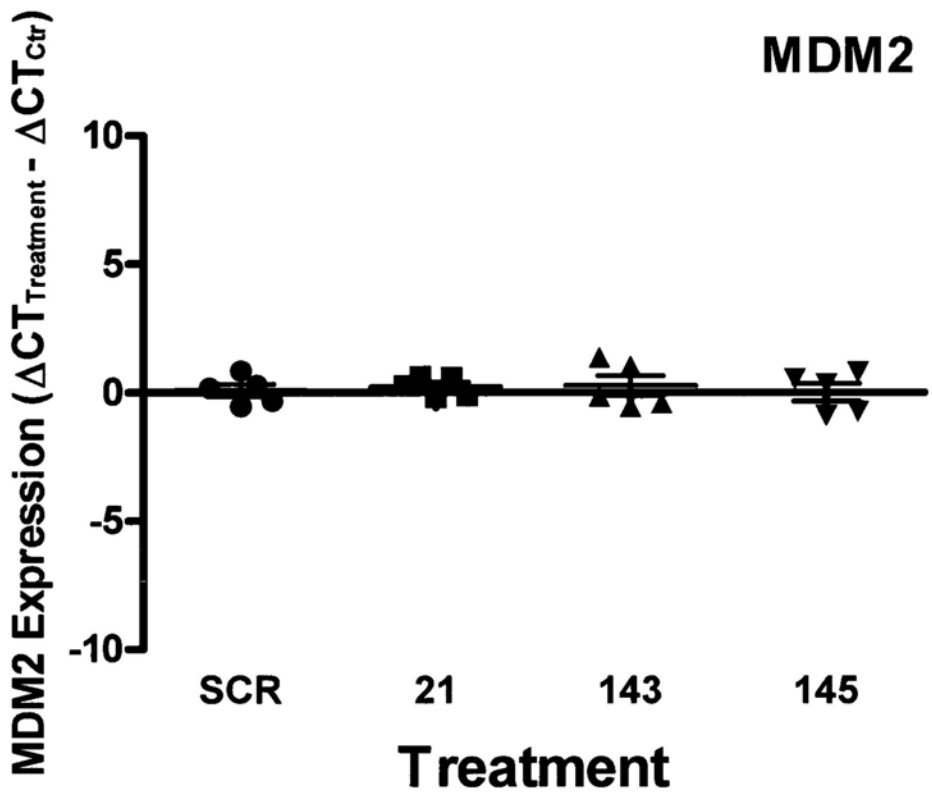

Figure 12.12. qPCR validation of MDM2 expression in scrambled pre-miR (SCR), pre-miR-21 (21), pre-miR-143 (143) and pre-miR-145 (145) transfected HCE cells. Kruskal Wallis test, * $p < 0.05$.

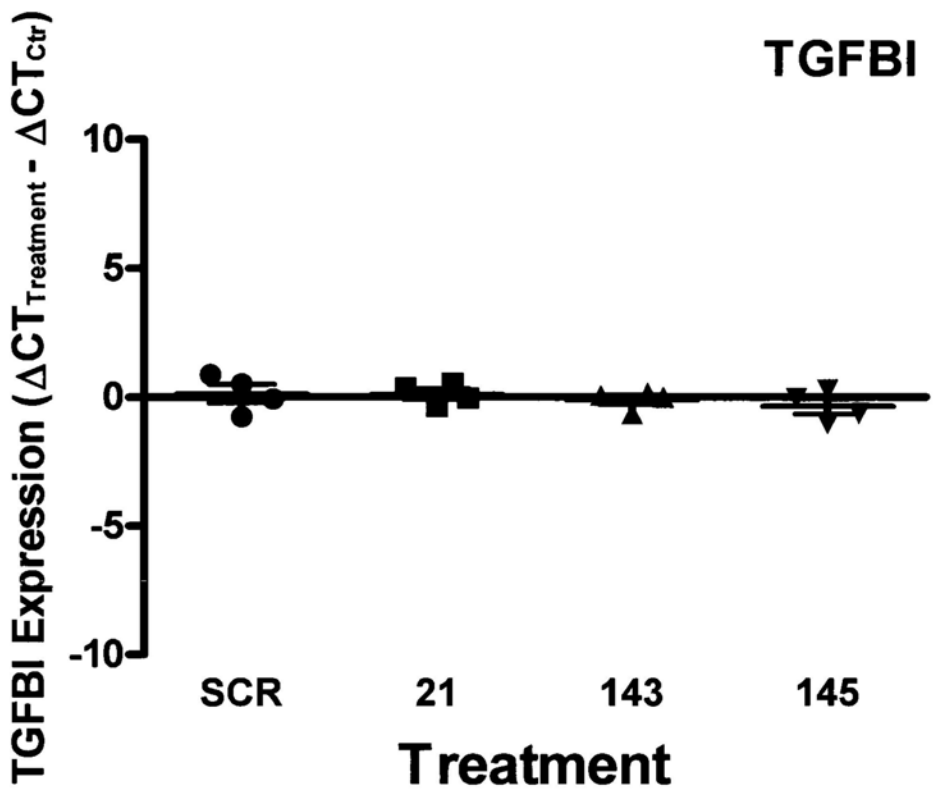

Figure 12.13. qPCR validation of TGFBI expression in scrambled pre-miR (SCR), pre-miR-21 (21), pre-miR-143 (143) and pre-miR-145 (145) transfected HCE cells. Kruskal Wallis test, * $p < 0.05$.

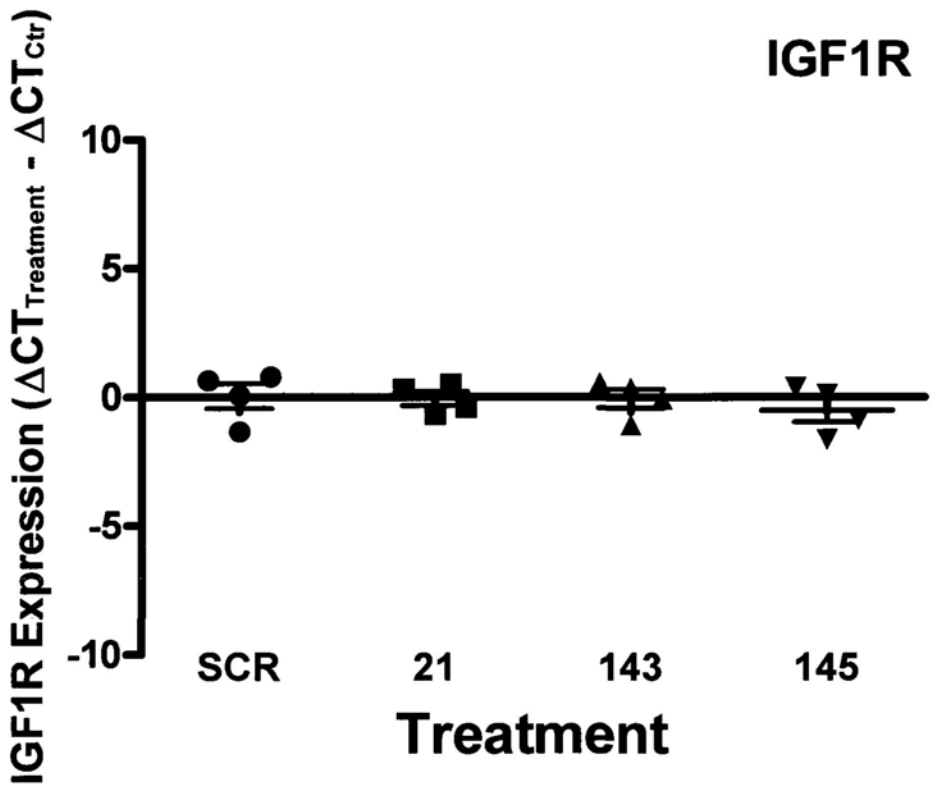

Figure 12.14. qPCR validation of IGF1R expression in scrambled pre-miR (SCR), pre-miR-21 (21), pre-miR-143 (143) and pre-miR-145 (145) transfected HCE cells. Kruskal Wallis test, * $p < 0.05$.

Part IV
Further Study and Conclusion

13

Further Study

13.1. Significance and Overview

The findings presented above shed lights on the possibility that limbus specific microRNA possess regulatory functions on CEPC. However, further experiments are suggested for depicting the roles of these candidates in details, which includes,

(a) confirming the role of miR-145 on IFNBI upregulation by protein analysis;

(b) elucidating the downstream or upstream genes in pathways that IFNBI involved (IFN/Toll receptor pathways, Role of AP-1 in regulation of cellular metabolism, and IFN alpha/beta signaling pathway);

(c) validating the remaining miRNA prediction targets obtained from the gene and transcription microarray;

(d) characterising miR-21, 143 and 145 over-expressed cells through the transfection of GFP-conjugated Human pre-microRNA Expression Construct (SBI);

(e) long term culture of human CEPC for expanding the therapeutic application of our candidate miRNAs to be the functional marker for CEPC culture before transplant;

(f) characterizing CEPC which is sorted by the four parameter sorting method as

described in Chapter 7;

(g) defining the role of miR-145 as a small molecule therapeutics in cell based treatment;

(h) discerning the role of miRNAs, possibly miR-21 and 143, in toll-like receptor regulation in cornea neovascularisation model;

(i) comparing the expression of miR-145 in limbal epithelium to miR-145 expression in colorectal tumors - because colorectal cancer also originates from epithelial cells but lining the gastrointestinal tract. We hope to shed lights on one of our long term goals of the present microRNA study, which is to use limbal epithelial stem cells, or CEPC that we have been using in this thesis, to be the model cell for understanding better cancer biology (Please refer to Chapter 5, section 5.2.3).

Of the above eight suggestions, a number of them have actually been underway and the methods are setting up. Some of the set ups are worth discussion here.

13.2. Characterising miR-21, 143 and 145 over-expressed cells through the transfection of GFP conjugated human pre-microRNA expression construct

Although the use of short double stranded precursor microRNA in the present study has enabled efficient transfection, we are unable to identify the cell which has high endogenous amount of the transfected microRNA and which has a change in

morphology and or protein expression. As the next step to validate our findings, we performed transfection by using GFP-conjugated human pre-microRNA expression lenti-vector construct for overexpressing microRNAs. From our preliminary results, we found that the transfection efficiency for expression lenti-miR-143 and lenti-miR-145 constructs was less than 1 % in HCE cells. But in cells transfected with lenti-miR-145, we discerned a few populations of cells which resemble colony morphology as depicted in Figure 11.1 in Day 3. The protocol needs further optimization.

13.3. Setting up the long term culture of human corneal epithelial cells

Cornea is always precious especially in the Chinese population. Cultured CEPC has been used as a source of cells for treating limbal stem cell deficiency. However, CEPC must be characterized before transplanting onto patient's eye. We attempt to establish microRNA as one of the markers for assessing CEPC quality before transplantation. Furthermore, we would like to evaluate any change in miRNA expression in long term culture for better understanding CEPC biology. To begin with, we have reviewed all the media that are currently avaliable for CEPC culture, including CNT20, CNT30, CNT50, defined KSFM, KSFM supplemented, SHEM and LS medium. From Figure 11.2, we observed that CEPC cultured in CNT20 for two weeks could grow cohesively into a colony (Figure 11.2A). However, for CEPC cultured in other media, for example, SHEM, were more wide spread and polarized. Figure 11.3A-D shows the morphology and characteristic of human CEPC culturing in CNT20 medium for four weeks. We

noted that the cells remained proliferative and cobblestone shape, expressed stem cell marker vimentin (Figure 11.3C) and alpha-enolase (Figure 11.3D) but not the differentiation marker Cx43 (Figure 11.3B). On the contrary, we discerned that SHEM induced expression of differentiation marker CK3/12 in human CEPC culture (Figure 11.3E). As shown in Figure 11.4, HCE cells cultured in CNT20 for four weeks could maintain Notch1 expression, as substantiated from the the immunostaining and Western blot analysis. In addition, after four weeks culture of the primary human CEPC in CNT20, half of the cells could abid to G0/G1 phase (red peak in the histogram of Figure 11.5) and preserved their proliferation potential. We therefore will use CNT20 as our medium for culturing human CEPC in further experiments.

13.4. Defining the role of miRNAs in toll-like receptor regulation in cornea neovascularisation model

Being the most external ocular surface, cornea has its own rapidly deployable innate immune system to evade pathogens. Important components of this immune system include the physical barrier to pathogen entry, the presence of antimicrobial molecules in the tear film, and pattern recognition receptors such as the cellular toll-like receptors (TLRs). Activation of TLRs promotes the release of cytokines, chemokines, and other molecules, which participate in inflammatory responses that coupled with increase vascular permeability and blood flow to the affected area, initiated by regional vasodilation and followed by enhanced angiogenesis to facilitate the wound healing process (Frantz et al., 2005). Two microRNAs are now known to be the regulator of

TLRs, including miR-105, which modulates TLR2 protein expression in human oral keratinocytes (Benakanakere et al., 2009), and let-7i, which controls TLR4 in human biliary epithelial cells (Chen et al., 2007a). Giving these miRNAs regulate TLRs exclusively in cells belonging to the epidermis, we here speculate that microRNAs may also regulate TLRs in mammalian corneal epithelial cells and may shed light on the unexplained role of miR-21 and 143 in limbal epithelium in this study.

To begin with, we first set up a chemical injury model as a cause for cornea neovascularisation and so angiogenesis in the cornea. Figure 11.5 shows the procedures that we have established. Briefly, right eye of the anesthetized mice was dipped in silver nitrate and potassium nitrate at appropriate concentration for less than 10 seconds. Any excess chemicals were washed away in large amount of water and the mice were warmed during recovery period. After five days when cornea angiogensis appeared, we collected the singlet cornea epithelial cells by using the procedures as described in Chapter 2. The cells were analysed by flow cytometry to observe any changes in cell size and TLR expression between the untreated and injuried eye. As shown in Figure 11.6, we found that the expression of TLR2 and TLR6 were increased in injuried eye when compared to the untreated control. The FSC and SSC plot in Figure 11.7 suggested that cells of larger size, which were likely the central cornea epithelial cell that we have injuried, were much reduced. In addition, cells stained with TLR2 were throughout the collected corneal epithelial cell population; however, cells expressing TLR6 were limited to the smaller cell population, which may be the cells at the limbus region and so the CEPC. For the other TLRs, including TLR3 and 4, we

could not obtain observable difference between the untreated and injuried eye, though its expression has been reported in cornea inflammation (Johnson et al., 2008; Rodriguez-Martinez et al., 2006).

Interestingly, co-expression of TLR2 and TLR6 substantiates the theory that TLR2 form heteromers with TLR6 to attain specificity for the diverse bacterial lipopeptides repertoire (Ozinsky et al., 2000; Takeuchi et al., 2001). Hise et al stated that activation of TLR2/TLR6 responses in the cornea could lead to infiltration of neutrophils to the corneal stroma (Hise et al., 2007), and TLR2 alone or the TLR2/TLR6 complex can regulate the production of IFN-gamma (Benson and Ernst, 2009; Weigt et al., 2004), which is a molecule pertaining to the family of IFNβ. This results therefore form the basis for our further study in defining the roles of microRNAs in corneal TLRs.

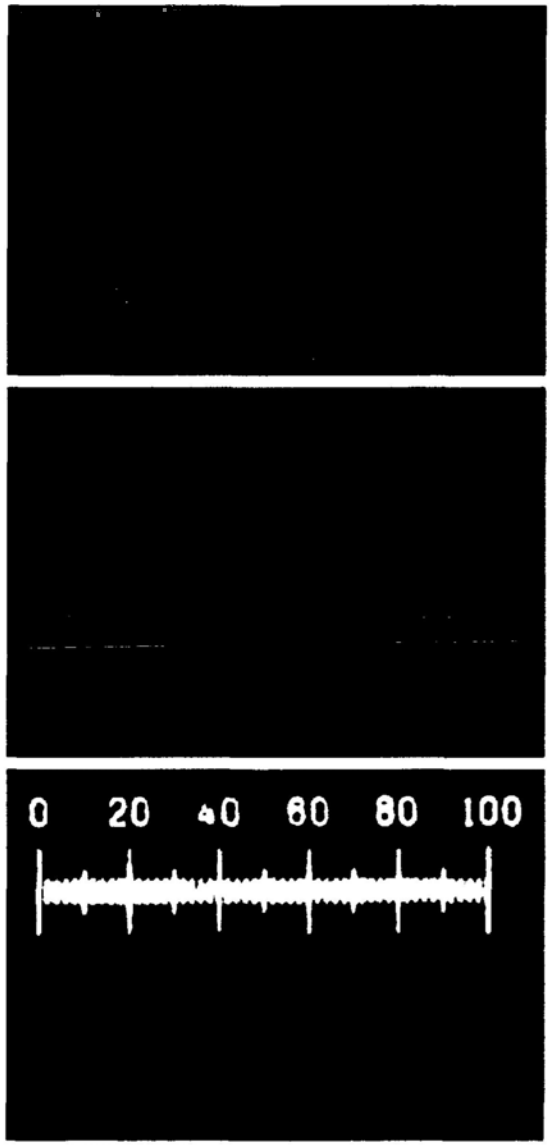

Figure 13.1. Morphology of cells transfected with human pre-microRNA expression construct lenti-miR-145.

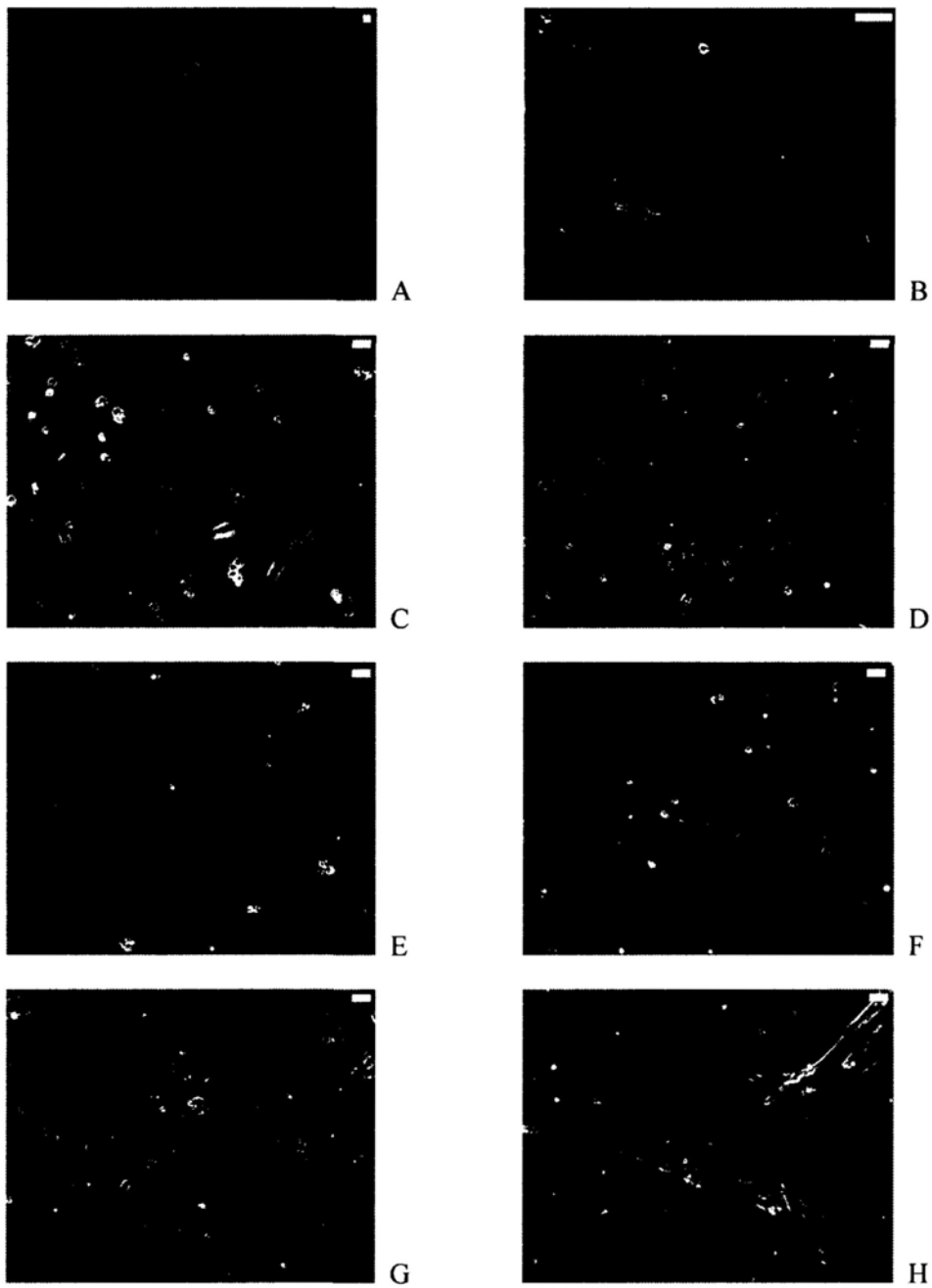

Figure 13.2. Cells culturing in different media present different morphology. A, and B, CNT20, C, CNT30, D, CNT50, E, defined KSFM, F, KSFM supplmented, G, SHEM, H, LS medium. Bar, 20μm.

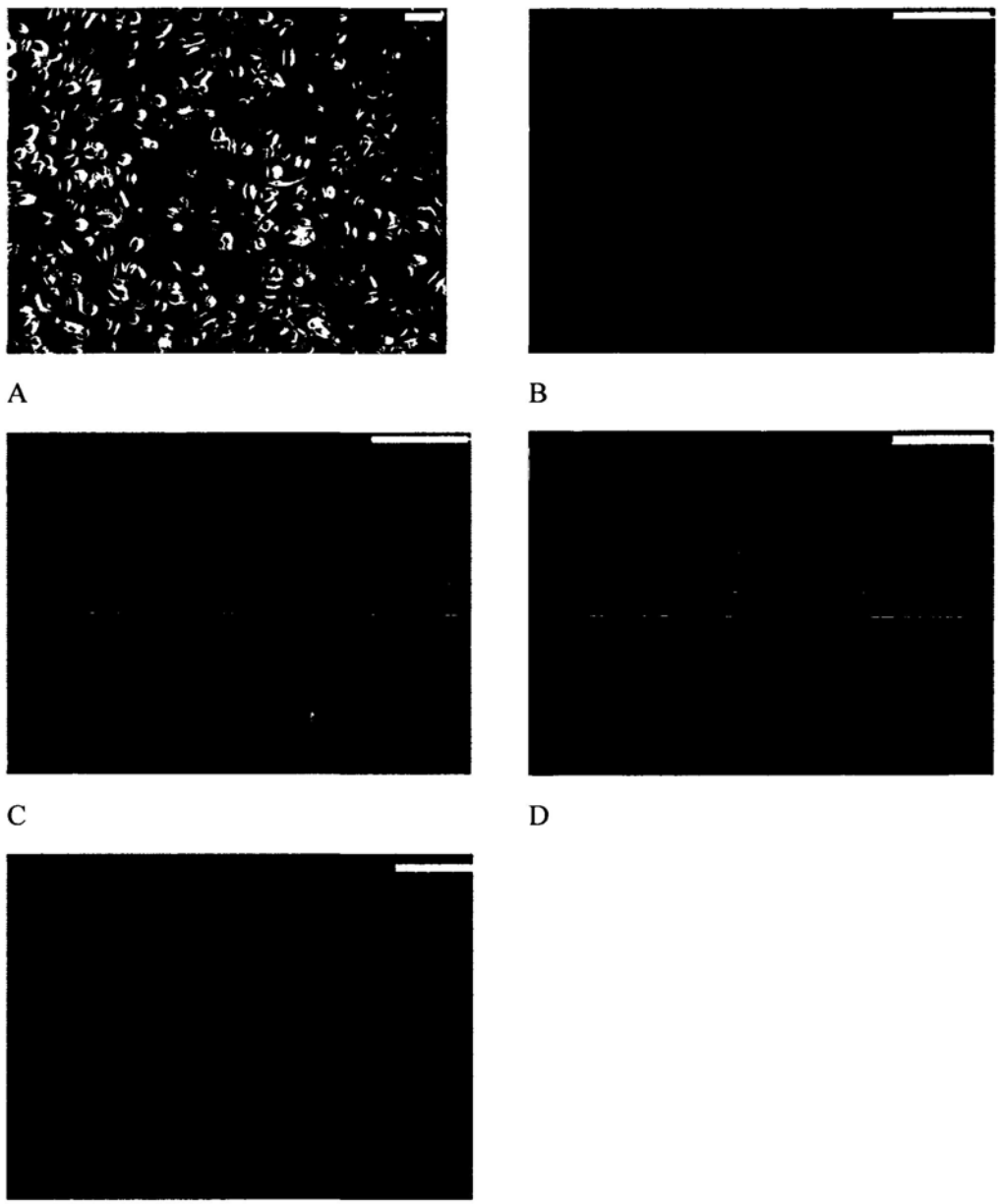

Figure 13.3. Morphology and characteristic of human CEPC culturing in CNT20 medium for 4 weeks. (A) morphology under phase contrast microscope; immunostaining of (B) Cx43, (C) vimentin, (D) alpha-enolase; (E) positive immunostaining of CK3/12 of human CEPC culturing in SHEM. Bar, 20 μm.

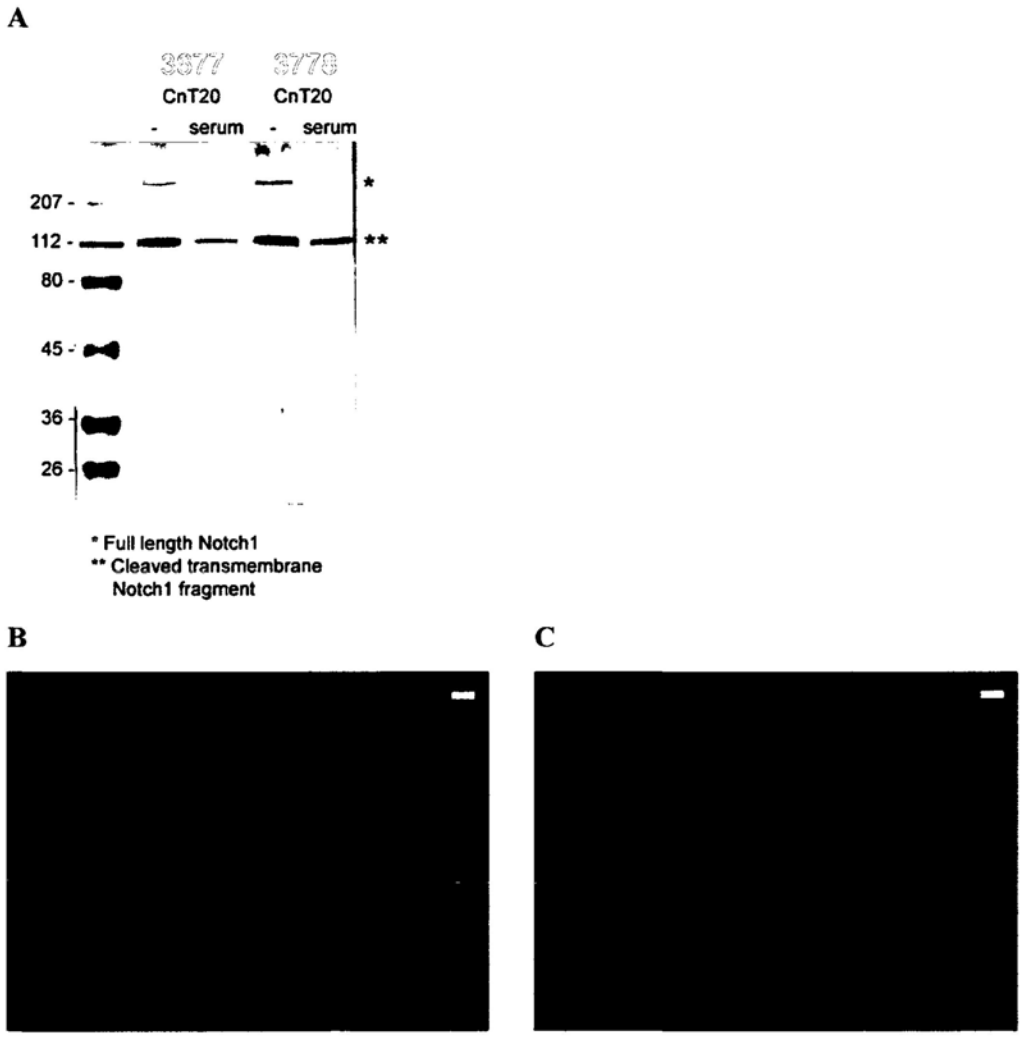

Figure 13.4. Expression of Notch1 in CEPC culturing in CNT20 for four weeks.

(A) Western blot showing the expression of Notch1 in CEPC culturing in supplemented and unsupplmented CNT20 medium; (B) and (C) immunostaining of Notch1 (green) and DAPI (blue) in CEPC cultured in CNT20 medium , 20x. Bar, 20 μm.

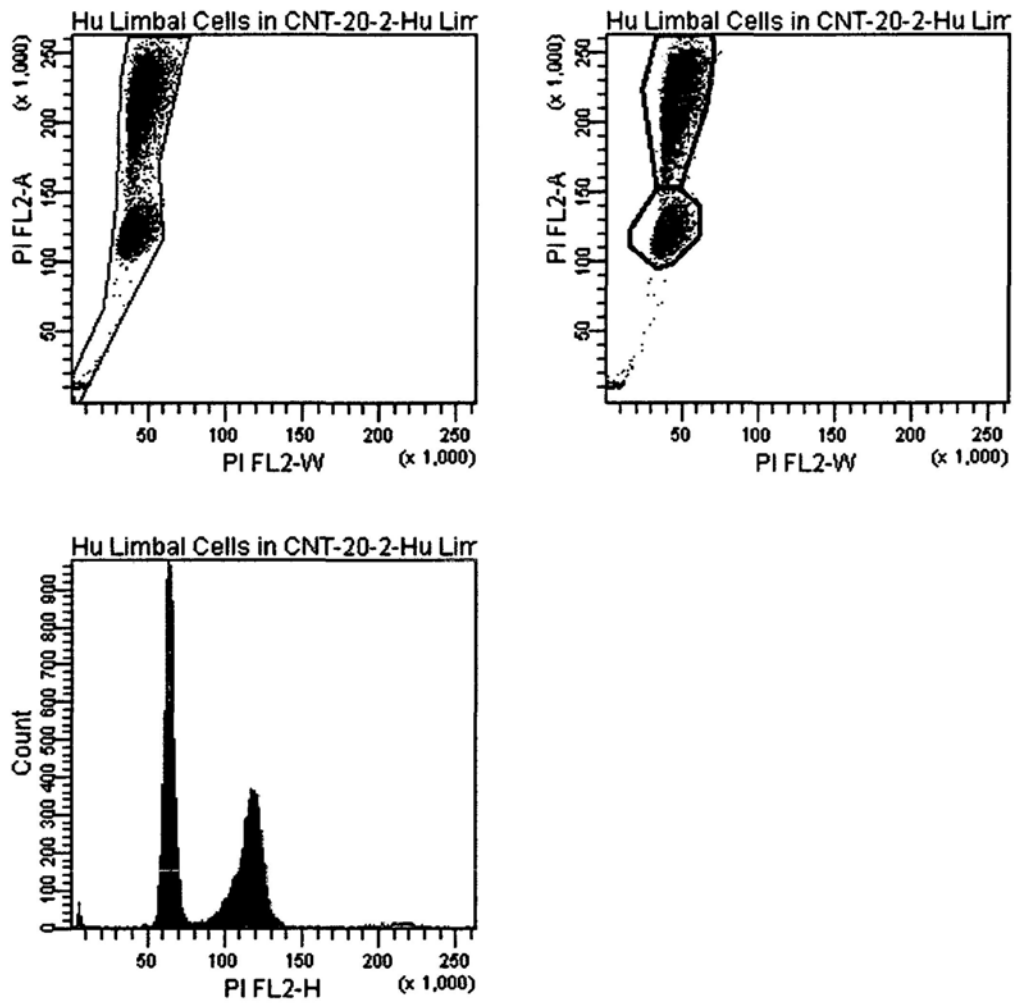

Figure 13.5. Cell cycle of human CEPC cultured for 4 weeks in CNT20 medium, n=1.

1

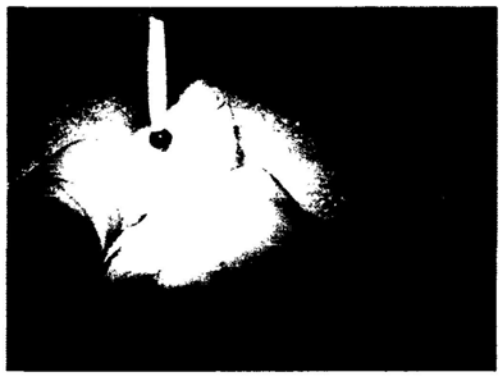

2

3

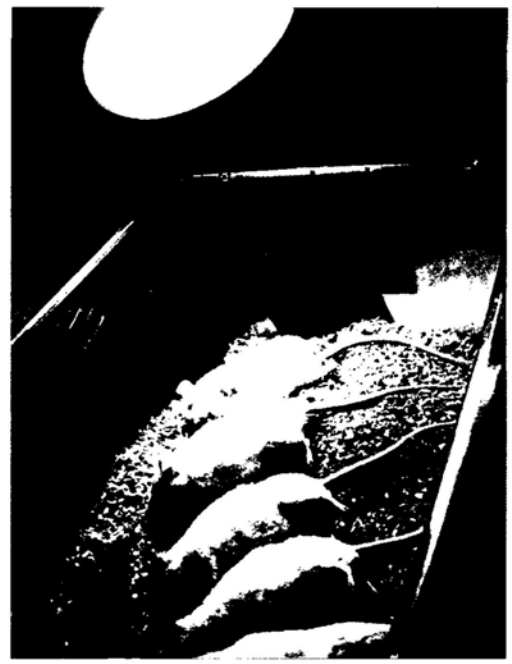

4

Figure 13.6. Procedures for inducing chemical injuries in our animal model using BALB/c mice.

(1) Anesthetize mice systemically with 1:1 xylaxine and ketamine and locally with one to two drops AlconeTM Alcaine; (2) Soak cotton bud with 75 % silver nitrate and 25 % potassium nitrate. Apply on the central cornea for aroud 10s; (3) Rinse cornea with water; (4) Warm mice under lamp during their recovery period.

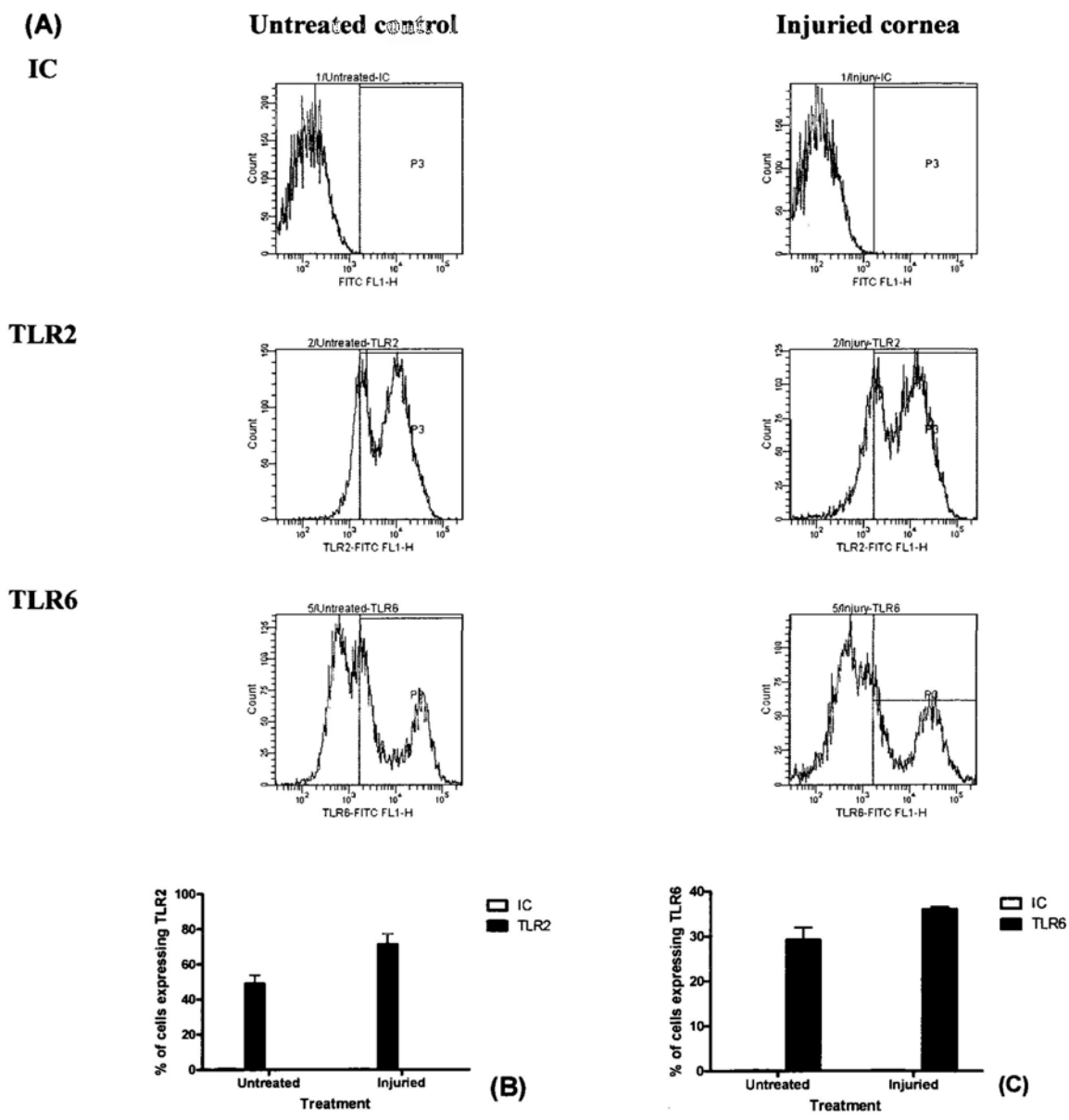

Figure 13.7. Toll-like receptors 2 and 6 expression in cornea epithelial cells.

(A) Flow cytometry histogram analysis showing the expression of Toll-like receptors 2 and 6 in untreated control and injuried cornea. (B) Bar graph showing the percentage of cells expressing TLR2 in untreated and injuried cornea. (C) Bar graph showing the percentage of cells expressing TLR6 in untreated and injuried cornea, n=2.

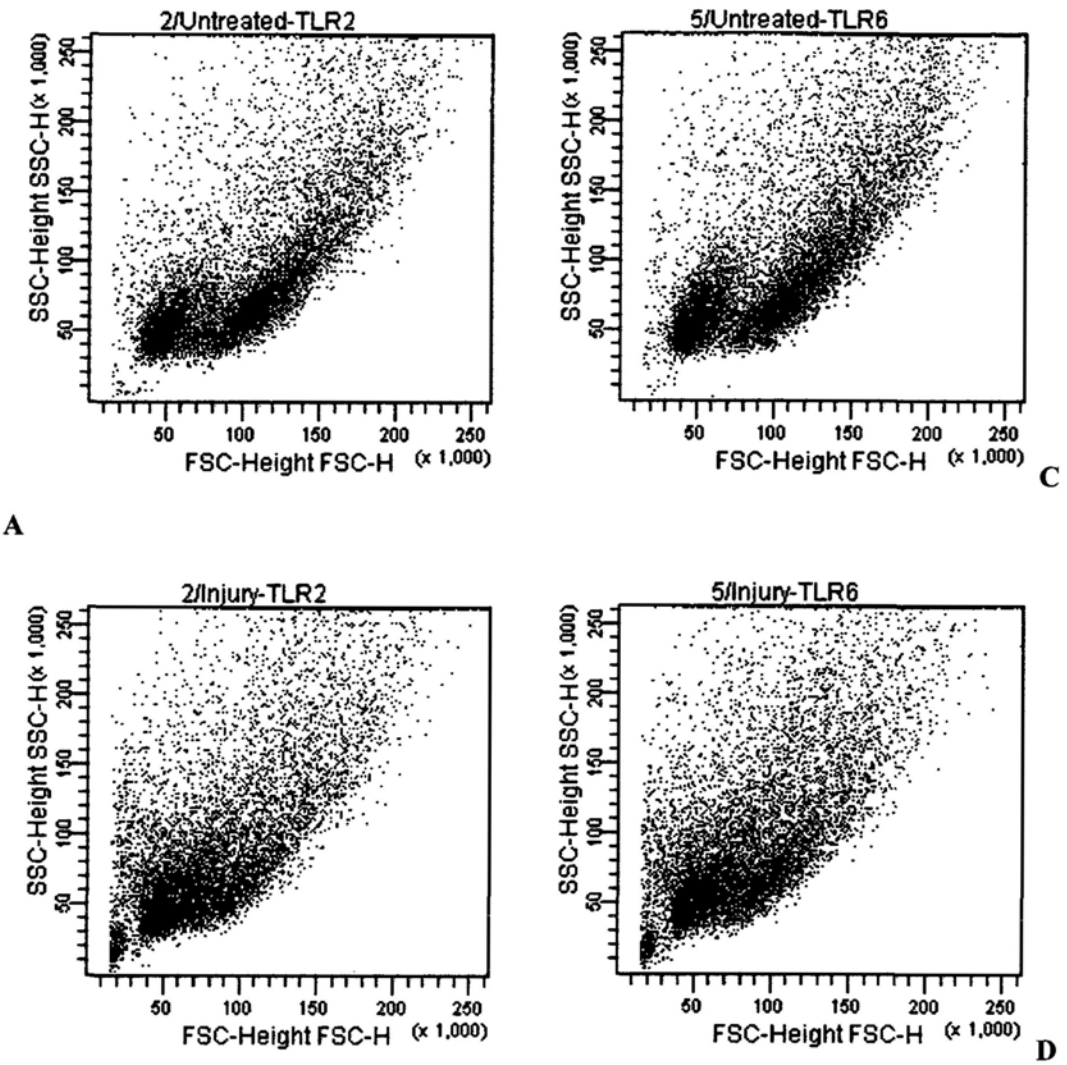

Figure 13.8. Flow cytometry analysis showing the relations of cell size and toll-like receptor expression in injuried and untreated cells.

A to D represents forward scatter (FSC) and side scatter (SSC) dot plots of (A,B) TLR2 and (C,D) TLR6 in (A,C) untreated control and (B,D) injuried cornea. The blue population indicates cells stained positively with either (A,B) TLR2 or (C,D) TLR6.

14

Summary and Conclusion

In this thesis, series of experiments elucidating the anatomical distribution and functional roles of microRNAs on the human cornea rims were performed with the aim to testifying the proposition that microRNAs participate in human cornea epithelial cell maintenance. To begin with, I first validated the morphology and phenotype of the human cornea rims collected from the Chinese Hong Kong population, followed by the development of several protocols which aim at enriching CEPC for further assays. For the first time a four parameter cell sorting system was devised which was envisaged as a useful tool in the prospective in vitro study. Likewise, three novel microRNAs (hsa-miR-21, 143 and 145) were identified to be precisely upregulated in the limbus region. Functionally miR-145 was shown to inhibit cell proliferation and generate small discrete ball-like colonies resembling holoclones in differenting human cornea epithelial cells. The downstream target of miR-145 was identified to be interferon beta 1 (IFNB1). These unprecedented results suggest miR-145 a faithful candidate for CEPC maintenance especially among the other two limbal microRNAs singled out in this thesis, possibly with the main function to inhibit cell growth through the indirect regulation of IFNB1 or its related pathway. Further research on the upstream and downstream target of IFNB1 are suggested, with the perspective to open up and decipher a novel cellular pathway that miR-145 is

participated. The regulatory functions of miR-145 on cell proliferation and survival has also suggested it a possible eyedrop therapy for limbal stem cell deficiency. Since I have also established the relations between miR-145, IFNB1 and cancer from literatures and our experimental results, miR-145 may be a useful switch in controlling the aberrantly regulated cancer stem cells. Further study on miR-145 in both healthy and cancerous limbal cells may help to unravel the myths of the origin of tumors cells and so to devise therapy in combating with the formidable cancers.

Bibliography

Akao, Y., Nakagawa, Y., Iio, A., and Naoe, T. (2009). Role of microRNA-143 in Fas-mediated apoptosis in human T-cell leukemia Jurkat cells. Leuk Res *33*, 1530-1538.

Akao, Y., Nakagawa, Y., Kitade, Y., Kinoshita, T., and Naoe, T. (2007). Downregulation of microRNAs-143 and -145 in B-cell malignancies. Cancer Sci *98*, 1914-1920.

Amaral, F.C., Torres, N., Saggioro, F., Neder, L., Machado, H.R., Silva, W.A., Jr., Moreira, A.C., and Castro, M. (2009). MicroRNAs differentially expressed in ACTH-secreting pituitary tumors. J Clin Endocrinol Metab *94*, 320-323.

Anderson, C., Catoe, H., and Werner, R. (2006). MIR-206 regulates connexin43 expression during skeletal muscle development. Nucleic Acids Res *34*, 5863-5871.

Arndt, G.M., Dossey, L., Cullen, L.M., Lai, A., Druker, R., Eisbacher, M., Zhang, C., Tran, N., Fan, H., Retzlaff, K., *et al.* (2009). Characterization of global microRNA expression reveals oncogenic potential of miR-145 in metastatic colorectal cancer. BMC Cancer *9*, 374.

Arpitha, P., Prajna, N.V., Srinivasan, M., and Muthukkaruppan, V. (2008a). A method to isolate human limbal basal cells enriched for a subset of epithelial cells with a large nucleus/cytoplasm ratio expressing high levels of p63. Microsc Res Tech *71*, 469-476.

Arpitha, P., Prajna, N.V., Srinivasan, M., and Muthukkaruppan, V. (2008b). A subset of human limbal epithelial cells with greater nucleus-to-cytoplasm ratio expressing high levels of p63 possesses slow-cycling property. Cornea *27*, 1164-1170.

Asangani, I.A., Rasheed, S.A., Nikolova, D.A., Leupold, J.H., Colburn, N.H., Post, S., and Allgayer, H. (2008). MicroRNA-21 (miR-21) post-transcriptionally downregulates tumor suppressor Pdcd4 and stimulates invasion, intravasation and metastasis in colorectal cancer. Oncogene *27*, 2128-2136.

Aschrafi, A., Schwechter, A.D., Mameza, M.G., Natera-Naranjo, O., Gioio, A.E., and Kaplan, B.B. (2008). MicroRNA-338 regulates local cytochrome c oxidase IV mRNA levels and oxidative phosphorylation in the axons of sympathetic neurons. J Neurosci *28*, 12581-12590.

Avissar, M., McClean, M.D., Kelsey, K.T., and Marsit, C.J. (2009). MicroRNA Expression in Head and Neck Cancer Associates with Alcohol Consumption and Survival. Carcinogenesis *30*, 2059-63.

Bagga, S., Bracht, J., Hunter, S., Massirer, K., Holtz, J., Eachus, R., and Pasquinelli, A.E. (2005). Regulation by let-7 and lin-4 miRNAs results in target mRNA degradation. Cell *122*, 553-563.

Bandres, E., Cubedo, E., Agirre, X., Malumbres, R., Zarate, R., Ramirez, N., Abajo, A., Navarro, A., Moreno, I., Monzo, M., *et al.* (2006). Identification by Real-time PCR of 13 mature microRNAs differentially expressed in colorectal cancer and non-tumoral tissues. Mol Cancer *5*, 29.

Barroso-del Jesus, A., Lucena-Aguilar, G., and Menendez, P. (2009). The miR-302-367 cluster as a potential stemness regulator in ESCs. Cell Cycle *8*, 394-398.

Bartel, D.P. (2004). MicroRNAs: genomics, biogenesis, mechanism, and function. Cell *116*, 281-297.

Basyuk, E., Suavet, F., Doglio, A., Bordonne, R., and Bertrand, E. (2003). Human let-7 stem-loop precursors harbor features of RNase III cleavage products. Nucleic Acids Res *31*, 6593-6597.

Benakanakere, M.R., Li, Q., Eskan, M.A., Singh, A.V., Zhao, J., Galicia, J.C., Stathopoulou, P., Knudsen, T.B., and Kinane, D.F. (2009). Modulation of TLR2 protein expression by miR-105 in human oral keratinocytes. J Biol Chem *284*, 23107-23115.

Benson, S.A., and Ernst, J.D. (2009). TLR2-dependent inhibition of macrophage responses to IFN-gamma is mediated by distinct, gene-specific mechanisms. PLoS One *4*, e6329.

Bernstein, E., Caudy, A.A., Hammond, S.M., and Hannon, G.J. (2001). Role for a bidentate ribonuclease in the initiation step of RNA interference. Nature *409*, 363-366.

Bernstein, E., Kim, S.Y., Carmell, M.A., Murchison, E.P., Alcorn, H., Li, M.Z., Mills, A.A., Elledge, S.J., Anderson, K.V., and Hannon, G.J. (2003). Dicer is essential for mouse development. Nat Genet *35*, 215-217.

Bhatt, R.I., Brown, M.D., Hart, C.A., Gilmore, P., Ramani, V.A., George, N.J., and Clarke, N.W. (2003). Novel method for the isolation and characterisation of the putative prostatic stem cell. Cytometry A *54*, 89-99.

Blake, C.R., Lai, W.W., and Edward, D.P. (2003). Racial and ethnic differences in ocular anatomy. Int Ophthalmol Clin *43*, 9-25.

Bohnsack, M.T., Czaplinski, K., and Gorlich, D. (2004). Exportin 5 is a RanGTP-dependent dsRNA-binding protein that mediates nuclear export of pre-miRNAs. RNA *10*, 185-191.

Borchert, G.M., Lanier, W., and Davidson, B.L. (2006). RNA polymerase III transcribes human microRNAs. Nat Struct Mol Biol *13*, 1097-1101.

Borralho, P.M., Kren, B.T., Castro, R.E., Moreira da Silva, I.B., Steer, C.J., and Rodrigues, C.M. (2009). MicroRNA-143 reduces viability and increases sensitivity to 5-fluorouracil in HCT116 human colorectal cancer cells. FEBS J. Epub ahead of print.

Brennecke, J., Hipfner, D.R., Stark, A., Russell, R.B., and Cohen, S.M. (2003). bantam encodes a developmentally regulated microRNA that controls cell proliferation and regulates the proapoptotic gene hid in Drosophila. Cell *113*, 25-36.

Bruchova, H., Merkerova, M., and Prchal, J.T. (2008). Aberrant expression of microRNA in polycythemia vera. Haematologica *93*, 1009-1016.

Bruchova, H., Yoon, D., Agarwal, A.M., Mendell, J., and Prchal, J.T. (2007). Regulated expression of microRNAs in normal and polycythemia vera erythropoiesis. Exp Hematol *35*, 1657-1667.

Bruchova, H., Yoon, D., Agarwal, A.M., Swierczek, S., and Prchal, J.T. (2009).

Erythropoiesis in polycythemia vera is hyper-proliferative and has accelerated maturation. Blood Cells Mol Dis *43*, 81-87.

Brueckner, B., Stresemann, C., Kuner, R., Mund, C., Musch, T., Meister, M., Sultmann, H., and Lyko, F. (2007). The human let-7a-3 locus contains an epigenetically regulated microRNA gene with oncogenic function. Cancer Res *67*, 1419-1423.

Buck, R.C. (1979). Cell migration in repair of mouse corneal epithelium. Invest Ophthalmol Vis Sci *18*, 767-784.

Budak, M.T., Alpdogan, O.S., Zhou, M., Lavker, R.M., Akinci, M.A., and Wolosin, J.M. (2005). Ocular surface epithelia contain ABCG2-dependent side population cells exhibiting features associated with stem cells. J Cell Sci *118*, 1715-1724.

Cai, X., Hagedorn, C.H., and Cullen, B.R. (2004). Human microRNAs are processed from capped, polyadenylated transcripts that can also function as mRNAs. RNA *10*, 1957-1966.

Calabrese, J.M., Seila, A.C., Yeo, G.W., and Sharp, P.A. (2007). RNA sequence analysis defines Dicer's role in mouse embryonic stem cells. Proc Natl Acad Sci U S A *104*, 18097-18102.

Cancelas, J.A., Koevoet, W.L., de Koning, A.E., Mayen, A.E., Rombouts, E.J., and Ploemacher, R.E. (2000). Connexin-43 gap junctions are involved in multiconnexin-expressing stromal support of hemopoietic progenitors and stem cells. Blood *96*, 498-505.

Card, D.A., Hebbar, P.B., Li, L., Trotter, K.W., Komatsu, Y., Mishina, Y., and Archer, T.K. (2008). Oct4/Sox2-regulated miR-302 targets cyclin D1 in human embryonic stem cells. Mol Cell Biol *28*, 6426-6438.

Carthew, R.W., and Sontheimer, E.J. (2009). Origins and Mechanisms of miRNAs and siRNAs. Cell *136*, 642-655.

Ceci, M., Gaviraghi, C., Gorrini, C., Sala, L.A., Offenhauser, N., Marchisio, P.C., and Biffo, S. (2003). Release of eIF6 (p27BBP) from the 60S subunit allows 80S ribosome assembly. Nature *426*, 579-584.

Center, R., Lukeis, R., Dietzsch, E., Gillespie, M., and Garson, O.M. (1993). Molecular deletion of 9p sequences in non-small cell lung cancer and malignant mesothelioma. Genes Chromosomes Cancer *7*, 47-53.

Challen, G.A., Boles, N., Lin, K.K., and Goodell, M.A. (2009). Mouse hematopoietic stem cell identification and analysis. Cytometry A *75*, 14-24.

Challen, G.A., and Little, M.H. (2006). A side order of stem cells: the SP phenotype. Stem Cells *24*, 3-12.

Chan, J.A., Krichevsky, A.M., and Kosik, K.S. (2005). MicroRNA-21 is an antiapoptotic factor in human glioblastoma cells. Cancer Res *65*, 6029-6033.

Chan, S.H., Wu, C.W., Li, A.F., Chi, C.W., and Lin, W.C. (2008). miR-21 microRNA expression in human gastric carcinomas and its clinical association. Anticancer Res *28*, 907-911.

Chee, K.Y., Kicic, A., and Wiffen, S.J. (2006). Limbal stem cells: the search for a marker. Clin Experiment Ophthalmol *34*, 64-73.

Chen, H.C., Chen, G.H., Chen, Y.H., Liao, W.L., Liu, C.Y., Chang, K.P., Chang, Y.S., and Chen, S.J. (2009a). MicroRNA deregulation and pathway alterations in nasopharyngeal carcinoma. Br J Cancer *100*, 1002-1011.

Chen, J.F., Mandel, E.M., Thomson, J.M., Wu, Q., Callis, T.E., Hammond, S.M., Conlon, F.L., and Wang, D.Z. (2006). The role of microRNA-1 and microRNA-133 in skeletal muscle proliferation and differentiation. Nat Genet *38*, 228-233.

Chen, X., Guo, X., Zhang, H., Xiang, Y., Chen, J., Yin, Y., Cai, X., Wang, K., Wang, G., Ba, Y., *et al.* (2009b). Role of miR-143 targeting KRAS in colorectal tumorigenesis. Oncogene *28*, 1385-1392.

Chen, X.M., Splinter, P.L., O'Hara, S.P., and LaRusso, N.F. (2007a). A cellular micro-RNA, let-7i, regulates Toll-like receptor 4 expression and contributes to cholangiocyte immune responses against Cryptosporidium parvum infection. J Biol Chem *282*, 28929-28938.

Chen, Y.T., Li, W., Hayashida, Y., He, H., Chen, S.Y., Tseng, D.Y., Kheirkhah, A., and Tseng, S.C. (2007b). Human amniotic epithelial cells as novel feeder layers for promoting ex vivo expansion of limbal epithelial progenitor cells. Stem Cells *25*, 1995-2005.

Chen, Z., de Paiva, C.S., Luo, L., Kretzer, F.L., Pflugfelder, S.C., and Li, D.Q. (2004). Characterization of putative stem cell phenotype in human limbal epithelia. Stem Cells *22*, 355-366.

Chen, Z.H., Zhang, H., and Savarese, T.M. (1996). Gene deletion chemoselectivity: codeletion of the genes for p16(INK4), methylthioadenosine phosphorylase, and the alpha- and beta-interferons in human pancreatic cell carcinoma lines and its implications for chemotherapy. Cancer Res *56*, 1083-1090.

Chendrimada, T.P., Gregory, R.I., Kumaraswamy, E., Norman, J., Cooch, N., Nishikura, K., and Shiekhattar, R. (2005). TRBP recruits the Dicer complex to Ago2 for microRNA processing and gene silencing. Nature *436*, 740-744.

Cheng, L.C., Pastrana, E., Tavazoie, M., and Doetsch, F. (2009). miR-124 regulates adult neurogenesis in the subventricular zone stem cell niche. Nat Neurosci *12*, 399-408.

Cheng, Y., Ji, R., Yue, J., Yang, J., Liu, X., Chen, H., Dean, D.B., and Zhang, C. (2007). MicroRNAs are aberrantly expressed in hypertrophic heart: do they play a role in cardiac hypertrophy? Am J Pathol *170*, 1831-1840.

Choong, M.L., Yang, H.H., and McNiece, I. (2007). MicroRNA expression profiling during human cord blood-derived CD34 cell erythropoiesis. Exp Hematol *35*, 551-564.

Ciafre, S.A., Galardi, S., Mangiola, A., Ferracin, M., Liu, C.G., Sabatino, G., Negrini, M., Maira, G., Croce, C.M., and Farace, M.G. (2005). Extensive modulation of a set of microRNAs in primary glioblastoma. Biochem Biophys Res Commun *334*, 1351-1358.

Clape, C., Fritz, V., Henriquet, C., Apparailly, F., Fernandez, P.L., Iborra, F., Avances, C., Villalba, M., Culine, S., and Fajas, L. (2009). miR-143 interferes with ERK5

signaling, and abrogates prostate cancer progression in mice. PLoS One *4*, e7542.

Cordes, K.R., Sheehy, N.T., White, M.P., Berry, E.C., Morton, S.U., Muth, A.N., Lee, T.H., Miano, J.M., Ivey, K.N., and Srivastava, D. (2009). miR-145 and miR-143 regulate smooth muscle cell fate and plasticity. Nature *460*, 705-710.

Cotsarelis, G., Cheng, S.Z., Dong, G., Sun, T.T., and Lavker, R.M. (1989). Existence of slow-cycling limbal epithelial basal cells that can be preferentially stimulated to proliferate: implications on epithelial stem cells. Cell *57*, 201-209.

Crawford, T.Q., and Roelink, H. (2007). The notch response inhibitor DAPT enhances neuronal differentiation in embryonic stem cell-derived embryoid bodies independently of sonic hedgehog signaling. Dev Dyn *236*, 886-892.

Crick, F. (1970). Central dogma of molecular biology. Nature *227*, 561-563.

Crick, F.H. (1958). On protein synthesis. Symp Soc Exp Biol *12*, 138-163.

Crist, C.G., Montarras, D., Pallafacchina, G., Rocancourt, D., Cumano, A., Conway, S.J., and Buckingham, M. (2009). Muscle stem cell behavior is modified by microRNA-27 regulation of Pax3 expression. Proc Natl Acad Sci U S A *106*, 13383-13387.

Cui, X.S., Zhang, D.X., Ko, Y.G., and Kim, N.H. (2009). Aberrant epigenetic reprogramming of imprinted microRNA-127 and Rtl1 in cloned mouse embryos. Biochem Biophys Res Commun *379*, 390-394.

Dahiya, N., Sherman-Baust, C.A., Wang, T.L., Davidson, B., Shih Ie, M., Zhang, Y., Wood, W., 3rd, Becker, K.G., and Morin, P.J. (2008). MicroRNA expression and identification of putative miRNA targets in ovarian cancer. PLoS One *3*, e2436.

Danesh-Meyer, H.V., and Green, C.R. (2008). Focus on molecules: connexin 43--mind the gap. Exp Eye Res *87*, 494-495.

Davanger, M., and Evensen, A. (1971). Role of the pericorneal papillary structure in renewal of corneal epithelium. Nature *229*, 560-561.

Davoren, P.A., McNeill, R.E., Lowery, A.J., Kerin, M.J., and Miller, N. (2008). Identification of suitable endogenous control genes for microRNA gene expression analysis in human breast cancer. BMC Mol Biol *9*, 76.

de Paiva, C.S., Chen, Z., Corrales, R.M., Pflugfelder, S.C., and Li, D.Q. (2005). ABCG2 transporter identifies a population of clonogenic human limbal epithelial cells. Stem Cells *23*, 63-73.

Deo, M., Yu, J.Y., Chung, K.H., Tippens, M., and Turner, D.L. (2006). Detection of mammalian microRNA expression by in situ hybridization with RNA oligonucleotides. Dev Dyn *235*, 2538-2548.

Dickens, M.P., Fitzgerald, R., and Fischer, P.M. (2009). Small-molecule inhibitors of MDM2 as new anticancer therapeutics. Semin Cancer Biol. Epub ahead of print.

Dijckmeester, W.A., Wijnhoven, B.P., Watson, D.I., Leong, M.P., Michael, M.Z., Mayne, G.C., Bright, T., Astill, D., and Hussey, D.J. (2009). MicroRNA-143 and -205 expression in neosquamous esophageal epithelium following Argon plasma ablation of Barrett's esophagus. J Gastrointest Surg *13*, 846-853.

Dixon-McIver, A., East, P., Mein, C.A., Cazier, J.B., Molloy, G., Chaplin, T., Andrew Lister, T., Young, B.D., and Debernardi, S. (2008). Distinctive patterns of microRNA expression associated with karyotype in acute myeloid leukaemia. PLoS One *3*, e2141.

Djalilian, A.R., Namavari, A., Ito, A., Balali, S., Afshar, A., Lavker, R.M., and Yue, B.Y. (2008). Down-regulation of Notch signaling during corneal epithelial proliferation. Mol Vis *14*, 1041-1049.

Dooley, R.T. (1958). Primary squamous cell carcinoma of the corneal-scleral limbus. J Okla State Med Assoc *51*, 413-414.

Dua, H.S., Miri, A., Alomar, T., Yeung, A.M., and Said, D.G. (2009). The role of limbal stem cells in corneal epithelial maintenance: testing the dogma. Ophthalmology *116*, 856-863.

Dua, H.S., Saini, J.S., Azuara-Blanco, A., and Gupta, P. (2000). Limbal stem cell deficiency: concept, aetiology, clinical presentation, diagnosis and management.

Indian J Ophthalmol *48*, 83-92.

Dua, H.S., Shanmuganathan, V.A., Powell-Richards, A.O., Tighe, P.J., and Joseph, A. (2005). Limbal epithelial crypts: a novel anatomical structure and a putative limbal stem cell niche. Br J Ophthalmol *89*, 529-532.

Duncan, A.W., Rattis, F.M., DiMascio, L.N., Congdon, K.L., Pazianos, G., Zhao, C., Yoon, K., Cook, J.M., Willert, K., Gaiano, N., *et al.* (2005). Integration of Notch and Wnt signaling in hematopoietic stem cell maintenance. Nat Immunol *6*, 314-322.

Durbin, J.E., Hackenmiller, R., Simon, M.C., and Levy, D.E. (1996). Targeted disruption of the mouse Stat1 gene results in compromised innate immunity to viral disease. Cell *84*, 443-450.

Dyrskjot, L., Ostenfeld, M.S., Bramsen, J.B., Silahtaroglu, A.N., Lamy, P., Ramanathan, R., Fristrup, N., Jensen, J.L., Andersen, C.L., Zieger, K., *et al.* (2009). Genomic profiling of microRNAs in bladder cancer: miR-129 is associated with poor outcome and promotes cell death in vitro. Cancer Res *69*, 4851-4860.

Ebato, B., Friend, J., and Thoft, R.A. (1987). Comparison of central and peripheral human corneal epithelium in tissue culture. Invest Ophthalmol Vis Sci *28*, 1450-1456.

Ebato, B., Friend, J., and Thoft, R.A. (1988). Comparison of limbal and peripheral human corneal epithelium in tissue culture. Invest Ophthalmol Vis Sci *29*, 1533-1537.

Edling, C.E., and Hallberg, B. (2007). c-Kit--a hematopoietic cell essential receptor tyrosine kinase. Int J Biochem Cell Biol *39*, 1995-1998.

Elia, L., Quintavalle, M., Zhang, J., Contu, R., Cossu, L., Latronico, M.V., Peterson, K.L., Indolfi, C., Catalucci, D., Chen, J., *et al.* (2009). The knockout of miR-143 and -145 alters smooth muscle cell maintenance and vascular homeostasis in mice: correlates with human disease. Cell Death Differ *16*, 1590-1598.

Esau, C., Kang, X., Peralta, E., Hanson, E., Marcusson, E.G., Ravichandran, L.V., Sun, Y., Koo, S., Perera, R.J., Jain, R., *et al.* (2004). MicroRNA-143 regulates adipocyte differentiation. J Biol Chem *279*, 52361-52365.

Essers, M.A., Offner, S., Blanco-Bose, W.E., Waibler, Z., Kalinke, U., Duchosal, M.A., and Trumpp, A. (2009). IFNalpha activates dormant haematopoietic stem cells in vivo. Nature *458*, 904-908.

Eulalio, A., Huntzinger, E., and Izaurralde, E. (2008). Getting to the root of miRNA-mediated gene silencing. Cell *132*, 9-14.

Eulalio, A., Rehwinkel, J., Stricker, M., Huntzinger, E., Yang, S.F., Doerks, T., Dorner, S., Bork, P., Boutros, M., and Izaurralde, E. (2007). Target-specific requirements for enhancers of decapping in miRNA-mediated gene silencing. Genes Dev *21*, 2558-2570.

Feber, A., Xi, L., Luketich, J.D., Pennathur, A., Landreneau, R.J., Wu, M., Swanson, S.J., Godfrey, T.E., and Litle, V.R. (2008). MicroRNA expression profiles of esophageal cancer. J Thorac Cardiovasc Surg *135*, 255-260; discussion 260.

Felli, N., Fontana, L., Pelosi, E., Botta, R., Bonci, D., Facchiano, F., Liuzzi, F., Lulli, V., Morsilli, O., Santoro, S., *et al.* (2005). MicroRNAs 221 and 222 inhibit normal erythropoiesis and erythroleukemic cell growth via kit receptor down-modulation. Proc Natl Acad Sci U S A *102*, 18081-18086.

Feng, Y., and Simpson, T.L. (2008). Corneal, limbal, and conjunctival epithelial thickness from optical coherence tomography. Optom Vis Sci *85*, E880-883.

Filipowicz, W., Bhattacharyya, S.N., and Sonenberg, N. (2008). Mechanisms of post-transcriptional regulation by microRNAs: are the answers in sight? Nat Rev Genet *9*, 102-114.

Fontana, L., Pelosi, E., Greco, P., Racanicchi, S., Testa, U., Liuzzi, F., Croce, C.M., Brunetti, E., Grignani, F., and Peschle, C. (2007). MicroRNAs 17-5p-20a-106a control monocytopoiesis through AML1 targeting and M-CSF receptor upregulation. Nat Cell Biol *9*, 775-787.

Fountain, J.W., Karayiorgou, M., Ernstoff, M.S., Kirkwood, J.M., Vlock, D.R., Titus-Ernstoff, L., Bouchard, B., Vijayasaradhi, S., Houghton, A.N., Lahti, J., *et al.* (1992a). Homozygous deletions within human chromosome band 9p21 in melanoma.

Proc Natl Acad Sci U S A *89*, 10557-10561.

Fountain, J.W., Karayiorgou, M., Taruscio, D., Graw, S.L., Buckler, A.J., Ward, D.C., Dracopoli, N.C., and Housman, D.E. (1992b). Genetic and physical map of the interferon region on chromosome 9p. Genomics *14*, 105-112.

Frankel, L.B., Christoffersen, N.R., Jacobsen, A., Lindow, M., Krogh, A., and Lund, A.H. (2008). Programmed cell death 4 (PDCD4) is an important functional target of the microRNA miR-21 in breast cancer cells. J Biol Chem *283*, 1026-1033.

Frantz, S., Vincent, K.A., Feron, O., and Kelly, R.A. (2005). Innate immunity and angiogenesis. Circ Res *96*, 15-26.

Fre, S., Huyghe, M., Mourikis, P., Robine, S., Louvard, D., and Artavanis-Tsakonas, S. (2005). Notch signals control the fate of immature progenitor cells in the intestine. Nature *435*, 964-968.

Fujita, S., Ito, T., Mizutani, T., Minoguchi, S., Yamamichi, N., Sakurai, K., and Iba, H. (2008). miR-21 Gene expression triggered by AP-1 is sustained through a double-negative feedback mechanism. J Mol Biol *378*, 492-504.

Fulci, V., Chiaretti, S., Goldoni, M., Azzalin, G., Carucci, N., Tavolaro, S., Castellano, L., Magrelli, A., Citarella, F., Messina, M., *et al.* (2007). Quantitative technologies establish a novel microRNA profile of chronic lymphocytic leukemia. Blood *109*, 4944-4951.

Gabriely, G., Wurdinger, T., Kesari, S., Esau, C.C., Burchard, J., Linsley, P.S., and Krichevsky, A.M. (2008). MicroRNA 21 promotes glioma invasion by targeting matrix metalloproteinase regulators. Mol Cell Biol *28*, 5369-5380.

Georgantas, R.W., 3rd, Hildreth, R., Morisot, S., Alder, J., Liu, C.G., Heimfeld, S., Calin, G.A., Croce, C.M., and Civin, C.I. (2007). CD34+ hematopoietic stem-progenitor cell microRNA expression and function: a circuit diagram of differentiation control. Proc Natl Acad Sci U S A *104*, 2750-2755.

Goldberg, M.F., and Bron, A.J. (1982). Limbal palisades of Vogt. Trans Am Ophthalmol Soc *80*, 155-171.

Goodell, M.A., Brose, K., Paradis, G., Conner, A.S., and Mulligan, R.C. (1996). Isolation and functional properties of murine hematopoietic stem cells that are replicating in vivo. J Exp Med *183*, 1797-1806.

Grishok, A., Pasquinelli, A.E., Conte, D., Li, N., Parrish, S., Ha, I., Baillie, D.L., Fire, A., Ruvkun, G., and Mello, C.C. (2001). Genes and mechanisms related to RNA interference regulate expression of the small temporal RNAs that control C. elegans developmental timing. Cell *106*, 23-34.

Hamilton, A.J., and Baulcombe, D.C. (1999). A species of small antisense RNA in posttranscriptional gene silencing in plants. Science *286*, 950-952.

Han, J., Lee, Y., Yeom, K.H., Kim, Y.K., Jin, H., and Kim, V.N. (2004). The Drosha-DGCR8 complex in primary microRNA processing. Genes Dev *18*, 3016-3027.

Han, J., Lee, Y., Yeom, K.H., Nam, J.W., Heo, I., Rhee, J.K., Sohn, S.Y., Cho, Y., Zhang, B.T., and Kim, V.N. (2006). Molecular basis for the recognition of primary microRNAs by the Drosha-DGCR8 complex. Cell *125*, 887-901.

Hayashi, K., and Kenyon, K.R. (1988). Increased cytochrome oxidase activity in alkali-burned corneas. Curr Eye Res *7*, 131-138.

Hayashi, R., Yamato, M., Sugiyama, H., Sumide, T., Yang, J., Okano, T., Tano, Y., and Nishida, K. (2007). N-Cadherin is expressed by putative stem/progenitor cells and melanocytes in the human limbal epithelial stem cell niche. Stem Cells *25*, 289-296.

He, X., He, L., and Hannon, G.J. (2007). The guardian's little helper: microRNAs in the p53 tumor suppressor network. Cancer Res *67*, 11099-11101.

Higa, K., Shimmura, S., Miyashita, H., Kato, N., Ogawa, Y., Kawakita, T., Shimazaki, J., and Tsubota, K. (2009). N-cadherin in the maintenance of human corneal limbal epithelial progenitor cells in vitro. Invest Ophthalmol Vis Sci *50*, 4640-4645.

Hise, A.G., Daehnel, K., Gillette-Ferguson, I., Cho, E., McGarry, H.F., Taylor, M.J., Golenbock, D.T., Fitzgerald, K.A., Kazura, J.W., and Pearlman, E. (2007). Innate immune responses to endosymbiotic Wolbachia bacteria in Brugia malayi and

Onchocerca volvulus are dependent on TLR2, TLR6, MyD88, and Mal, but not TLR4, TRIF, or TRAM. J Immunol *178*, 1068-1076.

Houbaviy, H.B., Murray, M.F., and Sharp, P.A. (2003). Embryonic stem cell-specific MicroRNAs. Dev Cell *5*, 351-358.

Hu, S.J., Ren, G., Liu, J.L., Zhao, Z.A., Yu, Y.S., Su, R.W., Ma, X.H., Ni, H., Lei, W., and Yang, Z.M. (2008). MicroRNA expression and regulation in mouse uterus during embryo implantation. J Biol Chem *283*, 23473-23484.

Huang, Q., Choy, K.W., Cheung, K.F., Lam, D.S., Fu, W.L., and Pang, C.P. (2003). Genetic alterations on chromosome 19, 20, 21, 22, and X detected by loss of heterozygosity analysis in retinoblastoma. Mol Vis *9*, 502-507.

Huang, X.H., Wang, Q., Chen, J.S., Fu, X.H., Chen, X.L., Chen, L.Z., Li, W., Bi, J., Zhang, L.J., Fu, Q., *et al.* (2009). Bead-based microarray analysis of microRNA expression in hepatocellular carcinoma: miR-338 is downregulated. Hepatol Res *39*, 786-794.

Huttmann, A., Liu, S.L., Boyd, A.W., and Li, C.L. (2001). Functional heterogeneity within rhodamine123(lo) Hoechst33342(lo/sp) primitive hemopoietic stem cells revealed by pyronin Y. Exp Hematol *29*, 1109-1116.

Hutvagner, G., McLachlan, J., Pasquinelli, A.E., Balint, E., Tuschl, T., and Zamore, P.D. (2001). A cellular function for the RNA-interference enzyme Dicer in the maturation of the let-7 small temporal RNA. Science *293*, 834-838.

Ichimi, T., Enokida, H., Okuno, Y., Kunimoto, R., Chiyomaru, T., Kawamoto, K., Kawahara, K., Toki, K., Kawakami, K., Nishiyama, K., *et al.* (2009). Identification of novel microRNA targets based on microRNA signatures in bladder cancer. Int J Cancer *125*, 345-352.

Ikeda, J.I., Morii, E., Kimura, H., Tomita, Y., Takakuwa, T., Hasegawa, J.I., Kim, Y.K., Miyoshi, Y., Noguchi, S., Nishida, T., *et al.* (2006). Epigenetic regulation of the expression of the novel stem cell marker CDCP1 in cancer cells. J Pathol *210*, 75-84.

Iorio, M.V., Ferracin, M., Liu, C.G., Veronese, A., Spizzo, R., Sabbioni, S., Magri, E.,

Pedriali, M., Fabbri, M., Campiglio, M., *et al.* (2005). MicroRNA gene expression deregulation in human breast cancer. Cancer Res *65*, 7065-7070.

Iorio, M.V., Visone, R., Di Leva, G., Donati, V., Petrocca, F., Casalini, P., Taccioli, C., Volinia, S., Liu, C.G., Alder, H., *et al.* (2007). MicroRNA signatures in human ovarian cancer. Cancer Res *67*, 8699-8707.

Itoh, T., Nozawa, Y., and Akao, Y. (2009). MicroRNA-141 and -200a are involved in bone morphogenetic protein-2-induced mouse pre-osteoblast differentiation by targeting distal-less homeobox 5. J Biol Chem *284*, 19272-19279.

Ji, R., Cheng, Y., Yue, J., Yang, J., Liu, X., Chen, H., Dean, D.B., and Zhang, C. (2007). MicroRNA expression signature and antisense-mediated depletion reveal an essential role of MicroRNA in vascular neointimal lesion formation. Circ Res *100*, 1579-1588.

Jiang, L., Li, J., and Song, L. (2009). Bmi-1, stem cells and cancer. Acta Biochim Biophys Sin (Shanghai) *41*, 527-534.

Jin, Z.B., Hirokawa, G., Gui, L., Takahashi, R., Osakada, F., Hiura, Y., Takahashi, M., Yasuhara, O., and Iwai, N. (2009). Targeted deletion of miR-182, an abundant retinal microRNA. Mol Vis *15*, 523-533.

Johannsdottir, H.K., Jonsson, G., Johannesdottir, G., Agnarsson, B.A., Eerola, H., Arason, A., Heikkila, P., Egilsson, V., Olsson, H., Johannsson, O.T., *et al.* (2006). Chromosome 5 imbalance mapping in breast tumors from BRCA1 and BRCA2 mutation carriers and sporadic breast tumors. Int J Cancer *119*, 1052-1060.

Johnnidis, J.B., Harris, M.H., Wheeler, R.T., Stehling-Sun, S., Lam, M.H., Kirak, O., Brummelkamp, T.R., Fleming, M.D., and Camargo, F.D. (2008). Regulation of progenitor cell proliferation and granulocyte function by microRNA-223. Nature *451*, 1125-1129.

Johnson, A.C., Li, X., and Pearlman, E. (2008). MyD88 functions as a negative regulator of TLR3/TRIF-induced corneal inflammation by inhibiting activation of c-Jun N-terminal kinase. J Biol Chem *283*, 3988-3996.

Jones, D.L., and Wagers, A.J. (2008). No place like home: anatomy and function of the

stem cell niche. Nat Rev Mol Cell Biol *9*, 11-21.

Jongen-Lavrencic, M., Sun, S.M., Dijkstra, M.K., Valk, P.J., and Lowenberg, B. (2008). MicroRNA expression profiling in relation to the genetic heterogeneity of acute myeloid leukemia. Blood *111*, 5078-5085.

Jorgensen, F., and Kurland, C.G. (1990). Processivity errors of gene expression in Escherichia coli. J Mol Biol *215*, 511-521.

Jost, C.A., Marin, M.C., and Kaelin, W.G., Jr. (1997). p73 is a simian [correction of human] p53-related protein that can induce apoptosis. Nature *389*, 191-194.

Ju, X., Li, D., Shi, Q., Hou, H., Sun, N., and Shen, B. (2009). Differential microRNA expression in childhood B-cell precursor acute lymphoblastic leukemia. Pediatr Hematol Oncol *26*, 1-10.

Kanellopoulou, C., Muljo, S.A., Kung, A.L., Ganesan, S., Drapkin, R., Jenuwein, T., Livingston, D.M., and Rajewsky, K. (2005). Dicer-deficient mouse embryonic stem cells are defective in differentiation and centromeric silencing. Genes Dev *19*, 489-501.

Kaplan, B.B., Gioio, A.E., Hillefors, M., and Aschrafi, A. (2009). Axonal protein synthesis and the regulation of local mitochondrial function. Results Probl Cell Differ *48*, 225-242.

Kapuscinski, J., and Darzynkiewicz, Z. (1987). Interactions of pyronin Y(G) with nucleic acids. Cytometry *8*, 129-137.

Karali, M., Peluso, I., Marigo, V., and Banfi, S. (2007). Identification and characterization of microRNAs expressed in the mouse eye. Invest Ophthalmol Vis Sci *48*, 509-515.

Kenyon, K.R. (1989). Limbal autograft transplantation for chemical and thermal burns. Dev Ophthalmol *18*, 53-58.

Kenyon, K.R., and Tseng, S.C. (1989). Limbal autograft transplantation for ocular surface disorders. Ophthalmology *96*, 709-722; discussion 722-703.

Ketting, R.F., Fischer, S.E., Bernstein, E., Sijen, T., Hannon, G.J., and Plasterk, R.H. (2001). Dicer functions in RNA interference and in synthesis of small RNA involved in developmental timing in C. elegans. Genes Dev *15*, 2654-2659.

Khudayberdiev, S., Fiore, R., and Schratt, G. (2009). MicroRNA as modulators of neuronal responses. Commun Integr Biol *2*, 411-413.

Khvorova, A., Reynolds, A., and Jayasena, S.D. (2003). Functional siRNAs and miRNAs exhibit strand bias. Cell *115*, 209-216.

Kim, H.K., Lee, Y.S., Sivaprasad, U., Malhotra, A., and Dutta, A. (2006). Muscle-specific microRNA miR-206 promotes muscle differentiation. J Cell Biol *174*, 677-687.

Kim, M., Cooper, D.D., Hayes, S.F., and Spangrude, G.J. (1998). Rhodamine-123 staining in hematopoietic stem cells of young mice indicates mitochondrial activation rather than dye efflux. Blood *91*, 4106-4117.

Kim, Y.J., Hwang, S.J., Bae, Y.C., and Jung, J.S. (2009). miR-21 Regulates Adipogenic Differentiation Through the Modulation of TGF-beta Signaling in Mesenchymal Stem Cells Derived from Human Adipose Tissue. Stem Cells. Epub ahead of print.

Kinoshita, S., Kiorpes, T.C., Friend, J., and Thoft, R.A. (1982). Limbal epithelium in ocular surface wound healing. Invest Ophthalmol Vis Sci *23*, 73-80.

Kiriakidou, M., Tan, G.S., Lamprinaki, S., De Planell-Saguer, M., Nelson, P.T., and Mourelatos, Z. (2007). An mRNA m7G cap binding-like motif within human Ago2 represses translation. Cell *129*, 1141-1151.

Koizumi, N., Inatomi, T., Suzuki, T., Sotozono, C., and Kinoshita, S. (2001a). Cultivated corneal epithelial stem cell transplantation in ocular surface disorders. Ophthalmology *108*, 1569-1574.

Koizumi, N., Inatomi, T., Suzuki, T., Sotozono, C., and Kinoshita, S. (2001b). Cultivated corneal epithelial transplantation for ocular surface reconstruction in acute phase of Stevens-Johnson syndrome. Arch Ophthalmol *119*, 298-300.

Koster, M.I., Kim, S., Mills, A.A., DeMayo, F.J., and Roop, D.R. (2004). p63 is the molecular switch for initiation of an epithelial stratification program. Genes Dev *18*, 126-131.

Koster, M.I., Kim, S., and Roop, D.R. (2005). P63 deficiency: a failure of lineage commitment or stem cell maintenance? J Investig Dermatol Symp Proc *10*, 118-123.

Krichevsky, A.M., Sonntag, K.C., Isacson, O., and Kosik, K.S. (2006). Specific microRNAs modulate embryonic stem cell-derived neurogenesis. Stem Cells *24*, 857-864.

Kutay, H., Bai, S., Datta, J., Motiwala, T., Pogribny, I., Frankel, W., Jacob, S.T., and Ghoshal, K. (2006). Downregulation of miR-122 in the rodent and human hepatocellular carcinomas. J Cell Biochem *99*, 671-678.

Lagos-Quintana, M., Rauhut, R., Lendeckel, W., and Tuschl, T. (2001). Identification of novel genes coding for small expressed RNAs. Science *294*, 853-858.

Lau, N.C., Lim, L.P., Weinstein, E.G., and Bartel, D.P. (2001). An abundant class of tiny RNAs with probable regulatory roles in Caenorhabditis elegans. Science *294*, 858-862.

Lawrie, C.H., Soneji, S., Marafioti, T., Cooper, C.D., Palazzo, S., Paterson, J.C., Cattan, H., Enver, T., Mager, R., Boultwood, J., *et al.* (2007). MicroRNA expression distinguishes between germinal center B cell-like and activated B cell-like subtypes of diffuse large B cell lymphoma. Int J Cancer *121*, 1156-1161.

Lee, E.J., Gusev, Y., Jiang, J., Nuovo, G.J., Lerner, M.R., Frankel, W.L., Morgan, D.L., Postier, R.G., Brackett, D.J., and Schmittgen, T.D. (2007). Expression profiling identifies microRNA signature in pancreatic cancer. Int J Cancer *120*, 1046-1054.

Lee, R.C., and Ambros, V. (2001). An extensive class of small RNAs in Caenorhabditis elegans. Science *294*, 862-864.

Lee, R.C., Feinbaum, R.L., and Ambros, V. (1993). The C. elegans heterochronic gene lin-4 encodes small RNAs with antisense complementarity to lin-14. Cell *75*, 843-854.

Lee, Y., Ahn, C., Han, J., Choi, H., Kim, J., Yim, J., Lee, J., Provost, P., Radmark, O., Kim, S., *et al.* (2003). The nuclear RNase III Drosha initiates microRNA processing. Nature *425*, 415-419.

Lee, Y., Kim, M., Han, J., Yeom, K.H., Lee, S., Baek, S.H., and Kim, V.N. (2004). MicroRNA genes are transcribed by RNA polymerase II. EMBO J *23*, 4051-4060.

Lemp, M.A., and Mathers, W.D. (1989). Corneal epithelial cell movement in humans. Eye *3 (Pt 4)*, 438-445.

Lena, A.M., Shalom-Feuerstein, R., Rivetti di Val Cervo, P., Aberdam, D., Knight, R.A., Melino, G., and Candi, E. (2008). miR-203 represses 'stemness' by repressing DeltaNp63. Cell Death Differ *15*, 1187-1195.

Levis, H., and Daniels, J.T. (2009). New technologies in limbal epithelial stem cell transplantation. Curr Opin Biotechnol *20*, 593-7.

Li, Q., Wang, G., Shan, J.L., Yang, Z.X., Wang, H.Z., Feng, J., Zhen, J.J., Chen, C., Zhang, Z.M., Xu, W., *et al.* (2009a). MicroRNA-224 is upregulated in HepG2 cells and involved in cellular migration and invasion. J Gastroenterol Hepatol. Epub ahead of print.

Li, S.S., Yu, S.L., Kao, L.P., Tsai, Z.Y., Singh, S., Chen, B.Z., Ho, B.C., Liu, Y.H., and Yang, P.C. (2009b). Target identification of microRNAs expressed highly in human embryonic stem cells. J Cell Biochem *106*, 1020-1030.

Li, W., Hayashida, Y., Chen, Y.T., and Tseng, S.C. (2007a). Niche regulation of corneal epithelial stem cells at the limbus. Cell Res *17*, 26-36.

Li, W., Hayashida, Y., He, H., Kuo, C.L., and Tseng, S.C. (2007b). The fate of limbal epithelial progenitor cells during explant culture on intact amniotic membrane. Invest Ophthalmol Vis Sci *48*, 605-613.

Lin, K.K., and Goodell, M.A. (2006). Purification of hematopoietic stem cells using the side population. Methods Enzymol *420*, 255-264.

Lin, Y.C., Kuo, M.W., Yu, J., Kuo, H.H., Lin, R.J., Lo, W.L., and Yu, A.L. (2008).

c-Myb is an evolutionary conserved miR-150 target and miR-150/c-Myb interaction is important for embryonic development. Mol Biol Evol *25*, 2189-2198.

Liu, J., Song, G., Wang, Z., Huang, B., Gao, Q., Liu, B., Xu, Y., Liang, X., Ma, P., Gao, N., *et al.* (2007). Establishment of a corneal epithelial cell line spontaneously derived from human limbal cells. Exp Eye Res *84*, 599-609.

Liu, S.P., Fu, R.H., Yu, H.H., Li, K.W., Tsai, C.H., Shyu, W.C., and Lin, S.Z. (2009a). MicroRNAs Regulation Modulated Self-Renewal and Lineage Differentiation of Stem Cells. Cell Transplant. *18*, 1039-45.

Liu, X., Sempere, L.F., Galimberti, F., Freemantle, S.J., Black, C., Dragnev, K.H., Ma, Y., Fiering, S., Memoli, V., Li, H., *et al.* (2009b). Uncovering growth-suppressive MicroRNAs in lung cancer. Clin Cancer Res *15*, 1177-1183.

Lo, K.C., Brugh, V.M., 3rd, Parker, M., and Lamb, D.J. (2005). Isolation and enrichment of murine spermatogonial stem cells using rhodamine 123 mitochondrial dye. Biol Reprod *72*, 767-771.

Love, T.M., Moffett, H.F., and Novina, C.D. (2008). Not miR-ly small RNAs: big potential for microRNAs in therapy. J Allergy Clin Immunol *121*, 309-319.

Lui, W.O., Pourmand, N., Patterson, B.K., and Fire, A. (2007). Patterns of known and novel small RNAs in human cervical cancer. Cancer Res *67*, 6031-6043.

Lujambio, A., Calin, G.A., Villanueva, A., Ropero, S., Sanchez-Cespedes, M., Blanco, D., Montuenga, L.M., Rossi, S., Nicoloso, M.S., Faller, W.J., *et al.* (2008). A microRNA DNA methylation signature for human cancer metastasis. Proc Natl Acad Sci U S A *105*, 13556-13561.

Lund, E., Guttinger, S., Calado, A., Dahlberg, J.E., and Kutay, U. (2004). Nuclear export of microRNA precursors. Science *303*, 95-98.

MacRae, I.J., Zhou, K., and Doudna, J.A. (2007). Structural determinants of RNA recognition and cleavage by Dicer. Nat Struct Mol Biol *14*, 934-940.

Macrae, I.J., Zhou, K., Li, F., Repic, A., Brooks, A.N., Cande, W.Z., Adams, P.D., and

Doudna, J.A. (2006). Structural basis for double-stranded RNA processing by Dicer. Science *311*, 195-198.

Maes, O.C., Sarojini, H., and Wang, E. (2009). Stepwise up-regulation of microRNA expression levels from replicating to reversible and irreversible growth arrest states in WI-38 human fibroblasts. J Cell Physiol *221*, 109-119.

Magrelli, A., Azzalin, G., Salvatore, M., Viganotti, M., Tosto, F., Colombo, T., Devito, R., Di Masi, A., Antoccia, A., Lorenzetti, S., *et al.* (2009). Altered microRNA Expression Patterns in Hepatoblastoma Patients. Transl Oncol *2*, 157-163.

Majo, F., Rochat, A., Nicolas, M., Jaoude, G.A., and Barrandon, Y. (2008). Oligopotent stem cells are distributed throughout the mammalian ocular surface. Nature *456*, 250-254.

Manley, J.L. (1978). Synthesis and degradation of termination and premature-termination fragments of beta-galactosidase in vitro and in vivo. J Mol Biol *125*, 407-432.

Markou, A., Tsaroucha, E.G., Kaklamanis, L., Fotinou, M., Georgoulias, V., and Lianidou, E.S. (2008). Prognostic value of mature microRNA-21 and microRNA-205 overexpression in non-small cell lung cancer by quantitative real-time RT-PCR. Clin Chem *54*, 1696-1704.

Maroney, P.A., Yu, Y., Fisher, J., and Nilsen, T.W. (2006). Evidence that microRNAs are associated with translating messenger RNAs in human cells. Nat Struct Mol Biol *13*, 1102-1107.

Mathe, E.A., Nguyen, G.H., Bowman, E.D., Zhao, Y., Budhu, A., Schetter, A.J., Braun, R., Reimers, M., Kumamoto, K., Hughes, D., *et al.* (2009). MicroRNA expression in squamous cell carcinoma and adenocarcinoma of the esophagus: associations with survival. Clin Cancer Res *15*, 6192-6200.

Matic, M., Evans, W.H., Brink, P.R., and Simon, M. (2002). Epidermal stem cells do not communicate through gap junctions. J Invest Dermatol *118*, 110-116.

Matic, M., Petrov, I.N., Chen, S., Wang, C., Dimitrijevich, S.D., and Wolosin, J.M.

(1997). Stem cells of the corneal epithelium lack connexins and metabolite transfer capacity. Differentiation *61*, 251-260.

Matsuda, M., Ubels, J.L., and Edelhauser, H.F. (1985). A larger corneal epithelial wound closes at a faster rate. Invest Ophthalmol Vis Sci *26*, 897-900.

McKenzie, J.L., Takenaka, K., Gan, O.I., Doedens, M., and Dick, J.E. (2007). Low rhodamine 123 retention identifies long-term human hematopoietic stem cells within the Lin-CD34+CD38- population. Blood *109*, 543-545.

Melkamu, T., Zhang, X., Tan, J., Zeng, Y., and Kassie, F. (2009). Alteration of microRNA expression in vinyl-carbamate-induced mouse lung tumors and modulation by the chemopreventive agent indole-3-carbinol. Carcinogenesis. Epub ahead of print.

Meng, F., Henson, R., Lang, M., Wehbe, H., Maheshwari, S., Mendell, J.T., Jiang, J., Schmittgen, T.D., and Patel, T. (2006). Involvement of human micro-RNA in growth and response to chemotherapy in human cholangiocarcinoma cell lines. Gastroenterology *130*, 2113-2129.

Meng, F., Henson, R., Wehbe-Janek, H., Ghoshal, K., Jacob, S.T., and Patel, T. (2007). MicroRNA-21 regulates expression of the PTEN tumor suppressor gene in human hepatocellular cancer. Gastroenterology *133*, 647-658.

Merkerova, M., Vasikova, A., Belickova, M., and Bruchova, H. (2009). MicroRNA expression profiles in umbilical cord blood cell lineages. Stem Cells Dev. Epub ahead of print.

Michael, M.Z., SM, O.C., van Holst Pellekaan, N.G., Young, G.P., and James, R.J. (2003). Reduced accumulation of specific microRNAs in colorectal neoplasia. Mol Cancer Res *1*, 882-891.

Mills, A.A., Zheng, B., Wang, X.J., Vogel, H., Roop, D.R., and Bradley, A. (1999). p63 is a p53 homologue required for limb and epidermal morphogenesis. Nature *398*, 708-713.

Mimeault, M., and Batra, S.K. (2008). Recent progress on tissue-resident adult stem cell biology and their therapeutic implications. Stem Cell Rev *4*, 27-49.

Miyashita, H., Higa, K., Kato, N., Kawakita, T., Yoshida, S., Tsubota, K., and Shimmura, S. (2007). Hypoxia enhances the expansion of human limbal epithelial progenitor cells in vitro. Invest Ophthalmol Vis Sci *48*, 3586-3593.

Mizuno, Y., Yagi, K., Tokuzawa, Y., Kanesaki-Yatsuka, Y., Suda, T., Katagiri, T., Fukuda, T., Maruyama, M., Okuda, A., Amemiya, T., *et al.* (2008). miR-125b inhibits osteoblastic differentiation by down-regulation of cell proliferation. Biochem Biophys Res Commun *368*, 267-272.

Mootz, D., Ho, D.M., and Hunter, C.P. (2004). The STAR/Maxi-KH domain protein GLD-1 mediates a developmental switch in the translational control of C. elegans PAL-1. Development *131*, 3263-3272.

Mosmann, T. (1983). Rapid colorimetric assay for cellular growth and survival: application to proliferation and cytotoxicity assays. J Immunol Methods *65*, 55-63.

Motoyama, K., Inoue, H., Takatsuno, Y., Tanaka, F., Mimori, K., Uetake, H., Sugihara, K., and Mori, M. (2009). Over- and under-expressed microRNAs in human colorectal cancer. Int J Oncol *34*, 1069-1075.

Murata, T., Ishibashi, T., and Inomata, H. (1993). Localizations of epidermal growth factor receptor and proliferating cell nuclear antigen during corneal wound healing. Graefes Arch Clin Exp Ophthalmol *231*, 104-108.

Nakagawa, R., Hara, Y., Arakawa, H., Nishimura, S., and Komatani, H. (2002). ABCG2 confers resistance to indolocarbazole compounds by ATP-dependent transport. Biochem Biophys Res Commun *299*, 669-675.

Nakagawa, Y., Iinuma, M., Naoe, T., Nozawa, Y., and Akao, Y. (2007). Characterized mechanism of alpha-mangostin-induced cell death: caspase-independent apoptosis with release of endonuclease-G from mitochondria and increased miR-143 expression in human colorectal cancer DLD-1 cells. Bioorg Med Chem *15*, 5620-5628.

Nam, E.J., Yoon, H., Kim, S.W., Kim, H., Kim, Y.T., Kim, J.H., Kim, J.W., and Kim, S. (2008). MicroRNA expression profiles in serous ovarian carcinoma. Clin Cancer Res *14*, 2690-2695.

Navarro, A., Gaya, A., Martinez, A., Urbano-Ispizua, A., Pons, A., Balague, O., Gel, B., Abrisqueta, P., Lopez-Guillermo, A., Artells, R., *et al.* (2008). MicroRNA expression profiling in classic Hodgkin lymphoma. Blood *111*, 2825-2832.

Naylor, C.S., Jaworska, E., Branson, K., Embleton, M.J., and Chopra, R. (2005). Side population/ABCG2-positive cells represent a heterogeneous group of haemopoietic cells: implications for the use of adult stem cells in transplantation and plasticity protocols. Bone Marrow Transplant *35*, 353-360.

Nottrott, S., Simard, M.J., and Richter, J.D. (2006). Human let-7a miRNA blocks protein production on actively translating polyribosomes. Nat Struct Mol Biol *13*, 1108-1114.

O'Donnell, K.A., Wentzel, E.A., Zeller, K.I., Dang, C.V., and Mendell, J.T. (2005). c-Myc-regulated microRNAs modulate E2F1 expression. Nature *435*, 839-843.

O'Hara, A.J., Wang, L., Dezube, B.J., Harrington, W.J., Jr., Damania, B., and Dittmer, D.P. (2009). Tumor suppressor microRNAs are underrepresented in primary effusion lymphoma and Kaposi sarcoma. Blood *113*, 5938-5941.

Obernosterer, G., Martinez, J., and Alenius, M. (2007). Locked nucleic acid-based in situ detection of microRNAs in mouse tissue sections. Nat Protoc *2*, 1508-1514.

Odom, R.E. (1954). Epithelioma of the limbus. N C Med J *15*, 505-510.

Ohlsson Teague, E.M., Van der Hoek, K.H., Van der Hoek, M.B., Perry, N., Wagaarachchi, P., Robertson, S.A., Print, C.G., and Hull, L.M. (2009). MicroRNA-regulated pathways associated with endometriosis. Mol Endocrinol *23*, 265-275.

Olasode, B.J., Bankole, O.O., and Adeoye, A.O. (1996). Invasive squamous cell carcinoma of the limbus: case report. East Afr Med J *73*, 627-628.

Olopade, O.I., Bohlander, S.K., Pomykala, H., Maltepe, E., Van Melle, E., Le Beau, M.M., and Diaz, M.O. (1992a). Mapping of the shortest region of overlap of deletions of the short arm of chromosome 9 associated with human neoplasia. Genomics *14*, 437-443.

Olopade, O.I., Jenkins, R.B., Ransom, D.T., Malik, K., Pomykala, H., Nobori, T., Cowan, J.M., Rowley, J.D., and Diaz, M.O. (1992b). Molecular analysis of deletions of the short arm of chromosome 9 in human gliomas. Cancer Res *52*, 2523-2529.

Ozen, M., Creighton, C.J., Ozdemir, M., and Ittmann, M. (2008). Widespread deregulation of microRNA expression in human prostate cancer. Oncogene *27*, 1788-1793.

Ozinsky, A., Underhill, D.M., Fontenot, J.D., Hajjar, A.M., Smith, K.D., Wilson, C.B., Schroeder, L., and Aderem, A. (2000). The repertoire for pattern recognition of pathogens by the innate immune system is defined by cooperation between toll-like receptors. Proc Natl Acad Sci U S A *97*, 13766-13771.

Palmieri, A., Pezzetti, F., Brunelli, G., Martinelli, M., Lo Muzio, L., Scarano, A., Degidi, M., Piattelli, A., and Carinci, F. (2008). Peptide-15 changes miRNA expression in osteoblast-like cells. Implant Dent *17*, 100-108.

Park, J.K., Lee, E.J., Esau, C., and Schmittgen, T.D. (2009a). Antisense inhibition of microRNA-21 or -221 arrests cell cycle, induces apoptosis, and sensitizes the effects of gemcitabine in pancreatic adenocarcinoma. Pancreas *38*, e190-199.

Park, S.J., Wee, W.R., Lee, J.H., and Kim, M.K. (2009b). Primary sebaceous carcinoma of the corneaoscleral limbus with pagetoid recurrence. Korean J Ophthalmol *23*, 104-107.

Pasquinelli, A.E., Reinhart, B.J., Slack, F., Martindale, M.Q., Kuroda, M.I., Maller, B., Hayward, D.C., Ball, E.E., Degnan, B., Muller, P., *et al.* (2000). Conservation of the sequence and temporal expression of let-7 heterochronic regulatory RNA. Nature *408*, 86-89.

Pellegrini, G., Dellambra, E., Golisano, O., Martinelli, E., Fantozzi, I., Bondanza, S., Ponzin, D., McKeon, F., and De Luca, M. (2001). p63 identifies keratinocyte stem cells. Proc Natl Acad Sci U S A *98*, 3156-3161.

Pellegrini, G., Golisano, O., Paterna, P., Lambiase, A., Bonini, S., Rama, P., and De Luca, M. (1999). Location and clonal analysis of stem cells and their differentiated

progeny in the human ocular surface. J Cell Biol *145*, 769-782.

Pellegrini, G., Traverso, C.E., Franzi, A.T., Zingirian, M., Cancedda, R., and De Luca, M. (1997). Long-term restoration of damaged corneal surfaces with autologous cultivated corneal epithelium. Lancet *349*, 990-993.

Petersen, C.P., Bordeleau, M.E., Pelletier, J., and Sharp, P.A. (2006). Short RNAs repress translation after initiation in mammalian cells. Mol Cell *21*, 533-542.

Qi, H., Li, D.Q., Shine, H.D., Chen, Z., Yoon, K.C., Jones, D.B., and Pflugfelder, S.C. (2008). Nerve growth factor and its receptor TrkA serve as potential markers for human corneal epithelial progenitor cells. Exp Eye Res *86*, 34-40.

Qi, J., Yu, J.Y., Shcherbata, H.R., Mathieu, J., Wang, A.J., Seal, S., Zhou, W., Stadler, B.M., Bourgin, D., Wang, L., *et al.* (2009). microRNAs regulate human embryonic stem cell division. Cell Cycle *8*, 3729-3741.

Rasteiro, A., and Cunha-Vaz, J.G. (1976). Squamous cell carcinoma of the limbus with intraocular invasion. Ophthalmologica *172*, 332-336.

Rauz, S., and Saw, V.P. (2009). Serum eye drops, amniotic membrane and limbal epithelial stem cells-tools in the treatment of ocular surface disease. Cell Tissue Bank. Epub ahead of print.

Reinhart, B.J., Slack, F.J., Basson, M., Pasquinelli, A.E., Bettinger, J.C., Rougvie, A.E., Horvitz, H.R., and Ruvkun, G. (2000). The 21-nucleotide let-7 RNA regulates developmental timing in Caenorhabditis elegans. Nature *403*, 901-906.

Revoltella, R.P., Papini, S., Rosellini, A., and Michelini, M. (2007). Epithelial stem cells of the eye surface. Cell Prolif *40*, 445-461.

Ribas, J., Ni, X., Haffner, M., Wentzel, E.A., Salmasi, A.H., Chowdhury, W.H., Kudrolli, T.A., Yegnasubramanian, S., Luo, J., Rodriguez, R., *et al.* (2009). miR-21: an androgen receptor-regulated microRNA that promotes hormone-dependent and hormone-independent prostate cancer growth. Cancer Res *69*, 7165-7169.

Roberson, M.C. (1984). Corneal epithelial dysplasia. Ann Ophthalmol *16*, 1147-1150.

Rodriguez-Martinez, S., Cancino-Diaz, M.E., Miguel, P.S., and Cancino-Diaz, J.C. (2006). Lipopolysaccharide from Escherichia coli induces the expression of vascular endothelial growth factor via toll-like receptor 4 in human limbal fibroblasts. Exp Eye Res *83*, 1373-1377.

Romania, P., Lulli, V., Pelosi, E., Biffoni, M., Peschle, C., and Marziali, G. (2008). MicroRNA 155 modulates megakaryopoiesis at progenitor and precursor level by targeting Ets-1 and Meis1 transcription factors. Br J Haematol *143*, 570-580.

Romano, A.C., Espana, E.M., Yoo, S.H., Budak, M.T., Wolosin, J.M., and Tseng, S.C. (2003). Different cell sizes in human limbal and central corneal basal epithelia measured by confocal microscopy and flow cytometry. Invest Ophthalmol Vis Sci *44*, 5125-5129.

Rosendaal, M., Green, C.R., Rahman, A., and Morgan, D. (1994). Up-regulation of the connexin43+ gap junction network in haemopoietic tissue before the growth of stem cells. J Cell Sci *107 (Pt 1)*, 29-37.

Ruby, J.G., Jan, C., Player, C., Axtell, M.J., Lee, W., Nusbaum, C., Ge, H., and Bartel, D.P. (2006). Large-scale sequencing reveals 21U-RNAs and additional microRNAs and endogenous siRNAs in C. elegans. Cell *127*, 1193-1207.

Ruegsegger, U., Leber, J.H., and Walter, P. (2001). Block of HAC1 mRNA translation by long-range base pairing is released by cytoplasmic splicing upon induction of the unfolded protein response. Cell *107*, 103-114.

Ryan, D.G., Oliveira-Fernandes, M., and Lavker, R.M. (2006). MicroRNAs of the mammalian eye display distinct and overlapping tissue specificity. Mol Vis *12*, 1175-1184.

Sachdeva, M., Zhu, S., Wu, F., Wu, H., Walia, V., Kumar, S., Elble, R., Watabe, K., and Mo, Y.Y. (2009). p53 represses c-Myc through induction of the tumor suppressor miR-145. Proc Natl Acad Sci U S A *106*, 3207-3212.

Saito, Y., Liang, G., Egger, G., Friedman, J.M., Chuang, J.C., Coetzee, G.A., and Jones, P.A. (2006). Specific activation of microRNA-127 with downregulation of the

proto-oncogene BCL6 by chromatin-modifying drugs in human cancer cells. Cancer Cell *9*, 435-443.

Sanvito, F., Piatti, S., Villa, A., Bossi, M., Lucchini, G., Marchisio, P.C., and Biffo, S. (1999). The beta4 integrin interactor p27(BBP/eIF6) is an essential nuclear matrix protein involved in 60S ribosomal subunit assembly. J Cell Biol *144*, 823-837.

Sarkadi, B., Ozvegy-Laczka, C., Nemet, K., and Varadi, A. (2004). ABCG2 -- a transporter for all seasons. FEBS Lett *567*, 116-120.

Sayed, D., Rane, S., Lypowy, J., He, M., Chen, I.Y., Vashistha, H., Yan, L., Malhotra, A., Vatner, D., and Abdellatif, M. (2008). MicroRNA-21 targets Sprouty2 and promotes cellular outgrowths. Mol Biol Cell *19*, 3272-3282.

Schaap-Oziemlak, A., Raymakers, R.A., Bergevoet, S.M., Gilissen, C., Jansen, B.J., Adema, G.J., Kogler, G., le Sage, C., Agami, R., van der Reijden, B.A., *et al.* (2009). MicroRNA hsa-miR-135b regulates mineralization in osteogenic differentiation of human Unrestricted Somatic Stem Cells (USSCs). Stem Cells Dev. Epub ahead of print.

Schepeler, T., Reinert, J.T., Ostenfeld, M.S., Christensen, L.L., Silahtaroglu, A.N., Dyrskjot, L., Wiuf, C., Sorensen, F.J., Kruhoffer, M., Laurberg, S., *et al.* (2008). Diagnostic and prognostic microRNAs in stage II colon cancer. Cancer Res *68*, 6416-6424.

Schermer, A., Galvin, S., and Sun, T.T. (1986). Differentiation-related expression of a major 64K corneal keratin in vivo and in culture suggests limbal location of corneal epithelial stem cells. J Cell Biol *103*, 49-62.

Schinkel, A.H., Mayer, U., Wagenaar, E., Mol, C.A., van Deemter, L., Smit, J.J., van der Valk, M.A., Voordouw, A.C., Spits, H., van Tellingen, O., *et al.* (1997). Normal viability and altered pharmacokinetics in mice lacking mdr1-type (drug-transporting) P-glycoproteins. Proc Natl Acad Sci U S A *94*, 4028-4033.

Schmidt, W.M., Spiel, A.O., Jilma, B., Wolzt, M., and Muller, M. (2009). In vivo profile of the human leukocyte microRNA response to endotoxemia. Biochem Biophys

Res Commun *380*, 437-441.

Schwarz, D.S., Hutvagner, G., Du, T., Xu, Z., Aronin, N., and Zamore, P.D. (2003). Asymmetry in the assembly of the RNAi enzyme complex. Cell *115*, 199-208.

Seale, E.R. (1953). Carcinoma of limbus; report of 19 cases treated with radium and effect of gamma radiation upon eye. AMA Arch Derm Syphilol *68*, 286-295.

Shimazaki, J., Aiba, M., Goto, E., Kato, N., Shimmura, S., and Tsubota, K. (2002). Transplantation of human limbal epithelium cultivated on amniotic membrane for the treatment of severe ocular surface disorders. Ophthalmology *109*, 1285-1290.

Shirzadeh, E. (2008). Pigmented squamous cell carcinoma of the limbus area: a rare case. Indian J Ophthalmol *56*, 169.

Shortt, A.J., Secker, G.A., Munro, P.M., Khaw, P.T., Tuft, S.J., and Daniels, J.T. (2007). Characterization of the limbal epithelial stem cell niche: novel imaging techniques permit in vivo observation and targeted biopsy of limbal epithelial stem cells. Stem Cells *25*, 1402-1409.

Shortt, A.J., Secker, G.A., Rajan, M.S., Meligonis, G., Dart, J.K., Tuft, S.J., and Daniels, J.T. (2008). Ex vivo expansion and transplantation of limbal epithelial stem cells. Ophthalmology *115*, 1989-1997.

Si, M.L., Zhu, S., Wu, H., Lu, Z., Wu, F., and Mo, Y.Y. (2007). miR-21-mediated tumor growth. Oncogene *26*, 2799-2803.

Singh, S.K., Kagalwala, M.N., Parker-Thornburg, J., Adams, H., and Majumder, S. (2008a). REST maintains self-renewal and pluripotency of embryonic stem cells. Nature *453*, 223-227.

Singh, S.K., Pal Bhadra, M., Girschick, H.J., and Bhadra, U. (2008b). MicroRNAs--micro in size but macro in function. FEBS J *275*, 4929-4944.

Slaby, O., Svoboda, M., Fabian, P., Smerdova, T., Knoflickova, D., Bednarikova, M., Nenutil, R., and Vyzula, R. (2007). Altered expression of miR-21, miR-31, miR-143 and miR-145 is related to clinicopathologic features of colorectal cancer. Oncology *72*,

397-402.

Slack, F.J., Basson, M., Liu, Z., Ambros, V., Horvitz, H.R., and Ruvkun, G. (2000). The lin-41 RBCC gene acts in the C. elegans heterochronic pathway between the let-7 regulatory RNA and the LIN-29 transcription factor. Mol Cell *5*, 659-669.

Smirnova, L., Grafe, A., Seiler, A., Schumacher, S., Nitsch, R., and Wulczyn, F.G. (2005). Regulation of miRNA expression during neural cell specification. Eur J Neurosci *21*, 1469-1477.

Soliman Mahdy, M.A., and Bhatia, J. (2009). Treatment of primary pterygium: role of limbal stem cells and conjunctival autograft transplantation. Eur J Ophthalmol *19*, 729-732.

Song, B., Wang, Y., Kudo, K., Gavin, E.J., Xi, Y., and Ju, J. (2008). miR-192 Regulates dihydrofolate reductase and cellular proliferation through the p53-microRNA circuit. Clin Cancer Res *14*, 8080-8086.

Stiewe, T., and Putzer, B.M. (2002). Role of p73 in malignancy: tumor suppressor or oncogene? Cell Death Differ *9*, 237-245.

Suh, M.R., Lee, Y., Kim, J.Y., Kim, S.K., Moon, S.H., Lee, J.Y., Cha, K.Y., Chung, H.M., Yoon, H.S., Moon, S.Y., *et al.* (2004). Human embryonic stem cells express a unique set of microRNAs. Dev Biol *270*, 488-498.

Swan, K.C., Emmens, T.H., and Christensen, L. (1948). Experiences with tumors of the limbus. Trans Am Acad Ophthalmol Otolaryngol *52*, 458-469.

Swan, K.C., Emmens, T.H., and Christensen, L. (1950). Tumors of the limbus. Arch Ophthal *43*, 175.

Takagi, T., Iio, A., Nakagawa, Y., Naoe, T., Tanigawa, N., and Akao, Y. (2009). Decreased expression of microRNA-143 and -145 in human gastric cancers. Oncology *77*, 12-21.

Takanabe, R., Ono, K., Abe, Y., Takaya, T., Horie, T., Wada, H., Kita, T., Satoh, N., Shimatsu, A., and Hasegawa, K. (2008). Up-regulated expression of microRNA-143 in

association with obesity in adipose tissue of mice fed high-fat diet. Biochem Biophys Res Commun *376*, 728-732.

Takeuchi, O., Kawai, T., Muhlradt, P.F., Morr, M., Radolf, J.D., Zychlinsky, A., Takeda, K., and Akira, S. (2001). Discrimination of bacterial lipoproteins by Toll-like receptor 6. Int Immunol *13*, 933-940.

Takita, J., Hayashi, Y., Kohno, T., Yamaguchi, N., Hanada, R., Yamamoto, K., and Yokota, J. (1997). Deletion map of chromosome 9 and p16 (CDKN2A) gene alterations in neuroblastoma. Cancer Res *57*, 907-912.

Tatsuguchi, M., Seok, H.Y., Callis, T.E., Thomson, J.M., Chen, J.F., Newman, M., Rojas, M., Hammond, S.M., and Wang, D.Z. (2007). Expression of microRNAs is dynamically regulated during cardiomyocyte hypertrophy. J Mol Cell Cardiol *42*, 1137-1141.

Tetzlaff, M.T., Liu, A., Xu, X., Master, S.R., Baldwin, D.A., Tobias, J.W., Livolsi, V.A., and Baloch, Z.W. (2007). Differential expression of miRNAs in papillary thyroid carcinoma compared to multinodular goiter using formalin fixed paraffin embedded tissues. Endocr Pathol *18*, 163-173.

Thoft, R.A., and Friend, J. (1983). The X, Y, Z hypothesis of corneal epithelial maintenance. Invest Ophthalmol Vis Sci *24*, 1442-1443.

Thomas, P.B., Liu, Y.H., Zhuang, F.F., Selvam, S., Song, S.W., Smith, R.E., Trousdale, M.D., and Yiu, S.C. (2007). Identification of Notch-1 expression in the limbal basal epithelium. Mol Vis *13*, 337-344.

Toth, C.A., and Thomas, P. (1990). The effect of interferon treatment on 14 human colorectal cancer cell lines: growth and carcinoembryonic antigen secretion in vitro. J Interferon Res *10*, 579-588.

Tran, N., McLean, T., Zhang, X., Zhao, C.J., Thomson, J.M., O'Brien, C., and Rose, B. (2007). MicroRNA expression profiles in head and neck cancer cell lines. Biochem Biophys Res Commun *358*, 12-17.

Tsai, R.J., and Tseng, S.C. (1994). Human allograft limbal transplantation for corneal

surface reconstruction. Cornea *13*, 389-400.

Tsai, Z.Y., Singh, S., Yu, S.L., Kao, L.P., Chen, B.Z., Ho, B.C., Yang, P.C., and Li, S.S. (2009). Identification of microRNAs regulated by activin A in human embryonic stem cells. J Cell Biochem. Epub ahead of print.

Tseng, S.C. (1989). Concept and application of limbal stem cells. Eye *3 (Pt 2)*, 141-157.

Tseng, S.C., Prabhasawat, P., Barton, K., Gray, T., and Meller, D. (1998). Amniotic membrane transplantation with or without limbal allografts for corneal surface reconstruction in patients with limbal stem cell deficiency. Arch Ophthalmol *116*, 431-441.

Tsubota, K., Satake, Y., Kaido, M., Shinozaki, N., Shimmura, S., Bissen-Miyajima, H., and Shimazaki, J. (1999). Treatment of severe ocular-surface disorders with corneal epithelial stem-cell transplantation. N Engl J Med *340*, 1697-1703.

Umemoto, T., Yamato, M., Nishida, K., Kohno, C., Yang, J., Tano, Y., and Okano, T. (2005). Rat limbal epithelial side population cells exhibit a distinct expression of stem cell markers that are lacking in side population cells from the central cornea. FEBS Lett *579*, 6569-6574.

Umemoto, T., Yamato, M., Nishida, K., Yang, J., Tano, Y., and Okano, T. (2006). Limbal epithelial side-population cells have stem cell-like properties, including quiescent state. Stem Cells *24*, 86-94.

Varnholt, H., Drebber, U., Schulze, F., Wedemeyer, I., Schirmacher, P., Dienes, H.P., and Odenthal, M. (2008). MicroRNA gene expression profile of hepatitis C virus-associated hepatocellular carcinoma. Hepatology *47*, 1223-1232.

Vasilescu, C., Rossi, S., Shimizu, M., Tudor, S., Veronese, A., Ferracin, M., Nicoloso, M.S., Barbarotto, E., Popa, M., Stanciulea, O., *et al.* (2009). MicroRNA fingerprints identify miR-150 as a plasma prognostic marker in patients with sepsis. PLoS One *4*, e7405.

Vasudevan, S., Tong, Y., and Steitz, J.A. (2007). Switching from repression to

activation: microRNAs can up-regulate translation. Science *318*, 1931-1934.

Veasey, C.A. (1907). Sarcoma of corneal limbus. Trans Am Ophthalmol Soc *11*, 282-290.

Visvanathan, J., Lee, S., Lee, B., Lee, J.W., and Lee, S.K. (2007). The microRNA miR-124 antagonizes the anti-neural REST/SCP1 pathway during embryonic CNS development. Genes Dev *21*, 744-749.

Volinia, S., Calin, G.A., Liu, C.G., Ambs, S., Cimmino, A., Petrocca, F., Visone, R., Iorio, M., Roldo, C., Ferracin, M., *et al.* (2006). A microRNA expression signature of human solid tumors defines cancer gene targets. Proc Natl Acad Sci U S A *103*, 2257-2261.

von Hippel, P.H., and Yager, T.D. (1991). Transcript elongation and termination are competitive kinetic processes. Proc Natl Acad Sci U S A *88*, 2307-2311.

Wagner-Souza, K., Diamond, H.R., Ornellas, M.H., Gomes, B.E., Almeida-Oliveira, A., Abdelhay, E., Bouzas, L.F., and Rumjanek, V.M. (2008). Rhodamine 123 efflux in human subpopulations of hematopoietic stem cells: comparison between bone marrow, umbilical cord blood and mobilized peripheral blood CD34+ cells. Int J Mol Med *22*, 237-242.

Wakiyama, M., Takimoto, K., Ohara, O., and Yokoyama, S. (2007). Let-7 microRNA-mediated mRNA deadenylation and translational repression in a mammalian cell-free system. Genes Dev *21*, 1857-1862.

Walden, T.B., Timmons, J.A., Keller, P., Nedergaard, J., and Cannon, B. (2009). Distinct expression of muscle-specific microRNAs (myomirs) in brown adipocytes. J Cell Physiol *218*, 444-449.

Wang, C.J., Zhou, Z.G., Wang, L., Yang, L., Zhou, B., Gu, J., Chen, H.Y., and Sun, X.F. (2009a). Clinicopathological significance of microRNA-31, -143 and -145 expression in colorectal cancer. Dis Markers *26*, 27-34.

Wang, H., Tao, T., Tang, J., Mao, Y.H., Li, W., Peng, J., Tan, G., Zhou, Y.P., Zhong, J.X., Tseng, S.C., *et al.* (2009b). Importin 13 Serves as a Potential Marker for Corneal

Epithelial Progenitor Cells. Stem Cells *27*, 2516-2526.

Wang, L.L., Zhang, Z., Li, Q., Yang, R., Pei, X., Xu, Y., Wang, J., Zhou, S.F., and Li, Y. (2009c). Ethanol exposure induces differential microRNA and target gene expression and teratogenic effects which can be suppressed by folic acid supplementation. Hum Reprod *24*, 562-579.

Wang, M., Tan, L.P., Dijkstra, M.K., van Lom, K., Robertus, J.L., Harms, G., Blokzijl, T., Kooistra, K., van T'veer M, B., Rosati, S., *et al.* (2008a). miRNA analysis in B-cell chronic lymphocytic leukaemia: proliferation centres characterized by low miR-150 and high BIC/miR-155 expression. J Pathol *215*, 13-20.

Wang, P., Zou, F., Zhang, X., Li, H., Dulak, A., Tomko, R.J., Jr., Lazo, J.S., Wang, Z., Zhang, L., and Yu, J. (2009d). microRNA-21 negatively regulates Cdc25A and cell cycle progression in colon cancer cells. Cancer Res *69*, 8157-8165.

Wang, Q., Huang, Z., Xue, H., Jin, C., Ju, X.L., Han, J.D., and Chen, Y.G. (2008b). MicroRNA miR-24 inhibits erythropoiesis by targeting activin type I receptor ALK4. Blood *111*, 588-595.

Wang, Q., Wang, Y., Minto, A.W., Wang, J., Shi, Q., Li, X., and Quigg, R.J. (2008c). MicroRNA-377 is up-regulated and can lead to increased fibronectin production in diabetic nephropathy. FASEB J *22*, 4126-4135.

Wang, W., Edington, H.D., Rao, U.N., Jukic, D.M., Land, S.R., Ferrone, S., and Kirkwood, J.M. (2007a). Modulation of signal transducers and activators of transcription 1 and 3 signaling in melanoma by high-dose IFNalpha2b. Clin Cancer Res *13*, 1523-1531.

Wang, X., Tang, S., Le, S.Y., Lu, R., Rader, J.S., Meyers, C., and Zheng, Z.M. (2008d). Aberrant expression of oncogenic and tumor-suppressive microRNAs in cervical cancer is required for cancer cell growth. PLoS One *3*, e2557.

Wang, Y., Medvid, R., Melton, C., Jaenisch, R., and Blelloch, R. (2007b). DGCR8 is essential for microRNA biogenesis and silencing of embryonic stem cell self-renewal. Nat Genet *39*, 380-385.

Waring, G.O., 3rd, Roth, A.M., and Ekins, M.B. (1984). Clinical and pathologic description of 17 cases of corneal intraepithelial neoplasia. Am J Ophthalmol *97*, 547-559.

Weber, B., Stresemann, C., Brueckner, B., and Lyko, F. (2007). Methylation of human microRNA genes in normal and neoplastic cells. Cell Cycle *6*, 1001-1005.

Weber, J.M., and Calvi, L.M. (2009). Notch signaling and the bone marrow hematopoietic stem cell niche. Bone. Epub ahead of print.

Weigt, H., Muhlradt, P.F., Larbig, M., Krug, N., and Braun, A. (2004). The Toll-like receptor-2/6 agonist macrophage-activating lipopeptide-2 cooperates with IFN-gamma to reverse the Th2 skew in an in vitro allergy model. J Immunol *172*, 6080-6086.

Wightman, B., Burglin, T.R., Gatto, J., Arasu, P., and Ruvkun, G. (1991). Negative regulatory sequences in the lin-14 3'-untranslated region are necessary to generate a temporal switch during Caenorhabditis elegans development. Genes Dev *5*, 1813-1824.

Wightman, B., Ha, I., and Ruvkun, G. (1993). Posttranscriptional regulation of the heterochronic gene lin-14 by lin-4 mediates temporal pattern formation in C. elegans. Cell *75*, 855-862.

Williams, A.E., Moschos, S.A., Perry, M.M., Barnes, P.J., and Lindsay, M.A. (2007). Maternally imprinted microRNAs are differentially expressed during mouse and human lung development. Dev Dyn *236*, 572-580.

Wilson, K.D., Venkatasubrahmanyam, S., Jia, F., Sun, N., Butte, A.J., and Wu, J.C. (2009). MicroRNA profiling of human-induced pluripotent stem cells. Stem Cells Dev *18*, 749-758.

Winter, J., Jung, S., Keller, S., Gregory, R.I., and Diederichs, S. (2009). Many roads to maturity: microRNA biogenesis pathways and their regulation. Nat Cell Biol *11*, 228-234.

Wong, T.S., Liu, X.B., Wong, B.Y., Ng, R.W., Yuen, A.P., and Wei, W.I. (2008). Mature miR-184 as Potential Oncogenic microRNA of Squamous Cell Carcinoma of

Tongue. Clin Cancer Res *14*, 2588-2592.

Wu, H., Neilson, J.R., Kumar, P., Manocha, M., Shankar, P., Sharp, P.A., and Manjunath, N. (2007). miRNA profiling of naive, effector and memory CD8 T cells. PLoS One *2*, e1020.

Wu, L., Fan, J., and Belasco, J.G. (2006). MicroRNAs direct rapid deadenylation of mRNA. Proc Natl Acad Sci U S A *103*, 4034-4039.

Wylegala, E., Dobrowolski, D., Tarnawska, D., Janiszewska, D., Gabryel, B., Malecki, A., and Siekiera, U. (2008). Limbal stem cells transplantation in the reconstruction of the ocular surface: 6 years experience. Eur J Ophthalmol *18*, 886-890.

Xie, H., Lim, B., and Lodish, H.F. (2009). MicroRNAs induced during adipogenesis that accelerate fat cell development are downregulated in obesity. Diabetes *58*, 1050-1057.

Xu, N., Papagiannakopoulos, T., Pan, G., Thomson, J.A., and Kosik, K.S. (2009a). MicroRNA-145 regulates OCT4, SOX2, and KLF4 and represses pluripotency in human embryonic stem cells. Cell *137*, 647-658.

Xu, Z.Y., Chen, J.S., and Shu, Y.Q. (2009b). Gene expression profile towards the prediction of patient survival of gastric cancer. Biomed Pharmacother. Epub ahead of print.

Yang, A., Schweitzer, R., Sun, D., Kaghad, M., Walker, N., Bronson, R.T., Tabin, C., Sharpe, A., Caput, D., Crum, C., *et al.* (1999). p63 is essential for regenerative proliferation in limb, craniofacial and epithelial development. Nature *398*, 714-718.

Yantiss, R.K., Goodarzi, M., Zhou, X.K., Rennert, H., Pirog, E.C., Banner, B.F., and Chen, Y.T. (2009). Clinical, pathologic, and molecular features of early-onset colorectal carcinoma. Am J Surg Pathol *33*, 572-582.

Yeom, K.H., Lee, Y., Han, J., Suh, M.R., and Kim, V.N. (2006). Characterization of DGCR8/Pasha, the essential cofactor for Drosha in primary miRNA processing. Nucleic Acids Res *34*, 4622-4629.

Yi, R., Poy, M.N., Stoffel, M., and Fuchs, E. (2008). A skin microRNA promotes differentiation by repressing 'stemness'. Nature *452*, 225-229.

Yi, R., Qin, Y., Macara, I.G., and Cullen, B.R. (2003). Exportin-5 mediates the nuclear export of pre-microRNAs and short hairpin RNAs. Genes Dev *17*, 3011-3016.

Yoshida, S., Shimmura, S., Kawakita, T., Miyashita, H., Den, S., Shimazaki, J., and Tsubota, K. (2006). Cytokeratin 15 can be used to identify the limbal phenotype in normal and diseased ocular surfaces. Invest Ophthalmol Vis Sci *47*, 4780-4786.

Yu, J., Ryan, D.G., Getsios, S., Oliveira-Fernandes, M., Fatima, A., and Lavker, R.M. (2008). MicroRNA-184 antagonizes microRNA-205 to maintain SHIP2 levels in epithelia. Proc Natl Acad Sci U S A *105*, 19300-19305.

Yu, T., Wang, X.Y., Gong, R.G., Li, A., Yang, S., Cao, Y.T., Wen, Y.M., Wang, C.M., and Yi, X.Z. (2009). The expression profile of microRNAs in a model of 7,12-dimethyl-benz[a]anthrance-induced oral carcinogenesis in Syrian hamster. J Exp Clin Cancer Res *28*, 64.

Zeng, Y., Yi, R., and Cullen, B.R. (2003). MicroRNAs and small interfering RNAs can inhibit mRNA expression by similar mechanisms. Proc Natl Acad Sci U S A *100*, 9779-9784.

Zhang, H., Chen, Z.H., and Savarese, T.M. (1996). Codeletion of the genes for p16INK4, methylthioadenosine phosphorylase, interferon-alpha1, interferon-beta1, and other 9p21 markers in human malignant cell lines. Cancer Genet Cytogenet *86*, 22-28.

Zhang, X., Liu, S., Hu, T., He, Y., and Sun, S. (2009). Up-regulated microRNA-143 transcribed by nuclear factor kappa B enhances hepatocarcinoma metastasis by repressing fibronectin expression. Hepatology *50*, 490-499.

Zhang, Z., Li, Z., Gao, C., Chen, P., Chen, J., Liu, W., Xiao, S., and Lu, H. (2008). miR-21 plays a pivotal role in gastric cancer pathogenesis and progression. Lab Invest *88*, 1358-1366.

Zhao, J.J., Yang, J., Lin, J., Yao, N., Zhu, Y., Zheng, J., Xu, J., Cheng, J.Q., Lin, J.Y.,

and Ma, X. (2009). Identification of miRNAs associated with tumorigenesis of retinoblastoma by miRNA microarray analysis. Childs Nerv Syst *25*, 13-20.

Zhou, B., Wang, S., Mayr, C., Bartel, D.P., and Lodish, H.F. (2007). miR-150, a microRNA expressed in mature B and T cells, blocks early B cell development when expressed prematurely. Proc Natl Acad Sci U S A *104*, 7080-7085.

Zhou, S., Schuetz, J.D., Bunting, K.D., Colapietro, A.M., Sampath, J., Morris, J.J., Lagutina, I., Grosveld, G.C., Osawa, M., Nakauchi, H., *et al.* (2001). The ABC transporter Bcrp1/ABCG2 is expressed in a wide variety of stem cells and is a molecular determinant of the side-population phenotype. Nat Med *7*, 1028-1034.

Zhu, S., Si, M.L., Wu, H., and Mo, Y.Y. (2007). MicroRNA-21 targets the tumor suppressor gene tropomyosin 1 (TPM1). J Biol Chem *282*, 14328-14336.

Zhu, S., Wu, H., Wu, F., Nie, D., Sheng, S., and Mo, Y.Y. (2008). MicroRNA-21 targets tumor suppressor genes in invasion and metastasis. Cell Res *18*, 350-359.

Zimmer, R., and Thomas, P. (2002). Expression profiling and interferon-beta regulation of liver metastases in colorectal cancer cells. Clin Exp Metastasis *19*, 541-550.